Quantum States in Cosmological Spacetimes and Entanglement in Quantum Field Theory

By

SERGI NADAL GISBERT

VNIVERSITAT DE VALÈNCIA

Departament de Física Teòrica
UNIVERSITAT DE VALÈNCIA

A dissertation submitted to the University of Valencia, in accordance with the requirements of the "3126 Programa Oficial de Doctorat en Física"

APRIL 2024

Advisors:
Prof. José Navarro Salas
Prof. Iván Agulló Ródenas

Abstract

The theory of quantized fields (QFT) in curved spacetime presents two fundamental challenges. Firstly, there's the task of explicitly calculating vacuum expectation values of field products such as the stress-energy tensor. This necessitates new regularization and renormalization techniques to address ultraviolet divergences arising from spacetime curvature while maintaining general covariance. Secondly, there's the issue of selecting a preferred vacuum state. Typically, this is straightforward only for stationary spacetimes or adiabatic regions in expanding universes, where a natural choice of vacuum can be made. However, any physically acceptable quantum state should also satisfy the Hadamard condition, which specifies the singularity structure of the two-point function. The first goal of this thesis is to give new insights into these aspects in a cosmological context. Specifically, the first part of the thesis explores the construction of a pragmatic renormalization method in cosmological spacetimes and the construction of Hadamard vacuum states for homogeneous time-dependent spacetimes, together with its main consequences in a relevant early Universe cosmological scenario.

On the other hand, the incorporation of concepts from quantum information into QFT enables the investigation of fundamental questions regarding locality and information transmission in quantum fields across diverse spacetimes. In particular, the study of entanglement in QFT plays a pivotal role in discerning purely quantum processes and has broad implications ranging from quantum information processing to fundamental physics. The vacuum state of a QFT is a rich state regarding its entanglement structure as revealed by the Reeh-Schlieder theorem. This is usually supported by calculations of entanglement entropy between a region and its complementary one. The results discussed so far pertain to subsystems with infinitely many degrees of freedom, encompassing all field modes within a region. While crucial for grasping quantum field theory conceptually and mathematically, it's also important to consider finite-dimensional subsystems, as experimentalists only have access to a finite set of degrees of freedom. The second goal of this thesis is to provide an operational approach to study entanglement between a finite set of field modes supported at different regions of space. In addition, we apply these techniques to explore the entanglement structure of the quantum field that underlies in the protocol of Entanglement Harvesting.

Agraïments

Aquesta tesi no hauria estat possible sense l'ajuda i el suport de diverses persones que han estat al meu costat durant aquesta etapa. És per això que aprofite aquestes línies per a dirigir-me a elles i expressar-los el meu agraïment més sincer.

En primer lloc, als meus pares, Pili i Paco. Gràcies per haver confiat sempre en mi i per donar-me el vostre suport per a fer el que més m'agradava. També vos agraïsc haver-me inculcat valors que han estat fonamentals per a poder presentar aquest treball i haver gaudit del camí fins ací. A la meua germana Judit, que sempre has estat al meu costat compartint els bons moments, a més d'encoratjar-me en els dolents.

Aquesta tesi tampoc haguera estat possible sense els meus directors Pepe i Iván. A Pepe, que m'has guiat des del treball de fi de grau fins a la presentació d'aquesta tesi. Gràcies per haver confiat en mi, per contagiar-me la teua passió per la física i per tractar-me com un igual. A Iván, que em vas acollir a Louisiana com si fora un *Cajun* més. Gràcies per haver-me donat aquesta oportunitat i per ensenyar-me tanta física sempre amb alegria, il·lusió i passió. Tant Iván com Pepe sou uns exemples a seguir, com a persones i en la carrera investigadora. Espere poder continuar col·laborant amb vosaltres molts anys més.

Als meus companys i col·laboradors Antonio, Silvia, Pau, Patricia i Dimitris, que tots tenen mèrit en aquesta tesi. Si he gaudit d'aquesta etapa, és en gran part gràcies a vosaltres. Silvia, moltes gràcies per acollir-me al grup des del minut zero i animar-me en els moments durs del doctorat. M'emporte molt bon record de la visita a Londres que et vaig fer. Espere que continuem col·laborant junts i ens fem moltes visites més. Pau, tot i que féiem horaris amb poca superposició "xd", amb qui més hores he compartit al despatx és amb tu. Ha sigut un privilegi tindre't de company. D'aquests anys m'emporte una bona amistat i diferents anècdotes; des de ronquits infernals a un hotel, a pizzes americanes "més *crispies*". La tesi sense vosaltres dos no haguera sigut el mateix. També he compartit moltes hores de feina amb Patricia, i algun càlcul que ens ha fet suar bastant. He aprés moltíssim treballant amb tu i et desitge el millor en els últims anys de la tesi.

D'altra banda, també estic molt agraït a Gonzalo. Gràcies per tota l'ajuda que durant aquests anys m'has oferit, així com els bons consells que m'has donat. A Eduardo i al seu grup, per haver-me acollit a Waterloo, i per haver confiat en mi per a col·laborar. Al grup de LSU (juntament amb Mari i Javi), gràcies per haver-me acollit a Louisiana en la meua primera estada de la qual tinc molts bons records. A Cristina, per haver-me ajudat amb els incomptables tràmits burocràtics que hem de fer.

No puc oblidar-me dels meus amics de la carrera: Andreu, Joan, Jorge, Pelu i Torronet. Gràcies pels moments tan bons que m'heu fet passar durant aquests anys. Tampoc, dels amics que he fet al doctorat durant aquests anys, Andreu Masó i Andreu Anglés, Flavio, Leo, Fabio, Carlos, Dani, Irene, Arnau, Rafa, Nicola, Marco, Javi i Dani. Heu fet que el dia a dia a la universitat fora molt més alegre.

Finalment, vull dedicar un agraïment especial a Elena. No només perquè m'has ajudat a corregir el text en valencià. També, i més important, perquè has estat al meu costat animant-me i fent-me feliç durant aquesta etapa. Has estat el meu punt de suport principal. Sempre has confiat en mi, fins i tot quan jo mateix dubtava de les meues capacitats. Has estat una ajuda clau en els moments difícils i la millor alegria compartint els bons moments amb mi. Per tot això, moltes gràcies de tot cor.

Author's declaration

I declare that the work presented in this thesis was carried out in accordance with the requirements of the University's Regulations and Code of Practice for Research Degree Program.

The contents of chapters 3, 4, 5, 6 and 7 of the thesis are based on the following publications

- *"Note on the pragmatic mode-sum regularization method: Translational-splitting in a cosmological background "*; P. Beltrán-Palau, A. Del Río, S. Nadal-Gisbert and J. Navarro-Salas, *Phys. Rev. D* **103** 105002 (2021).
- *"Renormalization, running couplings, and decoupling for the Yukawa model in a curved spacetime "*; A. Ferreiro, S. Nadal-Gisbert and J. Navarro-Salas, *Phys. Rev. D* **104** 2 (2021).
- *"Hadamard and boundary conditions for the Big Bang quantum vacuum "*; P. Beltrán-Palau, S. Nadal-Gisbert and J. Navarro-Salas, and S.Pla *J.Phys.Conf.Ser.* **103** 105002 (2023).
- *"Low-energy states and CPT invariance at the big bang"* S. Nadal-Gisbert, J. Navarro-Salas and S.Pla *Phys. Rev. D* **107** 8 (2023)
- *"How ubiquitous is entanglement in quantum field theory"* I. Agullo, B. Bonga, P. Ribes-Metidieri, D.Kranas and S. Nadal-Gisbert *Phys. Rev. D* **108** 085005 (2023)

The content of Chapter 8 is based on yet unpublished work.

The text presented here should be understood as a dissertation submitted to the University of Valencia as required to obtain the degree of Doctor of Philosophy in Physics.

Except where indicated by specific reference in the text, this is the candidate's own work, done in collaboration with, and/or with the assistance of, the candidate's supervisors and collaborators. Any views expressed in the thesis are those of the author.

Introducció i resum en valencià

La descripció física de la natura pretén donar explicació a tots els fenòmens que ocorren en l'univers, des de les interaccions entre les partícules elementals, fins a la formació i evolució del mateix univers. La caracterització dels diferents fenòmens físics, s'agrupa en diverses teories matemàtiques, vàlides en un rang d'escales d'energia. Entre aquestes, cal destacar les dos teories més fonamentals que coneguem, la Relativitat General (RG) i la Teoria Quàntica de Camps (TQC). Per una banda, la Teoria Quàntica de Camps unifica forces i matèria. Ambdues es descriuen com a camps que habiten a l'espai-temps i interaccionen entre ells. Aquesta exitosa teoria ha resultat en la creació del Model Estàndard de partícules [1]. D'altra banda, la Relativitat General formulada per Einstein a principis del segle XX, ens descriu la deformació de l'espai-temps a causa d'una distribució d'energia i conseqüentment dona explicació a la gravetat [2].

La tensió entre aquestes dues teories s'intueix directament de les mateixes equacions d'Einstein,

$$R_{ab} - \frac{1}{2} g_{ab} R + \Lambda g_{ab} = 8\pi G \, T_{ab} \,.$$

La part esquerra de les equacions descriu la geometria de l'espai-temps i la part dreta, amb el tensor energia-moment T_{ab}, representa el contingut d'energia que genera aquesta geometria. Aquestes equacions tenen una descripció clàssica amb un rang ampli de validesa. De fet, la gravetat d'Einsten ens permet explicar tots els fenòmens gravitatoris que observem a diferents escales, des de les ones gravitacionals i l'expansió de l'univers, fins a l'atracció gravitatòria que sentim a la terra. No obstant això, sabem que la matèria té un caràcter quàntic a nivell fonamental, i permet fenòmens que no tenen cabuda en la Relativitat General, com és el cas de la superposició d'una partícula en dos llocs diferents a la vegada. Llavors, la part dreta d'aquestes equacions admet una descripció quàntica, la qual és incompatible amb la part esquerra, és a dir, amb la descripció clàssica de la geometria .

Aquesta inconsistència, assenyala que cal una teoria més completa que acomode la interacció entre la matèria quàntica i la gravetat. A més a més, en els règims pròxims a l'escala de Planck, com per exemple a l'inici del Big Bang o a la proximitat de la singularitat d'un forat negre, la Relativitat General deixa de ser una teoria vàlida, i els efectes quàntics són rellevants. No obstant això, la formulació d'una teoria quàntica de la gravetat és una tasca altament complexa. Des dels anys 60 fins a hui dia, s'han formulat diferents propostes que donen una explicació quàntica de la gravetat. Entre les més conegudes hi ha la Teoria de Cordes [3] i la Gravetat Quàntica de Llaços [4, 5]. Tot i que aquestes han mostrat grans avanços en les últimes dècades, segueixen sent teories incompletes.

D'altra banda, als anys 70, en paral·lel a l'estudi de la Gravetat Quàntica, es va iniciar l'estudi de la Teoria Quàntica de Camps en espai-temps corbats [6, 7, 8, 9]. Aquesta és la formulació més general possible de la TQC i ens descriu els possibles efectes quàntics de la matèria en presència de gravetat. També, en l'aproximació de la gravetat *semiclàssica*, la TQC en espai-temps corbats acomoda els efectes que la matèria quàntica exerceix sobre la geometria clàssica de l'espai-temps. Una de les principals característiques de la formulació de la TQC en espai corbat, respecte a la formulació tradicional en espai-temps pla, és l'abandonament de la simetria de Poincaré i més concretament, de la simetria sota translacions temporals. Com a resultat, es deixa de tindre una noció única de partícula, i aquesta passa a ser una quantitat ambigua que depén de l'observador. La principal conseqüència d'aquest resultat és la creació espontània de partícules per espai-temps canviants. El primer a formular aquest fenomen va ser Leonard Parker [6, 10, 11] en un context cosmològic. Aquest resultat té unes fortes implicacions en l'univers primerenc. Les observacions cosmològiques indiquen que l'univers, uns segons després del Big Bang estava governat per una era espacialment plana, dominada per radiació [12], amb unes xicotetes pertorbacions escalars de l'espai-temps amb un espectre de potències inicial quasi invariant d'escala. Aquestes fluctuacions creixen a mesura que l'univers s'expandeix i evolucionen en la formació de galàxies i cúmuls de galàxies. Es creu que l'origen per a l'espectre de potències quasi invariant d'escala correspon amb fluctuacions quàntiques generades en una etapa inflacionària [13].

Poc després del treball de Parker, Stephen Hawking va aplicar les mateixes tècniques per a un espai-temps que descriu el col·lapse gravitatori formant un forat negre. Va observar que la presència de l'horitzó feia que la creació de partícules en la proximitat d'un forat negre es veiera com un flux de radiació de tipus tèrmic que emanava del forat negre [14]. Aquest fenomen dota el forat negre amb una temperatura,

$$T_H = \frac{\hbar c^3}{8\pi k_B G M} \, ,$$

inversament proporcional a la seua massa i una entropia proporcional a l'àrea de l'horitzó de successos. Estableix llavors, una profunda connexió amb les lleis de la termodinàmica. Aquest efecte i les seues implicacions han proporcionat les pistes més valuoses que ens guien cap a les característiques fonamentals que ha de tenir una teoria quàntica de la gravetat.

D'altra banda, la incorporació d'idees d'informació i òptica quàntica a la teoria de camps, permeten l'estudi de preguntes fonamentals sobre localitat i transmissió d'informació per a sistemes amb camps quàntics en espai-temps generals [15]. A més a més, la introducció de propietats únicament quàntiques com és el cas de l'entrellaçament, permet discernir si un procés relativista és purament quàntic o podria ser generat per altres mecanismes clàssics. L'entrellaçament ha estat àmpliament estudiat en diferents àrees amb diverses motivacions. Des de la informació quàntica, on l'entrellaçament quàntic s'utilitza com a recurs valuós per acomplir tasques computacionals, les quals no són possibles en la teoria de la informació clàssica [16, 17]; fins a la Gravetat Quàntica. En aquest cas l'entrellaçament quàntic s'ha proposat com a ingredient clau a partir del qual podria emergir l'espai-temps clàssic [18, 19, 20]. També per a la matèria condensada [21], on l'entrellaçament descriu les fases quàntiques de la matèria [22] i diagnostica els fenòmens crítics quàntics [23].

Particularment interessant és l'estudi de l'entrellaçament en les teories quàntiques de camps. L'entrellaçament en l'estat fonamental d'una Teoria Quàntica de Camps juga un paper important en diversos aspectes de la física. Alguns d'ells són: codifica els aspectes fonamentals de com fer coherents la relativitat i la teoria quàntica [24, 25, 26], l'entrellaçament es troba al centre de problemes oberts com la paradoxa de la informació dels forats negres [27, 28, 29] o pot ser l'eina per determinar l'origen quàntic de l'estructura a gran escala que observem en l'univers [30, 31]. Des d'una perspectiva de la tecnologia quàntica, l'entrellaçament de l'estat fonamental també pot ser utilitzat com a recurs potent en diferents protocols quàntics relativistes [32, 33, 34]. Amb tot, la quantificació de l'entrellaçament en sistemes relativistes i estats mixtos és una tasca altament complexa a causa dels infinits graus de llibertat, i a la diferència en la descripció dels espais d'estats entre la mecànica quàntica no-relativista (on usualment es defineix l'entrellaçament) i la Teoria Quàntica de Camps.

Els continguts d'aquesta tesi es poden separar en dues parts. La primera part s'engloba dins del marc de la Teoria Quàntica de Camps en espai-temps corbats, concretament en contextos cosmològics. S'hi investigarà diferents aspectes fonamentals de la renormalització en espai-temps de Friedmann-Lemaître-Robertson-Walker (FLRW) i algunes de les seues implicacions rellevants, mitjançant la creació espontània de partícules deguda a un univers en expansió. La segona part, per la seua banda, se centra en el tòpic de l'entrellaçament en la Teoria Quàntica de Camps. Concretament, aborda una investigació detallada de l'entrellaçament en l'espai de posició per a l'estat de buit d'un camp quàntic i en un espai-temps de Minkowski, centrant-se en un nombre finit de graus de llibertat del camp.

Teoria Quàntica de Camps en espai-temps cosmològics

La primera part de la tesi, corresponent als capítols 2, 3, 4 i 5, pretén estudiar algunes de les característiques essencials de la Teoria Quàntica de Camps en espai-temps cosmològics, principalment relacionats a la renormalització dels camps quàntics, així com estudiar algunes aplicacions concretes d'efectes quàntics en escenaris cosmològics rellevants.

El capítol 2 presenta una revisió de la TQC en espais corbats. L'objectiu d'aquest capítol no és presentar de manera exhaustiva i amb detall tot el que es coneix de la TQC, sinó introduir el lector no familiaritzat, a les eines i idees essencials què són necessàries per a entendre la resta de la tesi. D'aquesta manera, es presenta la quantització canònica d'un camp escalar en un espai-temps globalment hiperbòlic en $3+1$ dimensions. S'emfatitzarà en l'ambigüitat que apareix per definir un espai de Hilbert a causa de la manca de simetries. Seguidament, mitjançant les transformacions de Bogolubov, es mostra com aquesta ambigüitat resulta en el fenomen de creació espontània de partícules, degut a un espai-temps canviant. Finalment, l'última secció inclou les idees i tècniques usuals de renormalització en espai-temps corbats.

Al capítol 3, s'hi introdueix la tècnica de Levi i Ori (iniciada per Candelas [35]), [36, 37] per a obtenir un mètode de renormalització pragmàtic en espais-temps estacionaris. En aquesta tesi, la tècnica citada s'estén per a espais-temps dinàmics com els de Friedmann-Lemaître-Robertson-Walker (FLRW). La tècnica de Levi i Ori, parteix del mètode de renormalització general de *point-splitting*,

$$\left\langle \phi^2(x) \right\rangle_{\text{ren}} = \lim_{x' \to x} \left[\left\langle \{ \phi(x), \phi\left(x'\right) \} \right\rangle - G_{DS}^{(1)}\left(x, x'\right) \right] . \tag{1}$$

Donada la simetria temporal d'espai-temps estacionaris, el mètode utilitza representacions integrals dels termes de substracció, $G_{DS}^{(1)}\left(x, x'\right)$de l'expansió asimptòtica de Dewitt-Schwinger i proporciona una implementació numèrica d'integració sobre els modes del camp mitjançant integrals generalitzades,

$$\langle \phi^2(x) \rangle_{ren} = \int_m^\infty d\omega \left(|\psi_\omega(\vec{x})|^2 + a(\vec{x})\omega + c(\vec{x}) \frac{1}{\omega + m} \right) - \bar{d}(\vec{x}) . \tag{2}$$

on $a(\vec{x})$, $c(\vec{x})$ i $\bar{d}(\vec{x})$ són funcions reals de la mètrica. El mètode *pragmatic mode sum* de Levi i Ori s'ha aplicat fins ara exclusivament a espais-temps de forats negres estacionaris. En aquest capítol s'investiga com extendre aquest mètode a espais-temps dinàmics. Concretament, als espais-temps de (FLRW), especialment rellevants en estudis cosmològics, els quals són simètrics sota translacions espacials. Fent us d'aquestes simetries, esdevé natural actualitzar el mètode de *point-splitting* reescrivint el terme de resta $G_{DS}^{(1)}(x, x')$ com una integral en modes de moment $\vec{k}$, que representen les constants de moviment associades a les simetries de translació espacial. A més a més, la isotropia de la mètrica permet simplificar encara més les integrals, involucrant-hi només el valor absolut del moment, denotat com $|\vec{k}| = k$, resultant en

$$\langle \phi^2 \rangle_{ren} = \frac{1}{4\pi^2 a^3} \int_0^\infty dk k^2 \left[|h_k|^2 - \frac{1}{\omega} - \frac{(\frac{1}{6} - \xi)R}{2\omega^3} \right] - \frac{R}{288\pi^2} . \tag{3}$$

Al capítol s'exploren i implementen aquestes idees, revelant que les integrals de substracció són equivalents a les expressions derivades del mètode de regularització adiabàtica [38, 39, 40]. Aleshores, aquest treball ens permet entendre el mètode de renormalització adiabàtica com el mètode de renormalització natural que emergeix de la tècnica de *point-splitting*, quan apliquem les isometries espacials de la mètrica de FLRW.

El capítol 4 presenta, per a camps escalars, una revisió de la prescripció d'estats de baixa energia (SLE, per les sigles en anglès), què defineixen un candidat a estat de buit de tipus Hadamard en espai-temps de FLRW, i s'estén per primera vegada a camps de spin-1/2.

En TQC en espais corbats és ben sabut que, si el Hamiltonià d'un camp és depenent del temps, com en espais de FLRW; no hi ha una única elecció per a l'estat de buit, ja que l'energia canvia amb el temps [8]. No obstant això, qualsevol estat de buit físic ha de satisfer un comportament adequat en el règim ultravioleta. Concretament, el comportament d'alta energia de la funció de dos punts a l'estat de buit ha d'apropar-se al comportament en l'espai de Minkowski a un ritme que permeta la renormalització d'operadors compostos bàsics, com el tensor d'energia-moment. La condició asimptòtica que caracteritza completament el comportament singular de les funcions de dos punts s'anomena *Hadamard condition.* Els estats que la satisfan, que llavors són renormalitzables, s'anomenen *Hadamard states.*

Una proposta interessant per definir estats de buit que garanteix la condició Hadamard en espai-temps homogenis i isòtrops depenents del temps és la prescripció d'estats de baixa energia. Aquests s'obtenen minimitzant el valor d'expectació del Hamiltonià després de suavitzar-lo amb una funció de prova dependent del temps al llarg de la corba temporal d'un observador isòtrop.

$$\text{Min} : H[f] := \text{Min} : \int \mathrm{d}t \, \sqrt{g_{tt}} \, f^2(t) H(t) \, . \tag{4}$$

En general, la construcció d'aquests estats depén de l'elecció de la funció $f^2(t)$. Únicament per a espai-temps asimptòtics o altament simètrics, com de Sitter, la construcció de l'estat de baixa energia és independent de $f^2(t)$ [41, 42]. Els SLE es van introduir originalment només per a camps escalars (i per a acoblament mínim) [43]. En aquest capítol, la prescripció s'estén per a un acoblament a la curvatura general i també, per a camps de spin-1/2. Com a exemple, s'obté l'estat de buit d'un camp de spin-1/2 amb la prescripció d'estats de baixa energia en un espai-temps de Minkowski i es comprova que es recupera el buit usual de Minkowski.

Al capítol 5, s'aplica la prescripció d'estats de baixa energia per a definir un buit quàntic al voltant de la singularitat del Big Bang en un univers dominat per radiació i que respecta la simetria de reversió temporal.

Les observacions cosmològiques suggereixen un espai-temps dominat per radiació a temps primerencs amb una forma senzilla per al factor d'escala $a(\tau) \propto \tau$ (en temps conforme τ). Aquesta simplicitat ens motiva a estendre analíticament el paràmetre de temps conforme a valors negatius. El resultat és una simetria de la mètrica $ds^2 \propto \tau^2(d\tau^2 - d\vec{x}^2)$, sota la transformació $T : \tau \to -\tau$.

La simetria de reversió temporal s'ha explorat recentment a [44, 45] per a analitzar l'estat de buit, i ha donant lloc a l'estat $|0_T\rangle \propto |0_+\rangle + |0_-\rangle$. La selecció d'aquest buit depén del comportament asimptòtic a $|\tau| \to \infty$, on es poden definir solucions amb freqüències oscil·latòries positives $|0_\pm\rangle$. Aquest estat compleix la condició de Hadamard degut a la seua construcció en règims asimptòtics on el paràmetre de Hubble s'apropa a zero. No obstant això, definir l'estat d'aquesta manera implica proporcionar condicions inicials basades en el comportament a temps tardà de l'univers en expansió. Una caracterització més física implicaria definir l'estat de buit al voltant de $\tau \sim 0$ (el punt del Big Bang en temps conforme). En general, la construcció d'estats de buit al voltant de la singularitat del Big Bang resulta ser complexa a causa del seu caràcter divergent.

En aquest capítol es planteja el problema de construir estats de buit centrats en la singularitat del Big Bang $\tau \to 0$, en un univers dominat per radiació. Concretament, s'estudia la prescripció d'estats de baixa energia al voltant del Big Bang i es considera la simetria emergent sota reversió temporal, per imposar estats invariants CPT. En primer lloc, es caracteritza mitjançant els paràmetres $\{\theta_k, \Theta_k\}$, la possible família de buits invariants davall la simetria CPT per a camps escalars i fermiònics respectivament. Seguidament, s'estudia la creació de partícules en temps tardans donada per l'estat de buit, caracteritzat per $\{\theta_k, \Theta_k\}$. A continuació, s'obté la condició Hadamard per a aquets estats, en termes d'una expansió asimptòtica que han de satisfer $\{\theta_k, \Theta_k\}$,

$$\theta_k \sim \frac{\gamma^2}{8k^4} + \frac{5\gamma^4}{16k^8} + \frac{61\gamma^6}{24k^{12}} + \cdots , \tag{5}$$

$$\Theta_k \sim -\Big(\frac{\gamma}{4k^2} + \frac{\gamma^3}{6k^6} + \frac{4\gamma^5}{5k^{10}} + \cdots\Big) , \tag{6}$$

on $\gamma^2 = \frac{m^2a^2}{\tau^2}$ és una constant. Una vegada analitzats els possibles estats CPT, i el comportament ultravioleta que han de satisfer, es passa a estudiar la prescripció d'estats de baixa energia que satisfan la simetria CPT, obtenint com a resultat:

$$\theta_k = \frac{1}{2}\text{arctanh}\left(-\frac{\text{Re}(c_2)}{c_1}\right), \tag{7}$$

$$\Theta_k = \frac{1}{2}\arctan\left(\frac{\text{Im}(c_2)}{c_1}\right). \tag{8}$$

S'estudien, també, els possibles estats de baixa energia al voltant del Big Bang i es comprova que satisfan la condició Hadamard. Finalment, dins d'un context cosmològic on es requereix una cancel·lació exacta de l'anomalia conforme, hi ha un candidat natural de matèria fosca. Aquest és un *right-handed* neutrí massiu què està desacoblat de la resta del Model Estàndar. Aleshores, solament pot ser produït per creació espontània de partícules degut a la ràpida expansió de l'univers. Aquest capítol finalitza amb l'analisi de quina és la possible massa del neutrí, la qual depén de l'estat de buit inicial considerat.

Entrellaçament a l'espai real en Teoria Quàntica de Camps

La segona part de la tesi, corresponent als capítols 6, 7 i 8, se centra en estudiar l'entrellaçament d'un camp quàntic en espai de posició per a un nombre finit de graus de llibertat del camp. També pretén analitzar el mecanisme d'extracció d'entrellaçament del camp mitjançant detectors de partícules, anomenat *Entanglement Harvesting* i l'estructura d'entrelleçament del camp subjacent en aquest mecanisme.

El capítol 6 presenta la manera d'extraure un nombre finit de graus de llibertat del camp, localitzats en una regió V de l'espai. També introdueix els conceptes de mecànica quàntica d'estats Gaussians amb variable contínua, essencials per a l'estudi de l'entrellaçament entre un nombre finit de graus de llibertat, tant per a estats purs, com per a estats mixtes. Aquests conceptes s'utilitzen als capítols 7 i 8 per a estudiar l'entrellaçament d'un camp escalar en el buit de Minkowski entre un nombre finit de modes.

El contingut d'entrellaçament en la Teoria Quàntica de Camps ve suggerit pel teorema de Reeh-Schlieder [25]. Aquest teorema ens revela que l'estat de buit d'un camp quàntic és extraordinàriament ric en termes d'entrellaçamanent. En particular, si es consideren dos subsistemes A i B que contenen tots els graus de llibertat del camp suportats en les respectives regions V_A i V_B, i les dues regions estan separades espacialment, els subsistemes A i B estan sempre entrellaçats quan el camp es troba en l'estat de buit [46, 47]. No obstant això, els resultats discutits fins al moment involucren un nombre infinit de graus de llibertat en cada subsistema. És interessant extendre la discussió a sistemes de dimensió finita, ja que des d'un punt de vista pràctic, experimentalment només tenim accés a un nombre finit de modes del camp. Seguint aquesta filosofia, al present estudi s'introdueix la forma de definir modes individuals del camp de manera canònica, on és manté una estreta analogia amb sistemes amb un nombre finit d'oscil·ladors harmònics. Llavors, els modes individuals del camp es caracteritzen com un parell d'operadors lineals que no commuten

$$\left[\hat{O}_v \, , \, \hat{O}_{v'}\right] = i\Omega^{\alpha\beta} v_\alpha v'_\beta \neq 0 \, ,$$

on $\Omega^{\alpha\beta}$ és la inversa de l'estructura complexa que proporciona les relacions de commutació. Aquests operadors són definits mitjançant funcions de suport compacte (elements de l'espai de fase) de la següent manera

$$\hat{O}_{\vec{v}} := v_\alpha \hat{r}^\alpha = \int_{\Sigma_t} d^D x \left(f(\vec{x}) \, \hat{\phi}(\vec{x}, t) + g(\vec{x}) \, \hat{\pi}(\vec{x}, t) \right) .$$

Seguidament, aquest capítol presenta les tècniques de mecànica quàntica amb variable contínua necessaries per a l'estui de l'entrellaçament. Ací en presentem un resum. Donat un nombre finit de modes en un estat Gaussià, com és el cas de l'estat de buit, el sistema es caracteritza mitjançant la matriu de covariància σ, la qual conté tota la informació del sistema. La matriu de covariància es construeix a partir de les correlacions simètriques entre els diferents operadors que defineixen els modes del sistema

$$\sigma^{ij} = \langle \{ \hat{O}^i \, , \, \hat{O}^j \} \rangle \, , \tag{9}$$

on les claus $\{\ \}$ representen l'anticommutador. La informació continguda en la matriu de covariància pot ser descrita d'una manera elegant pels seus autovalors simplèctics ν_I. Aquests són els autovalors que es deriven de la matriu $i\,\sigma^{il}\Omega_{lk}$. A partir d'aquests autovalors es pot calcular l'entropia de von Neumann $S[\tilde{\sigma}]$ d'un estat reduït, $\tilde{\sigma}$, per a estats Gaussians; o la *Mutual Information*, $\mathcal{I}(A, B)$, entre un subsistema A amb N_A modes i un subsistema B amb N_B modes. La *Mutual Information* descriu les correlacions totals entre ambdós subsistemes, tant clàssiques com quàntiques. Per a evaluar les correlacions purament quàntiques, és a dir, l'entrellaçament entre el sistema A i B, s'utilitza la *Logarithmic Negativity*. Es tracta d'un quantificador fidel d'entrellaçament per a estats Gaussians quan un dels dos subsistemes conté un únic grau de llibertat. Si ambdós contenen més d'un grau de llibertat, un resultat no nul de *Logarithmic Negativity* és una condició suficient per a l'entrellaçament. Aquesta mesura s'obté aplicant l'operació local de transposició parcial a la matriu de covariància del sistema complet i se n'obtenen els seus autovalors simplètics $\tilde{\nu}_J$

$$E_{\mathcal{N}} = \sum_{J=1}^{N_A+N_B} \max\{0, -\log_2 \tilde{\nu}_J\} \,. \tag{10}$$

La *Logarithmic Negativity* és el quantificador d'entrellaçamanet que farem servir als capítols 7 i 8 per a avaluar entrellaçament entre diferents conjunts finits de modes.

El capítol 7, presenta una anàlisi detallada del contingut d'entrellaçament entre un nombre finit de modes suportats en regions separades de l'espai, per a l'estat de buit d'un camp escalar en l'espai-temps de Minkowski. S'estudia l'entrellaçament de diferents conjunts de modes rellevants: com varia depenent del suport; i com decau amb la distància i amb l'augment de la dimensió espacial.

El teorema de Reeh-Schlieder estableix que els graus de llibertat del camp dins de regions compactes separades estan entrellaçats. No importa com de separades estiguen ambdues regions. A més a més, per a qualsevol mode A del camp, localitzat en una regió V_A, el teorema garanteix que hi ha com a mínim un mode B entrellaçat amb A dins d'una altra regió V_B separada de la primera. Aquests resultats impliquen que l'entrellaçament és *ubic* en la Teoria Quàntica de Camps, fins i tot dins de subsistemes de dimensionalitat finita [46, 47]. En particular se sol assumir que qualsevol parell de modes estan entrellaçats en la Teoria Quàntica de Camps. No obstant això, el teorema no especifica com de complex és el mode B entrellaçat amb el mode A, ni ens diu quants modes en V_B estan entrellaçats amb A. Suposar que qualsevol parell de modes, un de cada regió, estan entrellaçats en l'estat de buit, és una extrapolació no justificada del contingut real del teorema. En aquest capítol s'analitza l'entrellaçamanent entre un conjunt accessible de modes. Aquests són definits mitjançant el *smearing* de l'operador camp i l'operador moment amb funcions de suport compacte, és a dir,

$$\begin{aligned} \hat{\phi}_i &:= \int \mathrm{d}^D x \, f_i(\vec{x}) \, \hat{\phi}(\vec{x}) \,, \\ \hat{\pi}_i &:= \int \mathrm{d}^D x \, f_i(\vec{x}) \, \hat{\pi}(\vec{x}) \,. \end{aligned} \tag{11}$$

on $f_i(\vec{x})$ és la funció de suport compacte. Intuitivament, cadascun d'aquests modes defineix un *píxel* en la teoria de camps, on la regió de suport indica la superfície del píxel, i la forma de $f_i(\vec{x})$ ens n'indica la sensibilitat. Llavors, aquest estudi, tot i mantindre una estructura matemàtica ben defininda amb modes covariants i locals, també es presenta com un estudi operacional amb una estreta connexió al possible accés experimental del camp. Els principals avantatges d'aquesta estratègia són que es poden utilitzar directament les tècniques de mecànica quàntica presentades al capítol 6 de manera consistent i també que desapareixen les divergències en considerar infinits graus de llibertat.

Aquest capítol mostra la dificultat d'obtindre parells de modes entrellaçats, els quals es troben suportats en regions disjuntes de l'espai, separades per una distància major que zero (Fig. 1.1). Aquesta dificultat augmenta amb la dimensionalitat de l'espai, de manera que per a una dimensió espacial $D \geq 2$ cal seleccionar curosament els modes i les seues regions de suport per tal de trobar entrellaçament. De manera que, tot i que existeix entrellaçament entre dues regions en la Teoria Quàntica de Camps, es troba distribuït d'una manera subtil.

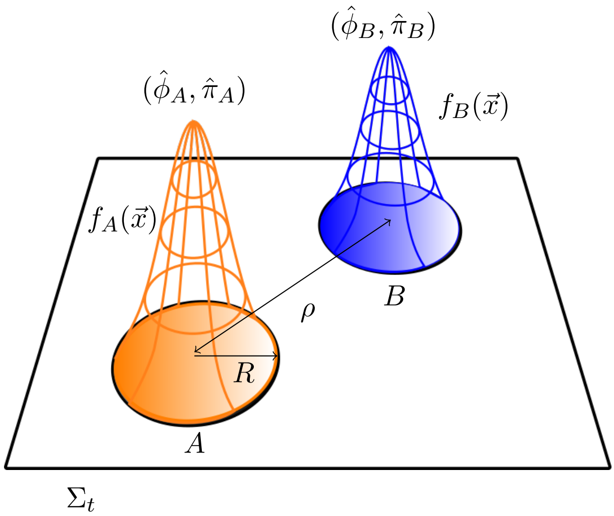

Figure 0.1: Esquema de dues boles espacialment separades de radi R en una t=constant hipersuperfície de Cauchy en un espai-temps de Minkowski amb $D+1$-dimensions. Una funció $f_{A(B)}(\vec{x})$ de suport compacte en la regió A (B) defineix un mode $(\hat{\phi}_{A(B)}, \hat{\pi}_{A(B)})$.

El capítol 8 explora el mecanisme d'extracció d'entrellaçament del camp anomenat *Entanglement Harvesting*, mitjançant l'acoblament local de detectors de tipus d'Unruh-DeWitt al camp. Seguidament, estudia l'estructura d'entrellaçament del camp que és rellevant en el protocol de *Harvesting*.

Per a obtenir informació d'un camp quàntic cal deixar-lo interaccionar amb un altre sistema extern, és a dir, amb algun tipus de detector. En el context de l'estudi de l'entrellaçament de l'estat de buit d'un camp quàntic, es planteja de manera natural la següent pregunta: podem extraure entrellaçament de l'estat de buit d'un camp quàntic, mitjançant la interacció local d'un parell de detectors amb el camp ? Valentini [48] i més tard per Reznik [49, 50], respongueren afirmativament aquesta qüestió. L'extracció d'entrellaçament del camp mitjançant un parell de detectors que localment s'hi acoblen, ha sigut àmpliament estudiada fins a dia de hui, en diferents contextos (mireu per exemple [51, 52, 53]). Aquest mecanisme és conegut com a *Entanglement Harvesting*.

Al protocol d'*Entanglement Harvesting* es consideren usualment un parell de detectors de tipus Unruh-DeWitt. Aquests són sistemes no relativistes amb dos nivells d'energia que acoblen localment al camp amb el següent Hamiltonià d'interacció:

$$H_I(t) = \sum_{j=A,B} \lambda_j \chi_j(t) \hat{\mu}_j(t) \hat{\phi}[f_j](t) \,, \tag{12}$$

on $\hat{\phi}[f_j](t)$ és el camp integrat amb la funció de *smearing* $f_j(\vec{x})$, que ens indica la regió espacial d'acoblament del detector j amb el camp. λ_j és la constant d'acoblament de la interacció. $\chi_j(t)$ és la funció de *switching* que controla el temps d'interacció i $\hat{\mu}_j(t)$ és el moment monopol del detector. Llavors, si es consideren dos detectors A i B localment acoblats al camp i interaccionant-hi de manera que n'estan causalment desconectats durant la interacció (i així no es poden transmetre informació entre ells), s'investiga si els detectors son capaços d'extraure entrellaçament de l'estat de buit del camp.

El capítol 8 es divideix en dues parts. La primera part presenta una revisió del protocol d'*Entanglement Harvesting*. S'hi emfatitzen els aspectes clau necessaris per a l'extracció de l'entrellaçament. A més, presenta alguns resultats propis on s'extrau entrellaçament de l'estat de buit del camp mitjançant aquest protocol amb un parell de detectors causalment desconnectats. Per a l'acoblament camp-detector, s'utilitza la mateixa família de funcions de *smearing* que s'utilitza al capítol 7.

Sorprenentment, els resultats d'*Entanglement Harvesting* semblen estar en contradicció amb els del capítol 7, ja que el parell de modes donats per $\hat{\phi}[f_A]$ i $\hat{\phi}[f_B]$, que acoblen al detector (mireu (12)), no estan entrellaçats en ningun instant de temps t. Llavors, com és possible que els detectors adquirisquen entrellaçament després de la interacció ?

La segona part del capítol 8 se centra en donar resposta a aquesta aparent tensió. Concretament, es mostra que cada detector explora una família contínua de modes del camp, donada per l'evolució temporal d'aquest. Llavors, tot i que no existisca entrellaçament entre parells de modes del camp, pot existir entrellaçament multimode entre les dues famílies contínues d'infinits modes que cada detector explora. Per a demostrar que aquest és el cas, es presenta la següent estratègia on a partir de l'evolució temporal del camp, s'extrau un conjunt finit de modes del camp, els quals els detectors exploren durant la interacció. Seguidament, es calcula l'entrellaçament entre aquests dos conjunts de modes. En concret, es demostra que existeix entrellaçament *multimode* entre els dos conjunts de modes del camp que cada detector és capaç d'explorar, per a la mateixa configuració on també existeix *Entanglement Harvesting.*

Metodologia i formació

Els mètodes emprats en aquesta tesi són principalment teòrics i computacionals. Entre els mètodes teòrics s'engloba: Investigació bibliogràfica, càlcul d'observables d'interès físic, extensió i aplicació de mètodes específics i idees d'unes arees d'investigació a unes altres (per exemple, aplicació de tècniques i idees d'informació quàntica a la Teoria Quàntica de Camps); resolució d'equacions diferencials, càlcul d'expansions asimptòtiques i altres. A nivell computacional s'ha fet ús de programari de càlcul avançat com ara *Mathematica* (incloent-hi el paquet *xAct* per a càlcul tensorial) i *Matlab.* També s'ha fet ús del cluster d'ordinadors de l'universitat de València (LluisVives). Les eines emprades en aquesta tesi provenen de diverses àrees de la física i les matemàtiques, com la teoria clàssica i quàntica de camps, la relativitat general, la cosmologia, la informació quàntica, l'òptica quàntica, la geometria diferencial, les equacions diferencials, i l'anàlisi real i complex,. També ha requerit una col·laboració intensa entre diversos investigadors, tant nacionals com internacionals.

Amb l'objectiu d'ampliar els meus coneixements bàsics i com a part de la formació doctoral, he assistit a diferents cursos que han tractat temes diversos d'interés dins de la física teòrica, i malgrat que els primers anys de la tesi s'engloben dins del període de la pandèmia Covid-19, també he assistit a diferents escoles internacionals de física.

- *"Selected topics on black hole physics"*. València (Espanya) 2019.

- *"Gravitational collapse and black holes"*. València (Espanya) 2020.

- *"Group Theory"*.València (Espanya) 2021.

- *" TAE 21. International workshop in high energy physics"* . Benasque (Espanya) 2021.

- *"Estate cuantística international school on Gravity, Cosmology, and Mathematical Physics"*. Scalea (Italia) 2022

- *"Loops 22 summer school on loop quantum gravity, black hole physics and general relativity"*. Marsella (França) 2022

- *"Basics of quantum gravity"*. Online school 2023 .

Així com també he realitzat dues estades internacionals a la Lousiana State university (EEUU) i a la university of Waterloo (Canadà). D'altra banda, he millorat les meves habilitats de comunicació assistint i participant en diferents conferències internacionals (per exemple, al Marcel Grossmann Meeting- MG16), tallers i seminaris.

Conclusions

Aquesta tesi agrupa els principals resultats realitzats durant el doctorat amb col·laboració amb els directors de tesi i altres investigadors. Aquesta investigació engloba dues disciplines diferents que s'inclouen dins el marc conceptual de la Teoria Quàntica de Camps. A la primera part de la tesi hem investigat alguns aspectes de la renormalització de camps quàntics en espais cosmològics, juntament amb la caracterització d'estats quàntics i les seues implicacions per a l'univers primerenc. A la segona part, hem estudiat l'entrellaçament de l'estat de buit d'una Teoria Quàntica de Camps en espai-temps de Minkowski. Aquest estudi l'hem realitzat des d'un punt de vista pràctic centrant-se en un nombre finit de graus de llibertat.

Al capítol 3 hem contribuit a estendre el mètode de renormalització de *point-splitting* a un mètode pragmàtic de renormalització. Aquest considera les substraccions dintre de la suma de modes de moment $\vec{k}$ en un espai-temps de FLRW. El mètode és útil per tal de realitzar una implementació numèrica de la renormalització de camps quàntics en espais cosmològics depenents del temps. Concretament, hem estés el *pragmatic mode-sum regularization method* a espais-temps dinàmics, ja que fins al moment aquest ha estat introduït en el context d'espais-temps estacionaris [36, 37]. Aquesta extensió ha sigut possible gràcies a la isometria sota translacions espacials de la mètrica d'espais-temps plans de FLRW. Els resultats obtinguts estan d'acord amb la prescripció coneguda de regularització adiabàtica, que fou desenvolupada per Parker i Fulling als anys 70. Llavors, la regularització adiabàtica es pot entendre com el mecanisme natural de renormalització que emergeix d'aplicar el mètode de *point-splitting* utilitzant les isometries espacials de la mètrica de FLRW.

Al capítol 4 hem presentat la prescripció d'estats de baixa energia (SLE) per a camps escalars [43] i hem contribuït extenent-la a camps de spin-1/2. El concepte d'estats de baixa energia sembla ser una prescripció molt útil per a seleccionar estats de buit en espais-temps depenents del temps, concretament, per a espais-temps de FLRW. Aquesta construcció selecciona l'estat de buit minimitjant el valor d'expectació del Hamiltonià suavitzat amb una funció depenent del temps. Té com a principal virtut que l'estat resultant satisfà la condició Hadamard.

Al capítol 5 hem fet servir el formalisme d'estats de baixa energia per a analitzar els estats de buit quàntic al voltant de la singularitat del Big Bang. En un univers dominat per radiació, i per a camps escalars i de spin-1/2. En aquest context motivat per les observacions cosmològiques, la mètrica de l'espai-temps és lineal amb el temps conforme τ a temps primerencs, i permet una extensió analítica a temps negatius del paràmetre conforme [54]. Realitzant aquesta extensió, apareix de forma natural una simetria de reversió temporal per a la mètrica. En aquest escenari cosmològic sembla natural imposar la simetria CPT al Big Bang com una condició extra que ha de satisfer l'estat de buit d'un camp quàntic.

Al capítol 5 hem caracteritzat la família d'estats de baixa energia que respecten la simetria CPT tant per a camps escalars, com per a camps de spin-1/2. Una possible elecció d'estat de buit és el proposat a [44, 45], $|0_T\rangle \propto |0_+\rangle + |0_-\rangle$. Des del punt de vista dels estats de baixa energia, aquest estat correspon a definir la funció de *smearing* temporal f^2 amb suport a qualsevol $\tau \to \pm\infty$ imposant també la simetria extra CPT. En aquest cas l'estat resultant és independent de la funció de *smearing*, ja que el seu suport està situat en regions adiabàtiques de l'espai-temps. No obstant això, aquest estat suposa donar condicions inicials basades en el comportament a temps tardans d'un univers en expansió. Una opció alternativa és definir l'estat de buit utilitzant una finestra temporal al voltant de $\tau \to 0$. Hem realitzat una anàlisi curosa per a la minimització de la densitat d'energia suavitzada amb la funció temporal, incloent-hi els factors apropiats provinents de l'element de volum. Seguidament hem comprovat que aquesta elecció és totalment consistent amb els requisits físics al règim ultravioleta, és a dir, que l'estat satisfà la condició Hadamard tant per als camps escalars com per als fermiònics. Per tant, aquests estats són candidats adequats com a buits efectius al Big Bang des del punt de vista de la Teoria Quàntica de Camps. El comportament a l'infraroig d'aquests estats és sensible a la funció de *smearing* temporal. Aquesta ambigüitat podria ser interpretada de forma natural, almenys de manera heurística, com a codificació dels efectes de la Gravetat Quàntica d'una teoria més fonamental.

Finalment, els estats obtinguts amb aquest mètode permeten fer algunes prediccions físiques interessants. En primer lloc, les ones gravitacionals primordials poden ser produïdes tot i que l'estat inicial de l'univers està descrit per una època dominada per la radiació. En segon lloc, en un escenari on es requereix completa cancel·lació de l'anomalia conforme al Big Bang, la massa del candidat natural per a la matèria fosca, és a dir, un neutrí *right-handed* ν_R; és de l'ordre de $10^8 GeV$. La predicció exacta per a la massa depèn lleugerament de la selecció de l'estat de buit.

La segona part de la tesi, centrada en l'estudi de l'entrellaçament quàntic de l'estat de buit d'un camp escalar a l'espai-temps de Minkowski, comença al capítol 6. En aquest capítol hem presentat un formalisme per a extraure modes del camp de manera canònica. També hem introduït les tècniques de mecànica quàntica per a estats gaussians i variable contínua que fem servir als següents capítols per a estudiar l'entrellaçament del camp escalar entre un nombre finit de graus de llibertat. Concretament, el formalisme es basa en extraure graus de llibertat (modes) individuals del camp localitzats en una regió compacta de l'espai, mitjançant el *smearing* del camp i el seu moment conjugat amb funcions de suport compacte. Cada mode defineix una àlgebra isomorfa a l'àlgebra d'un oscil·lador harmònic ordinari. Aquesta estratègia proporciona una manera d'extreure un conjunt finit de modes del camp de forma local i covariant, a la qual es poden aplicar les eines estàndard de la mecànica quàntica per avaluar l'entrellaçament. La nostra estratègia està lliure de divergències que afecten altres aproximacions. El focus amb un nombre finit de modes està motivat per les capacitats finites dels observadors.

Al capítol 7, hem realitzat un estudi detallat de l'entrellaçament de l'estat de buit d'un camp escalar a l'espai-temps de Minkowski en $D+1$ dimensions, entre un nombre finit de modes del camp. El conjunt específic de modes que hem considerat depèn de la selecció de les funcions de *smearing*. Al llarg d'aquest estudi, hem investigat diverses famílies d'aquestes funcions, centrant-nos en resultats comuns a aquestes. Per a certes funcions de *smearing* s'han obtingut resultats analítics per a D dimensions espacials, mentre que per a altres funcions s'han utilitzat mètodes numèrics. Fent us del caràcter gaussià de l'estat de buit, hem calculat l'estat reduït que defineix un subconjunt finit de modes i hem calculat la seua entropia, la *mutual information* i l'entrellaçament. Cal destacar que hem confirmat que l'estat reduït corresponent a subsistemes de dimensions finites és sempre mixte, en sintonia amb els resultats generals [55].

Els nostres resultats ens ensenyen que és difícil trobar parells de modes entrellaçats amb suport en regions espacialment separades per una distància no nul·la. Aquesta dificultat augmenta amb la dimensionalitat espacial. En particular, mentre que és relativament senzill trobar parells de modes entrellaçats en $D = 1$, la tasca esdevé notablement més difícil per a $D \geq 2$. De fet, observem que cal una selecció acurada de les regions de suport entre dos modes per a trobar entrellaçament en $D \geq 2$. Un exemple il·lustratiu on s'observa entrellaçament és quan un mode està confinat dins d'una esfera mentre que l'altre resideix en una closca esfèrica que l'envolta. Aquesta disposició minimitza la separació entre els modes i facilita la detecció de l'entrellaçament entre ells. Als casos on trobem entrellaçament entre parells o conjunts de modes, hem comprovat també, que en decau ràpidament amb la distància entre els subsistemes.

Amb tot, podem concloure que l'entrellaçament en la Teoria Quàntica de Camps no és tant prevalent com es creu. És ubic quan es consideren subsistemes amb infinits graus de llibertat, però no per a sistemes de dimensió finita. Aquest resultat és compatible amb el teorema de Reeh-Schlieder, que garanteix que donat un mode del camp amb suport en una regió R_A, i una segona regió R_B, hi ha com a mínim un mode a R_B que està entrellaçat amb el mode donat a R_A [47]. No obstant això, el teorema no indica quants modes a R_B estan entrellaçats amb el mode donat a R_A, ni com de complicat és aquest mode. Els nostres resultats mostren que es necessita seleccionar el mode a R_B de manera curosa per a trobar entrellaçament.

Els resultats del capítol 7 semblen estar en tensió amb el mecanisme d'*Entanglement Harvesting* en la Teoria Quàntica de Camps [49, 56]. El protocol acobla el camp quàntic a dos sistemes no relativistes que juguen el paper de detectors. Aquests s'engeguen durant una quantitat finita de temps i estan separats en l'espai de manera que romanen causalment desconnectats durant l'interval d'interacció. Els detectors estan preparats en els seus respectius estats fonamentals. Llavors, l'estat inicial del seu sistema és un estat producte sense entrellaçament. Després de la interacció, es vol saber si els dos detectors acaben en un estat entrellaçat. Si és així, degut a que els detectors no interactuen entre si ni tampoc a través del camp; aleshores, l'única possible font d'entrellaçament és el del propi camp. Aquest ha estat transferit als detectors mitjançant la interacció. En aquest sentit, es diu que els detectors extrauen entrellaçament del camp. Els càlculs del capítol

7 ens fan preguntar-nos d'on ve l'entrellaçament que adquireixen els detectors en el protocol d'*Entanglement Harvesting*, ja que parells de modes genèrics del camp no es troben entrellaçats.

La resposta a aquesta pregunta l'hem contestada al capítol 8. Per fer-ho, hem analitzat de manera detallada l'evolució temporal dels graus de llibertat del camp que acoblen a cada detector en el protocol de *Harvesting*. Hem mostrat que l'evolució temporal de cada grau de llibertat, sap sobre un conjunt infinit de modes. De fet, aquesta pot ser descrita com una família contínua de modes parametritzada pel temps t. Tots els modes d'aquesta família tenen suport a la mateixa hipersuperfície t_0. Llavors, cada detector en el protocol de *Harvesting* és capaç d'explorar un continuu de modes del camp a través de la interacció. D'aquesta manera, tot i que no existisca entrellaçament per al camp entre qualsevol parell de modes que acoblen als detector, pot existir entrellaçament multimode entre les dues famílies que cada detector explora. Per tal de demostrar-ho, al capítol 8 hem proposat una estratègia concreta on extraem un conjunt finit de modes de cada família i calculem l'entrellaçament entre ambdós conjunts mitjançant les tècniques emprades al capítol 7.

Els resultats ens mostren que existeix entrellaçament entre els dos conjunts discrets de modes del camp. Concretament obtenim els resultats per a una mateixa configuració geomètrica on els detectors són capaços d'extraure entrellaçament amb el protocol de *Entanglement Harvesting*. A més a més, aquest entrellaçament multimode del camp, sembla mostrar una tendència general a augmentar fins a arribar a un valor asimptòtic, quan incrementem també el nombre de modes. Aquest resultat està d'acord amb el teorema de Reeh-Schlieder i n'indica una realització directa d'aquest. Les dues regions espai-temporals R_A i R_B determinades per la interacció al protocol de *Harvesting*, contenen infinits graus de llibertat cadascuna. Ambdós conjunts d'aquests modes semblen estar entrellaçats, en concordança amb el teorema. A més a més, al nostre càlcul veiem que cal un nombre mínim de modes en cada regió per a trobar entrellaçament; i estan distribuïts d'una manera no trivial. Aquests resultats van en la línia de les conclusions del capítol 7. Ací s'indica que l'entrellaçament es distribueix de manera subtil, i que cal seleccionar els modes entre les dues regions de forma acurada per a trobar entrellaçament.

Amb tot, podem concloure que tot i que no hi ha entrellaçament entre cap parell de modes del camp que acoblen als detectors, existeix entrellaçament multimode entre les dues famílies de modes del camp que cada detector explora. Per tant, es possible que el protocol d'*Entanglement Harvesting* extraga entrellaçament d'aquesta estructura del camp.

Contents

Chapter 1

Introduction and summary

The physical description of nature aims to explain all phenomena that occur in the Universe, from interactions between elementary particles to the formation and evolution of the Universe itself. The characterization of different physical phenomena is grouped into different mathematical theories, valid within a range of energy scales. Among these, it is worth noting the two most fundamental theories, General Relativity (GR) and Quantum Field Theory (QFT). On one hand, quantum field theory unifies forces and matter. Both are described as fields inhabiting spacetime and interacting with each other. This successful theory has resulted in the creation of the Standard Model of particle physics [1]. On the other hand, general relativity, formulated by Einstein in the early 20th century, describes the deformation of spacetime due to an energy distribution, thereby explaining gravity [2].

The tension between these two theories is directly inferred from Einstein's equations:

$$R_{ab} - \frac{1}{2} g_{ab} R + \Lambda g_{ab} = 8\pi G \, T_{ab} \, .$$

The left-hand side describes the geometry of spacetime, and the right-hand side, with the energy-momentum tensor T_{ab}, represents the energy content generating this geometry. These equations have a classical description with a wide range of validity. In fact, Einstein's gravity allows us to explain all gravitational phenomena we observe at different scales, from gravitational waves and the expansion of the Universe to the gravitational attraction we feel on Earth. However, we know that matter has a quantum nature at a fundamental level, allowing phenomena that do not fit into the general relativity framework, such as the superposition of a particle in two different places at once. Thus, the right-hand side of these equations admits a quantum description, which is incompatible with the left-hand side, that is, the classical description of geometry [1, 2].

This inconsistency indicates the need for a more complete theory that accommodates the interaction between quantum matter and gravity. Moreover, in regimes close to the Planck scale, such as at the beginning of the Big Bang or near the singularity of a black hole, general relativity ceases to be a valid theory, and quantum effects are relevant. However, formulating a quantum theory of gravity is a highly complex task. From the 1960s to the present day, different proposals have been formulated to provide a quantum explanation of gravity. Among the most well-known being String Theory [3] and Loop Quantum Gravity [4, 5]. Although these have shown great advances in recent decades, they remain incomplete theories.

On the other hand, in the 1970s, parallel to the study of quantum gravity, the study of quantum field theory in curved spacetimes began [6, 7, 8, 9]. This is the most general formulation of QFT and describes the possible quantum effects of matter in the presence of gravity. Also, in the semiclassical gravity approximation, QFT in curved spacetimes accommodates the effects that quantum matter exerts on the classical geometry of spacetime. One of the main characteristics of the formulation of QFT in curved spacetimes, compared to the traditional formulation in flat spacetime, is the abandonment of Poincaré symmetry and, in particular, symmetry under temporal translations. As a result, there is no longer a unique notion of vacuum and particles, and they become ambiguous entities that depends on the observer. The main consequence of this result is the spontaneous creation of particles by changing spacetimes. The first to formulate this phenomenon was Leonard Parker [6, 10, 11] in a cosmological context. This result has strong implications in the early Universe. Cosmological observations indicate that the Universe, a few seconds after the Big Bang, was governed by a spatially flat era, dominated by radiation [12]. In top of that there are small scalar perturbations of spacetime with an initial almost scale invariant power spectrum. These fluctuations grow as the Universe expands and evolve into the formation of galaxies and clusters of galaxies. The origin of the almost scale invariant power spectrum is thought to correspond to quantum fluctuations generated in an hypothetical inflationary stage [13].

Shortly after Parker's work, Stephen Hawking applied the same techniques to a spacetime describing gravitational collapse forming a black hole. He observed that the presence of the horizon made the creation of particles appear as a flux of thermal type radiation which emanates from the black hole [14]. This phenomenon endows the black hole with a temperature,

$$T_H = \frac{\hbar c^3}{8\pi k_B G M}\,,$$

inversely proportional to its mass and an entropy proportional to the area of the event horizon, thus establishing a profound connection with the laws of thermodynamics. This effect and its implications have provided the most valuable clues that guide us towards the fundamental characteristics that a quantum theory of gravity must have.

On the other hand, the incorporation of quantum information and quantum optics ideas into field theory allows the study of fundamental questions about locality and information transmission for systems with quantum fields in general spacetimes [15]. Additionally, the introduction of purely quantum properties such as entanglement allows us to discern whether a relativistic process is purely quantum or could be generated by other classical mechanisms. Entanglement has been widely studied in various areas with diverse motivations. From quantum information, where quantum entanglement is used as a valuable resource for performing computational tasks that are not possible in classical information theory [16, 17]; to quantum gravity, where quantum entanglement has been proposed as a key ingredient from which classical spacetime could emerge [18, 19, 20]. Also to condensed matter [21], where entanglement describes the quantum phases of matter [22] and diagnoses quantum critical phenomena [23].

Particularly interesting is the study of entanglement in quantum field theories. Entanglement in the ground state of a quantum field theory plays an important role in various aspects of physics. Some of them are: it encodes the fundamental aspects of making relativity and quantum theory consistent [24, 25, 26];

entanglement is central to open problems such as the black hole information paradox [27, 28, 29], or it can be the tool to determine the quantum origin of large-scale structure we observe in the Universe [30, 31]. From a quantum technology perspective, the entanglement of the ground state can also be used as a powerful resource in different relativistic quantum protocols [32, 33, 34]. However, quantifying entanglement in relativistic systems and mixed states is a highly complex task due to the infinite number of degrees of freedom and the difference in the description of state spaces between non-relativistic quantum mechanics (where entanglement is usually defined) and quantum field theory.

The contents of this thesis can be separated into two parts. The first part falls within the framework of quantum field theory in curved spacetimes, specifically in cosmological contexts, where different fundamental aspects of renormalization in Friedmann-Lemaître-Robertson-Walker (FLRW) spacetimes are investigated, along with some of its relevant implications, through the spontaneous creation of particles due to an expanding universe. The second part focuses on the topic of entanglement in quantum field theory. Specifically, it addresses a detailed investigation of entanglement in position space of the ground state of a quantum field in Minkowski spacetime focusing on a finite number of degrees of freedom.

Quantum Field Theory in Cosmological Spacetimes

The first part of the thesis, corresponding to chapters 2, 3, 4, and 5, aims to study some of the essential characteristics of quantum field theory in cosmological spacetimes, mainly related to the renormalization of quantum fields, as well as to study some specific applications of quantum effects in relevant cosmological scenarios.

Chapter 2 presents a review of QFT in curved spaces. The objective of this chapter is not to present exhaustively and in detail everything known about QFT but to introduce the unfamiliar reader to the essential tools and ideas necessary to understand the rest of the thesis. Thus, the canonical quantization of a scalar field in a $3+1$ dimensional globally hyperbolic spacetime is presented, emphasizing the ambiguity that arises in defining a Hilbert space due to the absence of symmetries. Subsequently, through Bogolubov transformations, it is shown how this ambiguity results in the phenomenon of spontaneous particle creation due to a changing spacetime. Finally, the last section broadly introduces the usual ideas and techniques of renormalization in curved spacetimes.

In Chapter 3, the Levi and Ori technique (initiated by Candelas [35]) [36, 37] is introduced to obtain a pragmatic renormalization method in stationary spacetimes. In this thesis, this technique is extended to dynamic spacetimes such as Friedmann-Lemaître-Robertson-Walker (FLRW) spacetimes. The Levi and Ori technique is based on the general renormalization method of point-splitting,

$$\left\langle\phi^2(x)\right\rangle_{\text{ren}}=\lim_{x'\to x}\left[\left\langle\left\{\phi(x),\phi\left(x'\right)\right\}\right\rangle-G_{DS}^{(1)}\left(x,x'\right)\right],$$

Given the temporal symmetry of stationary spacetimes, the method uses integral representations of the point-splitting subtraction terms $G_{DS}^{(1)}\left(x,x'\right)$, obtained from the DeWitt-Schwinger representation of the Hadamard function and provides a numerical implementation of integration over field modes through generalized integrals,

$$\langle\phi^2(x)\rangle_{\text{ren}}=\int_m^\infty d\omega\left(|\psi_\omega(\vec{x})|^2+a(\vec{x})\omega+c(\vec{x})\frac{1}{\omega+m}\right)-\bar{d}(\vec{x})\,.$$

where $a(\vec{x})$, $c(\vec{x})$ and $\bar{d}(\vec{x})$ are real functions of the metric. The Levi and Ori "pragmatic mode sum" method has so far been exclusively applied to stationary black hole spacetimes. In this chapter, we investigate how to extend this method to dynamic spacetimes. Specifically, to FLRW spacetimes, especially relevant in cosmological studies, which are symmetric under spatial translations. By using these symmetries, it becomes natural to update the point-splitting method by rewriting the subtraction term $G_{DS}^{(1)}(x,x')$ as an integral over momentum modes $\vec{k}$, representing the constants of motion associated with spatial translation symmetries. Moreover, the metric isotropy further simplifies the integrals, involving only the absolute value of momentum, denoted as $|\vec{k}|=k$, resulting in

$$\langle\phi^2\rangle_{\text{ren}}=\frac{1}{4\pi^2a^3}\int_0^\infty dkk^2\left[|h_k|^2-\frac{1}{\omega}-\frac{(\frac{1}{6}-\xi)R}{2\omega^3}\right]-\frac{R}{288\pi^2}\,.$$

This chapter explores and implements these ideas, revealing that the subtraction integrals are equivalent to the expressions derived from the adiabatic regularization method [38, 39, 40]. Therefore, the adiabatic renormalization method can be understood as the natural renormalization procedure that emerges when the point-splitting technique is applied using the spatial isometries of the FLRW metric.

Chapter 4 presents, for scalar fields, a review of the states of low energy prescription (SLE), which defines a Hadamard-type vacuum state in FLRW spacetimes, and extends it for the first time to spin-1/2 fields.

It is well known in QFT in curved spaces that if the Hamiltonian of a field depends on time, as in FLRW spaces, there is no unique choice for the vacuum state minimizing the Hamiltonian, because energy changes with time [8]. However, any physically admissible vacuum state must exhibit suitable behavior in the ultraviolet regime. Specifically, the high-energy behavior of the two-point function in the vacuum state must approach the behavior in Minkowski space at a rate that allows for the renormalization of basic composite operators, such as the energy-momentum tensor. The asymptotic condition that fully characterizes the singular behavior of the two-point functions is called the *Hadamard condition.* States that satisfy it and are thus renormalizable in some sense, are called *Hadamard states.*

An interesting proposal for defining vacuum states that ensure the Hadamard condition in time-dependent spacetimes is the prescription of low energy states. These are obtained by minimizing the expectation value of the Hamiltonian after smoothing it with a time-dependent test function along the worldline of an isotropic observer

$$\text{Min} : H[f] := \text{Min} : \int \mathrm{d}t \, \sqrt{g_{tt}} \, f^2(t) H(t) \, .$$

In general, the construction of these states depends on the choice of the function $f^2(t)$. Only for asymptotically flat or highly symmetric spacetimes, such as de Sitter, the construction of the low-energy state is independent of $f^2(t)$ [41, 42]. The SLE were originally introduced only for scalar fields (and for minimal coupling) [43]. This chapter extends the prescription to a general coupling to the curvature and also extends the prescription to spin-1/2 fields. As an example, the vacuum state of a spin-1/2 field is obtained with the low energy state prescription in Minkowski spacetime, and it is verified that the usual Minkowski vacuum is recovered.

Chapter 5 applies the low energy state prescription defined in the previous chapter to define a quantum vacuum around the Big Bang singularity in a radiation-dominated universe respecting time reversal symmetry.

Cosmological observations suggest a radiation-dominated spacetime at the early times with a simple form for the scale factor $a(\tau) \propto \tau$, in conformal time τ. This simplicity motivates us to analytically extend the conformal time parameter to negative values, resulting in an emergent metric symmetry $ds^2 \propto \tau^2(d\tau^2 - d\vec{x}^2)$, under the transformation $T : \tau \to -\tau$.

The time reversal symmetry has been recently explored in [44, 45] to analyze the vacuum state, leading to the state $|0_T\rangle \propto |0_+\rangle + |0_-\rangle$. Selecting this vacuum depends on the asymptotic behavior at $|\tau| \to \infty$, where solutions with positive oscillatory frequencies $|0_\pm\rangle$ can be defined. This state satisfies the Hadamard condition due to its construction in asymptotic regimes where the Hubble parameter approaches zero. However, defining the vacuum state in this way implies providing initial conditions based on the late-time behavior of the expanding universe. A more physical characterization would involve defining the vacuum state around $\tau \sim 0$ (the Big Bang point in conformal time). In general, constructing vacuum states around the Big Bang singularity proves to be complex due to its divergent nature.

This chapter addresses the problem of constructing vacuum states around the Big Bang singularity $\tau \to 0$, in a radiation-dominated universe. Specifically, the prescription of low energy states around the Big Bang is studied, and the emergent symmetry under time reversal is considered to impose states invariant under CPT. First, the possible family of CPT-invariant vacuum states for scalar and fermionic fields is characterized through the parameters $\{\theta_k, \Theta_k\}$. Then, the particle creation at late times given by the vacuum state characterized by $\{\theta_k, \Theta_k\}$ is studied. Next, the Hadamard condition for these states is obtained in terms of an asymptotic expansion that $\{\theta_k, \Theta_k\}$ must satisfy,

$$\theta_k \sim \frac{\gamma^2}{8k^4} + \frac{5\gamma^4}{16k^8} + \frac{61\gamma^6}{24k^{12}} + \cdots \tag{1.1}$$

$$\Theta_k \sim -\left(\frac{\gamma}{4k^2} + \frac{\gamma^3}{6k^6} + \frac{4\gamma^5}{5k^{10}} + \cdots\right). \tag{1.2}$$

where $\gamma^2 = \frac{m^2a^2}{\tau^2}$ is a constant. Once the possible CPT states and their ultraviolet behavior are analyzed, the prescription of low energy states satisfying the CPT symmetry is obtained, getting as a result:

$$\theta_k = \frac{1}{2}\text{arctanh}\left(-\frac{\text{Re}(c_2)}{c_1}\right), \tag{1.3}$$

$$\Theta_k = \frac{1}{2}\arctan\left(\frac{\text{Im}(c_2)}{c_1}\right), \tag{1.4}$$

and the possible low-energy states around the Big Bang are studied, verifying that they satisfy the Hadamard condition. Finally, within a cosmological context where an exact cancellation of the conformal anomaly is required, there is a natural candidate for dark matter. This is a massive right-handed neutrino that is decoupled from the rest of the Standard Model. Therefore, it can only be produced by spontaneous particle creation due to the rapid expansion of the Universe. This chapter concludes by analyzing the possible mass of the neutrino, which depends on the initial vacuum state considered.

Entanglement in real space in Quantum Field Theory

The second part of the thesis, corresponding to chapters 6, 7, and 8, focuses on studying the entanglement of a quantum field in position space for a finite number of field degrees of freedom. It also analyzes the field entanglement structure underlying in the mechanism of "Entanglement Harvesting".

Chapter 6 presents a way to extract a finite number of field degrees of freedom located in a region V of space. It also introduces the essential concepts of quantum mechanics of Gaussian states with continuous variables for studying entanglement between a finite number of degrees of freedom, both for pure and mixed states. These concepts are used in chapters 7 and 8 to study the entanglement of a scalar field in the Minkowski vacuum between a finite number of modes.

The entanglement content in quantum field theory is suggested by the Reeh-Schlieder theorem [25]. This theorem reveals that the vacuum state of a quantum field is extraordinarily rich in terms of entanglement. In particular, if two subsystems A and B containing all the field degrees of freedom supported in their respective regions V_A and V_B are spatially separated, subsystems A and B are always entangled when the field is in the vacuum state [46, 47]. However, the results discussed so far involve an infinite number of degrees of freedom in each subsystem. It is interesting to extend the discussion to systems of finite dimension since, from a practical point of view, we can only have access to a finite number of field modes experimentally. Following this philosophy, this chapter introduces a way to define individual field modes canonically, maintaining a close analogy with systems with a finite number of harmonic oscillators. Thus, individual field modes are characterized as a pair of non-commuting linear operators

$$\left[\hat{O}_v\,,\,\hat{O}_{v'}\right] = i\Omega^{\alpha\beta}v_\alpha v'_\beta \neq 0\,,$$

where $\Omega^{\alpha\beta}$ is the inverse of the complex structure that provides the commutation relations between the elementary observables. These operators are defined by a pair of compactly supported functions (elements of the phase space) as follows

$$\hat{O}_{\vec{v}} := v_\alpha \hat{r}^\alpha = \int_{\Sigma_t} d^D x \left(f(\vec{x})\,\hat{\phi}(\vec{x},t) + g(\vec{x})\,\hat{\pi}(\vec{x},t)\right).$$

Subsequently, this chapter introduces techniques from quantum mechanics of continuous variables which are necessary to study entanglement. Here we provide a summary. Given a finite number of modes in a Gaussian state, such as the vacuum state, the system is characterized by the covariance matrix σ, which contains all the information of the system. The covariance matrix is constructed from symmetric correlations between the different operators defining the system modes

$$\sigma^{ij} = \langle\{\hat{O}^i, \hat{O}^j\}\rangle.$$

where the curly brackets $\{\ \}$ represent the anti-commutator. The information contained in the covariance matrix can be elegantly described by its symplectic eigenvalues ν_I. These are the eigenvalues derived from the matrix $i\,\sigma^{il}\Omega_{lk}$. From these, one can calculate the von Neumann entropy $S[\tilde{\sigma}]$ of a reduced state $\tilde{\sigma}$, or the Mutual Information $\mathcal{I}(A, B)$ between subsystem A with N_A modes and subsystem B with N_B modes. The Mutual Information describes the total correlations between both subsystems, both classical and quantum. To evaluate purely quantum correlations, i.e., the entanglement between system A and B, the Logarithmic Negativity is used. This is a faithful entanglement quantifier for Gaussian states when one of the two subsystems contains a single degree of freedom. If both contain more than one degree of freedom, a non-zero result of Logarithmic Negativity is a sufficient condition for entanglement. This measure is obtained by applying the local operation of partial transposition to the covariance matrix of the complete system and obtaining its symplectic eigenvalues $\tilde{\nu}_J$

$$E_{\mathcal{N}} = \sum_{J=1}^{N_A+N_B} \max\{0, -\log_2 \tilde{\nu}_J\}.$$

The Logarithmic Negativity is the entanglement quantifier that we will use in chapters 7 and 8 to evaluate entanglement between different finite sets of modes.

Chapter 7 presents a detailed analysis of the entanglement content between a finite number of modes supported in separate regions of space for the vacuum state of a scalar field in Minkowski spacetime. The entanglement between different mode sets is studied. This analysis includes how it varies depending on their support, and how it decays with the distance and by increasing the spatial dimension.

The Reeh-Schlieder theorem states that the degrees of freedom of the field within separate compact regions are entangled. Doesn't matter how separated the regions are. Moreover, for any mode A of the field, localized in a region V_A, the theorem guarantees that there is at least one mode B entangled with A within another separated region V_B. These results imply that entanglement is spatially distributed in quantum field theory, even within finite-dimensional subsystems [46, 47]. In particular, it is often assumed that any pair of modes, one from each region, are entangled in the vacuum state of a quantum field theory. However, the theorem does not specify how complex the entangled mode B with mode A is, nor does it tell us how many modes in V_B are entangled with A. Assuming that any pair of modes, one from each region, are entangled in the vacuum state is an unjustified extrapolation of the real content of the theorem. This chapter analyzes entanglement between an accessible set of modes. These are defined by smearing the field operator and the momentum operator with positive definite compactly supported functions, i.e.,

$$\begin{aligned} \hat{\phi}_i &:= \int \mathrm{d}^D x\, f_i(\vec{x})\, \hat{\phi}(\vec{x})\,, \\ \hat{\pi}_i &:= \int \mathrm{d}^D x\, f_i(\vec{x})\, \hat{\pi}(\vec{x})\,, \end{aligned} \tag{1.5}$$

where $f_i(\vec{x})$ is the positively defined compactly supported function. Intuitively, each of these modes defines a "pixel" in field theory, where the support region indicates the surface of the pixel, and the shape of $f_i(\vec{x})$ indicates its sensitivity. Thus, this study, while maintaining a well-defined mathematical structure with covariant and local modes, also presents itself as an operational study with a close connection to possible experimental access to the field. The main advantages of this strategy are that the techniques of quantum mechanics presented in chapter 6 can be directly applied consistently, and that the divergences of QFT due to its infinite degrees of freedom, disappear.

This chapter illustrates the difficulty of obtaining entangled mode pairs that are supported in disjoint regions of space, separated by a distance greater than zero (Fig. 1.1). This difficulty increases with the spatial dimensionality, so for a spatial dimension $D \geq 2$, it is necessary to carefully select the modes and their support regions in order to find entanglement. Therefore, although entanglement in quantum field theory exists between any two regions, it is distributed in a subtle manner.

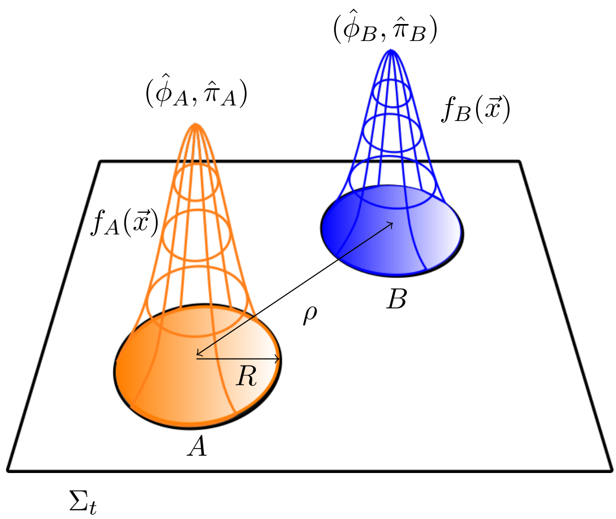

Figure 1.1: Illustration of two spacelike separated balls of radius R in a t=constant Cauchy hypersurface in $D+1$-dimensional Minkowski spacetime. A function $f_{A(B)}(\vec{x})$ compactly supported in region A (B) defines a single field-mode $(\hat{\phi}_{A(B)}, \hat{\pi}_{A(B)})$.

Chapter 8 explores the mechanism of extracting entanglement from the vacuum state of the field, through the local coupling of Unruh-DeWitt type detectors to the field. This protocol is known as “Entanglement Harvesting”. Subsequently, it studies the entanglement structure of the field that is relevant in the Harvesting protocol.

To obtain information from a quantum field, it is necessary to let it interact with another external system, i.e., with some type of detector. In the context of studying the entanglement of the vacuum state of a quantum field, the following question naturally arises: Can we extract entanglement from the vacuum state of a quantum field by locally coupling a pair of detectors to the field? This question was answered affirmatively by Valentini [48] and subsequently by Reznik [49, 50]. The extraction of entanglement from the field with a pair of detectors has been widely studied to date, in different contexts (see, for example, [51, 52, 53]). This mechanism is known as "Entanglement Harvesting."

In the protocol of "Entanglement Harvesting " a pair of Unruh-DeWitt type detectors are usually considered. These are non-relativistic systems with two energy levels, which locally couple to the field with the following interaction Hamiltonian:

$$H_I(t) = \sum_{j=A,B} \lambda_j \chi_j(t) \hat{\mu}_j(t) \hat{\phi}[f_j](t)\,,$$

where $\hat{\phi}[f_j](t)$ is the field integrated with the smearing function $f_j(\vec{x})$, which indicates the spatial region of coupling of detector j with the field. λ_j is the coupling constant of the interaction. $\chi_j(t)$ is the switching function that controls the interaction time, and $\hat{\mu}_j(t)$ is the detector's monopole moment. One considers two detectors A and B and let them interact with the field such that they are causally disconnected during the interaction (thus no information can be transmitted between them). Subsequently it is investigated whether the detectors are capable of extracting entanglement from the vacuum state of the field.

The first part of Chapter 8 presents a review of the Entanglement Harvesting protocol, emphasizing the key aspects necessary for entanglement extraction. Then presents some own results where entanglement is extracted from the vacuum state of the field with a pair of causally disconnected detectors. For the field-detector coupling, it is used the same family of smearing functions as in Chapter 7. Surprisingly enough, the Harvesting results seem to be in tension with the results of Chapter 7, since the pair of modes given by $\hat{\phi}[f_A]$ and $\hat{\phi}[f_B]$, which couple to the detector in the Harvesting protocol (see (12)), are not entangled at any given instant of time t. Thus, how is it possible that the detectors acquire entanglement after the interaction?

The second part of Chapter 8 focuses on addressing this apparent tension. Specifically, it is shown that each detector explores a continuous family of field modes, given by their temporal evolution. Therefore, although there is no entanglement between pairs of field modes, there can be multimode entanglement between the two continuous families of modes that each detector explores. To demonstrate that this is indeed the case, a strategy is proposed. First, one extracts a finite set of field modes that each detectors explore during the interaction time. Then, the entanglement between these two sets of modes is calculated. This chapter demonstrates that there is *multimode entanglement* between the two sets for the same configuration where Entanglement Harvesting also exists.

Finally, in Chapter 9, the conclusions and the main results of the thesis are presented.

1.1 Methodology and Training

The methods employed in this thesis are primarily theoretical and computational. Theoretical methods encompass literature research, calculation of physical observables, extension and application of specific methods and ideas from one research area to another (e.g., application of quantum information techniques to quantum field theory), solving differential equations, calculating asymptotic expansions, and others. On the computational side, advanced calculation software such as *Mathematica* (including the *xAct* package for tensor calculus) and *Matlab* were utilized. Additionally, the computing cluster at the University of Valencia (Lluis-Vives) was also employed. The tools used in this thesis stem from various areas of physics and mathematics, including classical and quantum field theory, general relativity, cosmology, quantum information, quantum optics, differential geometry, differential equations, real and complex analysis. Moreover, intense collaboration among various researchers, both nationally and internationally, was necessary.

In order to expand my foundational knowledge and as part of doctoral training, I have attended various courses covering diverse topics within theoretical physics and despite the initial years of the thesis coinciding with the Covid-19 pandemic, I also participated in several international physics schools:

- *"Selected topics on black hole physics"*. València (Espanya) 2019.

- *"Gravitational collapse and black holes"*. València (Espanya) 2020.

- *"Group Theory"*.València (Espanya) 2021.

- *"TAE 21. International workshop in high energy physics"* . Benasque (Espanya) 2021.

- *"Estate cuantística international school on Gravity, Cosmology, and Mathematical Physics"*. Scalea (Italia) 2022

- *"Loops 22 summer school on loop quantum gravity, black hole physics and general relativity"*. Marsella (França) 2022

- *"Basics of quantum gravity"*. Online school 2023 .

Additionally, I conducted two international visits to Louisiana State University (USA) and the University of Waterloo (Canada). Furthermore, I enhanced my communication skills by attending and participating in various international conferences (e.g., the Marcel Grossmann Meeting - MG16), workshops, and seminars.

Part I

Quantum field theory in cosmological spacetimes

Chapter 2

Quantum field theory in curved spacetime

Fundamental physics, as we know it today, is based on two independent theories: General Relativity and Quantum Field Theory. On one hand, General Relativity describes gravitation and the spacetime itself. In this theory, matter and energy instructs spacetime on how to curve. Simultaneously, the curvature of spacetime determines the dynamics of the matter residing within this spacetime. General relativity, since its formulation in 1915 until the present day, has demonstrated remarkable success in describing the macro-cosmos, predicting various observed phenomena such as light bending, the detection of gravitational waves, and the expansion of the universe.

On the other hand, quantum field theory describes the fundamental forces and the constituents of matter that we observe in the Universe. These are unified in the concept of fields that permeate all of spacetime. Particles cease to be fundamental and emerge from these fields as local excitations of the field. With the development of the Standard Model in the early sixties and the detection of all its particles, including the Higgs boson in 2012 at the LHC, quantum field theory lays the foundations for describing the micro-cosmos up to the present day.

One of the major challenges in fundamental physics is the incompatibility between these two theories. A consistent theory of quantum gravity is necessary to describe phenomena occurring at the Planck scale. However, the lack of experimental data at such energies makes this task extremely complex. In the absence of a quantum theory of gravity, quantum field theory in curved spaces has served as a crucial tool for describing quantum effects produced by gravitational interaction and for explaining how quantum fields might influence classical gravity. QFT in curved spacetimes accounts for various relevant phenomena occurring in our universe. In particular it has two main applications of great interest. The first is the creation of anisotropies observed in the cosmic microwave background, which later give rise to the large-scale structures that we observe in the Universe. These are due to quantum fluctuations in an inflationary expansion of the Universe. The second application is the gravitational creation of particles in the proximity of a black hole. This phenomenon, known as the Hawking effect, endows black holes with a radiation temperature and entropy, establishing a profound connection with the laws of thermodynamics. This effect and its implications provide us the most valuable clues to date, guiding toward the fundamental features that a consistent quantum theory of gravity should possess.

In this chapter, I will introduce the basic ideas regarding the quantization of fields in curved spaces. The intention is not to provide a detailed analysis of the subject but rather to offer the reader who is not familiar with the topic a general overview of the concepts and subtleties that arise when quantizing a field in curved spaces. This chapter will serve to contextualize the rest of the chapters presented in the thesis. For a detailed analysis of the quantum field theory in curved spaces, refer to [8, 7, 9, 57].

2.1 Canonical quantization

To show the main features in the quantization of fields in a curved spacetime, we will consider the quantization of a scalar field propagating in a globally hyperbolic spacetime (M, g_{ab}). [1] This guarantees the existence of a one-parameter family of Cauchy hypersurfaces Σ_t which foliates M and therefore ensures that there exists

[1] In the following we will use the $(+,-,-,-)$ metric sign convention

a well-posed initial value problem for the classical solutions to the equation of motion [9]. The action for the scalar field is given by,

$$S\left[\phi, \nabla_a \phi, g_{ab}\right] = \frac{1}{2}\int d^4x\sqrt{-g}\left(\nabla_a\phi\nabla^a\phi - m^2\phi^2\right)\,, \tag{2.1}$$

We are not including the $\xi R\phi^2$ term required for renormalization, because it is not relevant for the points that we want to stress in this section. From the principle of least action, $\delta S = 0$, we obtain the equation of motion

$$\left(\Box + m^2\right)\phi = 0\,. \tag{2.2}$$

Given two complex solutions f and g of (2.2), there exist the conserved scalar product over a time

$$(f, g) = i\int_{\Sigma_t} d^3x\sqrt{-h}\,n^a\left(f^*\nabla_a g - g\nabla_a f^*\right)\,, \tag{2.3}$$

where Σ_t is a spacelike hypersurface and n^a is a future-directed orthonormal vector to it and $\sqrt{-h}$ is the determinant of the induced metric on Σ_t. The product (f, g) is invariant under the choice of Σ_t. This product is usually called the Klein-Gordon product and it will play a pivotal role in the quantized theory when constructing a Hilbert space.

To quantize the theory we consider the field variable $\phi(x)$ and the canonical conjugated momentum

$$\pi(x) = \sqrt{-h}n^a\nabla_a\phi(x)\,,$$

and promote them to self-adjoint operators $(\hat{\phi}(x), \hat{\pi}(x))$ acting on a Hilbert space $\mathcal{H}$. The quantization follows by upgrading the Poisson bracket algebra of the classical observables to a commutation algebra for the quantum observables (representations of classical observables in the Hilbert space). In particular, the equal time commutation relations for field and conjugate momentum read

$$\left[\hat{\phi}(x,t), \hat{\pi}(x',t)\right] = i\hbar\,\delta(x,x')\,, \tag{2.4}$$

where $\delta(x,x') = \delta^3(\vec{x}-\vec{x}')$. In order to build a Hilbert space, we allow for complex solutions of (2.2), and split the space of complex solutions $\mathcal{S}_{\mathbb{C}}$ in [2]

[2]From now on we will use units $c = \hbar = 1$ and only reintroduce this factors when we want to show the quantum and relativistic character explicitly.

$$\mathcal{S}_{\mathbb{C}} = S_+ \oplus S_- \,, \tag{2.5}$$

where S_+ is a subspace of solutions with positive norm and $S_- = S_+^*$ its complex conjugate. Therefore for all $f^+ \in S_+$ and $f^- \in S_-$ we have

$$\left(f^+, f^+\right) > 0 \quad ; \quad \left(f^-, f^-\right) < 0 \quad ; \quad \left(f^+, f^-\right) = 0\,. \tag{2.6}$$

As a remark, it is easy to check that the positive frequency solutions in Minkowski spacetime $f^+ \propto e^{-i\omega t}$ have positive norm. Therefore, S_+ defines a Hilbert space in $\mathbb{C}$. Using the above structure we can define annihilation and creation operators for any $f \in S_{\mathbb{C}}$ by

$$\hat{a}(f) = (f^+, \hat{\phi}) \quad ; \quad \hat{a}^\dagger(f) = -a(f^*)\,. \tag{2.7}$$

Making use of (2.4) and of the K-G product (2.3) we can obtain the commutation relations for the annihilation and creation operators

$$[\hat{a}(f), \hat{a}(g)] = 0 \quad ; \quad \left[\hat{a}^\dagger(f), \hat{a}^\dagger(g)\right] = 0 \quad ; \quad \left[\hat{a}(f), \hat{a}^\dagger(g)\right] = (f^+, g^+)\,. \tag{2.8}$$

In particular, we can take an orthonormal basis $\left\{e_i^+\right\}$ spanning S_+ such that

$$\left(e_i^+, e_j^+\right) = \delta_{ij} \quad ; \quad \left(e_i^-, e_j^-\right) = -\delta_{ij} \quad ; \quad \left(e_i^+, e_j^-\right) = 0\,, \tag{2.9}$$

and define a basis of creation and annihilation operators

$$\hat{a}(e_i) \equiv \hat{a}_i = (e_i^+, \hat{\phi}) \quad ; \quad \hat{a}^\dagger(e_i) \equiv \hat{a}_i^\dagger = -\hat{a}(e_i^*)\,, \tag{2.10}$$

such that the commutation relations (2.8) for this basis satisfy

$$[\hat{a}_i, \hat{a}_j] = 0 \quad ; \quad [\hat{a}_i^\dagger, \hat{a}_j^\dagger] = 0 \quad ; \quad [\hat{a}_i, \hat{a}_j^\dagger] = \delta_{ij}\,. \tag{2.11}$$

In the Fock space representation, the vacuum state $|0\rangle$ is annihilated by any $\hat{a}_i$,

$$\hat{a}_i|0\rangle = 0\,.$$

The one-particle Hilbert space is spanned by the states created by acting with creation operators on the vacuum

$$|1_i\rangle = \hat{a}_i^\dagger|0\rangle\,.$$

The many particle states are created by the recursive action of creation operators in the vacuum state

$$|n_1, \cdots, n_l\rangle = \frac{\left(\hat{a}_1^\dagger\right)^{n_1}}{\sqrt{n_1!}} \cdots \frac{\left(\hat{a}_l^\dagger\right)^{n_l}}{\sqrt{n_l!}} |0\rangle\,,$$

where sub-indices $1...l$ refer to different one-particle states. $\hat{n}_i \equiv \hat{a}_i^\dagger \hat{a}_i$ is usually called the particle number operator, since it's expectation value on the state $|n_1, \cdots n_l\rangle$ give us the number of i particles in this state,

$$\langle n_1, \cdots n_l|\hat{n}_i|n_1, \cdots n_l\rangle = n_i\,.$$

The self-adjoint observable $\hat{\phi}(x)$ is represented in the Hilbert space by

$$\hat{\phi}(x) = \sum_i \hat{a}_i e_i^+(x) + \hat{a}_i^\dagger e_i^-(x)\,. \tag{2.12}$$

Note that, in a general spacetime, the decomposition $\mathcal{S}_\mathbb{C} = S_+ \oplus S_-$ is not unique and there is no preferred criteria to select a vacuum state out of which we build the Fock representation. Only for highly symmetrical spacetimes. In particular, for *stationary* spacetimes, which admit a time-like Killing vector field t^a, there is a natural decomposition for the field modes associated to this observer in terms of positive frequency solutions $\mathcal{L}_t e_i^+ = -i\omega_i e_i^+$ which have a well defined frequency $\omega_i > 0$. The temporal isometry of stationary spacetimes, renders a *time-independent* Hamiltonian for the t^a observer,

$$\hat{H} = \int_{\Sigma_t} \mathrm{d}^3x\sqrt{-h}\,\hat{T}_{ab}\,t^a n^b\,,$$

and therefore a conserved notion of energy over time. This quantity is independent of the hypersurfase Σ_t that we choose. The vacuum state is choosen to be the state with the minimum value for the vacuum expectation value of the Hamiltonian. As an example, in Minkowski spacetime, we have the Poincaré symmetry with the natural coordinates (t, x, y, z) associated to inertial observers. The vector ∂_t is a temporal Killing vector field of the metric and define the normalized positive frequency modes $e_{\vec{k}}^+ \propto e^{i(\vec{k}\vec{x}-\omega t)}$. These modes define the basis of annihilation and creation operators and thus the vacuum state $\hat{a}_{\vec{k}}|0\rangle = 0$. This definition of the vacuum state is the only one that is invariant under a Poincaré transformation. Moreover, the Hamiltonian with this mode decomposition is given by

$$\hat{H} = \int \frac{d^3\vec{k}}{(2\pi)^3}\omega_k(\,\hat{a}_{\vec{k}}^\dagger\hat{a}_{\vec{k}} + \frac{1}{2}\delta^3(0)\,), \tag{2.13}$$

which is time independent, and after rescaling the zero point energy gives $\langle 0| : \hat{H} : |0\rangle = 0$, which is the minimum energy possible. $|0\rangle$ is usually called the ground state of the Hamiltonian. As a final remark, note that the $\int \frac{d^3\vec{k}}{(2\pi)^3}\frac{1}{2}\omega_k$ term in (2.13), corresponds to the vacuum energy density of an infinite collection of harmonic oscillators and it is divergent. The process of rescaling the vacuum energy is called normal ordering. This is possible in Minkowski spacetime where we are only able to observe energy differences. The renormalization of this kind of divergences in curved spacetime requires a more involved analysis and will be outlined in section 2.3

2.2 Bogolubov transformations and particle creation

We have seen that the vacuum state is not unique in time-dependent spacetimes. Only for stationary spacetimes, or adiabatic regions in expanding universes (approximately stationary), one can naturally find a privileged definition of the vacuum. A major consequence of this ambiguity is the particle creation phenomena, as first discovered in cosmology [6, 10, 11, 58] and also in the vicinity of black holes [14]. To illustrate this phenomena, consider a different splitting for the complex space of solutions (2.5),

$$\mathcal{S}_{\mathbb{C}} = \bar{S}_{+} \oplus \bar{S}_{-}\,,$$

with the corresponding basis $\left\{g_i^+\right\}$ of $\bar{S}^+$ and $g_i^- = g_i^+$ The basis of annihilation and creation operators $\left\{\hat{A}_i\, \hat{A}_i^\dagger\right\}$ define a new vacuum state

$$\hat{A}_i|\bar{0}\rangle = 0 \quad \forall\, i\,.$$

Because $\left\{g_i^+, g_i^-\right\}$ and $\left\{e_i^+, e_i^-\right\}$ are complete basis of $\mathcal{S}_{\mathbb{C}}$, any element of $\mathcal{S}_{\mathbb{C}}$ can be written as a linear combination of the basis elements. In particular, we can write

$$g_i^+ = \sum_j \alpha_{ij} e_j^+ + \beta_{ij} e_j^-\,, \tag{2.14}$$

or inverting this expression,

$$e_i^+ = \sum_j \alpha_{ji}^* g_j^+ - \beta_{ji} g_j^-\,. \tag{2.15}$$

These are called Bogolubov transformations and the Bogolubov coefficients, α_{ij} and β_{ij}, for the above orthonormal basis, can be obtained computing the projections

$$\alpha_{ij} = (e_i^+, g_j^+) \quad ; \quad \beta_{ij} = -(e_i^+, g_j^-)\,. \tag{2.16}$$

We can decompose the field observable in the new basis as

$$\hat{\phi}(x) = \sum_i \hat{A}_i g_i^+(x) + \hat{A}_i^\dagger g_i^-(x)\,. \tag{2.17}$$

Equating (2.17) to (2.12) and making use of (2.14) and (2.15) we can obtain the following Bolgolubov transformations for the creation and annihilation operators

$$\hat{a}_i = \sum_j \alpha_{ij}^* \hat{A}_j - \beta_{ij}^* \hat{A}_j^\dagger\,, \tag{2.18}$$

or inverting this relation,

$$\hat{A}_i = \sum_j \alpha_{ji} \hat{a}_j + \beta_{ji}^* \hat{a}_j^\dagger\,, \tag{2.19}$$

To obtain this last expression we have made use of the orthonormalization of the basis modes (2.9). Applied to the Bogobulov coefficients the orthonormalization condition reads

$$\begin{aligned} \sum_l (\alpha_{il}^* \alpha_{kl} - \beta_{il}^* \beta_{kl}) &= \delta_{ik}\,, && (2.20)\\ \sum_l (\alpha_{il} \beta_{kl} - \beta_{il} \alpha_{kl}) &= 0\,. && (2.21) \end{aligned}$$

Note that if $\beta_{ij} \neq 0$, the two vacua are different. In fact, the expectation value of the particle number operator $\hat{N}_i \equiv \hat{A}_i^\dagger \hat{A}_i$ associated to the modes g_i^+ in the vacuum state of $|0\rangle$ is different from zero and given by

$$\begin{aligned} \langle 0|\hat{N}_i|0\rangle &= \langle 0| \sum_j \sum_l (\alpha_{ji}^* \hat{a}_j^\dagger + \beta_{ji} \hat{a}_j)(\alpha_{li} \hat{a}_l + \beta_{li}^* \hat{a}_l^\dagger)|0\rangle \\ &= \sum_j \sum_l (\beta_{ji} \beta_{li}^*) \langle 1_j | 1_l \rangle \\ &= \sum_l |\beta_{li}|^2\,. \end{aligned} \tag{2.22}$$

where in the last equality we have used that $\langle 1_j | 1_l \rangle = \delta_{jl}$. This calculation shows that the notion of particle in QFT is an observer dependent quantity. For example, if one considers asymptotic regions *in* and *out* where the spacetime can be treated as asymptotically flat in the remote past and future, there is a preferred vacuum state associated to the inertial observers in each regions ($|in\rangle$ and $|out\rangle$). The calculation (2.22) shows that the future observer perceives the $|in\rangle$ state, as an state full of particles [10]. Even in Minkwoski spacetime, the notion of particle is subjected to inertial observers. In fact, one can consider an accelerated observer (Rindler observer) and expand the Minkowski metric in his associated Rindler coordinates. Using the time-like Killing vector field associated to this observer, one can define creation and annihilation operators adapted to the accelerated observer. The Minkowski vacuum defined by inertial observers as the state containing no particle, is perceived by the accelerated observer as an state containing particles with a black-body spectrum with temperature $a/(2\pi)$, where a is the acceleration of Rindler observers. This effect is called the Fulling-Davies-Unruh effect [59, 60, 61].

As a final remark: From the mathematical side, one can regard the Bogolubov transformations (2.18) and (2.19) as a unitary transformation U, such that

$$U|0\rangle = |\bar{0}\rangle \,. \tag{2.23}$$

One can prove that this is well defined only when (see [62, 63])

$$\sum_{li} |\beta_{li}|^2 < \infty. \tag{2.24}$$

This has a clear interpretation: The total number of particles that a vacuum state contains in the other Fock space representation has to be finite [64].

From now on, in the following sections I will use $\phi(x)$ instead of $\hat{\phi}(x)$ to alleviate the notation.

2.3 Ultraviolet regularity

Many times in Quantum Field Theory one has to deal with quadratic operators of the field variables and derivatives of it evaluated at a single point. If one aims to study how quantum fields backreact on the geometry of the spacetime through the *semiclassical* Einstein equations, it is particularly interesting to evaluate the expectation value of the stress-energy tensor, $\langle T_{ab}(x)\rangle$, in curved spacetimes

$$R_{ab} - \frac{1}{2}Rg_{ab} + \Lambda g_{ab} = -8\pi G\langle T_{ab}\rangle\,. \tag{2.25}$$

The naive calculation of the expectation values of quantities such as $\langle\phi^2(x)\rangle$ and $\langle T_{ab}(x)\rangle$ shows that they are divergent. This is because the field observables $\phi(x)$ are not well defined operatirs in spacetime. In fact, they are operator valued distributions, and quantities such as $\langle\phi^2(x)\rangle$ involve taking the product of two distributions at the same spacetime point, which formally diverges. However, the product of $\langle\phi(x)\phi(x')\rangle$ is well defined as a bi-distribution. Already in Minkwoski spacetime, the vacuum expectation value of quadratic operators evaluated at a single point diverges. In flat spacetime the successful renormalizable theories, has taught us that these ultraviolet divergences can be reabsorbed in the *bare* parameters of the Lagrangian under consideration, since this parameters are not predictable from our theory and have to be measured experimentally. A major consequence of renormalization in Minkowski spacetime is the running of the couplings, this refers to the fact that the couplings of the theory acquire a different value depending on the energy scale of the problem under consideration.

In curved spacetimes, the systematics on renormalization have been known for several decades now (see [8, 7, 65] for a review). A formal way of renormalizing vacuum expectation values of composite operators, for example the two point function in a general spacetime, is by using the point-splitting approach [66, 67, 68]. This consists in taking the symmetric product of field operators $G^{(1)}(x,x') \equiv \langle\{\phi(x)\phi(x')\}\rangle$ (also usually called the Hadamard function) at different points and subtract the divergent terms of a locally constructed bi-distribution $G_H^{(1)}(x,x')$, which satisfies the Klein-Gordon equation (2.2) in both x and x', and that has an appropriate singular structure, such that it respects general covariance and recovers the singularity structure of Minkowski spacetime at an appropriate rate. Finally, one takes the coincident limit $x \to x'$ connecting these nearby points. The result of this procedure defines the renormalized two-point function:

$$\left\langle\phi^2(x)\right\rangle_{\text{ren}} = \lim_{x'\to x}\left[\left\langle\{\phi(x),\phi\left(x'\right)\}\right\rangle - G_H^{(1)}\left(x,x'\right)\right]\,, \tag{2.26}$$

where usually one substracts up to the last locally divergent term of $G_H^{(1)}$.

$G_H^{(1)}(x, x')$ has the following asymptotic formal solution [69]

$$G_H^{(1)}\left(x, x'\right) = \frac{\Delta^{1/2}\left(x, x'\right)}{(4\pi)^2}\left(\frac{2}{\sigma\left(x, x'\right)} + v\left(x, x'\right)\ln\sigma\left(x, x'\right) + w\left(x, x'\right)\right), \quad (2.27)$$

where

$$\Delta\left(x, x'\right) = -|g(x)|^{-1/2}\det\left[-\partial_\mu\partial_{\nu'}\sigma\left(x, x'\right)\right]\left|g\left(x'\right)\right|^{-1/2}$$

is the biscalar Van Vleck-Morette determinant and

$$\sigma\left(x, x'\right) = \frac{1}{2}\tau\left(x, x'\right)^2,$$

where $\tau\left(x, x'\right)$ is the proper distance along the geodesic between x and x'. $v(x, x')$ and $\omega(x, x')$ are analytic functions of $\sigma(x, x')$ admitting the following series

$$v\left(x, x'\right) = \sum_{n=0}^{\infty} v_n\left(x, x'\right)\sigma^n, \quad (2.28)$$

$$w\left(x, x'\right) = \sum_{n=0}^{\infty} w_n\left(x, x'\right)\sigma^n. \quad (2.29)$$

The coefficients $v_n\left(x, x'\right)$ can be determined by plugging (2.27) in to the field equation and solving recursively. There is freedom in setting the $\omega_0(x, x')$ coefficient in a symmetric manner. Once $\omega_0(x, x')$ is specified, the other $\omega_n(x, x')$ are completely satisfied . Note that in the coincidence limit ($x \to x'$; $\quad \sigma \to 0$), the divergences of $G_H^{(1)}(x, x')$ are all contained in the $1/\sigma$ and $\ln\sigma$ terms. The renormalized vacuum expectation value of the stress-energy tensor can be obtained by acting with a nonlocal operator to the symmetric part of the two-point function

$$\langle T_{\mu\nu}\rangle = \lim_{x\to x'}\mathcal{D}_{\mu\nu}(x, x')\left[\left\langle\left\{\phi(x), \phi\left(x'\right)\right\}\right\rangle - G_H^{(1)}(x, x')\right]. \quad (2.30)$$

This differential operator $\mathcal{D}_{\mu\nu}(x, x')$ contains different quadratic terms of covariant derivatives [70, 67];

Note that the Hadamard expansion (2.27) imposes an extra condition (usually called *Hadamard condition*) to the vacuum state $|0\rangle$ in curved spacetimes. This is because we require any physically admissible vacuum state to be ultraviolet regular. This means that vacuum expectation values of quantities such as $\langle\phi^2(x)\rangle$ can be renormalized. States that satisfy the Hadamard expansion (2.27) at all orders are called *Hadamard states.* This condition ensures the existence of any Wick polynomials of arbitrary order [71, 72, 73] and hence, the perturbative series of an interacting theory to be well-defined at any order. For highly symmetric spacetimes such as de Sitter, the Hadamard condition is sufficient to single out a unique vacuum state that is invariant under the symmetries of the spacetime. This is the so called Bunch-Davies vacuum in de Sitter spacetimes. For less symmetric spacetimes, in general this condition is not enough to univocally select a preferred vacuum state.

In the following three chapters, we will address three distinct aspects related to the renormalization of quantum fields in curved spaces. In the first chapter 3, we will demonstrate how, in a background possessing three-dimensional spatial symmetries, the point-splitting method can be upgraded into a pragmatic regularization method, ultimately reducing to the adiabatic regularization prescription. In the final two chapters 4 and 5, we will investigate how to define vacuum states in FLRW spacetimes that are compatible with renormalization, i.e., satisfying the Hadamard expansion (2.27). We will also provide a physically relevant example of particle creation due to an early expansion of the universe. With this chapter we will conclude the first part of the thesis related to different renormalization aspects of quantum fields in curved spacetimes.

Chapter 3

A pragmatic mode-sum regularization method in cosmology: Adiabatic regularization

The general prescriptions of renormalization in curved spacetimes are well known since last decades. Usually renormalization is performed by implementing the point-splitting technique. As it was shown in the previous chapter, this is a purely analytical procedure that involves taking limits of points along geodesics. However, getting the field modes in a given spacetime background requires solving complicated differential equations, which can only be addressed numerically but in exceptional cases. Hence, it is nearly imperative to develop a method that transforms the covariant point-splitting technique into a numerically implementable approach if quantum field theory intends to yield practically relevant results for a wide range of gravitational scenarios.

The first insight was given by Candelas, in the 1980s [35]. Candelas upgraded the point-splitting method for Schwarzschild spacetimes. Considering the temporal symmetry, he rewrote the subtraction terms in an integral representation of the frequencies ω that could be subtracted and integrated together with the mode part, thereby yielding a formally finite result upon which the limit of points could be taken before integrating in ω. However, the numerical implementation of these integrals was still a difficult task and this idea was not pursued further. Some years later Howard and Candelas [74, 75, 76] presented an alternative way of dealing with the problem which involved an analytical WKB-type approximation of the field and a Wick rotation to extend the metric to the Euclidean space. This method was successful in the Schwarzschild background and it was later extended for a general static and spherically symmetric metric by Anderson and collaborators [77, 78]. However, this procedure presents some problems when attempting to extend it to time-dependent backgrounds, as for instance in evaporating black-holes.

To address these issues, Levi and Ori developed the pragmatic mode-sum method of regularization [36, 37], which bypasses analytic approximations and can be applied to backgrounds with some isometry. This method utilizes integral representations of point-splitting subtraction terms and provides a successful numerical implementation of integration over field modes using generalized integrals. The technique has proven useful in numerically computing $\langle \phi^2(x) \rangle$ and $\langle T_{\mu\nu}(x) \rangle$ in various black hole backgrounds [79, 37, 80, 81, 82, 83, 84]. The importance of this new approach is that it can be applied to any metric provided that it has some symmetry. Let me review it for stationary spacetimes without going into the details. For instance, for a stationary spacetime one can define creation and annihilation operators, $A^\dagger_\omega$ and A_ω, by decomposing the field operator into positive and negative frequency parts,

$$\phi(x) = \int_m^\infty d\omega \left[A_\omega f_\omega(x) + A^\dagger_\omega f^*_\omega(x) \right] \,, \tag{3.1}$$

The notion of field modes f_ω, f^*_ω of positive and negative frequency ω can be introduced in a natural way by the conditions $\mathcal{L}_K f_\omega = -i\omega f_\omega$, $\mathcal{L}_K f^*_\omega = i\omega f^*_\omega$, where K is the infinitesimal generator of the isometry (i.e. the Killing vector field). Choosing a natural coordinate system $\{t, \vec{x}\}$ such that $K = \partial/\partial t$, this condition implies

$$f_\omega(x) = e^{-i\omega t}\psi_\omega(\vec{x}) \,, \tag{3.2}$$

where $\vec{x}$ is a shorthand for the three spatial coordinates x^k. The determination of the spatial functions $\psi_\omega(\vec{x})$ is achieved by solving numerically the Klein-Gordon equation. In this case, the point-splitting technique to renormalize the two-point function

$$\langle \phi^2(x) \rangle = \int_m^\infty d\omega \, |\psi_\omega(\vec{x})|^2 \,, \tag{3.3}$$

is described in (2.26). Following [36, 37], we can use the DeWitt-Schwinger representation of the Feynman propagator to obtain a particular asymptotic expansion for the Hadamard function. We will denote it as $G^{(1)}_{DS}(x, x')$ [65]. The point-splitting technique can be upgraded to a pragmatic regularization method by choosing $x = (t, \vec{x})$ and $x' = (t + \epsilon, \vec{x})$ with $\epsilon > 0$ an infinitesimal parameter. Splitting along this points, we localize the divergences of $G^{(1)}_{DS}(x, x')$, in the terms proportional to $\frac{1}{\epsilon^2}$ and $\log(m\epsilon)$. The interesting point is to express the ϵ-dependent terms as generalized integrals (in the distributional sense) with respect to ω. By doing this we can subtract the divergent part of the two-point function within the integral over modes, (3.3), finding the following expression for the renormalized two-point function:

$$\langle \phi^2(x) \rangle_{ren} = \lim_{\epsilon \to 0} \int_m^\infty d\omega \left(|\psi_\omega(\vec{x})|^2 + a(\vec{x})\omega + c(\vec{x}) \frac{1}{\omega + m} \right) \cos(\omega\epsilon) - \bar{d}(\vec{x}) \,, \tag{3.4}$$

where $a(\vec{x}), c(\vec{x})$, and $\bar{d}(\vec{x})$ are real functionals of the metric. Since the original point-splitting subtraction terms were capturing the divergences of the two point function. We expect the above integral to be convergent. Then, the limit and the integration can be interchanged and we finally obtain the following result for the renormalized two-point function:

$$\langle \phi^2(x) \rangle_{ren} = \int_m^\infty d\omega \left(|\psi_\omega(\vec{x})|^2 + a(\vec{x})\omega + c(\vec{x}) \frac{1}{\omega + m} \right) - \bar{d}(\vec{x}) \,. \tag{3.5}$$

Thus, with these manipulations the quantity $\langle \phi^2(x) \rangle_{ren}$ can, at least in principle, be computed using ordinary numerical techniques.

The pragmatic mode-sum regularization method has, so far, been exclusively applied to stationary black hole spacetimes. However, there is an inquiry into whether this approach can be extended to other symmetric spacetimes, potentially dynamic ones. Friedmann-Lemaitre-Robertson-Walker (FLRW) spacetimes, particularly relevant in cosmological studies, exhibit spatial translations through three spatial Killing vector fields. Leveraging these symmetries, it becomes natural to enhance the point-splitting method by rewriting the subtraction term $G^{(1)}_{DS}(x, x')$ as an integral in modes of momentum $\vec{k}$, representing the constants of motion associated with spatial translation symmetries. Additionally, the isotropy of the background metric allows further simplification of the integrals to involve only the absolute value of the Killing momentum, denoted as $|\vec{k}| = k$. This chapter explores and implements these ideas, revealing that the subtraction integrals align with expressions derived from the method of adiabatic regularization [38, 39, 40].

In the following section we will first introduce the adiabatic method of regularization for FLRW spacetimes. Continuously, we will extend the pragmatic mode-sum regularization method, considering the spatial translation simmetries os homogeneous spacetimes, revealing that the subtraction integrals align with expressions derived from the method of adiabatic regularization.

3.1 Adiabatic renormalization

Consider a scalar field $\phi(x)$ in a spatially flat FLRW spacetime $ds^2 = dt^2 - a^2(t)d\vec{x}^2$ which satisfies the Klein-Gordon equation,

$$(\Box + m^2 + \xi R)\phi = 0\,. \tag{3.6}$$

This spacetime does not admit a temporal Killing vector field which provides general positive frequency solutions. Given the isometries under spatial translations we can expand the field as

$$\phi(x) = \int d^3k \left[A_{\vec{k}} f_{\vec{k}}(x) + A^\dagger_{\vec{k}} f^*_{\vec{k}}(x) \right] \,, \tag{3.7}$$

where, $A_{\vec{k}}$ and $A^\dagger_{\vec{k}}$ refer to the annihilation and creation operators satisfying canonical commutation relations, and $f_{\vec{k}}(x)$ denote a complete orthonormal family of solutions to the field equation with positive norm such that $(f_{\vec{k}}, f_{\vec{k}'}) = \delta^3(\vec{k}-\vec{k}')$, $(f_{\vec{k}}, f^*_{\vec{k}'}) = 0$. The field modes satisfy $\mathcal{L}_{K^j} f_{\vec{k}} = ik^j f_{\vec{k}}$, where $\{K^j\}_{j=1,2,3}$ denote the three Killing vector fields associated with spatial translations. Thus, in a canonical coordinate chart $\{t, \vec{x}\}$ where $K^j = \partial/\partial x^j$ the field modes take the general form

$$f_{\vec{k}}(x) = \frac{e^{i\vec{k}\cdot\vec{x}}}{\sqrt{2(2\pi)^3 a(t)^3}} h_k(t) \,. \tag{3.8}$$

The orthonormalization condition is translated into a Wronskian condition for the modes h_k

$$h^*_k \dot{h}_k - \dot{h}^*_k h_k = -2i\,, \tag{3.9}$$

where the dot means derivative with respect to time t. The Klein-Gordon equation when substituting with the modes (3.8) reads

$$\ddot{h}_k + [\omega_k(t)^2 + \sigma(t)]h_k = 0\,, \tag{3.10}$$

with $\omega_k^2 = \frac{k^2}{a^2} + m^2$, $k^2 = \vec{k}^2$ and $\sigma = (6\xi - \frac{3}{4})(\frac{\dot{a}}{a})^2 + (6\xi - \frac{3}{2})\frac{\ddot{a}}{a}$. In FLRW spacetimes there is a very convinient way to renormalize quantities such as the two-point function

$$\langle \phi^2 \rangle = \frac{1}{(2\pi)^2 a(t)^3} \int_0^\infty dk k^2 |h_k(t)|^2\,. \tag{3.11}$$

This method is called the adiabatic method and it is based on an WKB asymptotic expansion of the fourier modes,

$$h_k(t) \sim \frac{1}{\sqrt{W_k(t)}} e^{-i\int^t W_k(t')dt'}\,, \tag{3.12}$$

which satisfies the Wronskian condition. The idea behind the adiabatic expansion lays in the fact that particles are not created in the absence of curvature. This is in the limit that the wave-length of a particle $\lambda = 2\pi/k$ is much smaller than the curvature terms $\dot{a}(t)^2/a^2$ and $\ddot{a}(t)/a(t)$ so that it doesn't feel it. Equivalently, we can say that the particle energy is much bigger than the energy scale of spacetime. Therefore, using the Fourier modes we can formulate an asymptotic expansion in terms of time derivatives of the metric or the scale factor $a(t)$ in this case. Thus we expand,

$$W_k = \omega_k + \omega_k^{(1)} + \omega_k^{(2)} + \omega_k^{(3)} + \omega_k^{(4)} + \cdots\,. \tag{3.13}$$

The coefficient $\omega_k^{(n)}$ depends on derivatives of $a(t)$ up to and including the order n, provided that n derivatives of $a(t) \equiv a$ exist. We note here that the square of frequency scale of the background $\sigma(t)$ is a function of adiabatic order two. The leading order of the expansion is $\omega_k^{(0)} \equiv \omega_k = \sqrt{k^2/a^2 + m^2}$ and the next-to-leading orders are obtained, by systematic iteration, from the relation

$$W_k^2 = \omega_k^2 + \sigma + \frac{3}{4}\frac{\dot{W}_k^2}{W_k^2} - \frac{1}{2}\frac{\ddot{W}_k}{W_k}\,, \tag{3.14}$$

derived from the mode equation (3.10). The adiabatic expansion of the modes is translated to an adiabatic expansion for the two point function $\langle \phi^2(x) \rangle \equiv G(x,x)$:

$$G_{Ad}(x,x) = \frac{1}{2(2\pi)^3 a^3} \int d^3k\, [\omega^{-1} + (W^{-1})^{(2)} + (W^{-1})^{(4)} + ...]\,. \tag{3.15}$$

The expansion is truncated to the minimal adiabatic order necessary to cancel all ultraviolet divergences that appear in the formal expression of the vacuum expectation value that one wishes to compute. The calculation of the renormalized variance $\langle\phi^2\rangle$ requires only second adiabatic order. The subtractions terms for the two point function are given by

$$^{(2)}G_{Ad}(x,x) = \frac{1}{4\pi^2 a^3}\int k^2 dk \left[\frac{1}{\omega} + \frac{(\frac{1}{6}-\xi)R}{2\omega^3} + \left(\frac{m^2\dot{a}^2}{2a^2\omega^5} + \frac{m^2\ddot{a}}{4a\omega^5} - \frac{5m^4\dot{a}^2}{8a^2\omega^7}\right)\right] . \tag{3.16}$$

where the last terms in the parentheses are finite and can be integrated to give

$$\frac{1}{4\pi^2 a^3}\int k^2 dk \left[\frac{m^2\dot{a}^2}{2a^2\omega^5} + \frac{m^2\ddot{a}}{4a\omega^5} - \frac{5m^4\dot{a}^2}{8a^2\omega^7}\right] = \frac{R}{288\pi^2} . \tag{3.17}$$

Thus the term obtained from the adiabatic expansion to be subtracted to (3.11) reads:

$$^{(2)}G_{Ad}(x,x) = \frac{1}{4\pi^2 a^3}\int_0^\infty dk k^2 \left[\frac{1}{\omega} + \frac{(\frac{1}{6}-\xi)R}{2\omega^3}\right] + \frac{R}{288\pi^2} . \tag{3.18}$$

And the renormalized value for the two-point function at coincidence reads:

$$\langle\phi^2\rangle_{ren} = \frac{1}{4\pi^2 a^3}\int_0^\infty dk k^2 \left[|h_k|^2 - \frac{1}{\omega} - \frac{(\frac{1}{6}-\xi)R}{2\omega^3}\right] - \frac{R}{288\pi^2} . \tag{3.19}$$

This method was developed by Parker and Fulling in the early 1970s for cosmological backgrounds and scalar fields [38, 39, 40] and it has been later extended for spin-1/2 fields [85, 86, 87, 88] and more recently also understood for spin-1 fields [89]).

In the following section we will arrive to the same result as in (3.19) applying the pragmatic mode sum regularization method. For this, we will consider the point-splitting prescription and split the points along the symmetric directions given by the spatial translations of a flat FLRW universe.

3.2 DeWitt-Schwinger representation of the Feynman propagator

In order to renormalize the two-point funtion $\langle\phi^2(x)\rangle$ using the point-splitting technique

$$\left\langle\phi^2(x)\right\rangle_{\text{ren}} = \lim_{x'\to x}\left[\left\langle\{\phi(x), \phi\left(x'\right)\}\right\rangle - G_{DS}^{(1)}\left(x,x'\right)\right] , \tag{3.20}$$

one needs to regularize the divergences of $G^{(1)}(x,x') \equiv \langle\{\phi(x),\phi(x')\}\rangle$ in terms of the geodesic distance between the two points as proposed in the formal Hadamard expansion (2.27). Following [67], we can achieve this goal by making use of the Dewitt-Schwinger proper-time expansion for the Feynman propagator. The Feynman green function and the Hadamard function are related by

$$G_F(x,x') = \bar{G}(x,x') - i\frac{1}{2}G^{(1)}(x,x'),$$

where $\bar{G}(x,x')$ is equal to one-half the sum of the advanced and retarded green function. Let us shortly review how to obtain the formal expansion for the Dewitt-Schwinger proper-time expansion for the Feynman propagator. Consider $G_F(x,x')$ satisfying,

$$(\Box_x + m^2 + \xi R)G_F\left(x,x'\right) = \sqrt{-g}\,\delta(x-x')\,. \tag{3.21}$$

We can write the symmetric operator

$$K_{xy} = (\Box_x + m^2 + \xi R)\frac{1}{\sqrt{-g(y)}}\,\delta(x-y)\,. \tag{3.22}$$

where defining

$$K^{-1}_{yz} = -G_F(y,z)\,, \tag{3.23}$$

these operators satisfy the property

$$\int d^n y\sqrt{-g(y)}K_{xy}K^{-1}_{yz} = \frac{1}{\sqrt{-g(z)}}\delta(x-z) \tag{3.24}$$

We can introduce a fictitious Hilbert space spanned by $|x\rangle$, where these states are eigenvectors of the formal operators $\hat{x}^a$, ($\hat{x}^a|x\rangle = x|x\rangle$) and there is a normalization condition given by

$$\langle x|x'\rangle = \frac{1}{\sqrt{-g(x)}}\delta(x-x')\,.$$

With the introduction of the Hilbert space we can write $G_F(x,x')$ and $K_{xx'}$ as

$$G_F(x,x') = \langle x|G_F|x'\rangle \tag{3.25}$$

$$K_{xx'} = \langle x|K|x'\rangle \tag{3.26}$$

where G_F and K are now operators acting on the Hilbert space. The equivalent of (3.23) in terms of these operators reads now $G_F = -K^{-1}$. At this point we can introduce the Schwinger parametrization, with the integral form for K^{-1} given by

$$\frac{1}{K-i\epsilon}=i\int_0^\infty e^{-i(K-i\epsilon)s}ds \tag{3.27}$$

where $\epsilon>0$ is introduced to have a formal convergent integral. With this, we can write the Feynman green function as

$$G_F(x,x')=-i\int_0^\infty \langle x|e^{-i\,K\,s}|x'\rangle ds=-i\int_0^\infty e^{-i(m^2-i\epsilon)s}\,\langle x,s|x',0\rangle ds \tag{3.28}$$

where $\langle x,s|x',0\rangle$ is usually called the Heat-Kernel and satisfies a Schrodinger's type equation

$$\mathrm{i}\frac{\partial}{\partial s}\left\langle x,s\mid x',0\right\rangle=\left(\square_x+\xi R\right)\left\langle x,s\mid x',0\right\rangle, \tag{3.29}$$

with a boundary condition, $\lim_{s\to 0}\langle x,s\mid x',0\rangle=\frac{1}{\sqrt{-g(x)}}\delta\left(x-x'\right)$. The Heat-Kernel represents the probability amplitude for one particle to propagate from x to x' in a proper time interval s [90]. Within the context of a WKB approximation, (3.29) has an asymptotic expansion in powers of s

$$\left\langle x,s\mid x',0\right\rangle=i(4\pi is)^{-n/2}\Delta^{1/2}\left(x,x'\right)\exp\left[\frac{\sigma\left(x,x'\right)}{2is}\right]\sum_{n=0}^{\infty}a_n(x,x')(is)^n \tag{3.30}$$

where $a_n(x,x')$ are the DeWitt coefficients, which can be solved recursively from (3.29), using $a_0(x,x')=1$, which satisfies the $s=0$ condition. These coefficients are regular when taking the coincidence limit $x\to x'$. $\sigma(x,x')$ is one-half of the geodesic distance connecting the nearby point x and x'. $\Delta(x,x')$ is the Van Vleck-Morette determinant defined as

$$\Delta(x,x')=-|g(x)|^{-1/2}\det\left[-\partial_\mu\partial_{\nu'}\sigma(x,x')\right]|g(x')|^{-1/2}\,. \tag{3.31}$$

The Feynman green function (3.28) therefore has the following expansion

$$G_F(x,x')=\frac{\Delta^{1/2}(x,x')}{(4\pi)^2}\int_0^\infty\frac{ds}{(is)^2}e^{-i(m^2s+\frac{\sigma}{2s})}\sum_{n=0}^{\infty}a_n(x,x')(is)^n\,. \tag{3.32}$$

In the coincidence limit $x\to x'$, this expression encodes the singular behaviour of the two point function in the two first terms of the expansion when $s\to 0$. (3.32) can be written in terms of Hankel functions which can be expanded in an asymptotic series in powers of σ. Restricting to the imaginary part of the Feynman green function, give us an expansion for the symmetric two-point function in terms of covariant quantities evaluated at x and the geodesic distance between x and x'. Including only the relevant terms needed in the calculation of the renormalized two-point function (i.e. up to second-order derivatives of the metric) we get

$$G^{(1)}_{DS} = \frac{1}{8\pi^2}\left[-\frac{1}{\sigma} + (m^2 + \bar{\xi}R)\left(\gamma + \frac{1}{2}\log\left(\frac{m^2|\sigma|}{2}\right)\right) - \frac{m^2}{2} + \frac{1}{12}R_{ab}\frac{\sigma^{;a}\sigma^{;b}}{\sigma}\right], \tag{3.33}$$

where $\bar{\xi} = (\xi - \frac{1}{6})$, γ is the Euler constant, R the scalar curvature at x and R_{ab} the Ricci tensor.

3.3 Pragmatic mode sum regularization of $\langle\phi^2(x)\rangle$ in an homogeneous spacetime

In order to extend the pragmatic-mode sum regularization method to a cosmological scenario with a FLRW spacetime $ds^2 = dt^2 - a^2(t)d\vec{x}^2$, we can take advantage of the translational symmetry of this spacetime, and consider equal-time points $x \equiv (t, \vec{x})$ and $x' \equiv (t, \vec{x} + \vec{\epsilon})$ to do the splitting. Expanding the field in Fourier modes as in (3.7) and (3.8), and using this splitting, the equal-time two-point function reads

$$\langle\phi(x)\phi(x')\rangle = \frac{1}{2(2\pi a(t))^3}\int d^3k|h_k(t)|^2 e^{i\vec{k}(\vec{x}'-\vec{x})} \tag{3.34}$$

and therefore the symmetric part can be written as,

$$\langle\{\phi(x), \phi(x')\}\rangle = \frac{1}{2(2\pi a(t))^3}\int d^3k|h_k(t)|^2\cos(\vec{k}\cdot\vec{\epsilon})\ . \tag{3.35}$$

Expressing the cosine in terms of exponentials we can perform the angular integration to reduce it to

$$\langle\{\phi(x), \phi(x')\}\rangle = \frac{1}{4\pi^2 a(t)^3}\int_0^\infty dk k^2|h_k(t)|^2\frac{\sin k\epsilon}{k\epsilon}\ , \tag{3.36}$$

where $k = |\vec{k}|$ and $\epsilon = |\vec{\epsilon}|$. In order to obtain an efficient numerical method of renormalization, we want to rewrite the DeWitt-Schwinger divergent term $G^{(1)}_{DS}(x, x')$ in (3.33) as an integral in momentum space so that it can be subtracted to (3.36) within the integral of k. For this purpose, we have to expand σ in a power series of ϵ. To this end, it is useful to use the Riemann normal coordinates

y^μ with origin at x. In these coordinates we have $\sigma(x,x') = \frac{1}{2}y_\mu y^\mu$. We follow [91] to expand y^μ in terms of $\Delta x^\mu = x'^\mu - x^\mu$, and obtain

$$\sigma = \frac{1}{2}\Delta t^2 - \frac{a^2}{2}\Delta\vec{x}^2 - \frac{a\dot{a}}{2}\Delta\vec{x}^2\Delta t - \frac{a\ddot{a}}{6}\Delta\vec{x}^2\Delta t^2 - \frac{a^2\dot{a}^2}{24}\Delta\vec{x}^4 + \cdots \ . \tag{3.37}$$

For the particular splitting that we are considering, $x \equiv (t,\vec{x})$ and $x' \equiv (t,\vec{x}+\vec{\epsilon})$, the above expansion can be given in terms of ϵ as

$$\sigma = -\frac{a^2}{2}\epsilon^2 - \frac{a^2\dot{a}^2}{24}\epsilon^4 - \frac{\left(a^2\dot{a}^4 + 3a^3\dot{a}^2\ddot{a}\right)}{720}\epsilon^6 + \mathcal{O}\left(\epsilon^8\right) \ . \tag{3.38}$$

The terms involving σ in (3.33) can be now expanded as follows [1]

$$\frac{1}{\sigma} = -\frac{2}{a^2\epsilon^2} + \frac{\dot{a}^2}{6a^2} + \mathcal{O}(\epsilon^2) \ . \tag{3.39}$$

$$R_{\alpha\beta}\frac{\sigma^{;\alpha}\sigma^{;\beta}}{\sigma} = 2\frac{\ddot{a}}{a} + 4\frac{\dot{a}^2}{a^2} + \mathcal{O}(\epsilon^2) \ . \tag{3.40}$$

plugging this expansions in (3.33) we get

$$G^{(1)}_{DS} = \frac{1}{4\pi^2}\left(\frac{1}{a^2\epsilon^2} + \frac{1}{2}(m^2+\bar{\xi}R)\left(\gamma + \log\left(\frac{ma}{2}\epsilon\right)\right) - \frac{m^2}{4} + \frac{R}{72}\right) + \mathcal{O}(\epsilon) \ , \tag{3.41}$$

The given expression is a function that relies only on the module of $\vec{\epsilon}$ as a result of the inherent isotropy of the FLRW metric. Our task is to rephrase the singularities in this expression as ϵ approaches zero, expressing them in the form of one-dimensional integrals in momentum space that include terms like $\frac{\sin k\epsilon}{k\epsilon}$. In order to achieve this, we explore the following integral transforms,

$$\int_0^\infty dk k\frac{\sin k\epsilon}{k\epsilon} = \frac{1}{\epsilon^2} \,, \tag{3.42}$$

$$\int_0^\infty dk \frac{k^2}{\omega^3}\frac{\sin k\epsilon}{k\epsilon} = -a^3\left(\gamma + \log\left(\frac{ma}{2}\epsilon\right)\right) + \mathcal{O}(\epsilon) \,, \tag{3.43}$$

where $\omega(t) = \sqrt{k^2/a^2(t) + m^2}$. These integrals have to be understood as generalized integrals where the convergence is understood by including a term $e^{-\alpha k}$ with $\alpha > 0$ in the integrand and at the end taking $\alpha \to 0_+$. Together with the identity,

$$\frac{1}{4\pi^2 a^3}\int_0^\infty dk \frac{\sin(k\epsilon)}{k\epsilon}\left[ka - \frac{k^2m^2}{2\omega^3} - \frac{k^2}{\omega}\right] = \frac{m^2}{16\pi^2} + \mathcal{O}(\epsilon) \,, \tag{3.44}$$

[1] As a remark, note that $\sigma^{;\alpha}$ must be calculated from (3.37) to do not miss any coefficient

we can substitute the terms depending on epsilon in (3.41) by the above integrals to obtain

$$G_{DS}^{(1)} = \frac{1}{4\pi^2 a^3} \int_0^\infty dk \frac{\sin(k\epsilon)}{k\epsilon} \left[\frac{k^2}{\omega} - \frac{k^2 \bar{\xi} R}{2\omega^3} \right] + \frac{R}{288\pi^2} + \mathcal{O}(\epsilon) \,, \tag{3.45}$$

where we have also made use of the identity (3.44) to simplify the expression. From (3.20) and with the above expression, we can write the two-point function at coincidence as

$$\langle \phi^2 \rangle_{ren} = \lim_{\epsilon \to 0} \frac{1}{4\pi^2 a^3} \int_0^\infty dk k^2 \frac{\sin k\epsilon}{k\epsilon} \left[|h_k|^2 - \frac{1}{\omega} - \frac{(\frac{1}{6} - \xi) R}{2\omega^3} \right] - \frac{R}{288\pi^2} \,. \tag{3.46}$$

We can interchange the limit and the integral since the above integral is convergent even in the limit $\epsilon \to 0$.

$$\langle \phi^2 \rangle_{ren} = \frac{1}{4\pi^2 a^3} \int_0^\infty dk k^2 \left[|h_k|^2 - \frac{1}{\omega} - \frac{(\frac{1}{6} - \xi) R}{2\omega^3} \right] - \frac{R}{288\pi^2} \,. \tag{3.47}$$

This result agrees exactly with the renormalized two-point function obtained by using the so-called adiabatic regularization method as shown in (3.19).

3.4 Pragmatic mode sum regularization of $\langle T_{ab}(x) \rangle$ in an homogeneous spacetime

We can also checked that the pragmatic mode sum regularization method agrees with the adiabatic regularization to higher orders. In particular, those required for the renormalization of the stress-energy tensor. Note from (2.30),

$$\langle T_{\mu\nu} \rangle = \lim_{x \to x'} \mathcal{D}_{\mu\nu}(x, x') \left[\langle \{ \phi(x), \phi(x') \} \rangle - G_{DS}^{(1)}(x, x') \right] \,, \tag{3.48}$$

that the renormalized vacuum expectation value of the stress-energy tensor can be obtained by acting with a nonlocal operator to the renormalized symmetric part of the two-point function, thus the divergences of the stress energy tensor are determined by the two-point function but including higher orders. Therefore, to compare the divergent terms of the stress energy tensor from the pragmatic mode sum regularization method with the divergent subtraction integrals from adiabatic renormalization, one needs a more complete form of the DeWitt-Schwinger expansion of the two-point function [67, 70] (we have added to (3.33) the contribution of the second DeWitt coefficient a_2)

$$\begin{aligned} G^{(1)}_{DS}\left(x,x'\right) \; &= \; \frac{\Delta^{1/2}}{8\pi^2}\left\{-\frac{1}{\sigma}+m^2\left(\gamma+\frac{1}{2}\ln\left|\frac{1}{2}m^2\sigma\right|\right)\left(1-\frac{1}{4}m^2\sigma\right)-\frac{1}{2}m^2+\frac{5}{16}m^4\sigma \right. \\ &\quad -a_1\left[\left(\gamma+\frac{1}{2}\ln\left|\frac{1}{2}m^2\sigma\right|\right)\left(1-\frac{1}{2}m^2\sigma\right)+\frac{1}{2}m^2\sigma\right] \\ &\quad \left. -\frac{1}{2}a_2\sigma\left[\gamma+\frac{1}{2}\ln\left|\frac{1}{2}m^2\sigma\right|-\frac{1}{2}\right]+\frac{a_2}{2m^2}\right\} , \end{aligned} \tag{3.49}$$

where a_1 and a_2 are the first DeWitt coefficients. The differential operator $\mathcal{D}_{\mu\nu}(x,x')$ contains different quadratic terms of covariant derivatives ($\nabla_\alpha\nabla_\beta, \nabla_\alpha\nabla_{\beta'}, \cdots$) [70, 67]; therefore, in order to regularize the divergences of the stress-energy tensor, we have to expand (3.49) up to and including the order $\mathcal{O}(\epsilon^2)$ because terms proportional to ϵ^2 can give rise to finite terms in $\langle T_{\mu\nu}\rangle$. Note also, that higher expansions in ϵ will result in a zero contribution when the coincidence limit $x \to x'$ is applied.

For simplicity we compute the case $\xi = \frac{1}{6}$. The following expansions are enough to build the renormalized stress-energy tensor ($\sigma^\alpha \equiv \sigma^{;\alpha}$):

$$\begin{aligned} \Delta^{1/2} = \quad & 1-\frac{1}{12}R_{\alpha\beta}\sigma^\alpha\sigma^\beta-\frac{1}{24}R_{\alpha\beta;\gamma}\sigma^\alpha\sigma^\beta\sigma^\gamma \\ & +\left(\frac{1}{288}R_{\alpha\beta}R_{\gamma\delta}+\frac{1}{360}R^{\rho}{}_{\alpha}{}^{\tau}{}_{\beta}R_{\rho\gamma\tau\delta}-\frac{1}{80}R_{\alpha\beta;\gamma\delta}\right)\sigma^\alpha\sigma^\beta\sigma^\gamma\sigma^\delta+\cdots , \end{aligned} \tag{3.50}$$

$$\begin{aligned} a_1 = \quad & \left[\frac{1}{90}R_{\alpha\rho}R^{\rho}{}_{\beta}-\frac{1}{180}R^{\rho\tau}R_{\rho\alpha\tau\beta}-\frac{1}{180}R_{\rho\tau\kappa\alpha}R^{\rho\tau\kappa}{}_{\beta}\right. \\ & \left.+\frac{1}{120}R_{\alpha\beta;\rho}{}^{\rho}-\frac{1}{360}R_{;\alpha\beta}\right]\sigma^\alpha\sigma^\beta+\cdots , \end{aligned} \tag{3.51}$$

$$a_2 = \quad -\frac{1}{180}R^{\rho\tau}R_{\rho\tau}+\frac{1}{180}R^{\rho\tau\kappa\iota}R_{\rho\tau\kappa\iota}-\frac{1}{180}R_{;\rho}{}^{\rho}+\cdots , \tag{3.52}$$

where σ^α is computed up to order ϵ^5 using the expansion (3.37). Expanding (3.49) with (3.50), (3.51), and (3.52) we obtain the following expansion for the two-point function up to and including the order $\mathcal{O}(\epsilon^2)$:

$$\begin{aligned} G^{(1)}_{DS}(x,x') \quad &= \frac{1}{4\pi^2\epsilon^2a^2}+\frac{1}{480\pi^2m^2}\left[10m^2\left(\frac{\ddot{a}}{a}+\frac{\dot{a}^2}{a^2}\right)-\left(\frac{a^{(4)}}{a}+\frac{\ddot{a}^2}{a^2}\right)\right. \\ &\quad \left.+3\left(\frac{\dot{a}^2\ddot{a}}{a^3}-\frac{a^{(3)}}{a^2}\dot{a}\right)+60m^4\left(\gamma-\frac{1}{2}+\log\left(\frac{m\epsilon}{2}a\right)\right)\right] \end{aligned}$$

$$+\frac{\epsilon^2}{2880\pi^2}\left[\left(\frac{3}{2}a^{(4)}a+6\ddot{a}^2-\frac{\dot{a}^4}{a^2}+\frac{21}{2}a^{(3)}\dot{a}+\frac{23}{2}\frac{\dot{a}^2\ddot{a}}{a}\right)\right.$$
$$+30m^2\left(a\ddot{a}+2\dot{a}^2\right)\left(\gamma-\frac{1}{2}+\log\left(\frac{m\epsilon}{2}a\right)\right)$$
$$\left.+45m^4a^2\left(\gamma-\frac{5}{4}+\log\left(\frac{m\epsilon}{2}a\right)\right)\right]+\mathcal{O}\left(\epsilon^3\right)\ , \tag{3.53}$$

where $a^{(4)} \equiv \ddot{\ddot{a}}$ and $a^{(3)} \equiv \dddot{a}$. As a remark, note that this expression contains terms with four derivatives of the metric $(a^{(4)}, \dot{a}^4, \dot{a}a^{(3)}, \cdots)$.

Replacing the ϵ terms in (3.53) the integral forms as in (3.42) and (3.43) (3.53) agrees with

$$^{(4)}G^{(1)}_{Ad}(x,x') = \frac{1}{4\pi^2a^3}\int_0^\infty k^2dk\frac{\sin k\epsilon}{k\epsilon}\left[\frac{1}{\omega}+\frac{(\frac{1}{6}-\xi)R}{2\omega^3}\right.$$
$$\left.+\frac{m^2\dot{a}^2}{2a^2\omega^5}+\frac{m^2\ddot{a}}{4a\omega^5}-\frac{5m^4\dot{a}^2}{8a^2\omega^7}+(W^{-1})^{(4)}\right]\ , \tag{3.54}$$

This equation is the expansion of adiabatic regularization at fourth adiabatic order [7]. The integral on $(W^{-1})^{(4)}$ is finite and contains terms with four derivatives of the metric.

Therefore, we have seen that the pragmatic mode-sum form of the divergent terms for the stress-energy tensor, when the translational symmetry is considered in homogeneous spacetimes, reduces to the renormalization terms of adiabatic regularization. The explicit formulas of interest required to do the direct numerical implementation can be obtained, for instance, from [92]. The present results make manifest the great versatility of the adiabatic method with numerical calculations [93, 94, 95, 96, 97, 98, 99].

3.5 Massless case and the renormalization scale μ

As a final remark, in this section we show how to extend the point-splitting prescription and the pragmatic-mode sum regularization method to massless fields, since for massless fields expression (3.33) is ill defined due to a logarithmic divergence. The usual approach to bypass this infrared divergence is to introduce an upper cutoff in the proper-time integral (3.32) [65], or to replace m^2 by an arbitrary mass scale μ^2 in the problematic logarithmic term. Here we will follow an alternative strategy based on [100]. This consists in replacing m^2 by $m^2+\mu^2$ in the exponent of the DeWitt-Schwinger integral form (3.32). The main advantage of this approach is that it leads to a natural decoupling mechanism for heavy massive fields. This approach has been recently extended to fermions and for a Yukawa model [101].Following this idea, we write the Feynman green function in the DeWitt-Schwinger representation as

$$G_F(x,x') = \frac{\Delta^{1/2}}{(4\pi)^2}\int_0^\infty \frac{ds}{(is)^2} e^{-i\left((m^2+\mu^2)s+\frac{\sigma}{2s}\right)} \sum_{n=0}^{\infty} \bar{a}_n (is)^n \ . \tag{3.55}$$

To ensure consistency with (3.32), the initial DeWitt coefficients must undergo the following modification: $\bar{a}_0(x,x')=1,\ \bar{a}_1(x,x')=a_1(x,x')+\mu^2,\ \bar{a}_2(x,x')=a_2(x,x')+a_1(x,x')\mu^2+\frac{1}{2}\mu^4$. Subsequently, one can proceed analogously to the case where $\mu=0$. We express (3.55) in terms of Hankel functions and expand them into asymptotic series, ultimately yielding the following expression for the subtraction term of the two-point function within the point-splitting renormalization method,

$$\begin{aligned} G^{(1)}_{DS}\left(x,x'\right) = \quad & \frac{1}{8\pi^2}\left[-\frac{1}{\sigma} + (m^2+(\xi-1/6)R)\left(\gamma+\frac{1}{2}\log\left(\frac{m^2+\mu^2}{2}|\sigma|\right)\right)\right. \\ & \left. -\frac{m^2+\mu^2}{2} + \frac{1}{12}R_{\alpha\beta}\frac{\sigma^{;\alpha}\sigma^{;\beta}}{\sigma}\right] \ . \end{aligned} \tag{3.56}$$

Note that the parameter μ^2 appears nontrivially in this expression. Not only does it appear in the logarithmic term but it also emerges in the constant term, and not in the usual combination $m^2+(\xi-1/6)R$ multiplying the logarithm. This effect is responsible of the decoupling of heavy particles in the computations of the renormalized energy-momentum tensor [100]. In other words, these nontrivial terms are responsible for quadratic μ^2 and quartic μ^4 (for the cosmological constant term) terms in the running of the couplings.

As it was done in the previous sections, if we consider a FLRW spatially flat spacetime we can write the generalized subtraction term with integrals in modes of k by using the translational symmetry. It is straightforward to do so from previous results, we just have to replace m^2 by $m^2_{\text{eff}}=m^2+\mu^2$ in (3.43) and use the integral representations of the divergent terms [Eqs. (3.42) and (3.43))] in

(3.56) to get

$$G^{(1)}_{\rm DS}(x,x') = \frac{1}{4\pi^2 a^3}\int_0^\infty dk \frac{\sin(k\epsilon)}{k\epsilon}\left[ka - \frac{k^2 m^2}{2\omega_{\rm eff}^3} + \frac{k^2(\frac{1}{6}-\xi)R}{2\omega_{\rm eff}^3}\right] - \frac{m_{\rm eff}^2}{16\pi^2} + \frac{R}{288\pi^2} + \mathcal{O}(\epsilon) \ , \tag{3.57}$$

where $\omega_{\rm eff}^2 = \frac{k^2}{a^2} + m^2 + \mu^2$. If we consider the identity (3.44) with m^2 replaced by $m_{\rm eff}^2$ we can rewrite the expression above as follows:

$$G^{(1)}_{\rm DS}(x,x') = \frac{1}{4\pi^2 a^3}\int_0^\infty dk k^2 \frac{\sin(k\epsilon)}{k\epsilon}\left[\frac{1}{\omega_{\rm eff}} + \frac{(\frac{1}{6}-\xi)R}{2\omega_{\rm eff}^3} + \frac{\mu^2}{2\omega_{\rm eff}^3}\right] + \frac{R}{288\pi^2} + \mathcal{O}(\epsilon) \ . \tag{3.58}$$

This represents the generalized subtraction term for the two-point function, expressed as an integral in terms of momentum modes k. It's noteworthy that a new term proportional to μ^2 emerges. This addition signifies the presence of a quadratic divergent term alongside the previously identified logarithmic divergence. This outcome aligns with adiabatic regularization, particularly when we introduce the arbitrary parameter μ, subject to identical conditions (see Appendix A for details).

Chapter 4

Low Energy States

One of the major issues of quantum field theory in general spacetimes is the dissapearence of the Poincaré symmetry of Minkowski spacetime. This lack of symmetry results in a non-unique or privileged way of constructing a vacuum state, specially when there is no time-translational symmetry as for FLRW spacetimes. If there is no time-like isometry, there is no conserved energy associated with the time-like Killing vector field (or observer), thus resulting in a time-dependent Hamiltonian. For time-independent Hamiltonians, there is a unique choice of vacuum state which renders the minimum possible value of the Hamiltonian. We usually call this state the ground state of the theory. However, when the Hamiltonian is time-dependent as in FLRW spacetimes, there is not a unique choice for the ground state, since energy varies in time. Only when the state is highly symmetric such as Minkowski spacetime, we can reduce the ambiguity to select a unique vacuum state, or in De-Sitter spacetime if we include regularity conditions (the so called Bunch-Davies vacuum).

For any quantum state $|0_{in}\rangle$ to be admitted as physically acceptable we should demand it to be ultraviolet regular. This means that the high-energy behaviour of the state must approach the behaviour of Minkowski space at a rate such that basic composite operators, as the stress-energy tensor, can be renormalized. In general spacetimes, the asymptotic condition that states have to satisfy to completely characterize the singular behaviour of two point functions is the *Hadamard condition*. This condition ensures the existence of any Wick polynomials of arbitrary order [71, 72, 73] and hence, the perturbative series of an interacting theory is well-defined at any order. The Hadamard condition, can be transformed into the *adiabatic condition* [63, 7, 102, 103] in homogeneous spacetimes. States satisfying the Hadamard condition are called Hadamard states or states of infinite adiabatic order.

Several approaches have been considered to select a preferred vacuum state at early times, based on different viewpoints [104, 105, 106, 107, 108, 109], from which one can predict late time quantum effects. An especially appealing proposal is the States of Low Energy (SLE) prescription [43, 110]. These states of low energy are obtained by minimizing the expectation value of the time-dependent Hamiltonian after smearing it with a time-dependent test function. This prescription ensures the Hadamard condition or, equivalently, adiabatic condition (at *all orders*) [7]. The SLE were introduced originally only for scalar fields (and for minimal coupling). It is easy to show that the Minkowski vacuum is the state of low energy, irrespectively of the specific form of the smearing function. For simple asymptotically flat regions, where the expansion factor $a(t)$ approaches constant values at $t \to \pm\infty$, the initial and final Minkowski vacua, corresponds to the state of minimal energy when the time averaging has support at early and late times respectively. For de Sitter spacetime, the Bunch-Davies vacuum is the state of low energy, irrespective of the particular form of the smearing function, as long as it has support at the distant past [41, 42]. However, the states of low energy depend, in general, on the choice of the smearing function.

The states of low energy have been recently studied in different context. In loop quantum cosmology, they have been considered to define the vacuum of cosmological perturbations [111, 42]. The method has been also applied to obtain physically motivated vacua in the Schwinger effect [112] and for scalar fields with Yukawa interaction [113]. More recently, the low energy states prescription has also been generalized to anisotropic Bianchi I spacetimes [114]

In the first section of this chapter we review the states of low energy prescription and upgrade it to include massive scalar fields with arbitrary coupling ξ to the scalar curvature. We will pay special attention to the terms that contain the divergences when we approach the Big Bang. We follow the prescription described in [43, 110]. In the second section of this chapter we extend the prescription of states of low energy to spin-1/2 fields. In the next chapters we apply these proposals to a radiation dominated universe, checking that the resulting states satisfy the Hadamard/adiabatic condition.

4.1 Low Energy States for scalar fields

Consider a massive scalar field ϕ, with an arbitrary coupling ξ to the scalar curvature propagating in a flat FLRW spacetime

$$\mathrm{d}s^2 = a^2(\tau)(\mathrm{d}\tau^2 - \mathrm{d}\vec{x}^2) \ . \tag{4.1}$$

We can expand the quantized field in Fourier modes adapted to the underlying homogeneity of the 3-space

$$\phi(\tau, \vec{x}) = \int \frac{\mathrm{d}^3k}{\sqrt{2(2\pi)^3}} \left(A_{\vec{k}} e^{i\vec{k}\vec{x}} \phi_k(\tau) + A^\dagger_{\vec{k}} e^{-i\vec{k}\vec{x}} \phi^*_k(\tau) \right) \ , \tag{4.2}$$

where $A_{\vec{k}}$ and $A^\dagger_{\vec{k}}$ are annihilation and creation operators satisfying canonical commutation relations $[A_{\vec{k}}, A^\dagger_{\vec{k}'}] = \delta^3(\vec{k} - \vec{k}')$, $[A_{\vec{k}}, A_{\vec{k}'}] = 0 = [A^\dagger_{\vec{k}}, A^\dagger_{\vec{k}'}]$. The normalization of the modes is fixed by the condition

$$\phi_k \phi'^*_k - \phi'_k \phi^*_k = \frac{2i}{a^2} \ , \tag{4.3}$$

where the prime denotes derivative with respect to the conformal time. The equation for the field modes reads:

$$\phi''_k + 2\frac{a'}{a}\phi'_k + \left(\omega^2 + 6\xi\frac{a''}{a}\right)\phi_k = 0 \,. \tag{4.4}$$

where $k^2 + a^2 m^2$.

The starting point to construct states of low energy is to fix a fiducial set of normalized modes $\phi_k(\tau)$ for the equation of motion (4.4). Then, one can parametrize a general set of modes $T_k(\tau)$ taking the linear combination

$$T_k(\tau) = \lambda_k \phi_k(\tau) + \mu_k \phi^*_k(\tau) \ , \tag{4.5}$$

where λ_k and μ_k are complex numbers that must obey $|\lambda_k|^2 - |\mu_k|^2 = 1$. The objective is to find for which values of λ_k and μ_k the vacuum expectation value for the smeared Hamiltonian over a temporal window function is minimal.

The vacuum expectation value of the Hamiltonian $H(\tau)$ for a scalar field ϕ, associated to a foliation of a spacelike Cauchy surface Σ_τ and a temporal vector characterizing an observer u^b is given by

$$H(\tau) = \int_{\Sigma_\tau} \mathrm{d}^3x \sqrt{|h|}\, \langle T_{ab} \rangle\, n^a u^b \ . \tag{4.6}$$

$\sqrt{|h|}$ is the determinant of the induced Riemann metric in Σ_τ, $\langle T_{ab}\rangle$ is the vacuum expectation value of the stress-energy tensor, n^a is the unit normal vector to the foliation. We should take $\langle T_{ab}\rangle$ to be the renormalized quantity. However, we are interested in the problem of minimizing the Hamiltonian observable, and since the subtraction terms in the renormalization are independent of the vacuum state we can ignore them. We will only consider the contributions of the modes, as in (4.8). Following [43], we choose the privileged isotropic observer, $u^a = n^a = (a^{-1}, 0, 0, 0)$ in conformal time coordinates, and the above expression reduces to

$$\begin{aligned} H(\tau) \qquad &= \int_{\Sigma_\tau} \mathrm{d}^3x \sqrt{|h|}\, \langle T_{ab}\rangle\, u^a u^b = \int_{\Sigma_\tau} \mathrm{d}^3x \sqrt{|h|}\, \langle \rho(\tau) \rangle \\ &= \int_{\Sigma_\tau} \mathrm{d}^3x \int \frac{\mathrm{d}^3k}{(2\pi)^{3/2}} \sqrt{|h|}\, \rho_k(\tau) \,, \end{aligned} \tag{4.7}$$

where $\rho_k(\tau)$ is the formal energy density of a given mode T_k. In conformal coordinates $\rho_k(\tau)$ is given by

$$\rho_k(\tau) = \frac{1}{4a^2} \left(|T_k'|^2 + \omega^2 |T_k|^2 + 6\xi \big(\frac{a'^2}{a^2} \, |T_k|^2 + \frac{a'}{a} \left(T_k T_k'^{*} + T_k^* T_k' \right) \big) \right) \,, \tag{4.8}$$

The smeared Hamiltonian is defined as

$$H[f] := \int \mathrm{d}\tau \sqrt{a^2}\, f^2(\tau) H(\tau) = \int \frac{\mathrm{d}^3k}{(2\pi)^{3/2}} \int_{\Sigma_\tau} \mathrm{d}^3x \int \mathrm{d}\tau \sqrt{|g|}\, f^2(\tau) \rho_k(\tau) \,, \tag{4.9}$$

where we have used (4.7), and where the smearing has been done with a positive definite window function f^2, along the curve of an isotropic observer. One can see that the minimization of the smeared Hamiltonian reduces to the minimization of the smeared energy density for each mode k with the appropriate factor $\sqrt{|g|}$

coming from the four-dimensional volume element. Therefore, from now on we will work directly with the smeared energy density

$$\mathcal{E}_k[f] \quad := \quad \int \mathrm{d}\tau \, \sqrt{|g|} \, f^2 \, \rho_k \, . \tag{4.10}$$

It is important to stress the appearance of $\sqrt{|g|}$ which in our case reduces to $\sqrt{|g|} = a^4$. This type of factors also appear in the analysis of Ref. [115] to smooth the Big Bang singularity via quantized fields. However, as we will see in the following chapter the smoothness of this factor is not enough in some cases to construct a low energy vacuum state around the Big Bang singularity.

In order to minimize $\mathcal{E}_k$, it is very convenient to express it explicitly in terms of the free parameters μ_k and λ_k, namely

$$\mathcal{E}_k = (2\mu_k^2 + 1)c_{k,1} + 2\mu_k \mathrm{Re}(\lambda_k c_{k,2}) \, , \tag{4.11}$$

where we have defined

$$\begin{aligned} c_1 \quad &\equiv \quad c_{k,1} = \frac{1}{4} \int \mathrm{d}\tau \, \sqrt{|g|} \, \frac{f^2}{a^2} \left(|\phi_k'|^2 + \omega^2 |\phi_k|^2 + 6\xi \big(\frac{a'^2}{a^2} \, |\phi_k|^2 + \frac{a'}{a} \, (\phi_k \phi_k'^* + \phi_k^* \phi_k') \big) \right) \, , \\ c_2 \quad &\equiv \quad c_{k,2} = \frac{1}{4} \int \mathrm{d}\tau \sqrt{|g|} \, \frac{f^2}{a^2} \left({\phi_k'}^2 + \omega^2 \phi_k^2 + 6\xi \big(\frac{a'^2}{a^2} \phi_k^2 + 2 \frac{a'}{a} \phi_k \phi_k' \big) \right) \, . \end{aligned} \tag{4.12}$$

In the above formulas it is assumed that c_1 is a positive quantity, as it is trivially satisfied for $\xi = 0$. It can be showed that if we take μ_k to be real and positive, the minimization problem over the parameters λ_k and μ_k determines a unique solution, namely

$$\mu_k = \sqrt{\frac{c_1}{2\sqrt{c_1^2 - |c_2|^2}} - \frac{1}{2}} \, ; \qquad \lambda_k = -e^{-i \mathrm{Arg} \; c_2} \sqrt{\frac{c_1}{2\sqrt{c_1^2 - |c_2|^2}} + \frac{1}{2}} \, . \tag{4.13}$$

The minimization is a well posed problem whenever $\frac{|c_2|}{c_1} < 1$ is satisfied. This is usually the case if ϕ_k do not contain singularities in the support of f^2 [43, 110]. This issue will be relevant around the Big Bang singularity, as we will see in the following sections. We remark that the resulting state of low energy is independent of the fiducial solution ϕ_k and it is a Hadamard state (i.e., a state of infinite adabatic order). The formal proof that states of low energy are Hadamard states was given in [43].

States of Low Energy for conformally coupled scalars

For conformally coupled scalar fields $\xi = 1/6$ it is convenient to work with the Weyl transformed modes $\mathcal{T}_k$ (i.e., $\mathcal{T}_k = a\, T_k$). The equation of motion for the Weyl modes read

$$\mathcal{T}_k''(\tau) + \left[k^2 + m^2 a^2\right] \mathcal{T}_k(\tau) = 0 \ , \tag{4.14}$$

and the energy density ρ_k in terms of the Weyl transformed mode takes the simple form

$$\rho_k(\tau) = \frac{1}{4a^4}\left(|\mathcal{T}_k'|^2 + \omega^2 |\mathcal{T}_k|^2\right) \ , \tag{4.15}$$

We stress that using the Weyl modes, all the divergent behavior at $\tau \to 0$ (Big Bang) is encapsulated in the term a^{-4}. We follow the minimization prescription as in Sec. 4.1. The smeared energy density to be minimized around takes the simple form

$$\mathcal{E}_k[f] := \int \mathrm{d}\tau \, \sqrt{|g|}\, f^2 \, \rho_k = \int \mathrm{d}\tau \, f^2 \, \frac{1}{4}\left(|\mathcal{T}_k'|^2 + \omega^2 |\mathcal{T}_k|^2\right) \ , \tag{4.16}$$

Note that the $\sqrt{|g|}$ has completely absorbed the divergent term for conformally coupled fields. Therefore,as we see in the above equation, conformally coupled scalar fields are less sensitive to the Big Bang singularity. We proceed to compute the integrals of c_1 and c_2 defining the states of low energy, which for conformally coupled scalar fields read

$$c_1 \equiv c_{k,1} = \frac{1}{4}\int \mathrm{d}\tau f^2 \, \left(|\varphi_k'|^2 + \omega^2 |\varphi_k|^2\right) , \tag{4.17}$$

$$c_2 \equiv c_{k,2} = \frac{1}{4}\int \mathrm{d}\tau f^2 \, \left(\varphi_k'^2 + \omega^2 \varphi_k^2\right) \ . \tag{4.18}$$

where $\{\varphi_k, \varphi_k^*\}$ are a pair of fiducial solutions of the Klein-Gordon equation. Any general mode is given by

$$\mathcal{T}_k(\tau) = \lambda_k \varphi_k(\tau) + \mu_k \varphi_k^*(\tau) \tag{4.19}$$

For the massless case we can take the conformal vacuum

$$\varphi_k(\tau) = \frac{e^{-ik\tau}}{\sqrt{k}}$$

as the fiducial mode and obtain that $c_2 = 0$ irrespectively of f^2. Therefore, using (4.13), we find $\mu_k = 0$ and $\lambda_k = 1$, and we conclude that the conformal vacuum minimizes the energy density at any τ. It is also independent of the test function.

This result reinforces the idea that low energy states are suitable candidates for preferred vacuum states.

For the massive case, we can consider a fiducial solution to the equation of motion and compute the above integrals for a given function f^2. The resulting state of low energy will depend now on the temporal window function. It is interesting to stress that for massive fields we can also define a Hadamard state around the Big Bang singularity by setting the support of f^2 around zero, since the Big Bang divergence has been absorbed by the volume element. In the following chapter we will see that this is also the case for fermionic fields since they behave as conformally coupled fields.

4.2 Low Energy States for fermionic fields

In this section, we extend the prescription to build States of Low Energy to spin-$\frac{1}{2}$ fields. We proceed here in analogy with the scalar field case. Although we do not present a formal proof that the states of low energy for spin-1/2 fields are Hadamard, we will check in the following chapter that the proposed states of low energy satisfy the Hadamard condition for a radiation dominated universe.

Let us consider now a spin one-half field Ψ propagating in the same background metric $\mathrm{d}s^2 = a^2(\tau)(\mathrm{d}\tau^2 - \mathrm{d}\vec{x}^2)$. The field equation $(i\underline{\gamma}^\mu \nabla_\mu - m)\Psi = 0$, where $\underline{\gamma}^\mu = \frac{1}{a}\gamma^\mu$ and γ^μ are the flat spacetime Dirac matrices, become

$$\left(\gamma^0 \partial_\tau + \vec{\gamma} \cdot \vec{\nabla} + \frac{3a'}{2a}\gamma^0 + ima\right)\Psi = 0 \; . \tag{4.20}$$

It is also convenient to perform a Weyl transformation for the spinor field of the form $\psi = a^{3/2}\Psi$. The mode expansion for the quantized ψ field is given by ($D_{\vec{k}h} = B_{\vec{k}h}$ for Majorana spinors)

$$\psi(x) = \int \mathrm{d}^3k \sum_h \left[B_{\vec{k}h} u_{\vec{k}h}(x) + D^\dagger_{\vec{k}h} v_{\vec{k}h}(x) \right] , \tag{4.21}$$

where the subindex h refers to the helicity, and the u-modes in the Dirac representation

$$\gamma^0 = \begin{pmatrix} I & 0 \\ 0 & -I \end{pmatrix} , \quad \vec{\gamma} = \begin{pmatrix} 0 & \vec{\sigma} \\ -\vec{\sigma} & 0 \end{pmatrix} , \tag{4.22}$$

can be written as (we have reexpressed the results in [85, 86] in terms of the conformal time, up to the above $a^{-3/2}$ Weyl rescaling factor)

$$u_{\vec{k}h}(x) = \frac{e^{i\vec{k}\cdot\vec{x}}}{\sqrt{(2\pi)^3}} \left(\begin{array}{c} h_k^I(\tau)\xi_h(\vec{k}) \\ h_k^{II}(\tau)\frac{\vec{\sigma}\cdot\vec{k}}{k}\xi_h(\vec{k}) \end{array} \right) , \tag{4.23}$$

and where ξ_h is a constant and normalized two-component spinor $\xi_h^\dagger \xi_{h'} = \delta_{h'h}$ that represent the helicity eigenstates. $v_{\vec{k}h}(x)$ is obtained by the charge conjugation operation. The Dirac equation for the functions $h_k^I(\tau)$ and $h_k^{II}(\tau)$ is transformed into

$$h_k'^I + ik\, h_k^{II} + i\, ma(\tau)\, h_k^I = 0\,, \tag{4.24}$$

$$h_k'^{II} + ik\, h_k^{I} - i\, ma(\tau)\, h_k^{II} = 0\,, \tag{4.25}$$

together with the normalization condition

$$|h_k^I|^2 + |h_k^{II}|^2 = 1\,. \tag{4.26}$$

The starting point to construct low energy states is now to fix a basis of solutions for the modes, namely, $\{h_k^I, h_k^{II}\}$. Any other set of modes can be parametrized in the form

$$\begin{aligned} t_k^I &= \lambda_k\, h_k^I + \mu_k\, h_k^{II*}\,, \\ t_k^{II} &= \lambda_k\, h_k^{II} - \mu_k\, h_k^{I*}\,. \end{aligned} \tag{4.27}$$

From the normalization condition, μ_k and λ_k should obey

$$|\lambda_k|^2 + |\mu_k|^2 = 1\,. \tag{4.28}$$

The smeared energy density over a temporal window function f^2 is given by (see Sec. 4.1)

$$\mathcal{E}_k[f] := \int \mathrm{d}\tau \sqrt{|g|}\, f^2\, \rho_k\,. \tag{4.29}$$

where $\sqrt{|g|} = a^4$, and where the energy density ρ_k associated with the set of fermionics modes $\{t_k^I, t_k^{II}\}$ reads

$$\rho_k(\tau) = \frac{2i}{a^4} \left(t_k^I \frac{\partial t_k^{I*}}{\partial \tau} + t_k^{II} \frac{\partial t_k^{II*}}{\partial \tau} \right) . \tag{4.30}$$

We can choose μ_k or λ_k to be real since $\{e^{i\alpha}\, t_k^I, e^{i\alpha}\, t_k^{II}\}$ is also a solution of the system of equations. For future convenience, and following similar arguments than in the scalar case [43], we assume that λ_k is real and positive $\lambda_k > 0$. The smeared energy density can be written, as in the scalar case, in terms of two constants $c_1 \equiv c_{k,1}$ and $c_2 \equiv c_{k,2}$, namely

$$\begin{aligned} \mathcal{E}_k &= (1 - 2|\mu_k|^2)c_1 + 2|\mu_k| \ \mathrm{Re}(\mu_k^* c_2) \\ &\equiv (1 - 2|\mu_k|^2)c_1 + 2|\mu_k|\sqrt{1 - |\mu_k|^2}\, |c_2| \cos(\mathrm{Arg} c_2 - \mathrm{Arg}\mu_k)\,, \end{aligned} \tag{4.31}$$

where

$$c_1 = 2i \int \mathrm{d}\tau f^2 \left(h_k^I \frac{\partial h_k^{I*}}{\partial \tau} + h_k^{II} \frac{\partial\, h_k^{II*}}{\partial \tau} \right), \tag{4.32}$$

$$c_2 = 2i \int \mathrm{d}\tau f^2 \left(h_k^I \frac{\partial h_k^{II}}{\partial \tau} - h_k^{II} \frac{\partial h_k^{I}}{\partial \tau} \right). \tag{4.33}$$

From now on, we assume that the fiducial modes are such that c_1 is a real, negative quantity. Note that this is the case for the standard mode solutions in Minkowski spacetime.

We find that $\mathcal{E}_k$ is trivially minimized with respect to $\mathrm{Arg}\mu_k$ for $\mathrm{Arg}\mu_k = \mathrm{Arg}c_2 + \pi$. Therefore, the task now is to minimize

$$\mathcal{E}_k = (1 - 2|\mu_k|^2)c_1 - 2|\mu_k|\sqrt{1 - |\mu_k|^2}\, |c_2|\,. \tag{4.34}$$

with respect to $|\mu_k|$. Taking $\partial_{|\mu_k|}\mathcal{E}_k = 0$ we obtain four possible solutions. Only two of them are real and positive for λ_k,

$$\lambda_k = \sqrt{\frac{1}{2} \mp \frac{c_1}{2\sqrt{c_1^2 + |c_2|^2}}}\,, \qquad |\mu_k| = \sqrt{\frac{1}{2} \pm \frac{c_1}{2\sqrt{c_1^2 + |c_2|^2}}}\,. \tag{4.35}$$

From the above solution, one can easily check that the one that minimizes the smeared energy density $\mathcal{E}_k$ is

$$\lambda_k = \sqrt{\frac{1}{2} - \frac{c_1}{2\sqrt{c_1^2 + |c_2|^2}}}\,, \qquad |\mu_k| = \sqrt{\frac{1}{2} + \frac{c_1}{2\sqrt{c_1^2 + |c_2|^2}}}\,. \tag{4.36}$$

and the minimum value of the smeared energy density $\mathcal{E}_k$ is $\mathcal{E}_k = -\sqrt{c_1^2 + |c_2|^2}$.

It is interesting to highlight that, unlike the analysis conducted for scalar fields, it is possible in this context to identify a maximum value for $\mathcal{E}_k$. By setting $\mathrm{Arg}\mu_k = \mathrm{Arg}c_2$ in equation (4.31) and subsequently calculating $\partial|\mu_k|\mathcal{E}_k = 0$, we arrive at the same expression as (4.35). Upon incorporating these values back into $\mathcal{E}_k$, we determine that it reaches its peak for the opposite solution (+ for λ_k and - for μ_k), resulting in $\mathcal{E}_k = \sqrt{c_1^2 + |c_2|^2}$. However, this corresponds to a nonphysical state in the sense that this would produces negative energies for the one particle/antiparticle state.

Low Energy States for fermions in Minkowski spacetime

As an example, we now perform the minimization of states of low energy 4.2 for fermions in a Minkowski spacetime. A general mode $\{t_k^I, t_k^{II}\}$ solution can be described by the following linear combination of fiducial solutions

$$\begin{aligned} t_k^I &= \lambda_k \, h_k^I + \mu_k \, h_k^{II*} \,, \\ t_k^{II} &= \lambda_k \, h_k^{II} - \mu_k \, h_k^{I*} \,. \end{aligned} \tag{4.37}$$

We take the well known postive and negative-frequency solutions of Minkowski spacetime as the fiducial solutions.

$$h_k^I = \sqrt{\frac{\omega + m}{2\omega}} e^{-i\omega\tau} \,, \qquad h_k^{II} = \sqrt{\frac{\omega - m}{2\omega}} e^{-i\omega\tau} \,. \tag{4.38}$$

By minimizing the smeared energy density for any arbitrary mode, we find that only when $\lambda_k = 1$ and $\mu_k = 0$, regardless of the chosen test function, does the smeared energy density $\mathcal{E}_k$ attain its minimum value. This solution, as evident from (4.37), corresponds to the standard positive frequency mode in Minkowski spacetime. The computation involves determining the coefficients c_1 and c_2 as given in (4.32) and (4.33). By substituting with (4.38) one arrives at

$$c_1 = -2\omega \int \mathrm{d}\tau \, f^2 \qquad c_2 = 0 \,. \tag{4.39}$$

Therefore, the two possible solutions that appears when minimizing $\mathcal{E}_k$ [see Eq. (4.34)] are given by

$$\lambda_k = \sqrt{\frac{1}{2} \mp \frac{-\omega}{2\omega}} \,, \qquad |\mu_k| = \sqrt{\frac{1}{2} \pm \frac{-\omega}{2\omega}} \,. \tag{4.40}$$

From the above solutions, the one that minimizes the smeared energy density is given by

$$\lambda_k = 1 \,, \qquad \mu_k = 0 \,, \tag{4.41}$$

which corresponds to the standard positive-frequency solution (4.38). If we compute the energy density we obtain

$$\rho_k = 2i \left(h_k^I \frac{\partial h_k^{I*}}{\partial \tau} + h_k^{II} \frac{\partial h_k^{II*}}{\partial \tau} \right) = -2\omega \,. \tag{4.42}$$

In other words, this choice gives the well-know state of low energy in Minkowski spacetime. This is the state of lowest energy for fermions which corresponds to the positive frequency solution from which we define the standard vacuum in Minkowski such that we have positive energies for the one particle/antiparticle state $H|k,s\rangle = \omega_k|k,s\rangle$. The other possible solution that we obtain when finding the extrems of $\mathcal{E}_k$ corresponds to $\lambda_k = 0$, $\mu_k = 1$. These are negative frequencies, which renders a nonphysical state. This would produces negative energies for the one particle/antiparticle state $H|k,s\rangle = -\omega_k|k,s\rangle$ In this case, the vacuum energy density results in $\rho_k = +2\omega$, which corresponds to its maximal value.

Chapter 5

CPT invariance and Hadamard condition for the Big Bang quantum vacuum

The investigation into the selection of a preferred vacuum state gains particular significance when considering a radiation-dominated universe. This specific expansion rate holds diverse motivations, being considered a plausible pre-inflationary phase, as recently discussed in [116, 117, 118]. In the context of this pre-de Sitter space, the vacuum evolution should seamlessly transition to a state that closely resembles the Bunch-Davies state for large wavenumbers k, yet deviates significantly from it at smaller wavenumbers.

Beyond the inflationary framework, defining a preferred vacuum in a radiation-dominated universe is also relevant. In particular within the Weyl curvature hypothesis proposed by Penrose [119]. This hypothesis offers a natural and well-motivated approach to address the initial singularity of the Big Bang, complementing Penrose's cosmic censorship hypothesis [120], which safeguards the external world from singularities predicted within black holes. Enforcing the Weyl curvature hypothesis consistently with observations is achieved through a

Friedmann-Lemaître-Robertson-Walker (FLRW) geometry for spacetime [121]. As we trace back in time, observations indicate that the expansion factor $a(\tau)$ follows a simple behavior in a radiation-dominated spacetime: $a(\tau) \propto \tau$, relative to the conformal time τ. This simplicity encourages the analytical extension of the conformal time parameter to negative values [54], resembling a bouncing geometry at the Big Bang.

In this chapter, we highlight the emerging symmetry of the metric, described by $ds^2 \propto \tau^2(d\tau^2 - d\vec{x}^2)$ under the transformation $T : \tau \to -\tau$. This time-reversal symmetry, has recently been explored in [44, 45], leading to the proposed vacuum state $|0_T\rangle \propto |0_+\rangle + |0_-\rangle$, where $|0_+\rangle$ is the adiabatic vacuum at $\tau \to \infty$ while $|0_-\rangle$ is its corresponding T-reversal image. The selection of this vacuum relies on the asymptotic behavior at $|\tau| \to \infty$ where one can define positive oscillatory frequency solutions. This state satisfies the Hadamard condition [9] due to their construction in asymptotic regimes where the Hubble rate approaches zero. However, defining the state in this way involves giving initial conditions by knowing the late-times behaviour of the expanding universe. A more physical characterization would involve defining the vacuum state around $\tau \sim 0$ (the Big Bang point in conformal time). Constructing sensible vacuum states around the Big Bang singularity proves more intricate.

In the subsequent sections, we delve into the challenge of constructing a vacuum state around $\tau \sim 0$ in a radiation dominated spacetime. We address this issue by applying the Low Energy States prescription around the Big Bang, leveraging the emergent time-reversal symmetry to impose well-established CPT symmetry at the Big Bang. This symmetry is further extended to the vacuum state by requiring CPT invariance for the Low Energy States defined around $\tau \to 0$. Specifically, we will characterize the possible CPT invariant states for scalars and spin-1/2 fields at the Big Bang event $\tau = 0$ and obtain a $\{\theta_k, \Theta_k\}$-family of Hadamard states for scalars and spin-1/2 field after studying its ultraviolet behaviour. We will study the possible CPT-invariant States of Low Energy in a radiation-dominated universe and analyze whether the smeared energy density can be minimized around the Big Bang for both scalar and spin-$\frac{1}{2}$ fields. We check that the resulting family of CPT-invariant states of low energy, indeed satisfy the Hadamard/adiabatic condition. Finally, within the context of the Weyl curvature hypothesis and a Time reversal symmetric universe, we will study a relevant scenario of gravitational dark matter production due to the expansion of the Universe.

5.1 CPT-invariant states for scalars in a radiation-dominated spacetime

Let us begin by considering a massive scalar field ϕ propagating in a flat FLRW spacetime

$$\mathrm{d}s^2 = a^2(\tau)(\mathrm{d}\tau^2 - \mathrm{d}\vec{x}^2) \ . \tag{5.1}$$

We assume a radiation-dominated universe where the expansion factor is given, in conformal time, by

$$a(\tau) \propto \tau \ . \tag{5.2}$$

We can split the quantized field in Fourier modes adapted to the underlying homogeneity of the 3-space

$$\phi(\tau, \vec{x}) = \int \frac{\mathrm{d}^3 k}{\sqrt{2(2\pi)^3}} \left(A_{\vec{k}} e^{i\vec{k}\vec{x}} \phi_k(\tau) + A^\dagger_{\vec{k}} e^{-i\vec{k}\vec{x}} \phi^*_k(\tau) \right) \ , \tag{5.3}$$

where the creation and annihilation operators satisfy the usual commutation relations ($[A_{\vec{k}}, A^\dagger_{\vec{k}'}] = \delta^3(\vec{k} - \vec{k}')$, etc). From the Klein-Gordon product, we obtain the normalization condition of the modes

$$\phi_k \phi'^*_k - \phi'_k \phi^*_k = \frac{2i}{a^2} \ , \tag{5.4}$$

where the prime denotes derivative with respect to the conformal time. In the following, we will work with the rescaled Weyl field $\varphi \equiv a\,\phi$ and the rescaled modes $\varphi_k \equiv a\,\phi_k$. The field equation for these modes implies

$$\varphi''_k(\tau) + \left[k^2 + \gamma^2\tau^2\right] \varphi_k(\tau) = 0 \ , \tag{5.5}$$

where we have defined γ by $a^2(\tau)m^2 = \gamma^2\tau^2$. The normalization condition is given by

$$\varphi_k \varphi'^*_k - \varphi'_k \varphi^*_k = 2i \ . \tag{5.6}$$

The general solution of (5.5) can be expressed in terms of parabolic cylindrical functions $D_\nu(z)$ [122]

$$\varphi_k(\tau) = C_{k,1}\, S_k(\tau) + C_{k,2}\, S^*_k(-\tau) \, , \tag{5.7}$$

where

$$S_k(\tau) = \frac{1}{(2\gamma)^{1/4}} D_{-\frac{1}{2}-2i\kappa}\left(e^{i\frac{\pi}{4}}\sqrt{2\gamma}\,\tau\right), \tag{5.8}$$

and $\kappa = \frac{k^2}{4\gamma}$. Any choice of k-functions $C_{k,1}$ and $C_{k,2}$ satisfying the normalization condition defines a set of modes characterizing a given vacuum state. By construction, these vacuum states are invariant under the continuous symmetries of spatial rotations and translations, and also under the discrete symmetries of parity and charge conjugation. Time translation is not a symmetry for expanding universes, and this is why there is not a preferred way of constructing a Fock vacua. Time-reversal has not been considered so far. In a radiation dominated spacetime, one can analytically extend the metric to negative values of the conformal time parameter and by imposing the emergent time reversal symmetry of the background to the quantum fields $\tau \to -\tau$, we can further reduce the freedom in choosing a vacuum representation.

In general the action of charge conjugation C, parity P, and time-reversal T on the Weyl transformed scalar field φ is given by [123]

$$C : \varphi(\tau, \vec{x}) \to \xi_c^* \varphi^*(\tau, \vec{x}) \;\; ; \;\; P : \varphi(\tau, \vec{x}) \to \xi_p^* \varphi(\tau, -\vec{x}) \;\; ; \;\; T : \varphi(\tau, \vec{x}) \to \xi_t^* \varphi^*(-\tau, \vec{x}) \, .$$

[The ξ's are the associated phases of the C, P, T transformations]. In the quantum theory, C and P are represented as unitary operators, while T is an anti-unitary operator. In our case C and P are already satisfied by directly looking at the Fourier expansion decomposition of the field. Enforcing T is the key ingredient. Because the complete CPT symmetry is a fundamental symmetry of the physical laws, as given by the CPT theorem [123] it seems natural to impose CPT at the Big Bang and by extension to enforce CPT all at once for the quantum fields [furthermore, we also choose $\xi_c \xi_p \xi_t = 1$ [124]; therefore $CPT\varphi(x)(CPT)^{-1} = \varphi(-x)^\dagger$]. For practical purposes, the condition for a CPT-invariant vacuum state takes a very simple form on the time-dependent part of scalar field modes,

$$\varphi_k(-\tau) = \varphi_k^*(\tau) \, . \tag{5.9}$$

This condition implies $C_{k,1} = C_{k,2}^*$, as can be checked using standard properties of the parabolic cylindrical functions. As a remark, note that when the T transformation is directly applied on the original scalar field $\phi(x)$ there will be a difference of sign with respect to the transformation defined here. We have removed this sign by absorbing it in the phase ξ_t^* or by redefining the (Weyl transformed) modes $\varphi_k \to i\varphi_k$ to keep our choices (e.g., $\xi_c\xi_p\xi_t = 1$), and hence, the final form of the CPT transformation unaltered. We follow the conventions adopted in [45, 44].

Within the context of a radiation dominated spacetime with a CPT invariant Big Bang, the natural way to characterize a CPT-invariant vacuum state is by specifying initial data satisfying the symmetries at $\tau = 0$. By taking (5.9) we easily find

$$\begin{aligned} \varphi_k(0) &= \varphi_k^*(0)\,, \\ \varphi_k'(0) &= -\varphi_k^{*\prime}(0)\,. \end{aligned} \tag{5.10}$$

The general solution with the above constraints and the normalization condition (5.6) can be parametrized as

$$\varphi_k(0) = \frac{1}{\sqrt{k}} e^{\theta_k}\,, \tag{5.11}$$

$$\varphi_k'(0) = -i\sqrt{k}\, e^{-\theta_k}\,, \tag{5.12}$$

where θ_k is an arbitrary real function. A potential sign ambiguity in (5.11-5.12) has been removed by matching the sign with the standard initial conditions for a massless (conformal) field $\varphi_k(0) = \frac{1}{\sqrt{k}}$, $\varphi_k'(0) = -i\sqrt{k}$. Note that we have used the freedom to phase-rotate the modes to make them real and non-negative at $\tau = 0$. In summary, the CPT requirement reduces the space of possible vacuum states to a family of states characterized by the hyperbolic initial ($\tau = 0$) phase θ_k. In terms of this parameter, the functions $C_1(k)$ and $C_2(k)$ read[1]

$$C_{k,1} = 2^{i\kappa}\sqrt{\pi} e^{\pi\kappa} \left(\frac{e^{-\frac{i\pi}{4}} e^{\theta_k}}{\kappa^{\frac{1}{4}}\Gamma(\frac{1}{4} - i\kappa)} + \frac{i\,\kappa^{\frac{1}{4}} e^{-\theta_k}}{\Gamma(\frac{3}{4} - i\kappa)} \right), \tag{5.13}$$

with $C_{k,2} = C_{k,1}^*$. In other words, any CPT-invariant solution can be written in terms of the θ_k angle as

$$\varphi_k^{CPT}(\tau) = C_{k,1}\, S_k(\tau) + C_{k,1}^*\, S_k^*(-\tau)\,, \tag{5.14}$$

with $C_{k,1}$ given above. Note that, with this characterization, in the Heisenberg picture we do understand now the time reversal vacuum state $|0\rangle$ as defined by giving initial data $\varphi_k^{CPT}(\tau_0)$ at $\tau_0 = 0$.

[1]The final expression for C_1 can be written in several ways by using some properties of the gamma functions. In particular we have used $\Gamma(z)\Gamma(z + \frac{1}{2}) = 2^{1-2z}\sqrt{\pi}\,\Gamma(2z)$ and $\Gamma(z)\Gamma(1 - z) = \frac{\pi}{\sin(\pi z)}$.

5.1.1 Particle production and the choice of θ_k

Particles are defined at $\tau \to +\infty$ as excitations of the *out*-vacuum $|0_+\rangle$. In this asymptotic region ($\tau \to \infty$), the general solution (5.7) behaves as a linear combination of positive and negative frequency solutions. The vacuum state is provided by the positive frequency solution,

$$\varphi_k^{(+)}(\tau) \sim \frac{e^{-i\int_\tau \omega(u)du}}{\sqrt{\omega(\tau)}} \sim \frac{e^{-i\left(\frac{\gamma}{2}\tau^2+\kappa\ln(2\gamma\tau^2)\right)}}{\sqrt{\gamma\tau}}\,, \tag{5.15}$$

where $\omega = \sqrt{k^2+m^2a^2}$. The constants $C_{k,1}$ and $C_{k,2}$ can be fixed imposing this late-time behavior. We directly find

$$C_{k,1} = \sqrt{2}\,e^{-\frac{\pi\kappa}{2}}e^{i\frac{\pi}{8}}\,, \qquad C_{k,2} = 0\,. \tag{5.16}$$

These family of Fourier modes define the *out*-vacuum $|0_+\rangle$. This vacuum is not CPT-invariant, since $C_{k,1} \neq C^*_{k,2}$. Note that an equivalent vacuum state $|0_-\rangle$ could be defined at the asymptotic region $\tau \to -\infty$. This vacuum is not CPT-invariant neither.

For each choice of initial vacuum $|0\rangle$, there is a different prediction for the spectrum of created particles at late times. The particle production rate can be obtained by the frequency-mixing approach [6]. It has been reviewed in [7, 8, 57, 125] and used extensively in the literature for decades (see, for instance, [126, 105, 54, 127, 128, 129, 130, 131, 132, 133]). In our case we can obtain a general expression for the average density number of created particles in the mode $\vec{k}$, depending on the vacuum state characterized by θ_k

$$n_k \equiv |\beta_k|^2 = -\frac{1}{2}+\frac{e^{-\pi\kappa}\cosh(2\pi\kappa)}{4\pi}\left(e^{-2\theta_k}\,\kappa^{\frac{1}{2}}\,|\Gamma(\tfrac{1}{4}+i\kappa)|^2+e^{2\theta_k}\,\kappa^{-\frac{1}{2}}\,|\Gamma(\tfrac{3}{4}+i\kappa)|^2\right), \tag{5.17}$$

where β_k is one of the Bogoliubov coefficients. It is interesting to remark that the above general expression can be re-expressed, after some manipulations, as

$$|\beta_k|^2 = \frac{1}{2}\Big(\cosh(2\eta_k)\cosh(\Lambda_k)-1\Big)\,, \tag{5.18}$$

where we have defined $\cosh(\Lambda_k) = \sqrt{1+e^{-4\pi\kappa}}$, and

$$2\eta_k = -2\theta_k + \frac{1}{2}\ln\Big(\frac{\kappa\cosh(2\pi\kappa)}{2\pi^2}|\Gamma(\tfrac{1}{4}+i\kappa)|^4\Big)\,. \tag{5.19}$$

From this we infer that the number of created particles is minimized when $\theta_k = \theta_k^{late}$, where

$$\theta_k^{late} = \frac{1}{4}\ln\left(\frac{\kappa\cosh(2\pi\kappa)}{2\pi^2}|\Gamma(\tfrac{1}{4}+i\kappa)|^4\right). \tag{5.20}$$

The vacuum defined by (5.20) is an equivalent characterization of the preferred CPT-invariant vacuum proposed in [45, 44], namely, $|0_T\rangle \propto |0_+\rangle + |0_-\rangle$. This vacuum minimizes the number of created particles at late times as well as the energy density in the asymptotic regions $|\tau| \to \infty$ since

$$\rho_k(\tau) \sim \omega_k|\beta_k|^2\ . \tag{5.21}$$

For this vacuum and for large-k, the particle number behaves as

$$n_k = \frac{1}{2}\left(\sqrt{1+e^{-4\pi\kappa}} - 1\right)\ . \tag{5.22}$$

At large k it has an exponential decay, $n_k \sim e^{-\frac{\pi k^2}{\gamma}}$.

An alternative choice for the vacuum state could be the minimal choice $\theta_k = 0$. This might seem physically reasonable because the field modes behave at the Big Bang as the modes of a massless conformally coupled field.

$$\varphi_k \sim \frac{1}{\sqrt{k}}e^{-ik\tau}\ . \tag{5.23}$$

This is consistent since the scalar curvature is $R = 0$ for a radiation dominated universe and the mass is negligible at $\tau \to 0$ as (5.5) suggests. Furthermore, if one analyzes the energy density or the Hamiltonian, as we will see in more detail in the following sections, this choice minimizes the energy density at $\tau = 0$ for $\xi = 1/6$. In this case, we have

$$\rho_k(\tau) \sim \frac{k}{a^4}\cosh(2\theta_k)\,. \tag{5.24}$$

For this choice and for large-k, the particle number behaves as

$$n_k \sim k^{-8}\,. \tag{5.25}$$

Despite the physical reasons for the selection of a vacuum state, another requirement that any vacuum has to satisfy is to be ultraviolet regular. In the following sections we will study the ultraviolet conditions within this cosmological context. We will study the construction of low energy states in a CPT-invariant radiation dominated universe and review the above vacuum states under the ultraviolet regularity conditions and relate them with the Low Energy States prescription.

5.1.2 Ultraviolet regularity and the Hadamard condition

An ultraviolet condition has to be imposed to any vacuum state $|0\rangle$ to be admitted as physically acceptable. This means that the local structure of products of field operators such as those defining the stress-energy tensor, should approach the same behaviour as in Minkowski spacetime to an appropiate rate. In particular, the specific rate of the behaviour for $\langle\phi(x)\phi(y)\rangle$ as $x \to y$, should be such that in the coincidence limit $\langle T_{\mu\nu}\rangle$ can be renormalized.

In cosmological backgrounds, the mode decomposition (5.3) allows us to write the formal vacuum expectation value of the stress-energy tensor as a sum over modes,

$$\langle T_{\mu\nu}\rangle = \int d^3k \; T_{\mu\nu}(\vec{k},\tau) \; . \tag{5.26}$$

Within this context, a very useful renormalization method, which captures the singular structure in momentum space at high energies, is the adiabatic renormalization method (see section 3.1). The method is based on the adiabatic WKB-type expansion of the field modes

$$\varphi_k(\tau) \sim \frac{1}{\sqrt{W_k(\tau)}} e^{-i\int^{\tau} W_k(\tau')d\tau'} \; , \tag{5.27}$$

where

$$W_k = \omega_k + \omega_k^{(2)} + \omega_k^{(4)} + \cdots \; , \tag{5.28}$$

with $\omega_k = \sqrt{k^2 + m^2a^2}$, and $\omega_k^{(n)}$ is the n-order term in a systematic adiabatic expansion. The adiabatic order is fixed by the number of τ-derivatives of the scale factor $a(\tau)$. The above expansion of the modes is translated to an adiabatic expansion of $T_{\mu\nu}(\vec{k},\tau)$.

In order to renormalize the stress energy tensor, this means having a convergent quantity for $\langle T_{\mu\nu}\rangle_{ren}$ (see section 3.1), one should require that the behaviour of the field modes φ_k, defining $|0\rangle$ should follow (5.27) for large k, up to at least order N=4 (in four spacetime dimensions). This asymptotic condition is called the *adiabatic condition to order 4*, and it is enough to renormalize $\langle T_{\mu\nu}\rangle_{ren}$. However if we allow for fluctuations of $\langle T_{\mu\nu}\rangle$ a more restrictive condition has to be imposed to ensure a regular behaviour. Also, when dealing with an interacting theory, we need to demand a higher renormalization condition allowing for the existence of Wick polynomials of any order [71, 72, 73]. Hence, we can construct a well defined perturbative series of an interacting theory at any order. For a general spacetime this condition is called the *Hadamard condition.* In a cosmological background, the *Hadamard condition* is equivalent to demanding the *adiabatic condition at all orders* [102].

Since the adiabatic modes $\varphi_k^{(N)}$ of order N satisfy the equation of motion at order N, adiabaticity is preserved in time. Therefore it is enough to state the adiabatic condition at a given instant of time to ensure the regularity of renormalized composite operators at any other instant. In the context of our analysis, it is useful to evaluate the complete adiabatic expansion of the modes (5.27) at $\tau = 0$. The explicit expansion (5.28) gives (we omit the details)

$$\varphi_k(0) \sim \frac{1}{\sqrt{k}} + \frac{\gamma^2}{8\,k^{9/2}} + \frac{41\gamma^4}{128\,k^{17/2}} + \cdots . \tag{5.29}$$

From this we infer the asymptotic expansion of θ_k

$$\theta_k \sim \frac{\gamma^2}{8k^4} + \frac{5\gamma^4}{16k^8} + \frac{61\gamma^6}{24k^{12}} + \cdots . \tag{5.30}$$

Thus, the recursive pattern of (5.30) is inherited from the recursive pattern of (5.28). The set of vacuum states that fits the above large k expansion to any order is referred as *adiabatic vacuum states of infinite order* or *Hadamard vacuum state.*

A consequence of having a Hadamard vacuum is that the number density of created particles in the mode $\vec{k}$ (i.e., n_k) with respect to the *out*-vacuum (which is also of infinite adiabatic order) decays faster than any power k^{-N} for large k. Typically, an exponential decay. This is the case of the θ_k^{late} vacuum state. Indeed, we have performed the large k expansion for θ_k^{late} and observed that it satisfies (5.30) as we increase the order of the expansion.

$$\theta_k^{late} = \frac{1}{4}\ln\Big(\frac{\kappa\cosh(2\pi\kappa)}{2\pi^2}|\Gamma(\tfrac{1}{4}+i\kappa)|^4\Big) \sim \frac{\gamma^2}{8k^4} + \frac{5\gamma^4}{16k^8} + \frac{61\gamma^6}{24k^{12}} + \cdots \tag{5.31}$$

In contrast, for a vacuum of a finite adiabatic order the decay is a power-law. If θ_k does not satisfy (5.30) at all orders, we get these kind of vacua. For instance, choosing $\theta_k = 0$ (zero adiabatic order) we find $n_k \sim k^{-8}$. Furthermore, for $\theta_k \sim 1/k^4$ we also get $n_k \sim k^{-8}$, except for the case $\theta_k = \gamma^2/(8k^4)$, for which $n_k \sim k^{-16}$. This behaviour ensures the UV convergence of the total number density of created particles,

$$\int \frac{d^3k}{(2\pi a)^3} n_k \ < +\infty \ . \tag{5.32}$$

In contrast, for $\theta_k \sim 1/k$ we get $n_k \sim k^{-2}$ and the integral evaluating the total number density is divergent.

5.1.3 CPT-invariant States of Low Energy for scalars

In general spacetimes there is not a prescription available to construct Hadamard states. Only when there is a temporal isometry, or in asymptotic regions where there exists a positive oscillatory frequency solution (as for $|0_+\rangle$ in (5.15)) the preferred state is a Hadamard state with an exponential decay for the spectra of created particles. For FLRW spacetimes a natural recipe to construct Hadamard states is possible using Low Energy States [43]. As introduced in chapter 4, these states are defined by minimizing the Hamiltonian or the energy density after averaging with a temporal window function in a smooth region, no matter how short. If the window function shrinks to a point, we recover the traditional method of instantaneous diagonalization of the Hamiltonian, which produced states that are not Hadamard. In this section we extend the Low Energy States precription for the CPT-invariant states in a radiation-dominated universe. If the minimization problem is restricted to the set of CPT-invariant states, we can re-parametrize the state of low energy using θ_k. For this we choose as a fiducial solution

$$\phi_k(\tau) = \frac{1}{a}\varphi_k^{CPT}(\tau, \theta_k = 0) \,, \tag{5.33}$$

with φ_k^{CPT} given in (5.14) and choosing $\theta_k = 0$. We impose CPT to the general solution

$$T_k(\tau) = \lambda_k \phi_k(\tau) + \mu_k \phi_k^*(\tau) \ , \tag{5.34}$$

using the CPT conditions at $\tau = 0$, [i.e., $\varphi_k(0) = \varphi_k^*(0)$ and $\varphi'_k(0) = -\varphi'^*_k(0)$] we arrive to

$$\lambda_k = \cosh(\theta_k) \,, \qquad \mu_k = \sinh(\theta_k) \,. \tag{5.35}$$

That is, λ_k and μ_k are real functions. The minimization of the smeared energy density $\mathcal{E}_k$ is performed with respect to θ_k

$$\mathcal{E}_k = (2\mu_k^2 + 1)c_1 + 2\mu_k \mathrm{Re}(\lambda_k c_2) \quad \rightarrow \quad \mathcal{E}_k = c_1 \cosh(2\theta_k) + \sinh(2\theta_k)\mathrm{Re}(c_2) \,.$$

Taking $\partial_{\theta_k} W = 0$ we end up with

$$\tanh(2\theta_k) = -\frac{\mathrm{Re}(c_2)}{c_1}\,. \tag{5.36}$$

So the state given by

$$T_k = \cosh(\theta_k)\phi_k + \sinh(\theta_k)\phi_k^*\,, \tag{5.37}$$

with ϕ_k given in (5.33) and

$$\theta_k = \frac{1}{2}\mathrm{arctanh}\left(-\frac{\mathrm{Re}(c_2)}{c_1}\right) \tag{5.38}$$

corresponds to the CPT-invariant state of low energy. As a remark note that while a specific fiducial solution is selected during the minimization process, the ultimate outcome (5.37) remains unaffected by this choice of basis. Nevertheless, it does, in a general sense, hinge on the selection of f^2.

The previously introduced vacuum states $|0_\pm\rangle$ and $|0_T\rangle \propto |0_+\rangle + |0_-\rangle$, can now be redefined as states of low energy, associated with smearing functions having support at $\tau \sim \pm\infty$ and satisfying symmetry requirements. By employing the general prescription (4.13) for any smearing function f^2 with support at $\tau \sim \pm\infty$, we derive the states $|0_\pm\rangle$. However, when CPT is imposed, the low-energy state for any window function with support at either $\tau \sim \pm\infty$ is given by $|0_T\rangle \propto |0_-\rangle + |0_+\rangle$, or expressed in terms of the initial phase (5.38),

$$\theta_k = \theta_k^{late}\,. \tag{5.39}$$

Here, θ_k^{late} is provided in Eq. (5.20). Notably, in the asymptotic regions $\tau \to \pm\infty$, the smeared energy density, incorporating conventional renormalization subtractions, is given by

$$\mathcal{E}_k\,[f] \propto \frac{1}{2}\int \mathrm{d}\tau\, f^2\,\omega\,|\beta_k|^2\,, \tag{5.40}$$

and it is minimized for the state that yields the least amount of particles, i.e., $\theta_k = \theta_k^{late}$. It is crucial to note that this state minimizes the (CPT-symmetric) smeared energy density at late times, irrespective of the chosen smearing function f^2. As anticipated, this state is Hadamard.

In the following section we analyze States of Low Energy with a window function f^2 supported around the Big Bang ($\tau = 0$) in the CPT-symmetric universe. As we will see, in this case we find that the result strongly depends on the choice of f^2, and also on ξ. For $\xi \neq \frac{1}{6}$ the issue is more subtle, and an extra condition has to be imposed on f^2. For $\xi = \frac{1}{6}$ this constraint is alleviated.

5.2 CPT-invariant States of Low Energy at $\tau = 0$ for scalars

In the last subsection, we have obtained a CPT-invariant state by minimizing the smeared energy density at $\tau \to \pm\infty$. Another physically sensitive choice of vacuum state would be a state that minimizes the smeared energy density around the Big Bang. Therefore, a simple question arises: can we obtain a Hadamard state by defining Low Energy State around $\tau = 0$? We will study the above question using a Gaussian smearing function

$$f_g^2(\tau) = \frac{1}{\sqrt{\pi}\epsilon} e^{-\frac{\tau^2}{\epsilon^2}} . \tag{5.41}$$

This function belongs to the Schwartz space. The behavior of the state with respect to the Big Bang singularity has also been studied with other functions with compact support around $\tau = 0$ rendering the same qualitative results.

In this section we work with minimally coupled scalars $\xi = 0$ for simplicity. The results can be generalized to other couplings except for the very special conformal coupling $\xi = 1/6$.

Massless case

Let us first analyze the massless case with a minimal coupling $\xi = 0$. This case is of particular interest because it is closely related to the question of the quantum creation of gravitons (quantum primordial gravitational waves). Tensor perturbations can be quantized in an expanding universe [134]. One can remove the gauge freedom by fixing the gauge. It is quite common to impose the transverse trace-free gauge. The two physical degrees of freedom, associated with the two polarizations (denoted by $\times$ and $+$), obey a scalar wave equation with

$m = 0 = \xi$.

$$h''_{\times,+} + a^2 \left(\frac{k^2}{a^2} + (\xi - \frac{1}{6})R \right) h_{\times,+} = 0 \quad , \tag{5.42}$$

Therefore, gravitons can be regarded, in this context, as a pair of massless minimally coupled scalar fields obeying the above equation. In a spatially flat radiation-dominated spacetime, the wave equation can not distinguish between conformal ($\xi = 1/6$) and minimal ($\xi = 0$) couplings. This is because $R = 0$. Therefore, one is tempted to define the vacuum for gravitons by the conformal vacuum with the modes

$$\phi_k^{\times,+} = \frac{e^{-ik\tau}}{a\sqrt{k}} \,. \tag{5.43}$$

The conformal vacuum is radiationless. Accordingly, one predicts that no gravitons are created by the expansion of the Universe during the radiation-dominated phase. One can further argue that the creation of gravitons in the very early Universe is a signal of a different expansion law, such as those linked to the inflationary universe. However, in the context of States of Low Energy we see that this is not the case if we define the vacuum state as the one that minimizes the smeared energy density around $\tau = 0$. Although the equation of motion does not distinguish between minimally coupled and conformally coupled fields, the stress-energy tensor, and correspondingly the Hamiltonian does. Therefore the statement that gravitons are not created in a radiation domianted spacetime requires to be revisited. This analysis goes beyond the purpose of this work and we leave it for a future study.

For the States of Low energy construction, we begin by taking a fiducial solution, which we take to be the conformal solution $\frac{e^{-ik\tau}}{a\sqrt{k}}$. We proceed to obtain the CPT-invariant state of low energy with the Gaussian function centered at $\tau = 0$, i.e., $f^2 = f_g^2$. For this we have to evaluate the integrals of c_1 and c_2.

$$\begin{aligned} c_1 &= \frac{1}{4} \int \mathrm{d}\tau \, \sqrt{|g|} \, \frac{f^2}{a^2} \left(|\phi'_k|^2 + \omega^2 |\phi_k|^2 + 6\xi \big(\frac{a'^2}{a^2} \, |\phi_k|^2 + \frac{a'}{a} \left(\phi_k \phi_k'^* + \phi_k^* \phi'_k \right) \big) \right) , \\ c_2 &= \frac{1}{4} \int \mathrm{d}\tau \sqrt{|g|} \, \frac{f^2}{a^2} \left(\phi_k'^{\,2} + \omega^2 \phi_k^2 + 6\xi \big(\frac{a'^2}{a^2} \phi_k^2 + 2 \frac{a'}{a} \phi_k \phi'_k \big) \right) . \end{aligned} \tag{5.44}$$

For $\xi = 0$ and $m = 0$ and using the conformal modes for the above integrals reduce to

$$c_1 = \frac{1}{4} \int \mathrm{d}\tau \, f_g^2 \left(\frac{1}{2k\tau^2} + k \right) = \frac{k}{4} - \frac{1}{4k\epsilon^2} \,, \tag{5.45}$$

$$c_2 \;=\; \frac{1}{4}\int \mathrm{d}\tau\, f_g^2\, e^{-2ik\tau}\left(\frac{1}{2k\tau^2}+\frac{i}{\tau}\right) = -\frac{e^{-k^2\epsilon^2}}{4k\epsilon^2}\,. \tag{5.46}$$

It is interesting to remark that the character of the singularity emerges in this construction when evaluating this integrals. In fact we have evaluated them making use of the distributional character of the integrand (see, for example, [115]). However, although this quantities give finite results, c_1 changes sign depending on the value of k, and therefore the quotient $\frac{|c_2|}{c_1}$ is not necessarily smaller than 1 for all k, thus the minimization prescription cannot be applied around $\tau = 0$ whenever we have a divergence in the above integrals. To bypass this problem and to be able to minimize the smeared energy density for all k we can require an extra condition to the window function,

$$\lim_{\tau\to 0}\frac{f^2(\tau)}{\tau^2} < \infty\,. \tag{5.47}$$

For example, using $f^2 = a^2\, f_g^2$ one obtains the following state of low energy for all k centered at $\tau = 0$

$$\theta_k^{m=0} = -\frac{1}{2}\coth^{-1}\left(e^{(\epsilon k)^2}\,\frac{1+(\epsilon k)^2}{1+2(\epsilon k)^2}\right)\,. \tag{5.48}$$

The resulting state is Hadamard, this can be seen because the large momentum expansion of θ_k decays faster than any power of k^{-n} [see Eq. (5.30) for $\gamma = 0$].

In section 4.1 we saw that for conformally coupled fields we don't need to require an extra condition for f^2. This is because the divergent terms τ^{-2} in the integrands of Eqs. (5.45) and (5.46) disappear for a conformally coupled field and the $\sqrt{|g|} = a^4$ factor from the volume element is enough to render both integrals finite. In contrast, the solution (5.48) depends on the test function that we use.

Massive case

For the massive field it is not possible to obtain analytical solutions to the integrals of c_1 and c_2 around $\tau = 0$. However, we can obtain an approximate state by expanding the mode part φ_k of the integrals around $\tau \to 0$ in a polynomial series. We have checked that the resulting state satisfies the adiabatic condition up to a given order, which increases as we increase the polynomial series in powers of τ.

This analysis can be done as follows. We begin from the definition of c_1 and c_2 given in Eqs. (5.44) with the fiducial modes ϕ_k proposed in Eqs. (5.33). Again we need to use $f^2 = a^2 f_g^2$ as the smearing function to ensure a well posed minimization problem, as it becomes explicit in (5.49) and (5.50). An approximated solution for the Hadamard state will be given if we expand the modes in powers of τ around $\tau = 0$ (where the center of the temporal window is located), and integrate

$$c_1 = \frac{1}{4}\int \mathrm{d}\tau\, a^2\, f_g^2 \left(\frac{1}{k\tau^2} + 2k + \frac{3\gamma^2\tau^2}{2k} - \frac{1}{9}\gamma^2 k\tau^4 \cdots\right), \tag{5.49}$$

$$c_2 = \frac{1}{4}\int \mathrm{d}\tau\, a^2\, f_g^2 \left(\frac{1}{k\tau^2} + 2k - \frac{8}{3}ik^2\tau - 2k^3\tau^2 + \frac{3\gamma^2\tau^2}{2k} \cdots\right). \tag{5.50}$$

We have computed the above integrals up to the order $O\left(\tau^{14}\right)$.

Finally, using Eq. (5.38), we can construct an approximated expression for the initial phase θ_k defining the state. Even more, if we expand the resulting θ_k for large k we recover order-by-order the expected asymptotic behavior (5.30), thus satisfying the Hadamard condition. As we include more terms of the τ expansion, more terms in the large k expansion are recovered. We have explicitly proved that for $\mathcal{O}\left(\tau^{14}\right)$ in (5.49) and (5.50) we obtain the expected large momentum expansion up to $\mathcal{O}\left(k^{-16}\right)$.

$$\theta_k \sim \frac{\gamma^2}{8k^4} + \frac{5\gamma^4}{16k^8} + \frac{61\gamma^6}{24k^{12}} + \mathcal{O}\left(k^{-16}\right). \tag{5.51}$$

A few interesting remarks. The asymptotic expansion is not sensitive to the particular smearing function f^2 that we are using: the particular choice of f^2 only matters in the infrared regime. This ambiguity included in the choice of smearing function could be naturally interpreted, at least heuristically, as encoding quantum gravity effects. We also note that the result above (5.51) is *independent of the scalar coupling* ξ. We have explicitly checked that the large k expansion of the hyperbolic angle θ_k obtained via the SLE prescription does not depend on ξ.

Summarizing the main ideas: With the prescription of States of Low Energy we can obtain a Hadamard state with a physical interpretation, a state that minimizes the smeared Hamiltonian with a temporal window. When we include a singular spacetime, we need to require an extra condition to the test function to smooth the singularity, except for conformally coupled fields. Although it is complicated to obtain analytical solutions for the vacuum state around the Big Bang, we can construct approximated Hadamard states which renders a finite $\langle T_{ab}\rangle$ after renormalization. These states can be used to study backreaction effects and particle production. Even more, we can improve our approximation by including more orders in the τ expansion and gain complete control of the renormalizability order of the state.

In the following sections we repeat the same analysis of for spin- 1/2 fields. First we parametrize the CPT-invariant states in a radiation dominated spacetime. Then we proceed to study States of Low energy within this context. Finally, we show an interesting application of gravitational dark matter production.

5.3 CPT-invariant states for fermions in a radiation-dominated spacetime

Consider a spin one-half field Ψ propagating in the same background metric $\mathrm{d}s^2 = a^2(\tau)(\mathrm{d}\tau^2 - \mathrm{d}\vec{x}^2)$. The Dirac field equation $(i\underline{\gamma}^\mu\nabla_\mu - m)\Psi = 0$, where $\underline{\gamma}^\mu = \frac{1}{a}\gamma^\mu$ and γ^μ are the flat spacetime Dirac matrices, in this spacetime become

$$\Big(\gamma^0\partial_\tau + \vec{\gamma}\cdot\vec{\nabla} + \frac{3a'}{2a}\gamma^0 + ima\Big)\Psi = 0\ . \tag{5.52}$$

As for the scalar fields we will perform a Weyl transformation for the spinor field of the form $\psi = a^{3/2}\Psi$. The mode expansion for the quantized ψ field is given by ($D_{\vec{k}h} = B_{\vec{k}h}$ for Majorana spinors)

$$\psi(x) = \int \mathrm{d}^3k \sum_h \Big[B_{\vec{k}h}u_{\vec{k}h}(x) + D^\dagger_{\vec{k}h}v_{\vec{k}h}(x)\Big]\ , \tag{5.53}$$

where the subindex h refers to the helicity, and where the u-modes in the Dirac representation can be written as (see the begining of section 4.2)

$$u_{\vec{k}h}(x) = \frac{e^{i\vec{k}\cdot\vec{x}}}{\sqrt{(2\pi)^3}}\begin{pmatrix} h^I_k(\tau)\xi_h(\vec{k}) \\ h^{II}_k(\tau)\frac{\vec{\sigma}\cdot\vec{k}}{k}\xi_h(\vec{k})\end{pmatrix}\ . \tag{5.54}$$

We recall that ξ_h is a constant and normalized two-component spinor $\xi^\dagger_h\xi_{h'} = \delta_{h'h}$ that represent the helicity eigenstates. $v_{\vec{k}h}(x)$ is obtained by the charge conjugation operation. The Dirac equation for the functions $h^I_k(\tau)$ and $h^{II}_k(\tau)$ is transformed into [we define again $ma = \gamma\tau$]

$$h'^I_k + ik\, h^{II}_k + i\,\gamma\tau\, h^I_k = 0\,, \tag{5.55}$$

$$h_k'^{II} + ik\, h_k^I - i\,\gamma\tau\, h_k^{II} = 0\,, \tag{5.56}$$

together with the normalization condition

$$|h_k^I|^2 + |h_k^{II}|^2 = 1\,. \tag{5.57}$$

The general solution to the mode equation is given in terms of parabolic cylindrical functions $D_\nu(z)$ as

$$h_k^I = C_{k,1}\, s_k^I(\tau) + C_{k,2}\, s_k^{II*}(-\tau)\,, \tag{5.58}$$
$$h_k^{II} = C_{k,1}\, s_k^{II}(\tau) + C_{k,2}\, s_k^{I*}(-\tau), \tag{5.59}$$

where

$$s_k^I = \frac{1}{\sqrt{2}} D_{-2i\kappa}(e^{\frac{i\pi}{4}}\sqrt{2\gamma}\,\tau)\,, \qquad s_k^{II} = e^{\frac{i\pi}{4}}\sqrt{\kappa}\, D_{-1-2i\kappa}(e^{\frac{i\pi}{4}}\sqrt{2\gamma}\,\tau)\,, \tag{5.60}$$

and where again $\kappa = \frac{k^2}{4\gamma}$. The complex functions $C_{k,1}$ and $C_{k,2}$ defining the vacuum state are constrained by the normalization condition (5.57).[2]

Equations (5.55) and (5.56) for the time-dependent part of the field modes h_k^I and h_k^{II} remain unchanged under the transformation $\tau \to -\tau$ and, simultaneously, $h_k^I \to h_k^{II*}$ and $h_k^{II} \to h_k^{I*}$. Therefore the vacuum will be CPT-invariant if the chosen modes verify the relation

$$h_k^I(\tau) = h_k^{II*}(-\tau)\,. \tag{5.61}$$

In terms of the functions $C_{k,1}$ and $C_{k,2}$ a CPT-invariant vacuum is characterized by the restriction $C_{k,1} = C_{k,2}^*$. As for the scalar field, we can easily constraint the CPT-invariant initial conditions at $\tau = 0$ as

$$h_k^I(0) = h_k^{II*}(0)\ . \tag{5.62}$$

Moreover, the normalization condition at $\tau = 0$

$$|h_k^I(0)|^2 + |h_k^{II}(0)|^2 = 1\ , \tag{5.63}$$

[2] In terms of $C_{k,1}$ and $C_{k,2}$ the normalization condition reads

$$\frac{e^{\pi\kappa}}{2}(|C_{k,1}|^2 + |C_{k2}|^2) + \frac{2\sqrt{\kappa}\,\sinh(2\pi\kappa)}{\sqrt{\pi}}\mathrm{Re}[e^{-i\frac{\pi}{4}}C_{k,1}C_{k,2}^*\Gamma(-2i\kappa)] = 1\,.$$

implies

$$|h_k^I(0)| = |h_k^{II}(0)| = \frac{1}{\sqrt{2}} \,. \tag{5.64}$$

Thus, the general ($\tau = 0$) solution to the conditions (5.62) and (5.64) can be written as

$$h_k^I(0) = \frac{e^{+i\Theta_k}}{\sqrt{2}} \,, \qquad h_k^{II}(0) = \frac{e^{-i\Theta_k}}{\sqrt{2}} \,, \tag{5.65}$$

where Θ_k is an arbitrary trigonometric angle. In terms of Θ_k, the constants $C_{k,1}$ and $C_{k,2}$ read

$$C_{k,1} = 2^{i\kappa}\sqrt{\pi}e^{\pi\kappa}\left(\frac{e^{i\Theta_k}}{\Gamma(\frac{1}{2}-i\kappa)} + \frac{\kappa^{\frac{1}{2}}e^{i\frac{3\pi}{4}}\,e^{-i\Theta_k}}{\Gamma(1-i\kappa)}\right), \tag{5.66}$$

$C_{k,2} = C_{k,1}^*$. Therefore, the CPT-invariant solution reads

$$h_k^{I;CPT} = C_{k,1}\, s_k^I(\tau) + C_{k,1}^*\, s_k^{II*}(-\tau) \,, \tag{5.67}$$

$$h_k^{II;CPT} = C_{k,1}\, s_k^{II}(\tau) + C_{k,1}^*\, s_k^{I*}(-\tau), \tag{5.68}$$

and with $C_{k,1}$ given above.

5.3.1 Particle production and the choice of Θ_k

As for the scalar case, we can define the late-times vacuum $|0_+\rangle$ in the asymptotic region $\tau \to \infty$. This is also called the adiabatic out-vacuum. This preferred solution at late times is a non CPT-invariant solution. It is given by the positive frequency solution of the field modes in the asymptotic region.

$$h_k^{I\,(+)}(\tau) \sim \sqrt{\frac{\omega+ma}{2\omega}}e^{-i\int_\tau \omega(u)du} \sim e^{-i\left(\frac{\gamma}{2}\tau^2+\kappa\ln(2\gamma\tau^2)\right)} \,, \tag{5.69}$$

$$h_k^{II\,(+)}(\tau) \sim \sqrt{\frac{\omega-ma}{2\omega}}e^{-i\int_\tau \omega(u)du} \sim \frac{\sqrt{\kappa}}{\sqrt{\gamma}\,\tau}e^{-i\left(\frac{\gamma}{2}\tau^2+\kappa\ln(2\gamma\tau^2)\right)} \,. \tag{5.70}$$

It leads to

$$C_{k,1} = \sqrt{2}e^{-\frac{\pi\kappa}{2}} \,, \qquad C_{k,2} = 0 \,. \tag{5.71}$$

This solution is not CPT-invariant since $C_{k,1} \neq C_{k,2}^*$. For completeness, we can also give the form of the preferred solution at ($\tau \to -\infty$) by imposing the late-times negative-frequency behaviour

$$h_k^{I\,(-)}(\tau) \sim \sqrt{\frac{\omega+ma}{2\omega}}e^{-i\int_\tau \omega(u)du} \sim -\frac{\sqrt{\kappa}}{\sqrt{\gamma}\,\tau}e^{+i\left(\frac{\gamma}{2}\tau^2+\kappa\ln(2\gamma(-\tau)^2)\right)} \,, \tag{5.72}$$

$$h_k^{II\,(-)}(\tau) \quad \sim \quad \sqrt{\frac{\omega - ma}{2\omega}} e^{-i\int_\tau \omega(u)du} \sim e^{+i\left(\frac{\gamma}{2}\tau^2 + \kappa \ln(2\gamma(-\tau)^2)\right)} \, . \tag{5.73}$$

From this condition we get $C_{k,1} = 0$ and $C_{k,2} = \sqrt{2}e^{-\frac{\pi\kappa}{2}}$. This defines the $|0_-\rangle$ vacuum state.

The number density of created particles at late times for any CPT-invariant vacuum state $|0\rangle$ is characterized by the trigonometric initial phase Θ_k. The vacuum $|0\rangle$ is perceived at late times as a collection of particles, defined as quantum excitations of the adiabatic out-vacuum $|0_+\rangle$. The number density of created particles is given by

$$\begin{aligned} n_{k,h} &= |\beta_{k,h}|^2 & (5.74)\\ &= \frac{1}{2} - \frac{e^{-\pi\kappa}\sinh(2\pi\kappa)\sqrt{\kappa}}{4\pi}\Big(e^{-2i\Theta_k}e^{i\frac{\pi}{4}}\Gamma(i\kappa)\Gamma(\tfrac{1}{2} - i\kappa) & (5.75)\\ &\quad + e^{2i\Theta_k}e^{-i\frac{\pi}{4}}\Gamma(-i\kappa)\Gamma(\tfrac{1}{2} + i\kappa)\Big) \ , \end{aligned}$$

where the subindex h refers to the helicity of the created fermionic particles. Note that (5.74) is independent of h. Equivalently to the scalar case, the above expression can be rewritten as

$$|\beta_{k,h}|^2 = \frac{1}{2}\big(1 - \cos(2\eta_k)\cos(\Lambda_k)\big) \ , \tag{5.76}$$

where $\cos(\Lambda_k) = \sqrt{1 - e^{-4\pi\kappa}}$ and

$$2\eta_k = 2(\Theta_k^{late} - \Theta_k) \, . \tag{5.77}$$

Therefore the number of created particles at late times is minimized for

$$\Theta_k = \Theta_k^{late} \equiv \frac{\pi}{8} + \frac{1}{2}\mathrm{Arg}[\Gamma(\tfrac{1}{2} - i\kappa)\Gamma(i\kappa)] \ , \tag{5.78}$$

resulting in

$$n_{k,h} = \frac{1}{2}\left(1 - \sqrt{1 - e^{-4\pi\kappa}}\right) \, . \tag{5.79}$$

This quantity decays exponentially for large k. This vacuum also minimizes the energy density at late times, as for the scalar case. The state Θ_k^{late} agrees with the preferred CPT-invariant fermionic vacuum proposed in [45, 44], i.e., $|0_T\rangle \propto |0_-\rangle + |0_+\rangle$. As for the scalar case, an alternative tempting vacuum could be the minimal choice

$$\Theta_k = 0 \, . \tag{5.80}$$

For this choice, the field modes behave as the conformal modes for $\tau \sim 0$, namely

$$h_k^{I,II} \sim \frac{1}{\sqrt{2}} e^{-ik\tau} \,, \tag{5.81}$$

and the particle number exhibits a power-law decay $n_{k,h} \sim k^{-4}$. This state minimizes the energy density at $\tau = 0$ since

$$\rho_k(\tau) = -\frac{2k}{a^4} \cos 2\Theta_k \,, \tag{5.82}$$

as we will see in the following sections.

5.3.2 Ultraviolet regularity of the CPT-invariant vacuum states

Similar to the scalar field case, it is crucial to investigate the ultraviolet regularity of vacuum states that are CPT-invariant. For cosmological backgrounds and spin-$\frac{1}{2}$ fields, this entails examining the behavior of the modes $h_k^I(\tau)$ and $h_k^{II}(\tau)$ for large k and matching them with the adiabatic expansion at all order. Analyzing the adiabatic expansion for spinors is more intricate compared to scalars, as it differs from the conventional WKB-type pattern applicable to scalar fields. Using the definitions (5.54) for the modes, the adiabatic expansion for spinors is expressed as follows:

$$\begin{aligned} h_k^I(\tau) &\sim \sqrt{\frac{\omega + ma}{2\omega}} \left(1 + F_k^{(1)} + F_k^{(2)} + \cdots \right) e^{-i\int^\tau \Omega_k(\tau')d\tau'} \,, \\ h_k^{II}(\tau) &\sim \sqrt{\frac{\omega - ma}{2\omega}} \left(1 + G_k^{(1)} + G_k^{(2)} + \cdots \right) e^{-i\int^\tau \Omega_k(\tau')d\tau'} \,, \end{aligned}$$

where $\omega^2 = k^2 + m^2a^2$, and $\Omega_k(\tau) = \omega + \omega_k^{(1)} + \omega_k^{(2)} + \cdots$. The recursive algorithm is detailed in [85, 86, 87, 88]. The above expansions establish the adiabatic condition for spin-$\frac{1}{2}$ fields, indicating that for large k, the modes $h_k^{I,II}$ should behave as this expansion at all orders. This is the equivalent to the adiabatic condition for scalar fields as defined in Eqs. (5.27) and (5.28).

To ascertain the desired asymptotic behavior for the trigonometric phase Θ_k, it is sufficient to evaluate the adiabatic expansion at $\tau = 0$, as adiabaticity is preserved in time. In this limit, and after a straightforward calculation, a well-defined large k asymptotic expansion is obtained:

$$h_k^I(0) \sim \frac{1}{\sqrt{2}} \Big(1 - i\frac{\gamma}{4k^2} - \frac{\gamma^2}{32k^4} - i\frac{21\gamma^3}{128k^6} - \frac{85\gamma^4}{2048k^8} + \cdots \Big) \,, \tag{5.83}$$

together with $h_k^{II}(0) \sim h_k^{I*}(0)$, this requires the following large k expansion for Θ_k:

$$\Theta_k \sim -\Big(\frac{\gamma}{4k^2} + \frac{\gamma^3}{6k^6} + \frac{4\gamma^5}{5k^{10}} + \cdots\Big) \,. \tag{5.84}$$

This establishes the appropriate rate for the decay of Θ_k as $k \to \infty$ to ensure a CPT-invariant vacuum of infinite adiabatic order. A vacuum meeting this asymptotic condition is considered a Hadamard state.

From (5.84) one can suspect that the minimal choice $\Theta_k = 0$ might not even render a finite stress energy tensor after renormalization $\langle T_{\mu\nu}\rangle_{ren}$. We give more details of this result in Appendix B . Although this state won't be good to study the backreaction of the semiclassical equations, we can obtain a state of low energy with a similar infrared behaviour (as we will see at the end of section 5.4), making the test function as short as we want. Therefore, the minimal solution Θ_k, can still be used as a good approximation to study the particle creation at late times.

5.3.3 CPT-invariant States of Low Energy for fermions

Let us characterize the States of Low Energy construction of section 4.2 including CPT-invariance. In this case, we begin by taking a convenient fiducial solution

$$h_k^I = h_k^{I;CPT}(\tau, \Theta_k = 0)\,, \qquad h_k^{II} = h_k^{II;CPT}(\tau, \Theta_k = 0)\,, \tag{5.85}$$

with $h_k^{I;CPT}$ and $h_k^{II;CPT}$ given in Eqs. (5.67) and (5.68) for $\Theta_k = 0$. The general modes are given by

$$\begin{aligned} t_k^I &= \lambda_k\, h_k^I + \mu_k\, h_k^{II*}\,, \\ t_k^{II} &= \lambda_k\, h_k^{II} - \mu_k\, h_k^{I*}\,. \end{aligned} \tag{5.86}$$

Imposing CPT-invariance to this solution we can write

$$t_k^I = \cos(\Theta_k) h_k^I + i \sin(\Theta_k) h_k^{II*}\,, \tag{5.87}$$

$$t_k^{II} = \cos(\Theta_k) h_k^{II} - i \sin(\Theta_k) h_k^{I*}\,. \tag{5.88}$$

and the ambiguity defining a vacuum state is reduced again to choosing the Θ_k parameter. The smeared energy density (4.34) is given by,

$$\mathcal{E}_k = \cos(2\Theta_k) c_1 + \sin(2\Theta_k) \mathrm{Im}(c_2)\,, \tag{5.89}$$

and minimizing this quantity with respect to Θ_k gives

$$-\sin(2\Theta_k)c_1+\cos(2\Theta_k)\mathrm{Im}(c_2)=0\,, \tag{5.90}$$

therefore

$$\tan(2\Theta_k)=\frac{\mathrm{Im}(c_2)}{c_1}\,. \tag{5.91}$$

The solution for the angle then reads

$$\Theta_k=\frac{1}{2}\arctan\left(\frac{\mathrm{Im}(c_2)}{c_1}\right)\,. \tag{5.92}$$

Up to irrelevant global phases, (5.92) characterizes a CPT-invariant low energy state, depending only on the smearing function f^2.

The state

$$\Theta_k=\Theta_k^{late}\equiv\frac{\pi}{8}+\frac{1}{2}\mathrm{Arg}[\Gamma(\tfrac{1}{2}-i\kappa)\Gamma(i\kappa)]\;, \tag{5.93}$$

which minimizes the number of particles at late times, also minimizes the smeared energy density at the asymptotic regions $\tau\to\pm\infty$ independently of f^2. This is so because

$$\mathcal{E}_k\,[f]\propto\frac{1}{2}\int\mathrm{d}\tau\,f^2\,\omega\,|\beta_k|^2\,. \tag{5.94}$$

Therefore Θ_k^{late} corresponds to the CPT-invariant state of low energy associated to any test function supported in the regions $\tau\to\pm\infty$. We have checked that Θ_k^{late} obeys the large k expansion (5.84) as we increase the orders of the expansion. This expansion together with the fact that $n_{k,h}$ decays exponentially for large k indicates that this state is Hadamard.

In the following section we study how to obtain a Hadamard state defined around the Big Bang singularity by using the low-energy states prescription. Finally, we will apply these constructions to study the creation of dark matter by an expanding universe in a cosmological scenario within the Weyl curvature hypothesis.

5.4 CPT-invariant States of Low Energy at $\tau=0$ for fermions

To define a State of Low energy with a test function supported around $\tau=0$ we will use a Gaussian function f_g^2 defined in Eq.(5.41). An interesting remark regarding fermions is that spin-1/2 behave like conformally coupled fields. Therefore, as it was shown in section 4.1, the energy density diverges with a^{-4} when $\tau \to 0$ and the $\sqrt{|g|} = a^4$ term from the volume element makes the integral of the smeared energy density perfectly finite. Let us analyse the massless and massive cases.

Massless case

We begin by considering the fiducial solution given in (5.85). This correspond to the conformal modes $h_k^I = \frac{1}{\sqrt{2}} e^{-ik\tau}$ and $h_k^{II} = \frac{1}{\sqrt{2}} e^{-ik\tau}$. We consider a Gaussian test function $f^2 = f_g^2$ and compute the integrals (4.32) and (4.33),

$$c_1 = -\frac{2k}{2} \int \mathrm{d}\tau \, f_g^2 = -\frac{k}{2} \, , \qquad c_2 = 0 \, . \tag{5.95}$$

Therefore directly applying (5.91) we get the state of low energy

$$\Theta_k^{m=0} = 0 \, . \tag{5.96}$$

This correspond to the conformal modes. Note that for massless spin-1/2 fields, this result is independent of the smearing function f^2. This is because $\Theta_k = 0$ minimizes the energy density

$$\rho_k(\tau) = -\frac{2k}{a^4} \cos 2\Theta_k \, , \tag{5.97}$$

for all τ. This is a unique feature of massless fields. As a final remark, we can see that $\Theta_k^{m=0} = 0$ satisfies the adiabatic condition (5.84) at all orders since $m = 0$ implies $\gamma = 0$.

Massive case

As for the scalars, we are not able to find analytical solutions for an state of low energy around $\tau = 0$ since the integrals to compute are highly involved. However, we can obtain an approximated Hadamard state, for which we have good control of its regularity, by expanding the modes h_k^I and h_k^{II} in the energy density function around $\tau \sim 0$. We explicitly compute its large-k behavior and check that it satisfies the adiabatic condition (5.84) up to a given order, that increases as we improve the orders of the expansion in τ. Thus satisfying the Hadamard or adiabatic condition.

Let us begin by taking a fiducial solution (5.85) and the Gaussian smearing function $f^2 = f_g^2$. Remember that since fermions behave as conformally coupled fields, the volume element $\sqrt{|g|} = a^4$ term is enough to absorb the singularity at $\tau = 0$ of the energy density of the modes, and we don't need to require an extra condition to f^2. In the following, we expand the modes in c_1 and c_2 in powers of τ around $\tau = 0$, and compute the resulting integrals to a given order $O(\tau^n)$.

$$\begin{aligned} c_1 &= 2i\int \mathrm{d}\tau f_g^2 \left(h_k^I \frac{\partial h_k^{I*}}{\partial\tau} + h_k^{II}\frac{\partial h_k^{II*}}{\partial\tau}\right) = \int \mathrm{d}\tau f_g^2\left(-4\sqrt{\gamma\kappa} - \frac{2}{3}\gamma^2\sqrt{\gamma\kappa}\tau^4 + \cdots\right), \\ c_2 &= 2i\int \mathrm{d}\tau f_g^2 \left(h_k^I \frac{\partial h_k^{II}}{\partial\tau} - h_k^{II}\frac{\partial h_k^{I}}{\partial\tau}\right) = i\int \mathrm{d}\tau f_g^2\left(4\sqrt{\gamma^3\kappa}\tau^2 - \frac{16}{3}\gamma^{5/2}\kappa^{3/2}\tau^4 + \cdots\right). \end{aligned}$$

Then, we can insert the results of this integrals in (5.91) and obtain an approximated solution for the initial phase Θ_k, and therefore for a vacuum state. Finally, we compute the large-k expansion of Θ_k, obtaining

$$\Theta_k = \frac{1}{2}\arctan\left(\frac{\mathrm{Im}(c_2)}{c_1}\right) \sim -\Big(\frac{\gamma}{4k^2} + \frac{\gamma^3}{6k^6} + \frac{4\gamma^5}{5k^{10}} + O\left(k^{-14}\right)\Big), \tag{5.98}$$

which fully agrees with the asymptotic expansion (5.84). We recover more terms of the adiabatic expansion as we increase the order of the polynomial expansion in τ. We have explicitly checked that for an expansion at order $O(\tau^{14})$ we recover the adiabatic expansion to $O\left(k^{-14}\right)$. This result gives strong evidence that the prescription of Low Energy States proposed in section 4.2 is consistent with the Hadamard/adiabatic condition for more general FLRW spacetimes. Note that (5.98) is insensitive to the details of f^2. Moreover, we have seen that this prescription allows to define Hadamard states with a physical meaning around the Big Bang singularity. In fact, these states correspond to the minimum of the smeared energy density around the initial singularity, $\tau = 0$. The infrared dependence with the f^2 function for a short temporal interval could be interpreted as including quantum gravity effects of a more fundamental theory.

To facilitate a comparison of physical predictions related to particle creation, it is intriguing to examine the behavior of the initial phase Θ_k in the infrared. For this purpose, we numerically compute Θ_k for various values of ϵ, representing the width of the Gaussian test function. The outcomes are depicted in Figure 5.1. It is evident that as the Gaussian becomes narrower, the state approaches $\Theta_k = 0$. In the limit $\epsilon \to 0$,

$$f^2 = \delta(\tau)\,, \tag{5.99}$$

resulting in a low-energy state with $\Theta_k = 0$. However, this state is neither Hadamard nor does it yield a renormalized vacuum expectation value of the stress-energy tensor, as discussed in Appendix (B) . On the contrary, as the Gaussian width increases, the state approaches $\Theta_k = \Theta_k^{late}$. This occurs because the dominant contribution of the Gaussian window arises from the asymptotic regions $\tau \sim \pm\infty$.

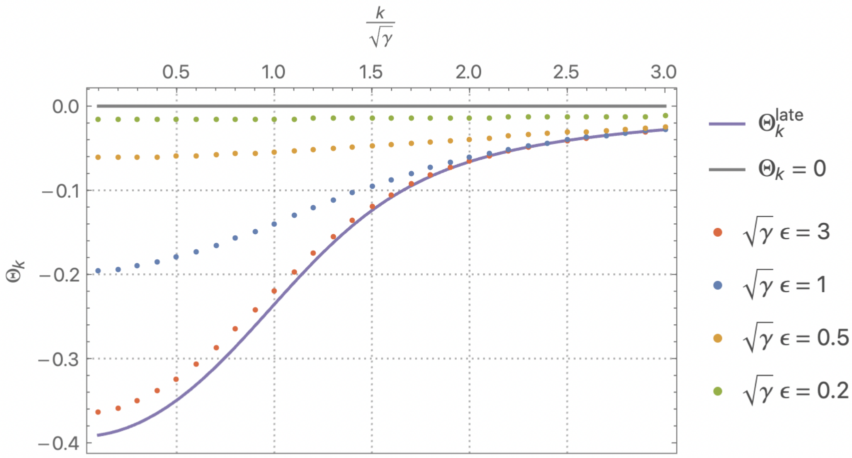

Figure 5.1: We represent Θ_k obtained with the states of low energy prescription for different values of ϵ, $\sqrt{\gamma}\epsilon = 3$ (red dots) and $\sqrt{\gamma}\epsilon = 1$ (blue dots), $\sqrt{\gamma}\epsilon = 0.5$ (orange dots) and $\sqrt{\gamma}\epsilon = 0.2$ (green dots). We also represent the two limiting cases $\Theta_k = 0$ (grey line) and $\Theta_k = \Theta_k^{late}$ (purple line).

In the next section we will illustrate how the above construction can be applied to a cosmological particle creation process of special relevance. It involves the production of heavy right-handed neutrinos by the early expansion in a radiation-dominated universe. To motivate the selection of this spin-$\frac{1}{2}$ field as a natural candidate for dark matter we will argue on the basis of conformal symmetry and anomaly cancellation.

5.5 Conformal symmetry, particle creation and dark matter

The very special character of the Big Bang singularity in the hot Big Bang theory suggested the formulation of the so called Weyl curvature hypothesis [119]. It essentially claims that the Weyl tensor vanishes at the initial singularity, in contrast with the typical black hole singularities. Writing the metric in conformal coordinates, $ds^2 = a^2(\tau)\left(d\tau^2 - d\vec{x}^2\right)$, it is explicitly manifested that the singularity is encoded in a conformal factor, a^2. Classically, this is a very smooth singularity, since massless conformally coupled fields do not "see" it. One can realize this by looking at the energy density of conformally coupled fields. As it was shown in (4.15) the energy density $\rho = u^a u^b T_{ab}$ for the Weyl modes $\varphi_k = a\phi_k$ associated to a conformal observer $u^a = (1/a, 0, 0, 0)$ is given by

$$\rho_k(\tau) = \frac{1}{4a^4}\left(|\varphi_k'|^2 + \omega^2|\varphi_k|^2\right) . \tag{5.100}$$

Under a conformal transformation [135],

$$\tilde{g}_{ab} = \Omega^{-2} g_{ab} \quad ; \quad \tilde{\phi} = \Omega\phi \tag{5.101}$$

$$\tilde{T}_{ab} = \Omega^2 T_{ab} \quad ; \quad \tilde{u}^a = \Omega u^a , \tag{5.102}$$

where $\tilde{u}^a$ is the rescaled conformal observer. This transformation leaves the action of a conformally coupled field invariant $S[\tilde{g}_{ab}, \tilde{\phi}] = S[g_{ab}, \phi]$. The energy density associated to $\tilde{u}^a$ reads

$$\rho_k(\tau) = \frac{\Omega^4}{4a^4}\left(|\varphi_k'|^2 + \omega^2|\varphi_k|^2\right) . \tag{5.103}$$

Therefore, the singularity in the energy density at $\tau = 0$ given by the $1/a^4$ factor is completely reabsorbed by the conformal factor Ω^4. Another consequence of having conformally coupled fields is that the trace of the stress energy tensor is zero, $T_a^a = 0$, in the classical theory. Penrose exploited the above properties by stressing that all matter fields behave as conformal fields as one approaches back to $\tau \to 0$ [135]. However, when quantizing the theory, the emergence of the trace anomaly appearing in the renormalization of the vacuum expectation values of the stress-energy tensor spoils the conformal character of the Big Bang singularity. For example for a conformally coupled scalar field the anomaly reads:

$$\langle T_a^a \rangle_{ren} = \frac{1}{2880\pi^2}\left(\Box R - \left(R^{ab}R_{ab} - \frac{1}{3}R^2\right)\right) , \tag{5.104}$$

which for a FLRW diverges as $1/a^8$. As we approach back to the Big Bang, the stress-energy tensor is fully dominated by the conformal anomaly contribution, and the conformally rescaled stress-energy tensor is no longer regular at $\tau \to 0$. This is in tension with the basic idea behind the Weyl curvature hypothesis.

To solve the conflict one could require an exact cancellation of the conformal anomaly in the Standard Model of particle physics. This has been further motivated in [136, 137]. In a first approximation, we can ignore interactions with the Higgs field and consider the free field content of the Standard Model living in a curved spacetime. By setting the Higgs field aside, the gauge and fermionic sectors from the standard model are Weyl invariant. After quantization of the Standard Model fields in a curved spacetime, the general expression for the conformal anomaly is given by

$$\langle T^{\mu}_{\mu} \rangle = cC^2 - aE \ , \tag{5.105}$$

where C^2 is the square of the Weyl tensor and E is the Euler density. We can omit the contribution proportional to $\Box R$ since it is ambiguous and can be removed by including a R^2 term in the Lagrangian [9, 7]. We are allowing geometries beyond exact FLRW, so C^2 does not need to be exactly zero. The interesting remark is that the coefficients a and c, which depend on the spin of the field [8],

$$\begin{aligned} a &= \frac{1}{360(4\pi)^2}[n_0 + \frac{11}{2}n_{1/2} + 62n_1] \ > 0 \\ c &= \frac{1}{120(4\pi)^2}[n_0 + 3n_{1/2} + 12n_1] \ > 0 \ , \end{aligned} \tag{5.106}$$

cannot cancel out. Where $n_0 \equiv$ number of scalar fields, $n_{1/2} \equiv$ number of spin-1/2 Weyl fields, $n_1 \equiv$ number of spin-1 fields. All conventional fields in the Standard Model contribute with the same sign. Note that we are not including spin-2 fields (gravitons) since they are not conformally coupled. [3]

The cancellation of the conformal anomaly requires the introduction of a special scalar fields ϕ'. These are conformally invariant scalar fields of dimension zero. Its action is expressed in terms of the unique conformally-invariant fourth order operator

$$S = \frac{1}{2}\int d^4x\sqrt{-g}\phi' \triangle_4 \ \phi' \ , \tag{5.107}$$

where $\triangle_4$ is given by [138, 139] (for other spin fields, see [140, 141])

$$\triangle_4 = \Box^2 + 2R^{\mu\nu}\nabla_\mu\nabla_\nu - \frac{2}{3}R\Box + \frac{1}{3}(\nabla^\mu R)\nabla_\mu \ . \tag{5.108}$$

These dimensionless scalar fields ϕ' contribute negatively to the conformal anomaly, with a contribution given by [142]

$$a = -\frac{28}{360(4\pi)^2} \qquad c = -\frac{8}{120(4\pi)^2} \ . \tag{5.109}$$

[3]The linearised gravitational field is not conformally coupled, and their trace contribution could spoil the Weyl curvature hypothesis. Nevertheless, the quantization of gravitational degrees of freedom, requires a more careful treatment which lives outside of this analysis.

The conformal anomaly is exactly cancelled for (see [143, 144])

$$n_{1/2} = 4n_1 = 48 \ , \qquad n_0' = 3n_1 = 36 \ , \qquad n_0 = 0 \, ,$$

at least to one-loop order. Surprisingly enough, this agrees with the current Standard Model, with exactly three generations of fermions, but with the following important caveats: i) one must include three right-handed neutrinos ν_R, (This corresponds to the minimal extension beyond the standard model where right handed neutrinos are typically included in order to explain neutrino masses and oscillations [1]). ii) The Higgs should be excluded as a fundamental field (it should emerge as a composite field). iii) One should also include 36 scalar fields ϕ'. These special fields are very peculiar because they do not have particle excitations. They only contribute to the vacuum state [145], so no new particles are required.

Therefore, in our context of an early CPT-invariant radiaton dominated universe, there is a natural candidate for dark matter. The heaviest right-handed Majorana neutrino ν^R, decoupled from all of the other particles in the Standard Model. It only interacts with gravity and therefore in a cosmological scenario it can only be produced due to a rapid expansion of the Universe [45]. As we have seen in (5.74) different vacuum states or Θ_k phases will produce a different spectra for this cold dark matter candidate.

It is noteworthy to recall that when considering the Hadamard State of Low Energy centered at the Big Bang, a very small window function $\epsilon \to 0$ can be applied. As illustrated in Figure 5.1, for $\epsilon \to 0$, the State of Low Energy (SLE) tends towards $\Theta_k = 0$ in the infrared regime. This behavior is also evident if we take the approximate SLE, where the analytical expression, when expanded for a very small window function, yields $\Theta_k^{SLE}|_{\epsilon\to 0} \sim 0 + O(\epsilon^2)$. It is crucial to emphasize this observation because the number density of created particles predominantly arises from the infrared regime. Consequently, nearly identical number densities of created particles are obtained whether utilizing $\Theta_k = 0$ or the state of low energy centered at the Big Bang with a very small window function. In Figure 5.2, we compare the predictions for the two different spectra given by $\Theta_k = \Theta_k^{late}$ and $\Theta_k = 0$. In the subsequent analysis, we will calculate the number density of created particles as a function of the state Θ_k. Subsequently, we will determine the resulting mass of the dark matter right-handed neutrino for the states $\Theta_k = \Theta_k^{late}$ and $\Theta_k = 0$.

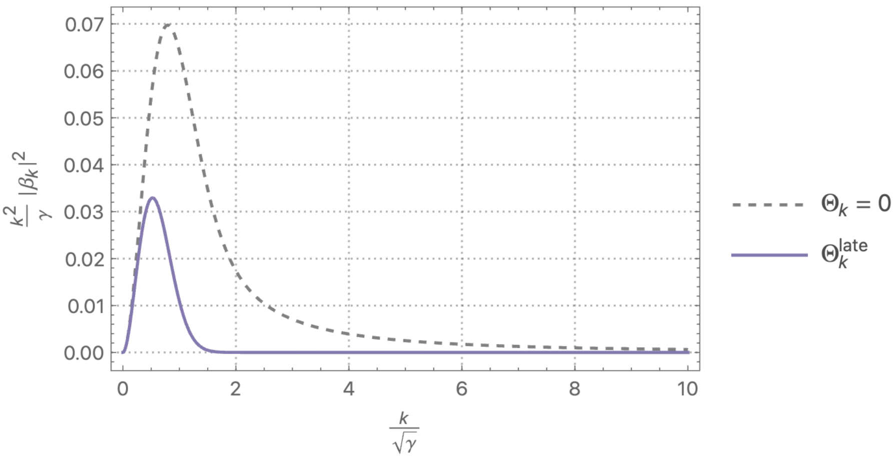

Figure 5.2: Comparison of the predicted spectra (cold dark matter) for two different vacua, namely Θ_k^{late} and $\Theta_k = 0$.

We begin by considering the comoving number density of created right-handed neutrinos,

$$n_{dm} = \sum_h \int \frac{d^3k}{(2\pi)^3}|\beta_k|^2 = (\gamma/\pi)^{3/2} I_{\Theta_k}\,. \tag{5.110}$$

I_{Θ_k} is the dimensionless integral given by (recall $\kappa = \frac{k^2}{4\gamma}$)

$$I_{\Theta_k} = \frac{4}{\sqrt{\pi}} \int_0^\infty d\kappa\sqrt{\kappa}|\beta_\kappa|^2\,, \tag{5.111}$$

where $|\beta_\kappa|^2$ is given by the right hand side of (5.74) and gives the spectra of created fermions at late times for a given state Θ_k. Furthermore, the physical energy density of the cold dark matter created is diluted in cosmological time t according to

$$\begin{aligned}\rho_{dm}(t) &= \frac{M_{\Theta_k} n_{dm}}{a^3} = \frac{M_{\Theta_k}}{a^3}\sum_h \int \frac{d^3k}{(2\pi)^3}|\beta_k|^2 \\ &= \frac{M_{\Theta_k}}{a^3}(\gamma/\pi)^{3/2} I_{\Theta_k} = \frac{M_{\Theta_k}}{(2\pi)^{3/2}}\left(\frac{M_{\Theta_k}}{t}\right)^{3/2} I_{\Theta_k}\,.\end{aligned} \tag{5.112}$$

To obtain a prediction for the mass of the dark matter candidate M_{Θ_k} from the observed value of the energy density, we follow now the argument in [44].

For the vacuum state Θ_k^{late} used in [44] one gets that $I_{\Theta_k^{late}} = 0.01276$ and then $M_{\Theta_k^{late}} = 4.8 \times 10^8 GeV$. If we now change the quantum state, the prediction for the mass changes accordingly

$$M^{5/2}_{\Theta_k^{late}} I_{\Theta_k^{late}} = M^{5/2}_{\Theta_k} I_{\Theta_k} \, . \tag{5.113}$$

For $\Theta_k = 0$ we have $I_{\Theta_k=0} = 0.06305$ and hence $M_{\Theta_k=0} = 2.6 \times 10^8 GeV$.

Part II

Entanglement in real space in Quantum Field Theory

Chapter 6

Entanglement in QFT

Entanglement is a unique property of quantum physics, and as such, it allows to distinguish between quantum and classical phenomena. Entanglement has been broadly studied in different areas with different motivations, ranging from quantum information theory, where quantum entanglement is used as an invaluable resource for performing computational tasks that are impossible to achieve in classical information theory [16, 17], in condensed matter [21], where entanglement describes quantum phases of matter [22] and diagnose quantum critical phenomena [23], and in quantum gravity where, quantum entanglement has been proposed as a key ingredient from which classical spacetime could emerge [18, 19, 20].

Particularly interesting is the study of entanglement in quantum field theories. Entanglement in the ground state of a quantum field theory plays an important role in different aspects of physics. Some of them are: It encodes the foundational aspects of how to make relativity and the quantum theory consistent [24, 25, 26], entanglement may be at the heart of understanding the black-hole information paradox [27, 28, 29], or it can be the toolkit to determine the quantum origin of the large scale structure that we observe in the Universe [30, 31]. From the quantum technology perspective, entanglement of the ground state can also be used as a powerful resource in different quantum relativistic protocols [32, 33, 34].

The vacuum state of a quantum field theory is a rich state regarding its entanglement structure as revealed by the Reeh-Schlieder theorem [25]. This theorem is applicable to both free and interacting theories. To delve into its implications within the most straightforward context, we will focus on a free real scalar field theory in $D+1$-dimensional Minkowski spacetimes. This ensures that the principles explored here are not a result of the interactions within the field theory in question; rather, they are inherent properties of any quantum field theory.

The Reeh-Schlieder theorem can be stated as follows: Consider operators of the form $\hat{\phi}_F := \int dV\, F(x)\, \hat{\phi}(x)$, where $F(x)$ is a smooth function, and dV is the spacetime volume element. These are known as smeared field operators, with $F(x)$ serving as smearing functions. Smearing ensures that $\hat{\phi}_F$ is a well-defined operator in the Hilbert space .[1] The Hilbert space of the theory can be generated from states of the form

$$|\Psi\rangle = \hat{\phi}_{F_1}\hat{\phi}_{F_2}\cdots\hat{\phi}_{F_N}|0\rangle\,, \tag{6.1}$$

i.e., any state can be approximated arbitrarily well by such states, for an appropriate choice of smearing functions $F_1(x),\cdots,F_N(x)$. This is expected, and indicates that any field excitation can be created by acting with a suitable combination of operators. Intuitively, an excitation with support in a small laboratory can be created by acting with a set of smeared operators supported within the laboratory.

What is rather surprising— and this is the content of the Reeh-Schlieder theorem— is that the entire Hilbert space can be generated from states of the form (6.1) even when we restrict the smearing functions to be supported within an arbitrarily small open region of spacetime. In simpler terms, one can excite the field in any corner of the Universe by acting on the vacuum with operators supported exclusively within our small lab. However, this fact cannot be used for faster-than-light communication [24, 146, 147].

[1] This implies that it maps states to other states. Without smearing, issues arise; for instance, $\hat{\phi}(x)$ acting on the vacuum produces a state with infinite norm, $\langle 0|\hat{\phi}(x)\hat{\phi}(x)|0\rangle \to \infty$, which is clearly outside the Hilbert space. Smeared field operators eliminate this problem and are suitable candidates for elementary observables, generating the full algebra of observables.

While initially puzzling, the situation bears a resemblance to the properties of maximally entangled states in quantum mechanics [24]. Let's consider two quantum mechanical systems, each with Hilbert spaces $\mathcal{H}_A$ and $\mathcal{H}_B$ of the same dimension n. Assume $|\Psi\rangle$ is a pure maximally entangled state. It's well-known that every state in $\mathcal{H}_A \otimes \mathcal{H}_B$ can be obtained by acting on $|\Psi\rangle$ with an *operator restricted to subsystem* A:

$$\forall\, |\alpha\rangle \in \mathcal{H}_A \otimes \mathcal{H}_B, \text{ there exists } \hat{O}_A \text{ such that } |\alpha\rangle = \hat{O}_A \otimes \hat{\mathbb{I}}_B |\Psi\rangle\,, \tag{6.2}$$

where $\hat{\mathbb{I}}_B$ is the identity operator in $\mathcal{H}_B$ (see, for instance, [148]). This holds not only for maximally entangled states, but also for any state whose Schmidt form is given by

$$|\Psi\rangle = \sum_i^n c_i\, |i\rangle_A |i\rangle_B\,, \tag{6.3}$$

where *all* coefficients c_i are different from zero. These are sometimes called totally entangled states (maximally entangled states correspond to $c_i = 1/\sqrt{n}$ for all i). The proof involves creating basis states $|i\rangle_A|j\rangle_B \in \mathcal{H}_A \otimes \mathcal{H}_B$ from $|\Psi\rangle$ by acting with operators $\frac{1}{c_j}|i\rangle\langle j|_A \otimes \hat{\mathbb{I}}_B$. This allows creating any basis element in $\mathcal{H}_A \otimes \mathcal{H}_B$. Therefore, for each state in $\mathcal{H}_A \otimes \mathcal{H}_B$, there exists a linear combination of such operators whose action on $|\Psi\rangle$ produces the desired state. Note that this argument fails if any of the coefficients c_j are equal to zero.

This scenario is similar to the Reeh-Schlieder theorem for quantum field theory if we identify the field degrees of freedom inside our small lab with subsystem A and the rest with subsystem B. The Reeh-Schlieder theorem reveals that the vacuum state is extraordinarily rich in terms of its entanglement structure [46]. In particular, it has been shown that the Reeh-Schlieder theorem implies that, if A and B are subsystems made up of all the field degrees of freedom contained within two regions of spacetime V_A and V_B, respectively, and the two regions are spacelike separated, subsystems A and B are always entangled when the field is prepared in the vacuum [46, 47]. The entanglement content of quantum field theory has been reinforced by calculations of the geometric entanglement entropy associated with an open region of space V (see [149, 150, 151, 152, 153, 154], and references therein).

These results teach us a profound lesson about quantum field theory: entanglement is "ubiquitous" in the vacuum, and since the short-distance behavior is the same for all states, entanglement is equally ubiquitous in any other state. This reflects the fact that entanglement between spatially separated regions is an intrinsic property of quantum field theory.

The results discussed so far involve subsystems containing *infinitely many* degrees of freedom, typically all the field modes supported within a region V. While this is crucial for understanding the conceptual and mathematical content of quantum field theory, it is desirable to extend the discussion to *finite-dimensional* subsystems of this theory, since from a practical point of view, experimentalists, have access only to a finite set of such field modes. This is the goal of the following two chapters.

In this chapter we will review the main concepts of quantum mechanics for continuous variable regarding entanglement and provide its consistent extension to quantum field theory. The organization of this chapter is as follows: In section 6.1 we will describe the way we isolate individual field degrees of freedom that are localized in a region of space in a free scalar theory. In section 6.2 we will describe how to compute the reduced state describing a finite number of such modes and how to compute the von Neumann entropy. In section 6.3 we will characterize mutual information and entanglement. In the following chapter, we will use the techniques presented here to analyse real space entanglement between finite modes in quantum field theory for the Minkowski vacuum in different situations.

6.1 Defining individual modes for the field

In order to fix the basic ideas that we will use to analyse entanglement in QFT, let us begin by reviewing some concepts of an analog situation in standard quantum mechanics. Consider the quantization of a system characterized by a $2N$-dimensional phase space, assuming a finite N. We will focus on linear systems in which the classical phase space Γ forms a vector space. It is possible to select global canonical coordinates x_I, p_I for $I = 1, \ldots, N$ in Γ such that the Poisson brackets satisfy $\{x_I, x_J\} = \{p_I, p_J\} = 0$ and $\{x_I, p_J\} = \delta_{IJ}$. This information can be succinctly conveyed by introducing the column vector $r^i = (x_1, p_1, \ldots, x_N, p_N)^\top$ —we will use lower case letters for indices in phase space, $i = 1, \ldots, 2N$— in terms of which all Poisson brackets read

$$\{r^i, r^j\} = \Omega^{ij}, \quad \text{where} \quad \Omega^{ij} = \oplus_N \begin{pmatrix} 0 & 1 \\ -1 & 0 \end{pmatrix}, \tag{6.4}$$

is the (inverse of) the symplectic structure. Observables are real functions of Γ in the classical theory, i.e., a map $O : \Gamma \to \mathbb{R}$. The vector r^i defines a "basis" of linear observables in the classical theory. Observables that are linear in the canonical variables can be written as $O_{\vec{v}} := v_i r^i$, (sum over repeated indices is understood) with $\vec{v} \in \mathbb{R}^{2N}$.

In the quantum theory, classical observables are promoted to operators acting on a Hilbert space and satisfying commutation relations. The basis of observables r^i are thus promoted to operators satisfying

$$[\hat{r}^i, \hat{r}^j] = i\,\Omega^{ij}\,. \tag{6.5}$$

A general linear observable can be written as $\hat{O}_{\vec{v}} := v_i \hat{r}^i$. Note that vectors $\vec{v}$ can be identified with elements of Γ^*, the dual of the classical phase space, establishing a correspondence between linear observables in the classical and quantum theories. Written in this way, all $\hat{O}_{\vec{v}}$'s have dimensions of action, and their commutation relations are given by the symplectic product of the corresponding $\vec{v}$'s,

$$[\hat{O}_{\vec{v}}, \hat{O}_{\vec{v}'}] = i\, v_i v'_j \Omega^{ij}\,. \tag{6.6}$$

For our subsequent computations, it is noteworthy to emphasize that any *noncommuting* pair of linear observables $(\hat{O}_{\vec{v}}, \hat{O}_{\vec{v}'})$ *defines a subsystem with a single degree of freedom* (referred to as "modes of the system"). To be more precise, the subsystem is characterized by the algebra generated by the pair $(\hat{O}_{\vec{v}}, \hat{O}_{\vec{v}'})$ [155]. For instance, subsystems corresponding to individual oscillators are determined by the pairs $(\hat{x}_I, \hat{p}_I)$, where $I = 1, \cdots, N$. However, the definition is more general and encompasses modes that are combinations of multiple oscillators. This methodology provides a straightforward approach to extract individual modes within our systems. We are interested in the extension of this concept to field theory to subsequently evaluate entanglement in field theory between a finite set of degrees of freedom.

In the realm of field theory, an infinite number of degrees of freedom exists, even when considering an arbitrarily small open region of space. Intuitively, at each spatial point $\vec{x}$, there exists an independent pair of canonically conjugated operators $(\hat{\phi}(\vec{x}), \hat{\pi}(\vec{x}))$, with each such pair defining a single mode of the system. Since any region encompasses an infinite number of points, it accommodates an equivalent number of independent modes. However, this intuitive understanding is only heuristic because neither of the entities $\hat{\phi}(\vec{x})$ nor $\hat{\pi}(\vec{x})$ are well-defined operators in spacetime. In reality, these are *operator-valued distributions*, and to establish well-defined operators it is necessary to smear them with test functions. The standard procedure is to smear the covariant operator $\hat{\phi}(x)$ against a test function in spacetime[2] $\hat{\phi}_F := \int dV F(x)\hat{\phi}(x)$, with $F(x)$ a smooth function compactly supported in a region V. This is the set of linear observables in the theory—in this covariant formulation, the conjugate momentum $\hat{\pi} = \frac{d}{dt}\hat{\phi}$ is not needed. Given two operators defined in this way, their commutation relations are

$$[\hat{\phi}_{F_1}, \hat{\phi}_{F_2}] = i\,\Delta(F_1, F_2)\,, \tag{6.7}$$

where

$$\Delta(F_1, F_2) := \int dV dV'\, F_1(x)F_2(x)\,\Delta(x, x')\,, \tag{6.8}$$

and $\Delta(x, x') := G_{\rm Ad}(x, x') - G_{\rm Ret}(x, x')$ is the difference between the advanced and retarded Green's functions of the Klein-Gordon equation. Equation. (6.7) is simply the smeared version of the familiar covariant commutation relations $[\hat{\phi}(x), \hat{\phi}(x')] = i\,\Delta(x, x')$.

With these definitions, for any two smearing functions F_1 and F_2 compactly supported in a region V where the associated field operators do not commute $[\hat{\phi}_{F_1}, \hat{\phi}_{F_2}] \neq 0$, the pair $(\hat{\phi}_{F_1}, \hat{\phi}_{F_2})$ establishes an individual mode of the system, which is localized within region V. This approach offers a straightforward method to extract individual degrees of freedom from the field theory that are specifically localized in a given region. It's crucial to bear in mind that within any open region V, there are infinitely many independent modes. A noncommuting pair $(\hat{\phi}_{F_1}, \hat{\phi}_{F_2})$ defines just one of these modes.

Finally, let us stress that the above discussion for defining individual modes in field theory can also be reformulated in a canonical manner. This reformulation

[2] Convenient choices for smearing functions in Minkowski spacetime are functions in Schwartz space [156] or functions of compact support sufficiently differentiable [157]). We will restrict to functions of compact support because this will allow us to localize field modes in compact regions.

resembles more to the example of N harmonic oscillators. We will use it in the following sections to quantify entanglement in field theory by borrowing standard techniques from continuous variable quantum mechanics. In the canonical picture, linear observables in field theory are of the form

$$\hat{O}_{\vec{v}} := v_\alpha \hat{r}^\alpha = \int_{\Sigma_t} d^D x \left(f(\vec{x})\, \hat{\phi}(\vec{x}, t) + g(\vec{x})\, \hat{\pi}(\vec{x}, t) \right), \tag{6.9}$$

where the integral is restricted to a Cauchy hypersurface Σ_t of a $D+1$-dimensional Minkowski spacetime, which for simplicity in this paper will be chosen to be a hypersurface defined by a constant value of the time coordinate t of any arbitrary inertial frame—although nothing will change in the discussion if we use a more complicated choice. In this case, the functions $f(\vec{x})$ and $g(\vec{x})$ are compactly supported in a region R of such Cauchy t =constant hypersurface, and $\hat{\pi}(\vec{x}, t) := \frac{d}{dt}\hat{\phi}(\vec{x}, t)$. As for the example of harmonic oscillators, we can identify $v_\alpha = (f(\vec{x}), g(\vec{x}))$ with elements of the dual phase space Γ^*, and $\hat{r}^\alpha = (\hat{\phi}(\vec{x}, t), \hat{\pi}(\vec{x}, t))$ as the basis of "observables". [3] The greek indices α in $v_\alpha \hat{r}^\alpha$ indicate summation over the $1, 2$ components and integration over the spatial coordinates $\vec{x}$. Note that operators defined from pairs of the form $(f(\vec{x}), 0)$ are called pure field operators; similarly, pairs of the form $(0, g(\vec{x}))$ are called pure momentum operators.

The commutation relations for two operators defined by $v_\alpha = (f(\vec{x}), g(\vec{x}))$ and $v'_\alpha = (f'(\vec{x}), g'(\vec{x}))$ are given by the symplectic product of the smearing functions

$$[\hat{O}_{\vec{v}}, \hat{O}_{\vec{v}'}] = i\, \Omega^{\alpha\beta} v_\alpha v'_\beta = i \int_t d^D x \; (f g' - g f'), \tag{6.10}$$

where we have used

$$\Omega^{\alpha\beta} = \begin{pmatrix} 0 & 1 \\ -1 & 0 \end{pmatrix} \delta(\vec{x} - \vec{x}'). \tag{6.11}$$

In this context, independent modes of the system that are localized in a region of space R are selected by choosing two pairs of functions (f, g) and (f', g') supported within R and such that the commutator in (6.10) is different from zero. This is the way we will define localized field modes in the following.

For completeness, we will end up this section by stressing the relation between the covariant and canonical pictures in non interacting theories. This can

[3] Remember that these are operator valued distributions. They are well-defined observables when we smeared them with the functions of compact support

be expressed through a mapping between functions F of compact support in spacetime and pairs of functions (f, g) that are compactly supported in space (for additional details, refer to [158, 159, 9]). This mapping will be given by the commutator bidistribution $\Delta(x, x')$ which satisfies the field equations in both of its variables. Consequently, by integrating the x' dependence of Δ with the function F, we obtain a solution to the field equations, denoted as

$$s(x) := \int dV \Delta(x, x') F(x') \,.$$

Extracting the Cauchy data from $s(x)$ corresponding to a hypersurface with constant time t, and defining

$$f(\vec{x}) = s(\vec{x}, t) \quad \text{and} \quad g(\vec{x}) = \frac{d}{dt} s(\vec{x}, t) \,,$$

we establish a correspondence $F(x) \to (f(\vec{x}), g(\vec{x}))$. This, in turn, defines a mapping $\hat{\phi}[F] \to \hat{O}_{f,g}$ between operators smeared in spacetime and operators smeared in space. This mapping is surjective but not invertible. The reason lies in the fact that the operator-valued distribution $\hat{\phi}[x]$ has a kernel, characterized by functions of the form $(\Box - m^2)G$, where G is a function with compact support in spacetime. In other words, $\hat{\phi}(x)$ smeared with $(\Box - m^2)G$ yields zero for all G. In transitioning to the canonical formulation, this kernel is conveniently eliminated by the mapping $F(x) \to (f(\vec{x}), g(\vec{x}))$ defined by $\Delta(x, x')$ since Δ shares the same kernel as $\hat{\phi}(x)$. Consequently, while the mapping $F \to \hat{\phi}_F$ possesses a kernel, implying that different smearing functions may not necessarily define distinct operators, the mapping $(f, g) \to \hat{O}_{f,g}$ is faithful. Note that this map preserves the commutation relations due to the properties of Δ, ensuring that $\Delta(F, F')$ is mapped to $\Omega((f, g), (f', g'))$ (see [158] for a concise proof).

6.2 Finite dimensional systems and reduced states

Now, let's consider a finite collection of independent modes of the field. These modes are characterized by a set of $2N$ operators $\hat{O}^i$, which can be easily normalized to satisfy the commutation relation

$$[\hat{O}^i, \hat{O}^j] = i\, \Omega^{ij}.$$

The algebra generated by these observables is isomorphic to the algebra of a quantum mechanical system featuring N harmonic oscillators. Mathematically, the associated Weyl algebra corresponds to a type I von Neumann algebra.

Therefore, by focusing on such a finite set of modes, we effectively navigate away from the inherent complexities of field theories. In this context, we find ourselves within the realm of standard quantum mechanics, enabling the definition of reduced states, entropies, and entanglement. From a physical standpoint, we can see this N-dimensional subsystem as encapsulating the degrees of freedom that a specific experimentalist might have the capability to measure.

In this section we review how to define the *reduce quantum state* for a finite set of modes in a *Gaussian state* and how to compute the *entanglement entropy* for the reduced state. In particular we will focus on the vacuum state of a field theory (see [160, 161] for previous similar calculations); the generalization to other Gaussian states is straightforward. In the vacuum state of a QFT, the reduced state obtained by considering a finite set of *physically acceptable* observables describing subsystems localized within a compact region of space is always a mixed state [46, 47, 55]. We will confirm this idea with different examples.

Given an arbitrary state $\hat{\rho}$ in the full theory, the task of finding the reduced state for a subsystem of N modes is complicated. However, there is a significant simplification when $\hat{\rho}$ is a Gaussian state. A Gaussian state within field theory finds complete and unique characterization through its one- and two-point distributions, denoted as $\langle\hat{\phi}(x)\rangle$ and $\langle\hat{\phi}(x)\hat{\phi}(x')\rangle$, respectively. The first and second moments for any field mode can be derived by smearing these distributions. In the case of the vacuum state, the one-point distribution is uniformly zero. Higher-order correlators can be obtained systematically from $\langle\hat{\phi}(x)\hat{\phi}(x')\rangle$. It's noteworthy that the reduced state of a Gaussian state maintains its Gaussian nature. Therefore, for a N-mode subsystem, the characterization of the reduced quantum state is fully encapsulated by the expectations $\langle\hat{O}^i\rangle$ and $\langle\hat{O}^i\hat{O}^j\rangle$. In the vacuum state, $\langle\hat{O}^i\rangle$ is zero for all i. Consequently, characterizing the reduced quantum state for our subsystem boils down to the computation of second moments $\langle\hat{O}^i\hat{O}^j\rangle$.

Additionally, we can dissect the second moments into their symmetric and antisymmetric components:

$$\langle 0|\hat{O}^i\hat{O}^j|0\rangle = \frac{1}{2}\,\langle 0|\{\hat{O}^i,\hat{O}^j\}|0\rangle + \frac{1}{2}\,\langle 0|[\hat{O}^i,\hat{O}^j]|0\rangle\,,$$

where curly brackets denote the standard anticommutator. Notably, the antisymmetric part, the commutator, equates to $i\,\Omega^{ij}$ and is independent of the state.

Consequently, all relevant information about the reduced state is encoded in the anticommutator part, commonly referred to as the *covariance matrix* of the reduced state:

$$\sigma^{ij} := \langle 0|\{\hat{O}^i, \hat{O}^j\}|0\rangle\,. \tag{6.12}$$

Therefore, the computation of the reduced state of an N-mode subsystem in the vacuum state simplifies to evaluating the covariance matrix σ. This matrix completely and uniquely characterizes the reduced state.

Some interesting features of the reduced state can be conveniently derived from the covariance matrix σ in an elegant manner. One notable example is Heisenberg's uncertainty principle, which manifests itself in the positivity semidefiniteness of the matrix $\sigma + i\Omega$. This positivity condition is expressed as $(\sigma^{ij} + i\,\Omega^{ij})\bar{v}_i v_j \geq 0$ for all $v_i \in \mathbb{C}^{2N}$. It is useful to introduce the $N \times N$ matrix

$$J^i_j = \sigma^{ik}\Omega_{kj}\,.$$

As a consequence of $\sigma + i\Omega \geq 0$, the matrix iJ^i_j has real eigenvalues which appear in pairs of opposite sign and magnitude equal or larger than one:

$$\mathrm{Eig}\,(\mathrm{i}J) = \pm\nu_I, \quad \text{with} \quad \nu_I \geq 1 \quad \text{and} \quad I = 1, \ldots, N \tag{6.13}$$

The eigenvalues ν_I, are called *symplectic eigenvalues.* The reduced state is pure if and only if the symplectic eigenvalues are all ± 1 (in this case, the pair $(\sigma^{ij}, \Omega_{ij})$ establishes a Kähler structure in a subspace of the classical phase space [159, 162]). We will employ this criterion to verify that all the reduced states derived from the Minkowski vacuum are indeed mixed.

The information encapsulated in the covariance matrix σ can be described by its *symplectic eigenvalues.* Numerous quantities of interest can be easily extracted from them. For instance, the von Neumann entropy of the reduced state, denoted as $S[\boldsymbol{\sigma}]$, is given by the expression [163]:

$$S[\boldsymbol{\sigma}] = \sum_I^N \left[\left(\frac{\nu_I + 1}{2}\right)\log_2\left(\frac{\nu_I + 1}{2}\right) - \left(\frac{\nu_I - 1}{2}\right)\log_2\left(\frac{\nu_I - 1}{2}\right)\right]\,. \tag{6.14}$$

This formula provides a clear and concise representation of the von Neumann entropy in terms of the symplectic eigenvalues, enabling a straightforward computation of the entropy from the covariance matrix σ.

6.3 Correlations and entanglement between a finite set of degrees of freedom

Let us consider two subsystems A and B made of N_A and N_B modes, respectively. In the following chapter, we will compute correlations and entanglement between them for different configurations. The correlations between concrete pairs of observables $\hat{O}^i$ and $\hat{O}^j$ can be computed straightforwardly from the covariance matrix (6.12). On the other hand, the total amount of correlations between the two subsystems can be quantified by means of the *mutual information* $\mathcal{I}(A,B)$, given by

$$\mathcal{I}(A,B) = S_A + S_B - S_{AB}\,, \tag{6.15}$$

where S_A, S_B, and S_{AB} are the von Neumann entropies of subsystems A, B and the joined system AB, respectively. With different examples we will check that the mutual information is different from zero in field theory, since correlations are ubiquitous in QFT. Nevertheless, it is important to emphasise that nonzero mutual information $\mathcal{I}(A,B)$ *does not* imply that the two subsystems are entangled. This is because $\mathcal{I}(A,B)$ quantifies all correlations, both of classical and quantum origins. To evaluate whether the subsystems are entangled, we need to go beyond mutual information.

Evaluating entanglement in quantum field theory between arbitrary subsystems is a subtle issue. The difficulty arises from the infinite number of degrees of freedom each subsystem may have. Note that entanglement entropy is not useful in this situation. Entanglement entropy is only a faithful quantifier for entanglement between A and B if the joined system AB is in a pure state. This is not the case in QFT if A and B are made of modes compactly supported in space.

Quantifying entanglement for mixed states is a subtle problem, and in general there is not a simple necessary and sufficient criterion for entanglement. In some restricted situations that we will study, there is a necessary and sufficient criterion for entanglement given by a non-zero value of the Logarithmic negativity. The logarithmic negativity (LN), denoted as $E_{\mathcal{N}}$, serves as a easily-computable measure of entanglement for both pure and mixed states [164, 165]. A nonzero LN value indicates a violation of the positivity of partial transpose (PPT) criterion [165], establishing it as a sufficient condition for entanglement in general quantum states, although not necessary. Notably, for Gaussian states with one subsystem consisting of a single mode, irrespective of the size of the other subsystem, LN is nonzero *if and only if* the state is entangled. Moreover, under these specific conditions, LN acts as a faithful quantifier of entanglement, meaning that a higher LN corresponds to a greater degree of entanglement [163]. [4]

The logarithmic negativity (LN) provides a direct measure of entanglement for Gaussian quantum states, particularly when expressed in terms of their covariance matrix. Let's consider a Gaussian state $\hat{\rho}$ with $N_A + N_B$ modes in a bipartite system, denoted by the covariance matrix σ_{AB}, where N_A and N_B are the mode counts in each subsystem. The computation of LN for this bipartition involves evaluating the expression:

$$E_{\mathcal{N}} = \sum_{J=1}^{N_A+N_B} \max\{0, -\log_2 \tilde{\nu}_J\}, \tag{6.16}$$

where $\tilde{\nu}_J$ represents the symplectic eigenvalues of $\tilde{\sigma}$. This $\tilde{\sigma}$ is obtained by applying the operation defined as

$$\widetilde{\sigma}_{AB} = \boldsymbol{T}\sigma_{AB}\boldsymbol{T}, \tag{6.17}$$

where $\boldsymbol{T}$ is a block matrix given by $\mathbb{I}_{2N_A} \oplus \boldsymbol{\Sigma}_{N_B}$, and $\boldsymbol{\Sigma}_{N_B}$ is a direct sum of N_B 2×2 Pauli-z matrices.

Understanding the relation between LN and the PPT criterion involves recognizing that $\tilde{\sigma}$ corresponds to the covariance matrix of the partially transposed density matrix $\hat{\rho}^{\top_B}$. This partial transposition is performed exclusively in the B subsystem. The nonpositivity of $\hat{\rho}^{\top_B}$ implies that some symplectic eigenvalues $\tilde{\nu}_I$ are less than 1, resulting in $E_{\mathcal{N}} > 1$ as detailed in, for instance, Ref. [163]. Therefore, having $(\tilde{\nu}_I < 1)$ is a sufficient condition for entanglement.

In the following sections, we will present the main results were we have computed correlations and entanglement between different subsystems A and B. We will analyze how entanglement varies with the space dimensionality, the distance and the number of modes per subsystem. We will mostly use the LN

[4]The LN is a lower bound for the entanglement that can be distilled from the system via local operations and classical communications. For Gaussian quantum states, the value of the LN has an operational meaning as the exact cost (where the cost is measured in Bell pairs or entangled bits) that is required to prepare or simulate the quantum state under consideration [166, 167]

in situations in which it is a necessary and sufficient condition (that is, when $N_A = 1$). Nevertheless, we will also analyze the LN of bipartitions of “many versus many” modes. This is also of interest since $E_{\mathcal{N}} > 0$ is always a sufficient condition for entanglement; although in this case it is not necessary, so $E_{\mathcal{N}} = 0$ does not imply the absence of entanglement. In any case, since the LN is a lower bound for distillable entanglement, $E_{\mathcal{N}} = 0$ indicates that whatever entanglement may be contained in the system cannot be distilled.

Chapter 7

Entanglement in real space in QFT between finite degrees of freedom

Entanglement has been extensively explored in QFT mostly by using the entanglement entropy linked to a spatial region R [168]. This quantity has been influential in various theoretical physics realms, ranging from black holes [152, 151, 150, 149] to the quantum nature of spacetime [169, 170, 153]. However, this entropy comes with challenges—it is intrinsically divergent and requires regularization to obtain a finite value, a process which introduces ambiguities. Additionally, the Hilbert space of the field theory can *not* be written in the form $\mathcal{H}_R \otimes \mathcal{H}_{\bar{R}}$, with $\mathcal{H}_R$ the Hilbert space of all the field degrees of freedom within region R and $\mathcal{H}_{\bar{R}}$ the field degrees of freedom for the complementary region $\bar{R}$. This implies that one is outside the standard realm to define entanglement in quantum mechanics. This makes unclear how to interpret the entropy in terms of entanglement between region R and its complement [47].

On the other hand, based on the Reeh-Schlieder theorem [25], it can be demonstrated that the field degrees of freedom within two separate compact regions, R_A and R_B, are entangled when they are separated from each other. The Reeh-Schlieder property ensures that this entanglement is finite [46, 47]. Even more, given a fixed field mode B compactly supported in a region R_B of spacetime, if we choose an arbitrary compact region R_A separated from the first, the Reeh-Schlieder theorem guarantees that there is at least one mode A within region R_A that is entangled to the fixed mode B in region R_B, when the field is in the vacuum state [47].

Motivated by the previous statements related to the Reeh-Schlieder theorem, it is usually thought that entanglement is *ubiquitous* in quantum field theory, even if we restrict to finite dimensional subsystems. In particular, it is commonly taken for granted that *any pair* of field degrees of freedom are entangled in the vacuum state. However, the theorem does not tell us how many modes in R_A are entangled with the fixed mode B, or how complicated such modes are. Since region R_A hosts infinitely many modes, the belief that any pair of modes, one in R_A and one in R_B, are entangled in the vacuum is an (unjustified) extrapolation of the actual content of the Reeh-Schlieder theorem.

In this chapter we will carefully analyze the entanglement content between a finite set of modes supported in disjoint regions of space for a free scalar field in Minkowski spacetime. We will do this by smearing field and conjugate momenta with functions compactly supported in a region where we define a mode. The smearing function can be intuitively thought of as defining a "pixel" of the field theory: the support of the smearing determines the size of the pixel, corresponding to the maximum resolution of a detector, while the shape of the smearing function determines the resolution of the detector within the pixel.

The main advantage of this strategy is that, given any two regions containing N_A and N_B degrees of freedom, respectively, one can use standard techniques from quantum mechanics to quantify correlations and entanglement. All the difficulties and subtleties intrinsic to quantum field theory are removed. In particular, the calculations do not contain the divergences that plague the calculation of the geometric entanglement entropy associated with a region in quantum field theory. A similar strategy has been used before in [171, 172, 160, 173, 161] to evaluate mutual information, entropy, quantum discord, and to search for violations of a type of Bell inequalities, with interesting applications in cosmology (see also [174]).

Following this proposal, we will see that it is difficult to find pairs of modes supported in disjoint regions of space separated by a nonzero distance that are entangled. The difficulty increases with the dimensionality of space. Namely, in $D = 1$ it is relatively easy to find pairs of such modes which are entangled, but this task becomes increasingly challenging for $D \geq 2$. In fact, we find that the regions of support of two modes need to be carefully chosen to find any entanglement for $D \geq 2$.

The rest of the chapter is organized in the following way: In section 7.1 we will present the family of modes that we will mostly consider in the rest of the chapter, then we will compute the mutual information and the logarithmic negativity between two modes located in disjoint regions of space. In section. 7.1.2 we will analyse entanglement between a mode supported within a sphere and another mode supported within a spherical shell surrounding the first. Finally, in section 7.2 we will compute logarithmic negativity for configurations where we increase the number of modes in one or both subsystems.

7.1 Correlations and Entanglement for two degrees of freedom

In this section, we apply the formalism introduced in chapter 6 to a straightforward yet illustrative scenario: two modes supported in spatially disjoint regions, each characterized by a pure field and a pure momentum operator. Our analysis includes the assessment of correlations, entropy, mutual information, and entanglement between these two modes. We will mainly focus on modes defined by smearing field and momentum operators on a *non-negative* function of compact support (see Fig. 7.1 and (7.1)), hence giving an observational and operational motivation to the selected modes. For massless fields, we select a family of functions which allows us to derive analytical expressions in any spatial dimension $D > 1$. However, the $D = 1$ case demands special attention due to potential infrared divergences, requiring the introduction of mass, which we handle through numerical solutions.

The main results of this section are that for two modes, each supported in a spherical region of D spatial dimensions, surprisingly, there is no entanglement

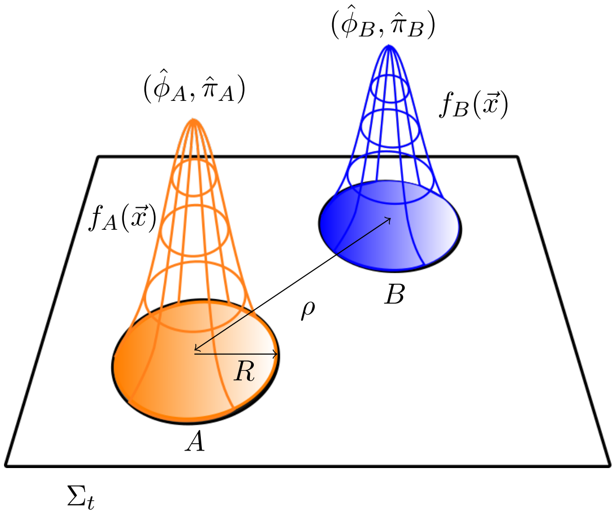

Figure 7.1: Illustration of two spacelike separated balls of radius R in a t=constant Cauchy hypersurface in $D+1$-dimensional Minkowski spacetime. A function $f_{A(B)}(\vec{x})$ compactly supported in region A (B) defines a single field-mode $(\hat{\phi}_{A(B)}, \hat{\pi}_{A(B)})$.

for $D > 1$. On the contrary, for a mode A supported in a sphere in D-spatial dimensions and a mode B supported in a shell surrounding the sphere, we can find entanglement between the two modes. These results contain a valuable message: entanglement in quantum field theory can be found in pairs of disjoint and compactly supported modes, but one needs to carefully choose their spatial configuration. This is in consonance with recent results in [175], which indicate that the entanglement between the modes supported in the spherical region and the surrounding shell is largely concentrated in modes sharply supported near the boundaries.

7.1.1 Entanglement between two spherical configurations in D-dimensions

We consider two D dimensional balls, A and B, with radius R in a $D+1$-dimensional Minkowski spacetime, and let ρ be the distance between their centers in units of R. The balls are assumed to be disjoint so that $\rho > 2$ (see Fig. 7.1). We explore two modes, each localized within the distinct regions A and B. Let's define these modes explicitly. The mode in region A is characterized by a pair of noncommuting operators given by

$$\begin{aligned}
\hat{\phi}_A &:= \int \mathrm{d}^D x \, f_A(\vec{x}) \, \hat{\phi}(\vec{x}) \, , \\
\hat{\pi}_A &:= c \int \mathrm{d}^D x \, f_A(\vec{x}) \, \hat{\pi}(\vec{x}) \, .
\end{aligned} \tag{7.1}$$

Here, $f_A(\vec{x})$ represents a function with compact support in region A, and c is an arbitrary constant with dimensions of inverse energy (entanglement between the two subsystems will not depend on the specific value of c, because changing c is equivalent to perform a locally symplectic transformation, which leaves entanglement invariant). In this section, we use the notation $(\hat{\phi}_A, \hat{\pi}_A)$ to represent the pair of noncommuting operators defining the modes of interest. This choice is distinct from the notation $(\hat{O}^1_A, \hat{O}^2_A)$ used in the previous section, highlighting that, in this case, we specifically select a pure field and pure momentum operators, respectively. The mode in region B is similarly defined using a function $f_B(\vec{x})$ with compact support in region B.

In this section, we will use the following one-parameter family of *non-negative* functions for $f_i(\vec{x})$, $i = A, B$

$$f_i^{(\delta)}(\vec{x}) = A_\delta \, \left(1 - \frac{|\vec{x} - \vec{x}_i|^2}{R^2}\right)^\delta \, \Theta\left(1 - \frac{|\vec{x} - \vec{x}_i|}{R}\right) \, , \tag{7.2}$$

where $\vec{x}_i$ is the center of the ball i, and $\Theta(x)$ is the Heaviside step function—this ensures that $f_i^{(\delta)}(\vec{x})$ is compactly supported within a ball of radius R centered at $\vec{x}_i$; A_δ is a normalization constant. The parameter δ determines the differentiability class of $f_i^{(\delta)}(\vec{x})$. For example, for $\delta = 0$, $f_i^{(\delta)}(\vec{x})$ reduces to the Heaviside function, which is discontinuous. For $\delta = 1$, the function is continuous, but its first derivative is not. The differentiability class of $f_i^{(\delta)}(\vec{x})$ is $C^{\delta-1}$ for integer δ. In order for the smeared operators $\hat{\phi}_i$ and $\hat{\pi}_i$ to be well defined, it suffices to choose $\delta \geq 1$. This is because for these values the field and momentum self-correlations will be bounded functions of δ. Fig. 7.2 shows the shape of $f_i^{(\delta)}(\vec{x})$ for different values of δ.

The main advantage of this family of smearing functions is that their Fourier transform has a simple expression in terms of Bessel functions in any spatial dimension D (see Appendix C) and we can obtain analytical expressions for the correlations and entanglement. In the following sections we will also consider

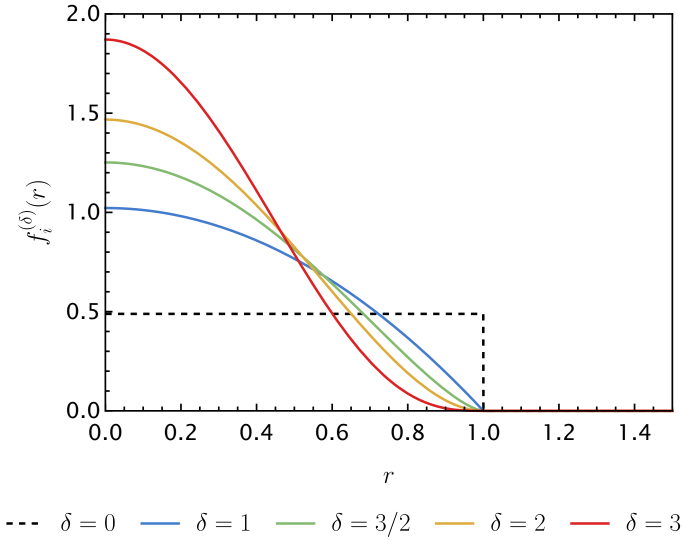

Figure 7.2: Shape of the smearing functions $f_i^{(\delta)}(\vec{x})$, centered at x_i for a different values of δ. Plotted as a function of the dimensionless radial coordinates $r := |\vec{x} - \vec{x}_i|/R$. Note that the larger δ is, the less support $f_i^{(\delta)}$ has near the boundary.

other families of smearing functions. The results are qualitatively similar, although in those cases we perform calculations numerically.

The commutator between the four operators ϕ_i, π_i, with $i = A, B$ are

$$\begin{aligned} [\hat{\phi}_A, \hat{\phi}_B] &= [\hat{\pi}_A, \hat{\pi}_B] = 0 \\ [\hat{\phi}_A, \hat{\pi}_B] &= [\hat{\phi}_B, \hat{\pi}_A] = i\, c \int d^D x\, f_A^{(\delta)}\, f_B^{(\delta)} = 0\,. \end{aligned} \tag{7.3}$$

The last integral vanishes because $f_A^{(\delta)}(\vec{x})$ and $f_B^{(\delta)}(\vec{x})$ are supported in disjoint regions. On the other hand,

$$[\hat{\phi}_i, \hat{\pi}_i] = i\, c \int d^D x\, (f_i^{(\delta)})^2 \neq 0\,, \quad i = A, B. \tag{7.4}$$

We fix the (dimensionful) constant A_δ in the definition of $f_i^{(\delta)}$ by demanding that $[\hat{\phi}_i, \hat{\pi}_i] = i$. This implies that

$$A_\delta = c^{-1/2}\, R^{-D/2} \pi^{-D/4} \sqrt{\frac{\Gamma(1 + D/2 + 2\delta)}{\Gamma(1 + 2\delta)}}\,. \tag{7.5}$$

The vacuum expectation values of symmetrized products of $\hat{\phi}_i$ and $\hat{\pi}_i$ are sufficient to construct the covariance matrix of the reduced state. It is easy to check that

$\langle\{\hat{\phi}_i, \hat{\pi}_j\}\rangle = 0$ and that $\langle\hat{\phi}_A\rangle = \langle\hat{\phi}_B\rangle =: \langle\hat{\phi}\rangle = 0$ (we are using the same smearing function in both regions) and $\langle\hat{\pi}_A\rangle = \langle\hat{\pi}_B\rangle =: \langle\hat{\pi}\rangle = 0$ in the Minkowski vacuum. The covariance matrix of the total system takes the general form

$$\sigma_{AB} = \begin{pmatrix} \sigma_A^{\text{red}} & C \\ C^T & \sigma_B^{\text{red}} \end{pmatrix} , \tag{7.6}$$

where

$$\sigma_A^{\text{red}} = \sigma_B^{\text{red}} = 2 \begin{pmatrix} \langle\hat{\phi}^2\rangle & 0 \\ 0 & \langle\hat{\pi}^2\rangle \end{pmatrix} , \tag{7.7}$$

is the covariance matrix of each reduced state , and $C = \text{diag}(\langle\{\hat{\phi}_A, \hat{\phi}_B\}\rangle \,, \langle\{\hat{\pi}_A, \hat{\pi}_B\}\rangle)$ describes the cross correlations between the subsystems. When the field is massless and for $D > 1$, we obtain (see Appendix C)

$$\langle\{\hat{\phi}_i, \hat{\phi}_j\}\rangle = 2\, N_\delta^2\, \frac{R}{c} \begin{cases} \mathcal{J}^D(-1,\delta) & i = j \\ \mathcal{L}^D(-1,\delta,\rho) & i \neq j \end{cases} , \tag{7.8}$$

$$\langle\{\hat{\pi}_i, \hat{\pi}_j\}\rangle = 2 N_\delta^2\, \frac{c}{R} \begin{cases} \mathcal{J}^D(1,\delta) & i = j \\ \mathcal{L}^D(1,\delta,\rho) & i \neq j \end{cases} , \tag{7.9}$$

where

$$\mathcal{J}^D(\lambda,\delta) = 2^{-1-2\delta+\lambda} \frac{\Gamma\left(\frac{D+\lambda}{2}\right)\Gamma\left(1+2\delta-\lambda\right)}{\Gamma\left(1+\delta-\frac{\lambda}{2}\right)^2 \Gamma\left(\frac{D-\lambda}{2}+2\delta+1\right)} , \tag{7.10}$$

$$\begin{aligned} \mathcal{L}^D(\lambda,\delta,\rho) =& \rho^{-(D+\lambda)} \frac{\Gamma\left(\frac{D+\lambda}{2}\right)\Gamma\left(D/2\right)}{2^{1+2\delta-\lambda}\Gamma\left(\frac{D}{2}+1+\delta\right)^2 \Gamma\left(-\frac{\lambda}{2}\right)} \times \\ & {}_3F_2 \left[\begin{matrix} 1+\frac{\lambda}{2}, \frac{D+\lambda}{2}, \frac{D+1}{2}+\delta \\ \frac{D}{2}+1+\delta, D+1+2\delta \end{matrix} ; \frac{4}{\rho^2} \right] , \end{aligned} \tag{7.11}$$

and

$$N_\delta^2 = \frac{2^{2\delta}\Gamma\left(1+\frac{D}{2}+2\delta\right)\Gamma\left(1+\delta\right)^2}{\Gamma\left(1+2\delta\right)\Gamma\left(D/2\right)} . \tag{7.12}$$

It is interesting to remark that, the field and momentum self-correlations are positive and bounded functions of δ for $\delta \geq 1$ (for $\delta = 0$, the momentum self-correlations diverge). On the other hand, these expressions show that the correlations between both modes behave, for large separations $\rho \gg 1$, as

$$\langle\{\hat{\phi}_A, \hat{\phi}_B\}\rangle = \rho^{-(D-1)} \frac{R}{c} \Big(u(\delta, D) + \mathcal{O}(\rho^{-2}) \Big) , \tag{7.13}$$

and

$$\langle\{\hat{\pi}_A, \hat{\pi}_B\}\rangle = -\rho^{-(D+1)}\frac{c}{R}\left(v(\delta, D) + \mathcal{O}(\rho^{-2})\right), \tag{7.14}$$

for $D > 1$, where

$$u(\delta, D) = \frac{2^{-2\delta-1}\Gamma\left(\frac{D-1}{2}\right)\Gamma(\delta+1)\Gamma\left(\frac{1}{2}(D+4\delta+2)\right)}{\Gamma\left(\delta+\frac{1}{2}\right)\Gamma\left(\frac{D}{2}+\delta+1\right)^2}$$

and

$$v(\delta, D) = \frac{2^{-2\delta}\delta\Gamma\left(\frac{D+1}{2}\right)\Gamma(\delta)\Gamma\left(\frac{1}{2}(D+4\delta+2)\right)}{\Gamma\left(\delta+\frac{1}{2}\right)\Gamma\left(\frac{D}{2}+\delta+1\right)^2}$$

are positive functions[1] that depend on δ and the spacetime dimension. We can evaluate from the expression how the correlations decay with the distance. This decaying behaviour has the expected dependence with the dimensionality of space, $\langle\{\hat{\phi}_A, \hat{\phi}_B\}\rangle \sim \rho^{-(D-1)}$ and $\langle\{\hat{\pi}_A, \hat{\pi}_B\}\rangle \sim -\rho^{-(D+1)}$ (See Fig. 7.3) , thus providing a good check to the above expressions.

Once we have calculated all correlations and constructed the total and reduced covariance matrices of systems A and B, we are in position to evaluate entanglement using logarithmic negativity between these degrees of freedom. However, before analysing the entanglement between these modes it is interesting to compute the von Neumann entropy for the reduced states, defined in (6.14) and the mutual information, defined in (6.15), which describes all existent correlations (classical and quantum) between the modes A and B.

Von Neumann entropy

To compute the von Neumann entropies of the reduced states for mode A and mode B, expression (6.14),

$$S[\boldsymbol{\sigma}] = \sum_{I}^{N}\left[\left(\frac{\nu_I+1}{2}\right)\log_2\left(\frac{\nu_I+1}{2}\right) - \left(\frac{\nu_I-1}{2}\right)\log_2\left(\frac{\nu_I-1}{2}\right)\right]. \tag{7.15}$$

[1] The correlator $\langle\{\hat{\pi}_A, \hat{\pi}_B\}\rangle$ is, therefore, negative. This, in turn, implies that the submatrix C of σ_{AB} is negative, even for positive definite smearing functions. Consequently, the covariance matrix σ_{AB} in (7.6) describes a Gaussian state which is not manifestly separable, according to Simon's separability criterion [176]. Additional calculations are needed to show that this state is indeed separable.

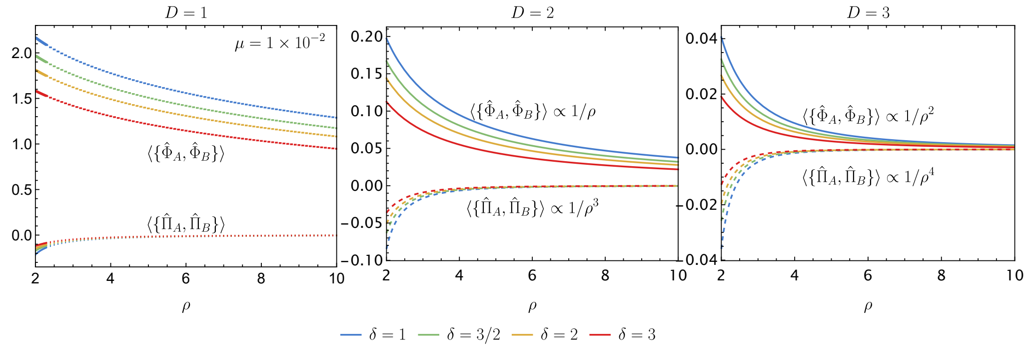

Figure 7.3: Correlations between two field modes versus the dimensionless distance between the centers of the spherical regions where each mode is supported. $\rho = 2$ corresponds to the two regions touching each other. The plots for $D = 2$ and $D = 3$ describe the correlations of a massless field and are obtained analytically, while for $D = 1$ we introduce a small mass $\mu = mR = 10^{-2}$ to avoid infrared divergences, and compute the correlations numerically. Correlations depend on the details of the smearing functions, particularly on the value of the parameter δ. On the other hand, at large separations the fall-off behavior of all correlations is as expected.

shows that all we need to compute is the symplectic eigenvalues of σ_A^{red} and σ_B^{red}. When the field is in the Minkowski vacuum, $\sigma_A^{\text{red}} = \sigma_B^{\text{red}}$, so their entropies are identical. Using the form of σ_A^{red} given in (7.7), this symplectic eigenvalue is, for $D > 1$,

$$\nu_A = 2\sqrt{\langle\hat{\phi}^2\rangle\,\langle\hat{\pi}^2\rangle} = \frac{\Gamma(\delta+1)^2\Gamma\left(\frac{D}{2}+2\delta+1\right)\sqrt{\frac{\Gamma\left(\frac{D-1}{2}\right)\Gamma\left(\frac{D+1}{2}\right)\Gamma(2\delta)\Gamma(2\delta+2)}{\Gamma\left(\frac{1}{2}(D+4\delta+1)\right)\Gamma\left(\frac{1}{2}(D+4\delta+3)\right)}}}{\Gamma\left(\frac{D}{2}\right)\Gamma\left(\delta+\frac{1}{2}\right)\Gamma\left(\delta+\frac{3}{2}\right)\Gamma(2\delta+1)}. \tag{7.16}$$

This quantity is larger than 1. This confirms that the reduced state corresponding to mode A is a mixed quantum state [161, 47], and equivalently for mode B, since $\nu_A = \nu_B$. From this, we obtain an analytical expression for S_A, which we plot in Fig. 7.4.

As for the case of correlation we observe that the entropy S_A depends on the smearing function characterized by δ. In particular, the larger δ is, the smaller the entropy is. Larger δ corresponds to smearing functions with more weight around the center of the region and less support close to the boundary. In other

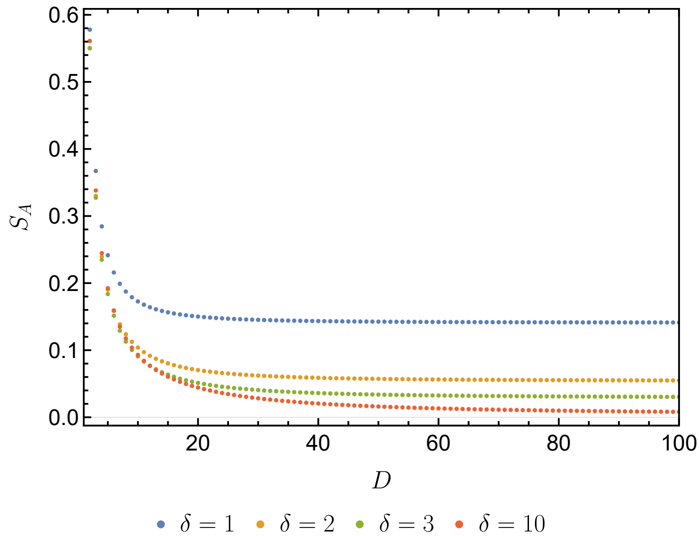

Figure 7.4: The von Neumann entropy S_A of a single mode as a function of the dimension of space D and different values of δ.

words, we find that modes supported closer to the boundary have larger entropy.

Mutual information

Mutual information is defined by (6.15)

$$\mathcal{I}(A, B) = S_A + S_B - S_{AB} \,. \tag{7.17}$$

From this expression, we see that the left ingredient needed to compute mutual information is the von Neumann entropy S_{AB} of the joined system AB. This quantity can also be obtained analytically for $D > 1$, by plugging in Eq. (6.14) the form of the two symplectic eigenvalues of σ_{AB}:

$$\nu_\pm = \sqrt{(2\,\langle\hat{\phi}^2\rangle \pm \langle\{\hat{\phi}_A, \hat{\phi}_B\}\rangle)(2\,\langle\hat{\pi}^2\rangle \pm \langle\{\hat{\pi}_A, \hat{\pi}_B\}\rangle)} \,. \tag{7.18}$$

Notice that, although both field and momentum correlations depend on the radius R of the regions where the modes are supported, this dependence cancels out in the combination of correlation functions appearing in (7.18). Consequently, $\nu_\pm$ and quantities derived from it, like mutual information, entropies, and entanglement, remain invariant under rescalings.

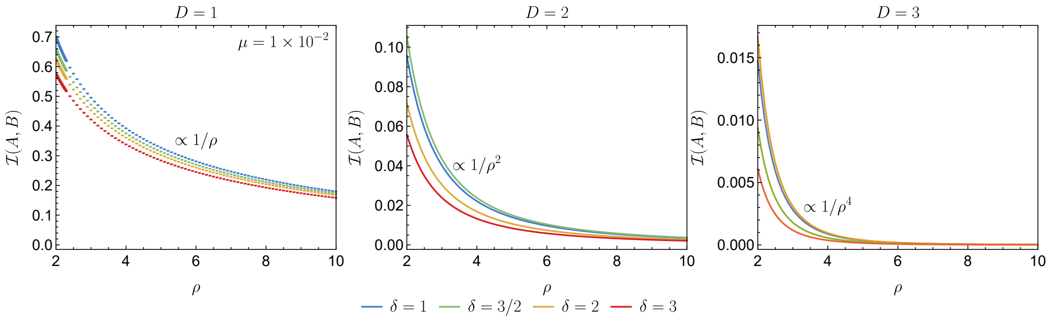

Figure 7.5: Mutual information for two field modes A and B versus the dimensionless distance between the centers of the spherical regions where each mode is supported. $\rho = 2$ corresponds to the two regions touching each other. All plots show that the short-distance behavior of the mutual information depends on the value of the parameter δ. However, at large distances the dependence on δ decreases and the fall-off behavior is as expected.

In Fig. 7.5, we plot the mutual information $\mathcal{I}_{AB}$ versus the distance between the two regions in, for $D = 1$ (left panel), $D = 2$ (middle figure), and when $D = 3$ (right panel), for different values of δ. We observed that, the short-distance behavior ($\rho \gtrsim 2$) changes with the smearing function. However, its long-distance behaviour ($\rho \gg 2$) is given by $\mathcal{I}(A,B) \sim \rho^{-2(D-1)}$ for $D > 1$ This is the expected result, and it is compatible with results obtained previously in [171, 160, 173] for $D = 3$.

The main lesson we learn from this analysis is that, for a fixed distance between the regions supporting two modes, the total correlations (classical and quantum) between them are weaker the larger the dimension D of space is.

Entanglement

As discussed in the preceding chapter, we employ the logarithmic negativity (LN) to assess the presence of entanglement in the correlations between two single modes. The LN, is defined as (6.16),

$$E_{\mathcal{N}} = \sum_{J=1}^{N_A+N_B} \max\{0, -\log_2 \tilde{\nu}_J\}, \tag{7.19}$$

where N_A and N_B are the respective number of modes in subsystem A and B, and $\tilde{\nu}_J$ are the symplectic eigenvalues of $\tilde{\sigma}_{AB}$, the partial transposition of the covariance matrix σ_{AB}. For the two mode covariance matrix, there are two different symplectic eigenvalues of the partially transposed covariance matrix, given by

$$\tilde{\nu}_{\pm} = \sqrt{(2\,\langle\hat{\phi}^2\rangle \pm \langle\{\hat{\phi}_A, \hat{\phi}_B\}\rangle)(2\,\langle\hat{\pi}^2\rangle \mp \langle\{\hat{\pi}_A, \hat{\pi}_B\}\rangle)}\,. \tag{7.20}$$

From (7.19) it is straightforward to see that LN is nonzero only if at least one of these symplectic eigenvalues is less than 1. Comparing this expression with (7.18) and considering that $\langle\{\hat{\pi}_A, \hat{\pi}_B\}\rangle$ is negative while $\langle\{\hat{\phi}_A, \hat{\phi}_B\}\rangle$ is positive for our smearing functions, it follows that $\tilde{\nu}_+ \geq \nu_+$, and $\tilde{\nu}_- \leq \nu_-$ (where $\nu_\pm$ are the symplectic eigenvalues of σ_{AB}). Since both $\nu_\pm$ are greater than 1, only $\tilde{\nu}_-$ can potentially contribute to the LN.

For $D = 1$, we compute the correlation functions numerically, and from this we evaluate $\tilde{\nu}_-$ and the LN, $E_{\mathcal{N}}$. The results are shown in Fig. 7.6 and Fig. 7.7.

Fig. 7.6 shows the LN versus the dimensionless mass μ, for a fixed distance ρ and for different values of δ. Since the LN decreases with ρ, we choose in this plot the minimum possible value of ρ, namely $\rho = 2$. The key insights drawn from this figure are as follows: (1) When $\delta = 1$, the LN is nonzero, indicating that the two modes *are entangled.* (2) For $\delta \geq 1.7$, the LN becomes zero for any mass value μ. This shows the high sensitivity of the LN to the shape of the smearing function. The smearing functions $f^{(\delta)}$ used in this section, with smaller δ, exhibits more support near the region's boundary. Since correlations decrease with distance, modes with greater support near the boundary (δ close to 1) are expected to be more correlated (and entangled) compared to modes defined with $\delta \geq 1$. Figure 7.6 confirms this intuition and additionally shows that the modes are not entangled at all when using $\delta \gtrsim 1.7$. (3) The LN between these two modes is highly responsive to the field's mass. For $\delta = 1$, the LN gets a maximum when $\mu \ll 1$. If we increase the mass, LN decreases rapidly around $\mu \approx 1$, and completely vanishes for $\mu \gtrsim 10$.

On the other hand, Fig. 7.7 shows the way the LN changes with the distance ρ between the centers of the two regions A and B. In Fig. 7.7 we use $\mu = 10^{-2}$, where we know that there is entanglement from Fig. 7.6. We observe that the

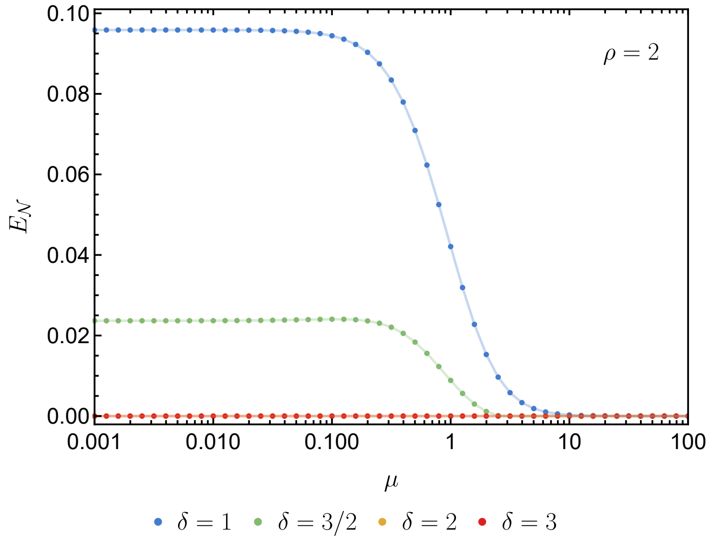

Figure 7.6: LN for $D = 1$ as a function of the dimensionless mass, $\mu = mR$ (R is the radius of the regions of support of modes A and B), when the regions A and B are kept at a fixed dimensionless distance $\rho = 2$. The LN reaches a maximum when $\mu \ll 1$, decreases monotonically, and vanishes when the mass of the field reaches a threshold that depends on the details of the smearing function. The LN is zero for all μ if $\delta \gtrsim 1.7$.

LN decreases rapidly with the distance and completely vanishes beyond $\rho \approx 2.2$ (i.e., when the separation between the boundaries of the two regions is about 20% of their radius). This fall off is much faster than the one we obtained for the mutual information $\mathcal{I}_{AB} \sim \rho^{-1}$.

For spatial dimensions greater than 1, analytical computation of the LN is feasible for massless fields. This is particularly interesting as entanglement is expected to be more prominent when $\mu \to 0$ (as observed earlier). Substituting the correlation function values from (7.8) and (7.9) into the expression (7.20), we find that $\tilde{\nu}_-$ remains greater than 1 for all distances ρ and all values of δ, including $\delta = 1$. Consequently, we derive

$$E_{\mathcal{N}} = 0 \quad \forall\, \delta \geq 1 \text{ and } \forall D > 1\,. \tag{7.21}$$

The observation of less entanglement in $D \geq 2$ compared to $D = 1$ aligns with the notion that correlations are stronger in lower dimensions, as demonstrated in the preceding subsection.

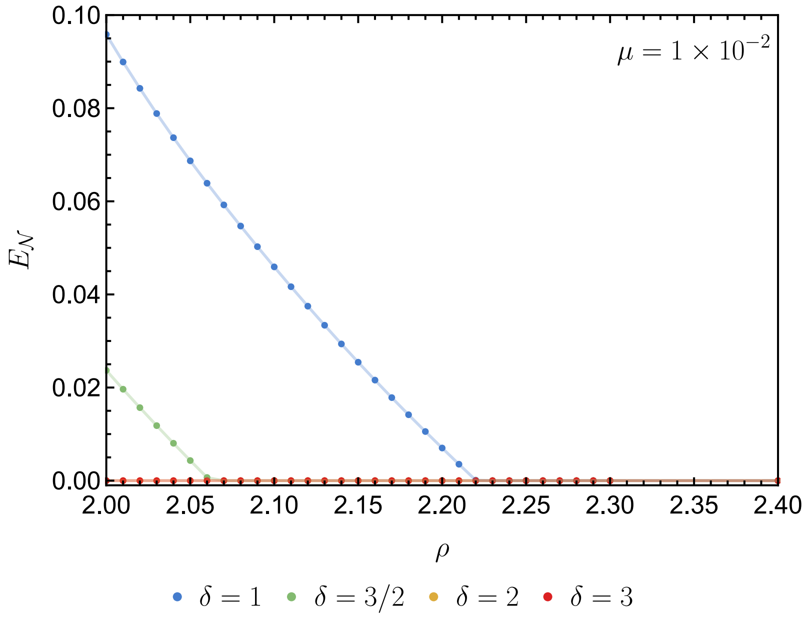

Figure 7.7: LN for $D = 1$ between the two field modes as a function of the dimensionless distance between the centers of the spherical regions where each mode is supported, for a fixed dimensionless mass of the scalar field ($\mu = 10^{-2}$) and for different smearing functions.

In summary, our findings indicate that the correlations quantified by the mutual information in the previous section primarily exhibit classical correlations and not entanglement. For the explored family of modes in this section, only in the specific case of $D = 1$, small mass μ, δ close to 1, and a small separation between the two regions, there is entanglement between the two modes. *In all other scenarios, the reduced state is separable.*

These conclusions are not peculiar to the concrete smearing functions used here. We have generalized our calculations in different directions, by (i) considering other families of smearing functions including some without a definite sign, and (ii) by mixing field and momentum operators. In none of these cases have we found entanglement between subsystems A and B in $D \geq 2$ for pairs of modes supported in disjoint spherical regions.

Other positive semi-definite functions

In addition to the smearing functions introduced in (7.2), we have also analyzed the following families of non-negative smearing functions, all spherically symmetric around a center $\vec{x}_i$ and where r is the distance to the center in units of the radius R of the region of support:

1. $h^{(n)}(r) = A_n \, \Theta(1-r) \cos^n\left(\frac{\pi}{2} r\right), \quad n > 1 \in \mathbb{N},$

   with A_n a normalization constant. This family has been used before in [177].

2. $g(r) = A \, \Theta(1-r) \exp\left(-\frac{1}{1-r^2}\right).$

3. $$w^{(\delta)}(r) = A_\delta \begin{cases} 1 & 0 < r \leq 1 \\ -\frac{1}{\delta}(r-1)+1 & 1 < r \leq 1+\delta \\ 0 & r > 1+\delta \end{cases}.$$

   This family has been used before in [172].

4. $j^{(n)}(r) = A_n \, \Theta(1-r)(1-r^n), \quad n > 1 \in \mathbb{N}.$

All these functions and their first derivatives are continuous ($g(r)$ is actually smooth) this is sufficient for our purposes [157].

Non-semi-positive definite smearing functions

We have considered the following family of L^2-orthonormal functions of compact support,

$$k^{(n)}(r) = \frac{\sin 2\pi n r}{2\pi n r} \Theta(1-r). \tag{7.22}$$

Again, these functions and their first derivatives are continuous. When these functions are used to define modes supported in disjoint regions, we find no entanglement between them.

Combinations of field and momentum

The field modes employed in the calculations outlined in the previous sections were all characterized by pairs of operators comprising a pure-field and a pure-momentum operator, denoted as $(\hat{\Phi}_i, \hat{\Pi}_i)$. These operators were both constructed from the same smearing function, with the exception of an exact factor c in $\hat{\Pi}_i$, which was necessary to ensure that both operators possessed identical units (action).

We extended here these calculations by considering modes defined from (the algebra generated by) pairs of canonically conjugated operators of the following form

$$\hat{O}_A^{(1)} = \frac{1}{\sqrt{2N}} \sum_{i=1}^{N} \left(\hat{\Phi}_A^{(2i-1)} - \hat{\Pi}_A^{(2i)} \right) , \tag{7.23}$$

$$\hat{O}_A^{(2)} = \frac{1}{\sqrt{2N}} \sum_{i=1}^{N} \left(-\hat{\Phi}_A^{(2i-1)} + \hat{\Pi}_A^{(2i)} \right) , \tag{7.24}$$

where $\hat{\Phi}_A^{(n)}$ and $\hat{\Pi}_A^{(n)}$ indicate field and momentum operators, respectively, smeared with the element $k^{(n)}(r)$ of the orthonormal family of functions written in (7.22). Therefore, each of these two operators $\hat{O}_A^{(i)}$ is made by combining pure-field and pure-momentum operators, each constructed from different smearing functions. The orthonormality of the smearing functions $k^{(n)}(r)$ ensures that $\hat{O}_A^{(1)}$ and $\hat{O}_A^{(2)}$ are canonically conjugate.

Subsystem B is similarly defined, with its support within a spherical region as close as possible to that of subsystem A. We have examined various values of N, ranging from 1 to 10 in (7.23), and in none of these case have we found entanglement between the two subsystems.

The analysis in this subsections reveals that the absence of entanglement in $D \geq 2$ between pairs of modes supported in two disjoint spherical regions is not unique to the smearing functions we have chosen, but a rather generic fact. In the following section we show how we can find entanglement between two modes by carefully selecting the regions of support.

7.1.2 Entanglement between sphere-shell configuration in D-dimensions

In this section we evaluate entanglement between a mode A supported in a sphere and a mode B supported in a shell surrounding the sphere. The motivation for this configurations is to maximize the "contact" between the two regions given that correlations decrease with the distance between the two subsystems. The region of support of each mode is illustrated in Fig. 7.8.

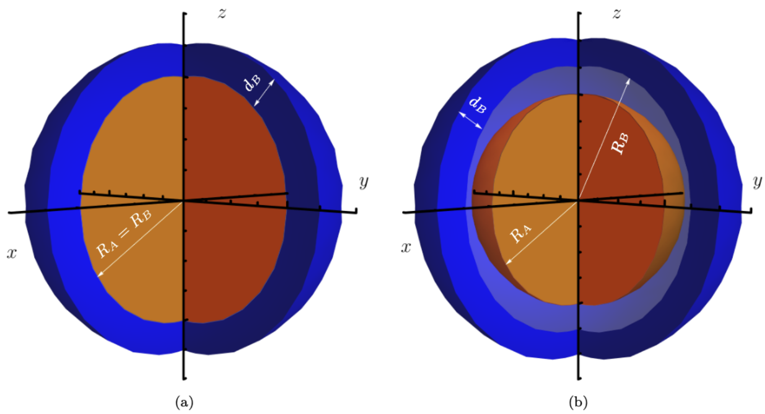

Figure 7.8: Regions of support for two field modes. The orange sphere is where the mode defining subsystem A is supported, while the mode in B is supported in the blue shell. The two panels illustrate the freedom we have in the distance between the sphere and the shell, as well as the thickness of the shell. (a) The distance between the sphere and the shell is zero, such that, $R_A = R_B$. (b) The sphere and the shell are separated by a nonvanishing distance, such that $R_B - R_A > 0$

We construct modes from pairs of operators of the form $(\hat{\phi}_i, \hat{\pi}_i)$, $i = A, B$, similarly to the previous section, with the difference that here we use the following smearing functions:

$$f_A(r; R_A) = \cos^2\left(\frac{\pi}{2}\frac{r}{R_A}\right)\Theta(R_A - r)\,, \tag{7.25}$$

for the sphere (subsystem A), and

$$f_B(r; R_B, d_B) = \begin{cases} \sin^2\left(\pi \frac{r-R_B}{d_B}\right) & R_B \le r \le R_B + d_B \\ 0, & \text{otherwise} \end{cases} \tag{7.26}$$

for the shell (subsystem B). These functions and their first derivatives are continuous.

Note that while the smearing function in the sphere depends only on one parameter (the radius R_A), the mode in the shell is parametrized by the inner radius R_B and the thickness of the shell d_B. We have checked that for a massless scalar field the logarithmic negativity is invariant if we rescale these three parameters simultaneously. Therefore, we have only two independent parameters, which we choose to be R_B and d_B measured in units of R_A. In the following, we will numerically compute the LN between subsystems A and B and the way it changes with R_B, d_B, and D. The main results are contained in Fig. 7.9, Fig. 7.11 and Fig. 7.10

Fig. 7.9 shows the value of the LN when there is no gap between the shell and the sphere ($R_A = R_B$) (the optimal case) and for a fixed value of d_B. The LN is evaluated as a function of the dimensionality of space D. The main lessons from this plot are that (i) the LN is different from zero, and (ii) it decreases in higher dimensions, completely vanishing for $D > 6$ for the values of d_B we have chosen.

Thus, interestingly enough, when trying to maximize the contact regions where the two modes are supported, we have found a configuration where there is entanglement for $D > 1$, Next, we study how the LN depends on the thickness of the shell d_B. Figure 7.10 shows a curious result: the LN is different from zero in a finite interval and vanishes when d_B is either bigger or smaller than this interval. We have obtained the same behaviour for different spatial dimensons.

Finally, we explore how the LN depends on the separation between A and B, as quantified by $R_B - R_A$ (see Fig. 7.8 b) for an illustration of the configuration). The results are presented in Fig. 7.11 for several values of D. As expected, the LN quickly falls off with the distance between both subsystems and completely vanishes beyond some threshold distance.

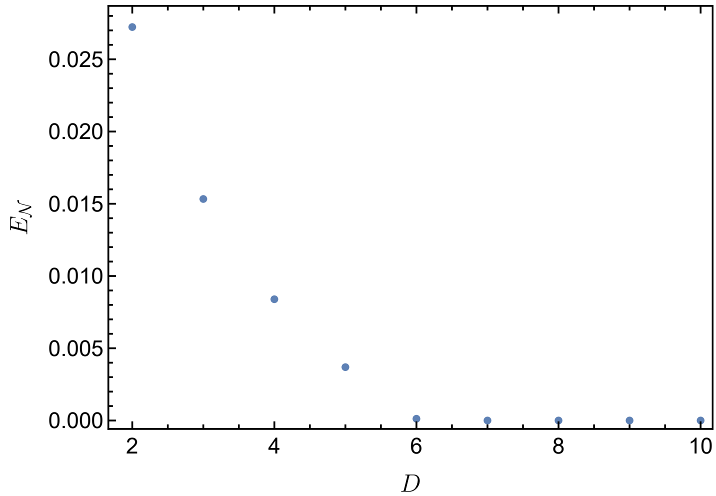

Figure 7.9: LN as a function of the spatial dimension, D, for the configuration of two modes depicted in Fig. 7.8 (a), i.e., when there is no gap between the sphere and the shell, $R_A = R_B = 1$. We choose $d_B = 0.5$ for this particular plot.

In this subsection, we have identified specific configurations of two modes, each compactly supported in disjoint spatial regions, that exhibit entanglement in spatial dimensions $D \geq 2$. However, the entanglement observed is delicate and sensitive to changes: it decreases as the separation between the modes or the spatial dimensionality increases. These findings convey a crucial message: while entanglement can be present in pairs of disjoint modes with compact support, the spatial arrangement of these modes must be thoughtfully chosen. This observation aligns with recent research in [175], emphasizing that the entanglement between regions R_A and R_B is predominantly concentrated in modes sharply localized near the boundaries.

7.2 Multimode entanglement

In this section we extend the previous calculations by enlarging the number of modes in our two subsystems in different manners. We will analyze several examples and show how in most of the cases enlarging the subsystems results in an enhancement of entanglement.

In this section, we will work with the smearing functions (7.2) for $D \geq 2$

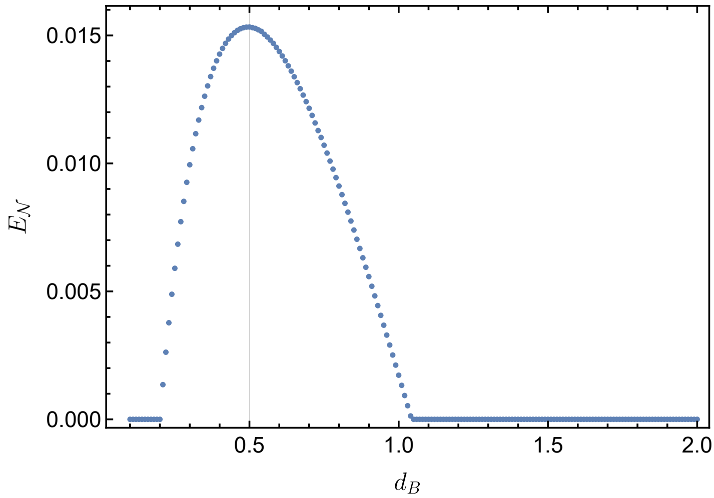

Figure 7.10: The LN $E_{\mathbb{N}}$ as a function of the width of the shell d_B, when there is no gap between the sphere and the shell. The LN is different from zero only in a finite interval of d_B.

spatial dimensions and massless scalar fields, where all the results can be obtained analitically. We will use smearing functions $f_i^{(\delta)}(\vec{x})$ with $\delta = 1$ since this is the case for which entanglement is more likely to appear as shown in section 7.1.1. The extension to other values of δ is straightforward.

The configurations that we will study involves $N_A + N_B$ modes distributed across disjoint regions, following a similar approach to section 7.1.1. The inclusion of more than two modes prompts the question of their spatial distribution. We will focus on arrangements that are more prone to exhibit bipartite entanglement—specifically, configurations where the two subsystems are in close proximity. In the context of spherical regions, this problem can be framed as maximizing the density of packed spheres in a D-dimensional space.

A natural extension of the findings from the preceding section involves introducing additional modes to subsystem B while minimizing their distance from subsystem A—the latter being composed of a single mode ($N_A = 1$). In $D = 2$, this can be accomplished as illustrated in Fig. 7.12, where the modes in subsystem B form a hexagonal configuration around mode A [178]. Figure 7.12 depicts the LN results between A and B as a function of N_B, considering the smallest possible distance between modes. The key observation from Fig. 7.12 is that

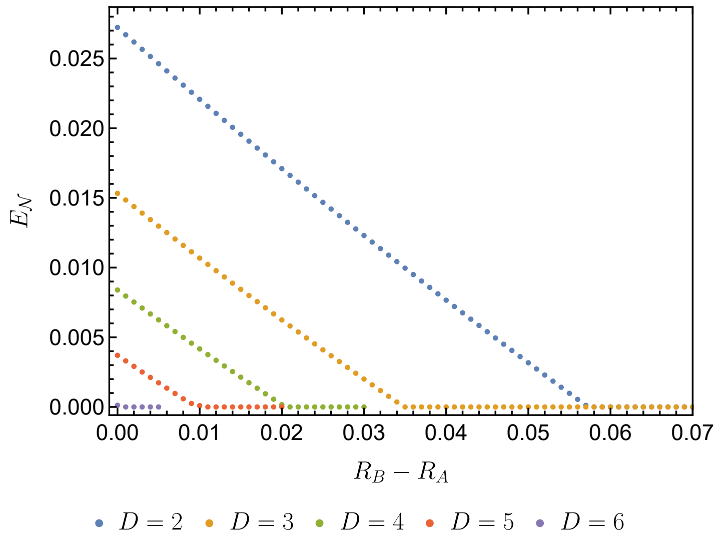

Figure 7.11: LN for the same configuration as in Fig. 7.9, now plotted versus the separation between the sphere and the shell, for different spatial dimensions D. We used $d_B = 0.5$ for the thickness of the shell (all distanced measured in units of R_A).

the LN becomes *nonzero only if* $N_B > 4$. It is noteworthy that for spherical configurations, unlike the $D = 1$ case, in two spatial dimensions, expanding our subsystems is necessary to detect any entanglement. Fig. 7.12 also shows that the LN saturates as the number of "layers" in subsystem B increases, in the sense that adding more layers does not change its value. The interpretation here is that the outer layers are too far away from subsystem A to contribute to the entanglement.

Next, we can explore how entanglement decreases with the distance. We can do this in many ways, In particular, in Fig. 7.13 we show an illustrative example, where we plot the LN versus the distance ρ for this system, containing $N_B = 6$ modes in subsystem B. We observe that the LN falls off very fast, completely vanishing when the distance between the surfaces of the regions is greater than the 8% of their radius.

Subsequently, we can explore setups in which both subsystems, A and B, comprise multiple modes (noting that when both N_A and N_B exceed 1, a nonzero LN is a sufficient but not a necessary condition for entanglement, unless). In such scenarios, numerous geometric configurations are possible. Here, we highlight a

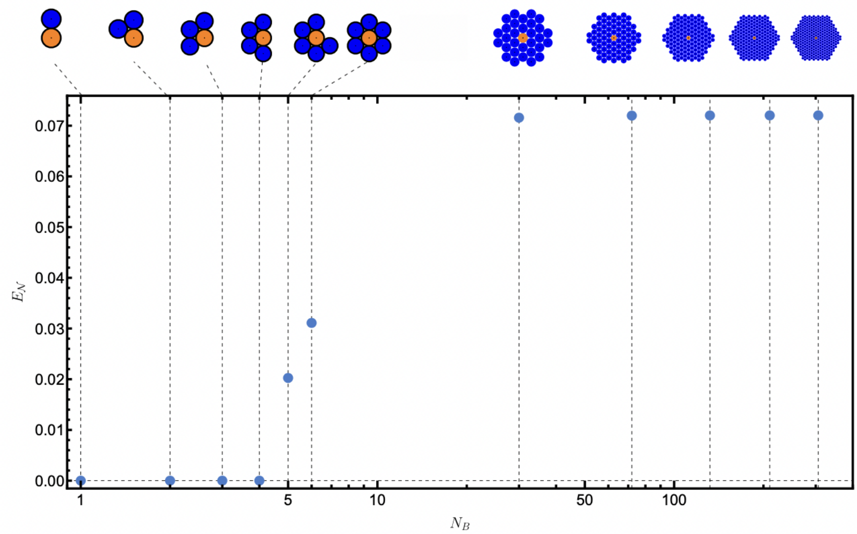

Figure 7.12: LN between subsystems A and B for different values of the number of modes N_B in subsystem B and $N_A = 1$, in two spatial dimensions, $D = 2$. The N_B modes are distributed in space as illustrated in the top part of the figure, where the orange central disk represents the region of support of the single mode in A, and the blue disks are the regions where each of the N_B modes are supported. We use smearing functions $f^{(\delta)}$ with $\delta = 1$ in this plot. The plot shows that A and B are entangled as long as $N_B \geq 5$.

particularly intriguing one. This is illustrated in Fig. 7.14 and involves $2N$ disjoint regions arranged linearly, with alternating regions assigned to each subsystem. This configuration is noteworthy because, for $N = N_A = N_B \geq 2$, the LN is nonzero and exhibits linear growth with N, as shown in Fig. 7.14.

Next, we extend these calculations to the case of $D = 3$ spatial dimensions. Firstly by adding new modes to subsystem B, supported in disjoint regions located close to subsystem A. In $D = 3$, the densest regular arrangement of spheres can be achieved by placing them either in a face-centered cubic configuration, or in a hexagonal close-packed configuration. We choose the latter. We illustrate one such configuration in Fig. 7.15.

We have computed the covariance matrix for this configuration, including up to $N_B = 1088$ modes in subsystem B, while keeping $N_A = 1$. Given the covariance matrix we have been able to compute the LN for a massless noninteracting scalar

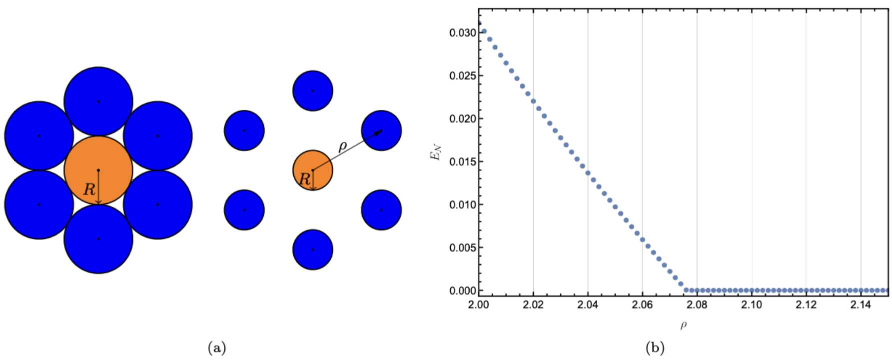

Figure 7.13: (a) The blue disks represent subsystem B made of six modes supported in the blue disks, while the orange disk is where mode in A is supported. (b) LN between subsystems A and B as a function of the distance between centers ρ units of the radius (hence, $\rho \geq 2$).

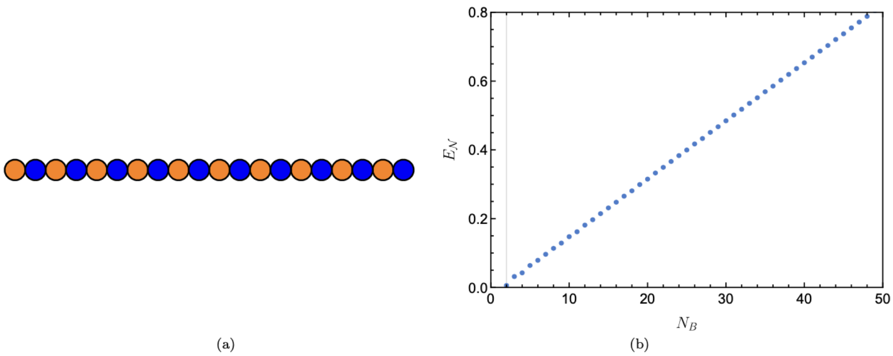

Figure 7.14: (a) Configuration in $D = 2$ consisting of $N_A = N_B = 10$ modes placed alongside a straight line. The orange discs represent the regions of support of the modes forming subsystem A, while the blue discs represent the regions of support of the modes that constitute subsystem B. (b) LN between subsystems A and B as a function of the number of modes N_B (N_A) within subsystem B (A).

field and for the family of smearing functions introduced in (7.2). In contrast to the scenario in $D = 2$, our observations in $D = 3$ reveal that the LN remains *zero* for N_B values up to 1088. This holds true even when employing smearing functions with δ equal to or close to 1, which exhibited entanglement in $D = 2$ for $N_B \geq 5$. This results confirms that entanglement is “weaker” or “sparser” in higher dimensions.

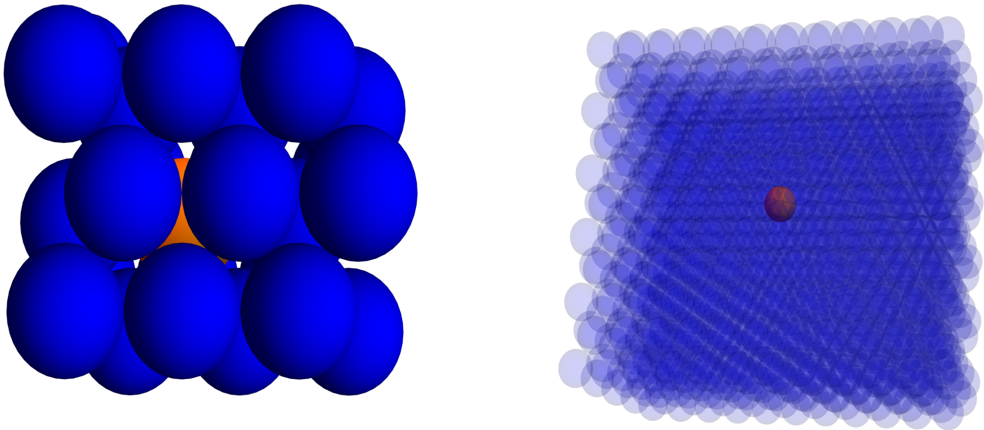

(a) (b)

Figure 7.15: (a) Configuration of modes in $D = 3$ in a hexagonal close-packed with a single mode in subsystem A and $N_B = 18$ modes in subsystem B. (b) Example of a configuration we used to compute the LN in $D = 3$. The blue spheres represent the regions of support of the $N_B = 1088$ modes, while the orange sphere is where the single mode in subsystem A is supported.

We have extended the calculations also by increasing the number of modes in subsystem A. The particular configuration studied is shown in Fig. 7.16. We have increased the number of modes to $N_A = 961$ and $N_B = 1922$ and obtained LN equal to *zero* in all cases. This shows that entanglement for $D = 3$ is too weak to be captured using the finite number of modes we have used so far.

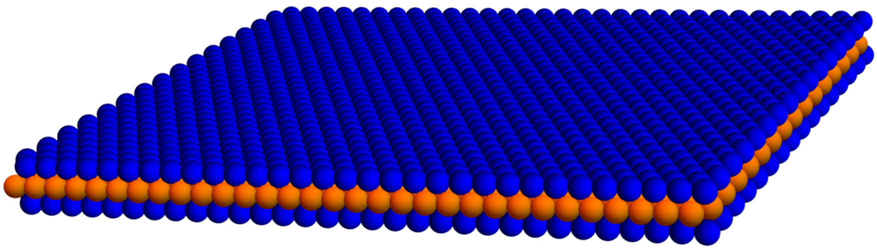

Figure 7.16: Configuration in $D = 3$. The blue spheres represent the regions of support of the $N_B = 1922$ modes, while the orange spheres represent the regions of support of the $N_A = 961$ modes in subsystem A. We find that LN vanishes in this configuration.

To finish this section we illustrate an example of an "onion like" configuration, see Fig. 7.17. This configuration is motivated by our previous results (see section 7.1.2) where we found entanglement between two modes supported in a sphere and a surrounding shell respectively and for $D = 3$. Subsequently, in Fig. 7.17 we increase the number of spherical shells and assign one mode per shell alternating between modes in subsystem A and B. Fig. 7.17 (b) shows that LN grows monotonically with the number of layers, as expected.

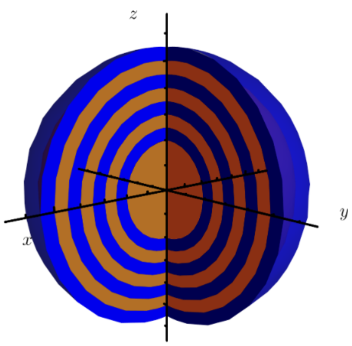

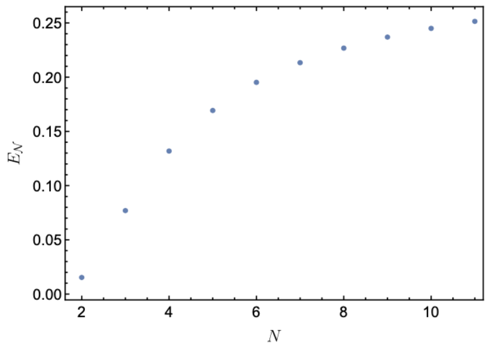

Figure 7.17: (a) Regions of support of modes in an onionlike configuration. The orange sphere and shells belong to subsystem A, and the blue shells belong to subsystem B. (b) LN as a function of the total number of degrees of freedom $N = N_A + N_B$. As expected from our previous results, the LN grows with the number of shells.

Chapter 8

Entanglement Harvesting

Quantifying the entanglement of a field's vacuum state across two disconnected spacetime regions is a complex task due to the involvement of an infinite number of degrees of freedom. While we have previously explored the quantification of entanglement between a finite number of modes supported in a specific spatial region, extending this approach to encompass all modes supported across a spacetime region—essentially addressing an infinite number of modes—presents a non-trivial challenge [47].

In the absence of this generalization, an alternative method for investigating entanglement in the vacuum state between two spacetime regions involves locally coupling a pair of probes (with a finite number of degrees of freedom), respectively to a pair of field modes in two disjoint regions of space and try to extract entanglement from the field after some interaction time. Additionally, when probing a field, it is necessary to allow it to interact with some kind of probe, for example an Unruh-Dewitt detector (also referred to as *particle detectors*). These detectors are non-relativistic two-energy level systems that locally couple to the field within a specific region of space. Consequently, when delving into the entanglement structure of the vacuum state in a field theory, a natural question arises: Can we extract entanglement from the field's vacuum state with a pair of particle detectors, even when these detectors are spacelike separated?

This question was affirmatively addressed initially by Valentini [48] and subsequently by Reznik [49, 50]. This phenomenon of extracting entanglement has come to be known as *"Entanglement Harvesting"* and has been extensively studied up to this day. Given that Unruh-DeWitt detectors can serve as a reasonable approximation to the interaction between light and matter in certain scenarios [179, 180], these groundbreaking findings suggest the potential to extract entanglement from the electromagnetic vacuum to atomic qubits. This extracted entanglement could then be utilized as a valuable resource in different quantum information protocols [181]. The Entanglement Harvesting has been extensively studied for quantum fields in flat spacetime for different spin fields [49, 50, 56, 51, 52, 182] and also for some curved spacetimes (see for example [53, 183]). Even more, some experimental implementations of the Entanglement Harvesting protocol are now within reach [184, 185, 186].

However, although there is a lot of evidence pointing toward the fact that spacelike separated particle detectors might be able to extract entanglement from the vacuum state of the field, it is less clear what is the entanglement structure of the quantum field that these detectors are able to harvest. In fact, there seems to be an apparent tension between our results in the previous chapter and the harvesting protocol. The interaction field-detector in the harvesting protocol is expressed as

$$S_{\text{int}} = \lambda \int dt\, \chi(t)\, f(\vec{x})\, \hat{\mu}(t)\, \hat{\phi}(\vec{x}, t)\,, \tag{8.1}$$

where $f(\vec{x})$ describes the spatial support of the detector, $\hat{\mu}(t)$ is an operator representing the detector's degrees of freedom, and $\chi(t)$ is a switching function defining the time duration of the interaction. It's important to note that in this action, the function $\chi(t)$ cannot be integrated against $\hat{\phi}[f]$ to define a field smeared in spacetime, as $\hat{\mu}(t)$ also carries time dependence. Instead, the natural interpretation is an interaction between $\hat{\mu}(t)$ and $\hat{\phi}[f](t)$ (the field smeared only in space), with $\lambda\chi(t)$ acting as a time-dependent coupling constant. Therefore, using the tools presented in chapter 6, we can assess whether the field modes $\hat{\phi}[f]$ to which two detectors are coupled are entangled. The calculations presented in chapter 7 indicate that pairs of such modes separated by a non-zero distance are generally not entangled at any given moment. From this point of view, it is unclear where the entanglement in the detectors is coming from, since pairs of field modes to which they are coupled are not entangled at any instant of time.

This chapter of the thesis, aims to shed some light on this issue. We will argue that, in fact, each detector in the harvesting protocol explores a continuous family of modes from the field through time evolution. Therefore, although there is not pair-wise entanglement between any pair of modes of the field at any given instant of time, there might exists *multimode entanglement* between the two continuous family of modes that couples to each detector. We will present a strategy to proved that indeed there is multimode entanglement between these two families of field modes, and this is the entanglement structure of the quantum field that produces Entanglement Harvesting.

The chapter is organized as follows. In section 8.1, we review the Harvesting protocol setup. In section 8.2, we present some results of our own of Entanglement Harvesting from the vacuum state of a massless scalar field in Minkowski spacetime, for causally disconnected detectors. In section 8.3 we argue that each detector is able to explore a continuous t-family of modes from the field through time evolution in the harvesting protocol. First we illustrate this idea in a simple example with a finite number of degrees of freedom, i.e an harmonic oscillator configuration. Then we push forward this idea in the continuum with field theory. We present a strategy to extract a discrete family of independent modes from the time evolution of the field, and to compute entanglement between the two families that each detector explores. Finally, in section 8.4 we compute logarithmic negativity between these two discrete families of modes as a function of the number of modes in each family, showing that there exists *multimode* entanglement between these two sets of modes for the same configuration where we find Entanglement Harvesting.

8.1 Harvesting setup

We will restrict attention to Minkowski spacetime with $(t, \vec{x})$ inertial coordinates and analyse Entanglement Harvesting of the vacuum state of a free scalar field,

$$\hat{\phi}(t, \vec{x}) = \int_{\infty}^{\infty} \frac{dk^3}{\sqrt{(2\pi)^3 2\omega_k}} \left(\hat{a}_{\vec{k}} e^{i(\vec{k}\vec{x}-\omega_k t)} + \hat{a}^{\dagger}_{\vec{k}} e^{-i(\vec{k}\vec{x}-\omega_k t)} \right) , \tag{8.2}$$

where the annihilation operators $\hat{a}_{\vec{k}}$ associated to the positive frequency solutions define the vacuum state $\hat{a}_{\vec{k}}|0\rangle_k = 0$. In the Harvesting protocol, we locally couple the scalar field to a pair of Unruh-DeWitt detectors, that we call A and B. The interaction field-detector is given by the following Hamiltonian in the interaction picture

$$H_I(t) = \sum_{j=A,B} \lambda_j \chi_j(t) \hat{\mu}_j(t) \hat{\phi}[f_j](t) , \tag{8.3}$$

with

$$\hat{\phi}[f_j](t) = \int d^3x f_j(\vec{x} - \vec{x}_j) \hat{\phi}(t, \vec{x}) , \tag{8.4}$$

where λ_j is the overall coupling strength, $\chi_j(t)$ is the switching function controling the interaction time, $f_j(\vec{x} - \vec{x}_j)$ is the smearing function which characterizes the sensitivity profile of the j detector, centered at $\vec{x}_j$. Finally, $\hat{\mu}_j(t)$ is the monopole moment of each detector given by

$$\hat{\mu}(t) = \hat{\sigma}^- e^{-i\Omega_j t} + \hat{\sigma}^+ e^{i\Omega_j t} ,$$

with $\sigma^- = |g\rangle\langle e|$ and $\sigma^+ = |e\rangle\langle g|$. $|g\rangle$ refers to the ground state of the detector and $|e\rangle$ refers to the exited state. Ω is the energy gap between the two energy levels. As a final remark, note that in this characterization, we are considering both detectors trajectories at rest with respect to the frame that we use to quantize the field. More general setup can be considered (see for example [187, 53]).

The detectors are prepared in their respective ground states, so the initial state of the system made of the two detectors is a product state with no entanglement. The field is assumed in the vacuum state, thus the initial state of the detectors-field system is given by

$$\hat{\rho}_0 = |0\rangle\langle 0| \otimes |g_A\rangle\langle g_A| \otimes |g_B\rangle\langle g_B| . \tag{8.5}$$

Time evolution is performed in the interaction picture where states evolve unitarily as $\hat{\rho} = \hat{U}_I \hat{\rho}_0 \hat{U}_I^\dagger$, where $\hat{U}_I$ given by the time-ordered exponential

$$\hat{U} = \mathcal{T} e^{-\mathrm{i} \int \mathrm{d}t \hat{H}_I(t)} . \tag{8.6}$$

We can evaluate this perturbatively via Dyson series expansion

$$U = \mathbb{I} \underbrace{- \mathrm{i} \int_{-\infty}^{\infty} \mathrm{d}t H_I(t)}_{U^{(1)}} \underbrace{- \int_{-\infty}^{\infty} \mathrm{d}t \int_{-\infty}^{t} \mathrm{d}t' H_I(t) H_I\left(t'\right)}_{U^{(2)}} + \ldots \tag{8.7}$$

This translates in a perturbative series for the density matrix describing the final state of the system

$$\hat{\rho} \quad = \quad \hat{\rho}_0 + \hat{\rho}^{(1)} + \hat{\rho}^{(2)} + O\left(\lambda^3\right) , \tag{8.8}$$

$$\hat{\rho}^{(j)} = \sum_{k+l=j} \hat{U}^{(k)} \hat{\rho}_0 \hat{U}^{(l)\dagger} \tag{8.9}$$

where $\rho^{(j)}$ is of order λ^j.

In order to compute the entanglement acquired by the detectors, we will be interested in the reduced density matrix between the two subsystems. Therefore, we have to trace over the field degrees of freedom: $\hat{\rho}_{AB} = \mathrm{Tr}_\phi \hat{\rho}$. We can evolve this quantity perturbatively to $O(\lambda^2)$ and obtain the following matrix

$$\hat{\rho}_{\mathrm{AB}} = \begin{pmatrix} 1 - \mathcal{L}_{\mathrm{AA}} - \mathcal{L}_{\mathrm{BB}} & 0 & 0 & \mathcal{M}^* \\ 0 & \mathcal{L}_{\mathrm{BB}} & \mathcal{L}_{\mathrm{AB}} & 0 \\ 0 & \mathcal{L}_{\mathrm{BA}} & \mathcal{L}_{\mathrm{AA}} & 0 \\ \mathcal{M} & 0 & 0 & 0 \end{pmatrix} + O\left(\lambda^4\right) \tag{8.10}$$

where we have two main contributing terms

$$\mathcal{L}_{ij} = \lambda^2 \int \mathrm{d}t\, \mathrm{d}t' \chi_i(t) \chi_j\left(t'\right) e^{-\mathrm{i}\Omega(t-t')} W\left(t, \vec{x}_i; t', \vec{x}_j\right) \tag{8.11}$$

$$\begin{aligned} \mathcal{M} = {} & -\lambda^2 \int \mathrm{d}t\, \mathrm{d}t' e^{\mathrm{i}\Omega(t+t')} \chi_{\mathrm{A}}(t) \chi_{\mathrm{B}}\left(t'\right) \times \\ & \left[\Theta\left(t-t'\right) W\left(t, \vec{x}_{\mathrm{A}}; t', \vec{x}_{\mathrm{B}}\right) + \Theta\left(t'-t\right) W\left(t', \vec{x}_{\mathrm{B}}; t, \vec{x}_{\mathrm{A}}\right)\right], \end{aligned} \tag{8.12}$$

where $\Theta\left(t-t'\right)$ is a heaviside step function and $W\left(t, \vec{x}_{\mathrm{A}}; t', \vec{x}_{\mathrm{B}}\right)$ refers to the smeared field's Wightman two-point function

$$W\left(t, \vec{x}_{\mathrm{A}}; t', \vec{x}_{\mathrm{B}}\right) = \langle \phi[f_A](t)\, \phi[f_B](t') \rangle . \tag{8.13}$$

We will focus in the case of identical detectors, i.e identical smearing functions centered at different points. In this case, the effect of smearing the field over a region of space contributes in the L and M terms by introducing a term $(2\pi)^{3/2}|f(k)|^2$ in the momentum integral $dk \to dk(2\pi)^{3/2}|f(k)|^2$ coming from the Fourier transform,

$$W\left(t, \vec{x}_{\mathrm{A}}; t', \vec{x}_{\mathrm{B}}\right) = \int \frac{d^3k}{(2\pi)^3 2\omega_k} |f(k)|^2 e^{i\vec{k}(\vec{x}_A - \vec{x}_B)} e^{-i\omega_k(t-t')} . \tag{8.14}$$

We will use Negativity to quantify entanglement between the two detectors. For a two qubits system, the negativity N of a density matrix $\hat{\rho}$ is defined by [188]

$$N(\rho) = \frac{||\rho^T|| - 1}{2}$$

where ρ^T is the partial transpose, and $||\rho^T||$ is the trace-norm of ρ^T. $N(\rho)$ corresponds to the absolute value of the sum of negative eigenvalues of ρ^T. Negativity does not increase under LOCC and it is an entanglement monotone function, therefore it is a faithful quantifier of entanglement. It is related to the Logarithmic Negativity through $E_{\mathcal{N}} = \log_2 (2N(\rho) + 1)$. For the density matrix $\hat{\rho}_{AB}$ of (8.10) at order $O(\lambda^2)$ we get

$$N(\hat{\rho}_{AB}) = \mathrm{Max}\{0, -E\} \tag{8.15}$$

where

$$E = \frac{1}{2}\left(\mathcal{L}_{AA} + \mathcal{L}_{BB} - \sqrt{(\mathcal{L}_{AA} - \mathcal{L}_{BB})^2 + 4|\mathcal{M}|^2}\right) + O(\lambda^4)\,. \tag{8.16}$$

For the case of identical detectors interacting during the same amount of time, we have that $\mathcal{L}_{AA} = \mathcal{L}_{BB} \equiv \mathcal{L}$ then the Negativity reduces to the simple expression

$$N(\rho) = \mathrm{Max}\{0, (|\mathcal{M}| - \mathcal{L})\} \tag{8.17}$$

This is the simplest possible configuration, but it is enough to capture the main features arising in the harvesting protocol in Minkowski spacetime. Finally, note that the $\mathcal{M}$ term explores the cross-correlations between the smeared field at the two different regions, and at different instants of time, $\langle \phi[f_A](t)\, \phi[f_B](t')\rangle$. In contrary, the $\mathcal{L}$ term explores self-correlations of each detector at different instants of time, $\langle \phi[f_i](t)\, \phi[f_i](t')\rangle$. Therefore, this term is usually interpreted as a local noise term for each detector. As a second remark, notice that the Wightman two point function can be split in the anti-commutator and commutator parts,

$$W(x, x') = \frac{1}{2}\langle 0|\{\phi(x), \phi(x')\}|0\rangle + \frac{1}{2}\langle 0|[\phi(x), \phi(x')]|0\rangle\,. \tag{8.18}$$

Since the commutator $[\phi(x), \phi(x')]$ is a c-number, the commutator part of the Wigthman function is state independent and it is 0 for causally disconnected points,

$$[\phi(x), \phi(x')]\big|_{(x-x')^\mu (x-x')_\mu < 0} = 0\,.$$

In order to study harvesting of entanglement and avoid classical transmission of information or state-independent contributions, we have to look at causally disconnected points, otherwise the detectors might acquire entanglement through the communication of the two detectors via the field. As we will see in the following section, Negativity can be different from zero in causally disconnected regions for some configurations of the detectors parameters.

Remark:

In the last part of this section we make a few comments regarding specific calculations in this setup. This part is not necessary to understand the main ideas that we want to stress, thus it can be skipped in a first read.

It is interesting to stress that we can write $\mathcal{M} = \mathcal{M}^+ + \mathcal{M}^-$ and $\mathcal{L} = \mathcal{L}^+ + \mathcal{L}-$, where the $+$ terms correspond to the symmetric part contribution of the correlations, and the $-$ terms correspond to the anti-symmetric part. For causally disconnected points the Negativity for identical detectors reduces to

$$N(\rho) = \text{Max}\{0, \left(|\mathcal{M}^+| - (\mathcal{L}^+ + \mathcal{L}^-)\right)\}\,. \tag{8.19}$$

We can obtain some interesting analytic results when considering a free massless scalar fiels and a configuration were both detectors, and switching functions are identical. In this case, the $\mathcal{M}^+$ term and the $\mathcal{L}^+$ and $\mathcal{L}^-$ terms can be written in the following momentum integral compact form

$$\frac{\mathcal{M}^+}{\lambda^2} = -\pi\int_0^\infty \frac{kdk}{(2\pi)^2}\frac{\sin(k|\Delta x|)}{k(\Delta x)}\chi(\Omega+k)\chi(\Omega-k) \tag{8.20}$$

$$\frac{\mathcal{L}^-}{\lambda^2} = \frac{\pi}{2}\int_0^\infty \frac{kdk}{(2\pi)^2}\left(|\chi(\Omega+k)|^2 - |\chi(\Omega-k)|^2\right) \tag{8.21}$$

$$\frac{\mathcal{L}^+}{\lambda^2} = \frac{\pi}{2}\int_0^\infty \frac{kdk}{(2\pi)^2}\left(|\chi(\Omega+k)|^2 + |\chi(\Omega-k)|^2\right) \tag{8.22}$$

For simplicity, in this calculation we didn't consider a spatial smearing. The extension to the case with spatial smearing is straightforward provided (8.14). A few interesting remarks can be make from the following expressions. 1) $\mathcal{L}^+ > \mathcal{L}^-$, so $\mathcal{L}$ can be interpreted as a noise term. 2) $|\mathcal{M}^+| - \mathcal{L}^+ < 0$. Therefore, $\mathcal{L}^-$ contributes positively to entanglement.[1] This term encodes the non-commutative

[1] The proof is very simple:

$$\begin{aligned}
\frac{|\mathcal{M}^+| - \mathcal{L}^+}{\lambda^2} &< \int_0^\infty \frac{\pi kdk}{(2\pi)^2}\left(|\chi(\Omega+k)\chi(\Omega-k)| - \frac{1}{2}|\chi(\Omega+k)|^2 - \frac{1}{2}|\chi(\Omega-k)|^2\right) \\
&\leq \int_0^\infty \frac{\pi kdk}{(2\pi)^2}\left(|\chi(\Omega+k)||\chi(\Omega-k)| - \frac{1}{2}|\chi(\Omega+k)|^2 - |\chi(\Omega-k)|^2\right) \\
&= -\frac{1}{2}\int_0^\infty \frac{\pi kdk}{(2\pi)^2}\left(|\chi(\Omega+k)| - |\chi(\Omega-k)|\right)^2 \\
&< 0\,,
\end{aligned} \tag{8.23}$$

where in the second inequality we have used the Cauchy-Scharwz inequality.

character of quantum mechanics. In addition, from the above expressions it can easily be proved that, if the switching function is a Dirac delta function $\chi(t) = \delta(t)$, then $\mathcal{L}^{-} = 0$ and consequently $N = 0$. Therefore, we can not harvest entanglement from an instantaneous interaction. These results illustrate the fact that time evolution is essential in the harvesting protocol. In the following section we will further analyse the entanglement structure of the field in the harvesting protocol.

8.2 Some results on Entanglement Harvesting

Let us consider the simplest case of a free massless scalar field coupled to a pair of identical detectors. We will consider compactly supported functions for the smearing functions $f_i(\vec{x})$.We will consider the one-dimensional version of the same family of functions for the switchings. It is important to consider compactly supported switchings in order to keep both detectors in causally disconnected regions during the interaction. Many times, this point is not strictly considered in the literature, and Gaussian switching functions that decay rapidly outside the interaction interval are often employed. The main reason for this is to obtain analytical results that help us better understand the outcomes. However, it is essential to carefully analyze harvesting with compactly supported switchings to avoid signalings due to information transmission.

In Fig. 8.1, we illustrate a spacetime diagram of the interaction. Detectors A and B are localized in space by spherically symmetric smearing functions f_A and f_B respectively. Detectors have to be separated a minimum distance of $\Delta x \geq \Delta T + 2R$, to be causally disconnected [2], where ΔT is the interaction time determined by the support of the switching function $\chi(t)$, and R is the radius of support of the smearing function. Note that, in this configuration, we use the same switching function for both detectors, and we make them interact with the field during the same time.

In this section, we analyse a concrete example of Entanglement Harvesting. We will see how it is possible to harvest entanglement for detectors localized in causally disconnected regions for some energy-gap interval and how entanglement

[2]We include the = because the field modes are compactly supported.

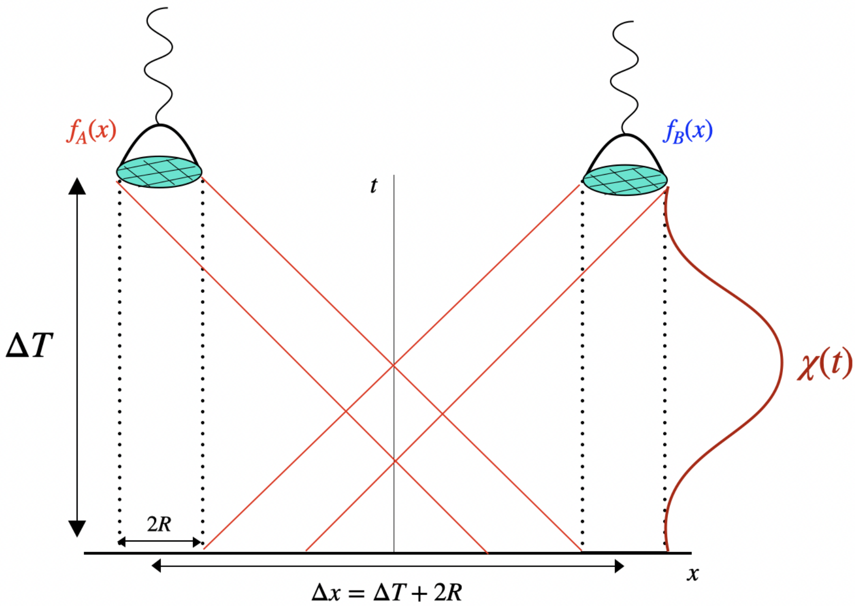

Figure 8.1: Scheme of the harvesting protocol for a pair of detectors characterized by the smearing functions $f_A(\vec{x})$ and $f_B(\vec{x})$. Both detectors interact during the same amount of time ΔT, determined by the switching function $\chi(t)$. The distance between the detectors in this interaction is such that both detectors are always causally disconnected, i.e., $\Delta x \geq \Delta T + 2R$.

rapidly decreases as we increase the distance between the detectors.

We consider a pair of detectors, each localized in a given region of space determined by the smearing function (7.2)

$$f_i^{(\delta)}(\vec{x}) = A_\delta \left(1 - \frac{|\vec{x} - \vec{x}_i|^2}{R^2}\right)^\delta \Theta\left(1 - \frac{|\vec{x} - \vec{x}_i|}{R}\right), \tag{8.24}$$

with $\vec{x}_i$ being the center of the ball ($i = A, B$), and $\Theta(x)$ the Heaviside step function —which ensures that $f_i^{(\delta)}(\vec{x})$ is compactly supported within a ball of radius R centered at $\vec{x}_i$, and δ characterizes the differentiability of the function. A_δ is a normalization constant. We use a similar family of compactly supported functions for the switching

$$\chi(t) = \left(1 - \frac{(t - t_i)^2}{(\Delta T/2)^2}\right)^{\delta_t} \Theta\left(1 - \frac{\sqrt{(t - t_i)^2}}{\Delta T/2}\right). \tag{8.25}$$

We fix $\delta_t = 2.5$ and $t_i = 0$ for both detectors.

In Fig. 8.2 we show the Negativity of the detectors as a function of the energy gap Ω in units of R^{-1}. In this configuration both detectors are switched on and off for the same period of $\Delta T = 40R$, the distance between the detectors is $\Delta x = \Delta T + 2R$. Fig. 8.2 shows us that there is a narrow window of Ω were it is possible to harvest entanglement for this configuration. We observe that it depends a lot in the sensitivity profile of the detectors. In particular, as δ increases, the detector is able to harvest less entanglement. For $\delta \geq 5$ we do not find entanglement within this window. This is in consonance with Fig. 7.2, which shows that smaller δ's have more support at the boundary. As it is argued in Appendix B of [157], for the above family of smearing functions, there always exists another function in $C_0^\infty(\mathbb{R}^D)$ producing the same physical predictions with arbitrarily high accuracy. This argument is extensible to the Entanglement Harvesting results found in this work, since the only thing that detectors sees from the field are its second moments.

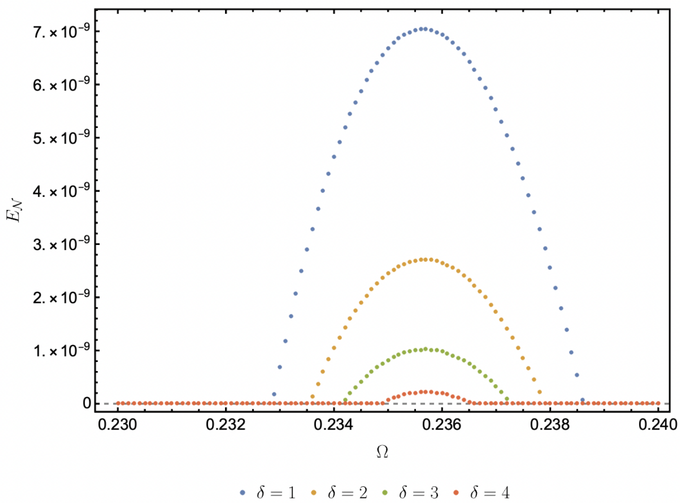

Figure 8.2: Negativity, $E_{\mathcal{N}}$, as a function of the energy gap of the detectors, Ω, in units of R^{-1}. We plot different values of δ for adistance between the detectors $\Delta x = \Delta T + 2R$.

In Fig. 8.3, we show the Negativity of the detectors as a function of the distance Δx in units of R. Again, both detectors are switched on and off for a period of $\Delta T = 40R$ and the energy gap is fixed to be $\Omega = 0.236$ in units of R^{-1}.

The right hand side of the vertical gray dashed line represents the region were the detectors are space-like separated. Fig. 8.3 shows us that entanglement decreases very fast with the distance and that it is possible to harvest entanglement in causally disconnected regions. Notice that there is a region at the right hand side of the vertical gray dashed line, with a non-zero negativity. Fig. 8.3 also shows that there is less entanglement for bigger δ's.

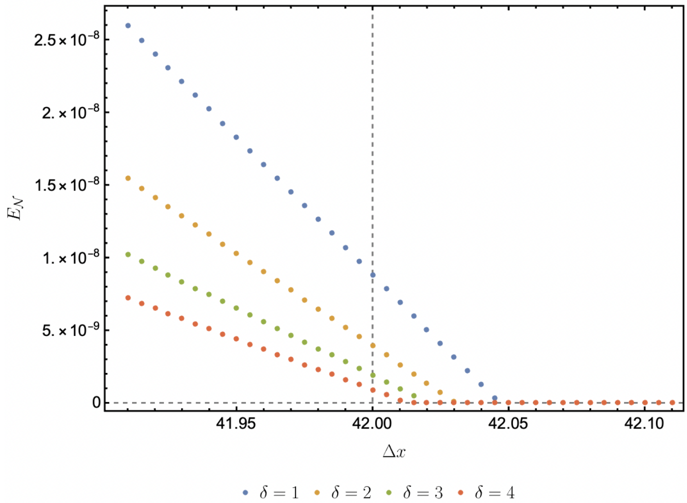

Figure 8.3: Negativity, $E_{\mathcal{N}}$, as a function of the distance between the centers of the detectors, Δx, for different values of δ. The energy gap between both detectos is $\Omega = 0.236$ in units of R^{-1}. The right hand side of the vertical gray dashed line, represents the region were the detectors are causally disconnected.

An apparent tension

The results of Entanglement Harvesting obtained in the last section are in apparent tension with our results of chapter 7. Recall that in chapter 7, we analyzed entanglement between a pair of degrees of freedom defined by the operators (7.1)[3]

$$\begin{aligned}\hat{\phi}_i = \hat{\phi}[f_i] &:= \int \mathrm{d}^D x\, f_i^{(\delta)}(\vec{x})\, \hat{\phi}(\vec{x})\,, \\ \hat{\pi}_i = \hat{\phi}[f_i] &:= \int \mathrm{d}^D x\, f_i^{(\delta)}(\vec{x})\, \hat{\pi}(\vec{x})\,.\end{aligned} \tag{8.26}$$

[3]Throughout the text, we will use both notations $\hat{\phi}_A$ or $\hat{\phi}[f_A]$. We will use them as needed, striving to maintain maximum clarity in each argument.

where $f_i^{(\delta)}$ refers to the functions (8.24) for two modes, A and B properly normalized. We have checked that, for a massless scalar field, the two field degrees of freedom $(\hat{\phi}_A, \hat{\pi}_A)$ and $(\hat{\phi}_B, \hat{\pi}_B)$ are not entangled at any given instant of time in $3+1$ dimensions. Furthermore, the Lorentz invariance of the Minkowski vacuum guarantees that such a pair of field modes is not entangled even if the two modes are defined at different times.

This seems to be in tension with the calculations of Entanglement Harvesting. In the harvesting example of the last section, the detector-field interaction is described by the following action

$$S_{\text{int}} = \lambda \int dt\, \chi(t)\, \hat{\mu}_A(t)\, \hat{\phi}[f_A](t) + \lambda \int dt\, \chi(t)\, \hat{\mu}_B(t)\, \hat{\phi}[f_B](t)\,, \tag{8.27}$$

were each detector A and B (we are considering identical detectors) couples with the individual degrees of freedom of the field, $(\hat{\phi}_A, \hat{\pi}_A)$ and $(\hat{\phi}_B, \hat{\pi}_B)$ respectively.[4] Moreover, from the M and L terms we see that the only information that the detectors see from the field are the field correlations between A and B at different instants of time

$$\langle 0|\hat{\phi}_A(t)\hat{\phi}_B(t')|0\rangle \quad ; \quad \langle 0|\hat{\phi}_i(t)\hat{\phi}_i(t')|0\rangle\,.$$

With this observation, one might be tempted to conclude that detectors can extract entanglement from the vacuum state of the field only if the individual modes $(\hat{\phi}_A, \hat{\pi}_A)$ and $(\hat{\phi}_B, \hat{\pi}_B)$ are entangled at some point in time during the interaction. However, this hasty conclusion creates a contradiction between the entanglement findings in field theory and the results obtained from the harvesting process discussed in the previous section. In the subsequent sections, we will delve into a detailed analysis of the temporal evolution to resolve this apparent tension.

8.3 A possible solution: Multimode entanglement

In this section, we argue that each detector in the harvesting protocol can probe a *continuous family of modes* from the field, through the integrals in time, rather than accessing a single degree of freedom. Consequently, although there may not

[4]Note that there is no coupling with the momentum $\hat{\pi}[f_i]$. Nevertheless this doesn't mean that we are loosing information about the reduced state of the field. The harvesting protocol is sensible to the Wightman function at different instants of time $\langle 0|\hat{\phi}_i(t)\hat{\phi}_i(t')|0\rangle$ and this contains the same information as the covariance matrix of the reduced state at a given t.

be pairwise entanglement between individual modes within each family, there could exist multimode entanglement between subsystem 1, comprising all the modes explored by detector A, and subsystem 2, consisting of all the modes explored by detector B.

We initiate our discussion in section 8.3.1 by gaining insight through a straightforward example involving harmonic oscillators, were we have a system with a finite number of degrees of freedom. Then in section 8.3.2 we will show how time evolution of the field modes can be associated with a continuous t-family of modes. In the subsequent subsections, we present an strategy to extract a finite set of modes from this continuous family and evaluate entanglement between the two subsets that couples to each detector.

8.3.1 Gaining intuition with harmonic oscillators

Before jumping to field theory, let us consider an illustrative example with a finite number of degrees of freedom. In this example we will have a configuration with 4, harmonic oscillators as represented in Fig. 8.4. We will separate subsystem 1 made of harmonic oscillator 1 and subsystem 2 which consists of harmonic oscillator 2, 3 and 4 which are coupled as described by the following Hamiltonian

$$H = \sum_{i=1}^{4} \left(\frac{\hat{p}_i^2}{2m} + \frac{1}{2} m \, \hat{x}_i^2 \omega^2 \right) + \frac{1}{2}\kappa^2 m (\hat{x}_2 - \hat{x}_3)^2 + \frac{1}{2}\kappa^2 m (\hat{x}_2 - \hat{x}_4)^2 \,. \tag{8.28}$$

We can study Harvesting of entanglement by coupling particle detectors to a pair of degrees of freedom. In particular, we couple harmonic oscillator 1 to particle detector A and harmonic oscillator 2 to particle detector B, as represented in Fig.8.4. Time evolution for the detectors is given in the interaction picture. The Hamiltonian of interaction is given by,

$$\hat{H}_I(t) = \hat{H}_A(t) + \hat{H}_B(t) \,, \tag{8.29}$$

with

$$\hat{H}_j(t) = \lambda_j \chi_j(t) \hat{\mu}_j(t) \hat{x}_j(t) \,, \quad j = A, B \,. \tag{8.30}$$

We examine a general state $|\Psi\rangle$ describing the oscillators and investigate the Entanglement Harvesting between detectors A and B. Following the harvesting protocol outlined in section 8.1, we arrive at the same outcome, (8.17), albeit with

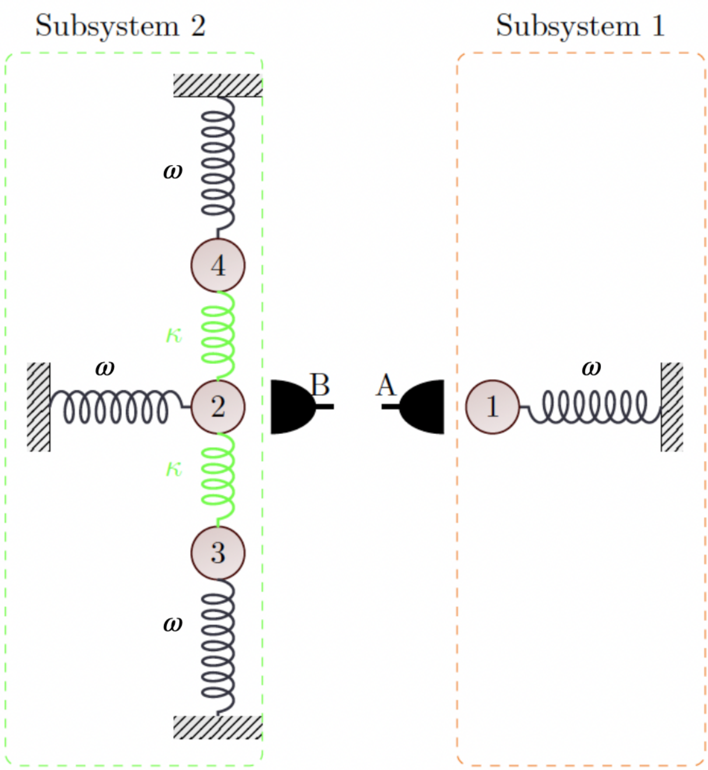

Figure 8.4: Schematic representation of the subsystems of harmonic oscillators from which the detectors can harvest entanglement.

the Wightman functions, $\langle 0|\hat{\phi}_i(t)\hat{\phi}_j(t')|0\rangle$, written in (8.12) and (8.11) substituted by

$$\langle \Psi|\hat{x}_i(t)\hat{x}_j(t')|\Psi\rangle \ .$$

Just like in the field theory case, a naive examination of this example suggests that the harvesting protocol could potentially extract entanglement from the harmonic oscillators only if $(\hat{x}_2, \hat{p}_2)$ and $(\hat{x}_1, \hat{p}_1)$ (to which the detectors are coupled) are entangled at any instant of time. However, further investigation reveals that upon a detailed analysis of the harmonic oscillator's temporal evolution, detectors are actually capable of probing the four independent degrees of freedom over time.

Time evolution

Let us carefully analyze the time evolution of the harmonic oscillators. Hamiltonians which are quadratic polynomials of the canonical variables, can be written as $\hat{H} = \frac{1}{2}\hat{r}^i h_{ij}\hat{r}^j + c$, where h_{ij} is a symmetric, positive definite, possibly time-dependent matrix, and c a constant. This family of Hamiltonians is the analog for a finite-dimensional system of the Hamiltonian for a free field theory. The time evolution matrix, determined from the Hamiltonian is given by $E = \mathcal{T}\exp\int_{t_0}^{t_1}\Omega\cdot h\,(t')\,dt'$, with $\mathcal{T}$ indicating the standard time-ordered product. Note that the $2N\times 2N$ matrix E (for a system with $2N$dimensional phase space) provides the evolution of the canonical variables in the Heisenberg picture:

$$\hat{r}^i\,(t_1) = E^i_j\hat{r}^j\,(t_0)$$

It is also exactly the same matrix that implements the Hamiltonian flow in the classical theory, in particular, $r^i(t) = E^i_j r^j\,(t_0)$ is a solution to the classical Hamilton's equations. Thus, given any linear observable, $\hat{O}_{\vec{v}} \equiv \vec{v}\cdot\hat{\vec{r}} = v_i\,\hat{r}^i$ [5], time evolution from t_0 to t is usually given by the evolution of the basis elements,

$$\hat{x}_2(t) \equiv \hat{O}_{\vec{v}_{x_2}}(t) = \vec{v}_{x_2\,i}\,\hat{r}^i(t) \quad \text{where} \quad \hat{r}^i(t) = E^i_j\hat{r}^j(t_0)\,.$$

Recall that Ω provides an isomorphism between elements of the phase space $\gamma^a \in \Gamma$ and elements of the dual $v_a \in \Gamma^*$, with $v_a = \Omega_{ab}\gamma^b$.[6] With this, we can characterize an observable also by its corresponding element in phase space $\hat{O}_{\vec{\gamma}}(t) = \Omega_{ab}\gamma^b\hat{r}^a(t)$. This will be convenient to analyze the time evolution in the field theory case. Note that, since time evolution is a symplectic transformation (and thus satisfies $(E_{tt_0})^T\,\Omega\,E_{tt_0} = \Omega$), we can also write a generic observable $\hat{O}_{\vec{\gamma}}(t)$ at time t as

$$\hat{O}_{\vec{\gamma}}(t) = \Omega_{ji}\gamma^i\hat{r}^j(t) = \Omega_{ji}\gamma^i(E_{tt_0}\hat{r}^j(t_0)) = \Omega_{ji}(E^{-1}_{tt_0}\gamma)^i\hat{r}^j(t_0) \equiv \hat{O}_{\vec{\gamma}_t} \tag{8.31}$$

Thus, we can define the observable $\hat{O}_{\vec{\gamma}}(t)$ at time t, by either evolving the basis of observables $\hat{r}(t_0)$ forward in time with the hamiltonian flow E_{tt_0}, or by evolving the phase space element $\vec{\gamma}$ "backwards" in time, $(E^{-1}_{tt_0}\cdot\vec{\gamma})$. In this simple example with harmonic oscillators, we can straightforwardly find the matrix E_{tt_0} and its inverse. There is, however, another way of understanding the action of the map $E^{-1}_{tt_0}$ when acting on $\vec{\gamma}$. Namely, *we can derive* $E^{-1}_{\tilde{t}t_0}\vec{\gamma}$ *by finding the*

[5] for example, $\vec{v}_{x_2} = (0,0,1,0,0,0,0,0,0)$, with the basis $\hat{r}^i = (\hat{x}_1,\hat{p}_1,\hat{x}_2,\hat{p}_2,\hat{x}_3,\hat{p}_3,\hat{x}_4,\hat{p}_4)$ gives observable $\hat{x}_2$.

[6] From now on, we will use the letter γ for elements of the phase space Γ, and the letter v for elements of the dual Γ^*.

particular solution to the equation of motion of the oscillators that satisfies the initial conditions $\vec{\gamma}$ at time $\tilde{t}$, and then evaluate this solution at time t_0. The latter is the method we will use in the following section to characterize a set of modes ($\gamma_{\phi,t_n} \equiv E^{-1}_{t_n,t_0}\gamma_\phi$, $\gamma_{\pi,t_n} \equiv E^{-1}_{t_n,t_0}\gamma_\pi$) in our calculation with quantum fields. We will use this method because in field theory we can not find a matrix representation for $E^{-1}_{tt_0}$ as for the harmonic oscillators case.

Whatever way of evolution we take for the harmonic oscillator case, it is crucial to stress that time evolution of a given harmonic oscillator knows about the original modes to which it is coupled to. In the above example, the harmonic oscillator 2 is coupled to the harmonic oscillators 3 and 4, and $\hat{x}_2(t)$ knows about the original modes through time evolution,

$$\begin{aligned}\hat{x}_2(t) &= a_2(t)\hat{x}_2(t_0) + a_3(t)\hat{x}_3(t_0) + a_4(t)\hat{x}_4(t_0) \\ &+ b_2(t)\hat{p}_2(t_0) + b_3(t)\hat{p}_3(t_0) + b_4(t)\hat{p}_4(t_0)\,, \end{aligned} \tag{8.32}$$

where $a_2(t), a_3(t), a_4(t), b_2(t), b_3(t), b_4(t)$ for the above particular Hamiltonian, are given in the footnote 7. [7] From (8.32) it is straightforward to check that, at any two instants of time t and t', any pair of modes for this subsystem are not independent (i.e., they do not commute), not even the same degree of freedom at two different times.

$$\left[\hat{x}_i(t)\,,\hat{x}_j(t')\right] \neq 0\,, \quad \left[\hat{x}_i(t)\,,\hat{p}_j(t')\right] \neq i\delta_{ij}\delta_{tt'}\,, \quad \left[\hat{p}_i(t)\,,\hat{p}_j(t')\right] \neq 0$$

Therefore, recalling that a *noncommuting* pair of observables $(\hat{O}_{\vec{\gamma}}, \hat{O}_{\vec{\gamma}'})$ *defines a subsystem with a single degree of freedom* (referred to as "modes of the system"), we see that, monitoring a single degree of freedom $(\hat{x}_2, \hat{p}_2)$ in the course of time, we are able to explore the three independent modes of subsystem 2. In other words, considering $(\hat{x}_2, \hat{p}_2)$ at three different instants of time, we might be able to extract three independent degrees of freedom from the system. This fact implies

[7]

$$\begin{aligned}\hat{x}_2(\tilde{t}) &= (E^{-1}_{\tilde{t}t_0}\cdot\vec{\gamma}_{x_2})^T\cdot\Omega\cdot\hat{\vec{r}}(t_0) = \frac{1}{3}\hat{x}_2(\cos(\omega(\tilde{t}-t_0)) + 2\cos(\omega_{++}(\tilde{t}-t_0))) \\ &+ \frac{1}{3}(\hat{x}_3+\hat{x}_4)(\cos(\omega(\tilde{t}-t_0)) - \cos(\omega_{++}(\tilde{t}-t_0))) \\ &+ \hat{p}_2\frac{(\omega_{++}\sin(\omega(\tilde{t}-t_0)) + 2\omega\sin(\omega_{++}(\tilde{t}-t_0)))}{3m\omega_{++}} + (\hat{p}_3+\hat{p}_4)\frac{(\omega_{++}\sin(\omega(\tilde{t}-t_0)) - \omega\sin(\omega_{++}(\tilde{t}-t_0)))}{3m\omega_{++}}\end{aligned} \tag{8.33}$$

where $\omega_+ = \sqrt{\omega^2 \pm \kappa^2}$ and $\omega_{++} = \sqrt{\omega^2 + 3\kappa^2}$

the following for the Harvesting protocol: Imagine that we prepare the state of the oscillator system in a Gaussian state with covariance matrix σ at t_0 in a configuration where there is not pair-wise entanglement between any pair of oscillators at any instant of time t. Specially, there is not entanglement at any t between $(\hat{x}_1, \hat{p}_1)$ and $(\hat{x}_2, \hat{p}_2)$ to which the detectors couple to. However, at t_0 the state is defined such that there exists *multimode entanglement* between subsystem 2 composed of the oscillators 2,3,4 and subsystem 1 made by oscillator 1. The total system of oscillators contains four independent modes. The detectors explore the Wightman function $\langle\Psi|\hat{x}_1(t)\hat{x}_2(t')|\Psi\rangle$ through the time integral in the $\mathcal{M}$ and $\mathcal{L}$ terms. Because $\hat{x}_2(t)$ knows about the original modes, *the detectors might be able to explore the multimode-entanglement between the four independent modes.*

Although in this simplified example we have checked that detectors are not able to harvest multimode entanglement from the original modes, it is an illustrative example to point out this possibility and to rise up the difficulty that will appear in QFT. Note that, when jumping to field theory, the time evolution of the smeared field $\hat{\phi}[f](t)$ in each subsystem will know about the infinitely many modes of the field to which it is coupled to. Detectors might be able to explore entanglement between all of them through the time integrals containing $\langle 0|\hat{\phi}[f_A](t)\hat{\phi}[f_B](t')|0\rangle$.

In the following section, we analyze the time evolution of the quantum field. We show that time evolution can be associated with a continuous t-family of modes and we present a strategy to extract two finite sets of modes from the field that each detector explores.

8.3.2 Time evolution as a continuous t-family of modes

For simplicity, we will restrict attention to the subset of degrees of freedom (8.26) that enters in the harvesting protocol of section 8.2. These are given by "pure" field and "pure" momentum operators,

$$\hat{\phi}[f_i](t) := v^{\phi}_{\alpha}\hat{r}^{\alpha}(t) = \int_t d^3x\, f_i^{(\delta)}(\vec{x})\,\hat{\phi}(\vec{x},t)\,, \tag{8.34}$$

and

$$\hat{\pi}[f_i](t) := v^{\pi}_{\alpha}\hat{r}^{\alpha}(t) = \int_t d^3x\, f_i^{(\delta)}(\vec{x})\,\hat{\Pi}(\vec{x},t), \tag{8.35}$$

where $f_i^{(\delta)}$ is given in (7.2). Using the symplectic structure, one can associate with the elements of the dual phase space unique phase space elements:

$$\begin{aligned} v_\alpha^\phi &= (f_I^{(\delta)}(\vec{x}) \quad 0) \quad \rightarrow \quad \gamma_\phi^\alpha = \Omega^{\alpha\beta} v_\beta^\phi = (0 \quad - f_I^{(\delta)}(\vec{x}))^T && (8.36) \\ v_\alpha^\pi &= (0 \quad f_I^{(\delta)}(\vec{x})) \quad \rightarrow \quad \gamma_\pi^\alpha = \Omega^{\alpha\beta} v_\beta^\pi = (f_I^{(\delta)}(\vec{x}) \quad 0)^T \,. && (8.37) \end{aligned}$$

As it was argued in the last subsection, time evolution is a symplectic transformation. Therefore we can write the time evolution of the operators (8.34) and (8.35) (characterized by the above phase space elements $\hat{\pi}[f_i](t) := \hat{O}_{\vec{\gamma}_\phi}(t)$ and $\hat{\phi}[f_i](t) := \hat{O}_{\vec{\gamma}_\pi}(t)$) as

$$\begin{aligned} \hat{O}_{\vec{\gamma}_\phi}(t) &= \Omega_{\beta\alpha}\gamma_\phi^\alpha (E_{tt_0}\hat{r}^\beta(t_0)) = \Omega_{\beta\alpha}(E_{tt_0}^{-1}\gamma_\phi)^\alpha \hat{r}^\beta(t_0) \equiv \hat{O}_{\vec{\gamma}_{\phi,t}} \,, && (8.38) \\ \hat{O}_{\vec{\gamma}_\pi}(t) &= \Omega_{\beta\alpha}\gamma_\pi^\alpha (E_{tt_0}\hat{r}^\beta(t_0)) = \Omega_{\beta\alpha}(E_{tt_0}^{-1}\gamma_\pi)^\alpha \hat{r}^\beta(t_0) \equiv \hat{O}_{\vec{\gamma}_{\pi,t}} \,. && (8.39) \end{aligned}$$

On the RHS of the previous equations, the operators $\hat{r}^\beta(t_0)$ are defined on the Cauchy hypersurface t_0, and γ_ϕ^α , γ_π^α can be understood as initial data (Eqs. (8.36), (8.37)) prescribed at time t. This initial data is evolved backwards in time to t_0 with $E_{tt_0}^{-1}$. The operator $E_{tt_0}^{-1} : \Gamma_t \rightarrow \Gamma_{t_0}$ maps elements of the phase space at time t to elements of the phase space at time t_0. Therefore, from γ_ϕ^α , γ_π^α, and the $E_{tt_0}^{-1}$ map, we can associate the time evolution of any observables $\hat{O}_{\vec{\gamma}_\phi}(t), \hat{O}_{\vec{\gamma}_\pi}(t)$ with a *continuous t-parameter family of modes* given by

$$\gamma_{\phi,t} \equiv E_{t,t_0}^{-1}\gamma_\phi \,, \; \gamma_{\pi,t} \equiv E_{t,t_0}^{-1}\gamma_\pi \tag{8.40}$$

with different supports at t_0. Note that at two different instants of time, the observables $\hat{O}_{\vec{\gamma}_{\phi,t'}}, \hat{O}_{\vec{\gamma}_{\phi,t}}$ do not commute,

$$[\hat{O}_{\vec{\gamma}_{\phi,t'}}, \hat{O}_{\vec{\gamma}_{\phi,t}}] = i \,\langle \vec{\gamma}_{\phi,t'}, \vec{\gamma}_{\phi,t} \rangle = i\Omega_{\alpha\beta}\gamma_{\phi,t'}^\alpha \gamma_{\phi,t}^\beta \neq 0 \,, \tag{8.41}$$

and equivalently for the momentum-momentum and field-momentum commutators. Therefore, in analogy with the harmonic oscillator case (8.32), at a given instant of time $t' > t_0$, $\hat{O}_{\vec{\gamma}_{\phi,t'}}$ knows about an infinite number of modes, and (8.40) gives us a recipe to extract a finite set of modes from the field through time evolution. In particular, we can consider an evolution time ΔT and a finite number N of instants of time, such that we can discretize ΔT in $N-1$ smaller intervals, $\Delta T = (N-1)\Delta t$. Using (8.40), it is straightforward to extract N modes, one per each instant of time,

$$\left\{ \gamma_{\phi,t_n} \equiv E_{t_n,t_0}^{-1}\gamma_\phi \;,\; \gamma_{\pi,t_n} \equiv E_{t_n,t_0}^{-1}\gamma_\pi \right\}_{n=0\cdots N-1} \,. \tag{8.42}$$

These modes are all supported at the t_0 hypersurface. However, they are not independent, i.e. they do not commute. Below we provide a strategy to obtain an independent set of modes from these ones and therefore apply the same tools of chapter 6 to compute entanglement between them. Note that, in the harvesting protocol, each detector might be able to explore a continuous family of modes through the integrals in time,

$$\mathcal{M} \propto \int dtdt'\chi(t)\chi(t')\cdots\langle\hat{O}_{\vec{\gamma}_{\phi_A},t'},\hat{O}_{\vec{\gamma}_{\phi_B},t}\rangle\,, \tag{8.43}$$

and the corresponding $\mathcal{L}$ terms. Therefore, it is interesting to define a strategy to prove if there exists entanglement between the two t-families of modes that each detector explores. Focusing on the configurations of section 8.2, were we found Entanglement Harvesting, we propose the following strategy: 1) Discretize the time interval of the harvesting interaction, ΔT, in N different instants of time, with a time distance of Δt between instants, see Fig.8.5. For each subsystem A and B, extract n modes from the field using (8.42), one per each instant of time. 2) This family of modes is not independent. Perform a symplectic version of a Gram-Schmidth algorithm to obtain an orthonormal family of modes. (We give details of this method in Appendix D). 3) Compute logarithmic negativity for the two subsystems (of field modes), and check if there exists multimode entanglement for the field in the same geometric configuration were we find harvesting. Study how entanglement changes if we increase the number of modes in each subsystem. A schematic representation of this checking proposal is given in Fig. 8.5.

In the following sections, we will implement this strategy and thereby demonstrate that, while there is no pair-wise entanglement between modes in subsystem A and B, there exists multimode entanglement. This indicates that detectors in the Harvesting protocol might be able to extract entanglement from this multimode structure.

8.3.3 t-family of mode solutions

In this section, we introduce a method for deriving an analytical expression representing the action of the $E^{-1}_{tt_0}$ map on a specific phase space element γ. Subsequently, we will utilize these solutions to generate a discrete set of N modes, each corresponding to a distinct moment in time within the interaction interval

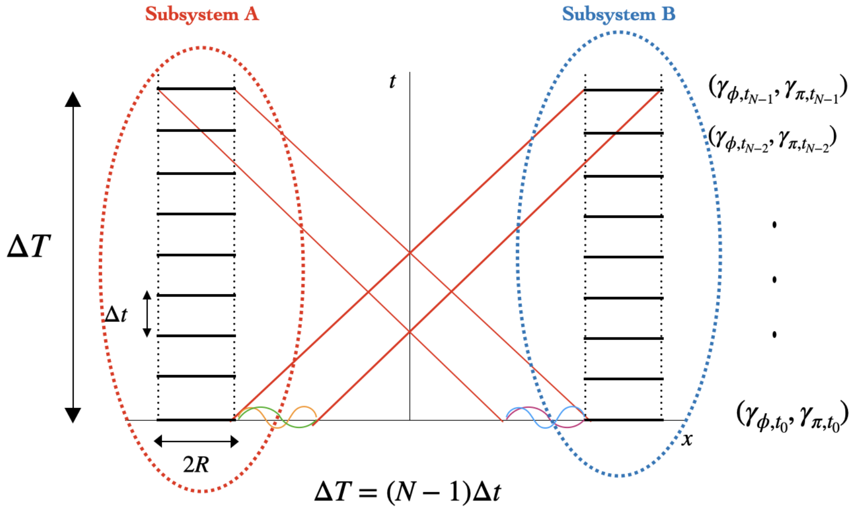

Figure 8.5: Same geometric configuration of Fig. 8.1. The time interval ΔT is discretized in N instants with a distance Δt between them. We extract one mode per each instant of time. Therefore, subsystem A which couples to detector A contains N modes and subsystem B which couples to detector B also contains N modes.

$\Delta T = (N-1)\Delta t.$, i.e,

$$\left\{\gamma_{\phi,t_n} \equiv E^{-1}_{t_n,t_0}\gamma_\phi \ , \ \gamma_{\pi,t_n} \equiv E^{-1}_{t_n,t_0}\gamma_\pi\right\}_{n=0\cdots N-1} . \tag{8.44}$$

In general, it is not possible to write the action of the map $E^{-1}_{tt_0}$ in a simple closed form. However, for a massless field and for spherically symmetric initial data, that is, $\gamma^\alpha_I = (f(r), g(r))$ where r refers to the radial coordinate, the action of $E^{-1}_{\tilde{t}t_0}$ can be computed in a closed form as follows: first, we find the solution $\varphi(r,t)$ to the corresponding equation of motion such that at time $\tilde{t}$ it satisfies

$$\varphi(r, t = \tilde{t}) = f(r)$$

and

$$\partial_t\varphi(r,t)|_{t=\tilde{t}} = g(r)\,.$$

Then, we find the action of $E^{-1}_{\tilde{t}t_0}$ by evaluating the resulting solution at time $t_0 < \tilde{t}$. The solution with spherical symmetry to the equation of motion of a massless scalar field in Minkowski spacetime with prescribed initial data $\gamma^i_I = (f(r), g(r))$ at time $\tilde{t}$ is given by

$$\varphi(r,t) = \frac{1}{r}\left(\varphi^u(u) + \varphi^v(v)\right) \tag{8.45}$$

with $u = r - (t - \tilde{t})$, $v = r + (t - \tilde{t})$, and

$$\varphi^u(u) = \frac{1}{2}\left(u\, f(u) - \int_0^{|u|} dz\, zg(z)\right) ,$$

$$\varphi^v(v) = \frac{1}{2}\left(v\, f(v) + \int_0^{|v|} dz\, zg(z)\right) ,$$

Let us denote by $\varphi^{(\phi)}(r,t)$ the solution obtained from prescribing the initial data (pure field), (8.36), at time $\tilde{t}$, i.e., satisfying $\varphi^{(\phi)}(r,t_0) = 0$ and $\partial_t\varphi^{(\phi)}(r,t_0) = -f_i^{(\delta)}(r)$, and by $\varphi^{(\pi)}(r,t)$ the solution obtained from prescribing the initial data (pure momentum), (8.37), at time $\tilde{t}$, i.e satisfying $\varphi^{(\pi)}(r,t_0) = f_i^{(\delta)}(r)$ and $\partial_t\varphi^{(\Pi)}(r,t_0) = 0$. For these initial data, we can obtain an analytic result for the solution in Eq. (8.45). These are explicitly given by:

$$\varphi^{(\phi)}(r,t) = \frac{R^2 A_\delta}{4(\delta+1)r}\left(\left(1-\left(\frac{v}{R}\right)^2\right)^{\delta+1}\Theta\left(1-\frac{|v|}{R}\right) - \left(1-\left(\frac{u}{R}\right)^2\right)^{\delta+1}\Theta\left(1-\frac{|u|}{R}\right)\right) ,$$

and

$$\varphi^{(\pi)}(r,t) = \frac{R\, A_\delta}{2r}\left(\frac{v}{R}\left(1-\left(\frac{v}{R}\right)^2\right)^{\delta}\Theta\left(1-\frac{|v|}{R}\right) + \frac{u}{R}\left(1-\left(\frac{u}{R}\right)^2\right)^{\delta}\Theta\left(1-\frac{|u|}{R}\right)\right) .$$

From these mode solutions, we can obtain a discrete family of modes in a straightforward manner. We consider a time interval ΔT discretized in N smaller Δt intervals. Subsequently, by prescribing the same initial data at the N different instants of times, we can generate a discrete family of N mode solutions $\{\gamma_{\phi,t_n}\ ,\ \gamma_{\pi,t_n}\}_{n=0\cdots N-1}$ evaluated at t_0:

$$\begin{aligned}
\gamma_{\phi,t_0} &= (\varphi^{(\phi)}(r,t_0), \partial_t\varphi^{(\phi)}(r,t_0))|_{\tilde{t}=t_0},\\
\gamma_{\pi,t_0} &= (\varphi^{(\pi)}(r,t_0), \partial_t\varphi^{(\pi)}(r,t_0))|_{\tilde{t}=t_0},\\
\gamma_{\phi,t_1} &= (\varphi^{(\phi)}(r,t_0), \partial_t\varphi^{(\phi)}(r,t_0))|_{\tilde{t}=t_1},\\
\gamma_{\pi,t_1} &= (\varphi^{(\pi)}(r,t_0), \partial_t\varphi^{(\pi)}(r,t_0))|_{\tilde{t}=t_1},\\
&\ \vdots \qquad\qquad\qquad\qquad\qquad\qquad\qquad\qquad\qquad (8.46)\\
\gamma_{\phi,t_{N-1}} &= (\varphi^{(\phi)}(r,t_0), \partial_t\varphi^{(\phi)}(r,t_0))|_{\tilde{t}=t_{N-1}},\\
\gamma_{\pi,t_{N-1}} &= (\varphi^{(\pi)}(r,t_0), \partial_t\varphi^{(\pi)}(r,t_0))|_{\tilde{t}=t_{N-1}}\,. \qquad (8.47)
\end{aligned}$$

Recall that these are elements of the phase space at time t_0. In other words, this family of modes have support at the same hypersurface. Fig. 8.6 and 8.7

show different phase space elements belonging to this family for $\delta = 2$, for the ϕ and π modes, respectively. The solid lines represent the first component of the solution as defined above, and the dashed lines, the second component. The initial data of the different phase space elements propagates in the light-cone, as expected for a massless scalar field. This is reflected in the fact that modes defined at different instants of time have different regions of support at the t_0 hypersurface.

It is important to stress that modes defined from prescribing the initial data at times t and t' such that $t - t' < 2R$, share a common region of support. Because of this, they are not independent (i.e., they do not commute). This can be checked explicitly by computing the symplectic product between these modes (see Appendix D). The fact that different phase space elements in this family of modes are not independent poses a problem if one intends to use them to compute multimode entanglement, because they don't define a proper canonical system and standard tools can not be used directly. However, given a discrete subset consisting of N elements of the family of modes in Eqs. (8.46) - (8.47), we can extract a set of N independent modes by means of a symplectic Gram-Schmidt procedure. This is a set of local operations in each subsystem that renders an orthonormal family of modes (the details of this algorithm can be found in Appendix D). Once we have obtained a canonical set of N symplectically orthonormal modes, $\{\tilde{\gamma}_{\phi,n}\ ,\ \tilde{\gamma}_{\pi,n}\}_{n=0\cdots N-1}$, [8], for both subystems A and B as represented in Fig. 8.5 we are in position to evaluate entanglement between these families. We will use logarithmic negativity as in chapter 6 to quantify entanglement between the two sets.

In the following section, we calculate the logarithmic negativity between two families of modes defined by the trajectories of particle detectors which are causally disconnected during the interaction period. We use the same geometric configuration as the one that we used to harvest entanglement in section 8.1. Our results prove that *there exists entanglement between the two families of field modes.*

8.4 Results in multimode entanglement

In the previous section we have learned to extract a canonical system of N independent modes from the continuous t-family of modes associated with the time

[8] we use the $\tilde{\gamma}$ notation to indicate that this set is orthonormal

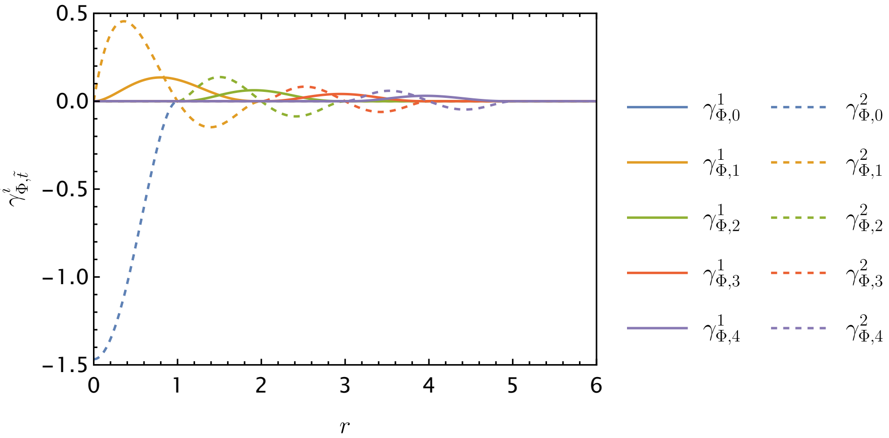

Figure 8.6: Phase space elements obtained from prescribing the initial data in (8.36) with $\delta = 2$ and $R = 1$ at time $\tilde{t}$ as a function of the radial distance, r. The solid (dashed) lines represent the first (second) components of the corresponding phase element.

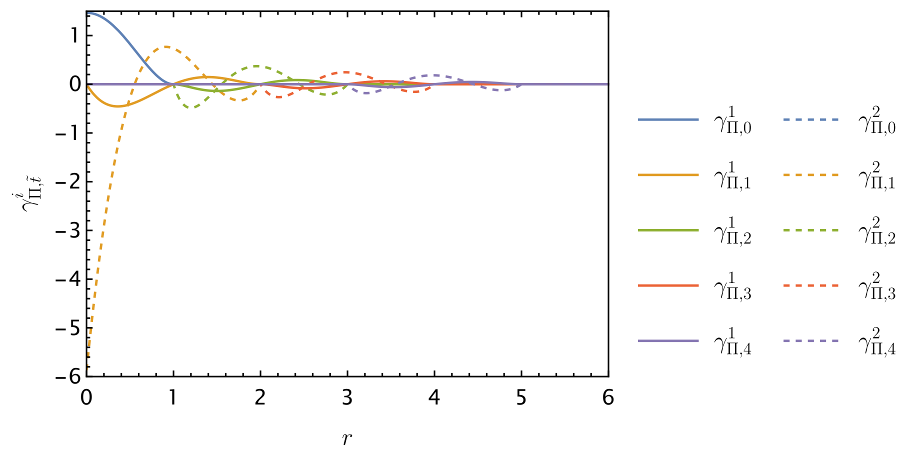

Figure 8.7: Phase space elements obtained from prescribing the initial data in (8.37) with $\delta = 2$ and $R = 1$ at time $\tilde{t}$ as a function of the radial distance, r. The solid (dashed) lines represent the first (second) components of the corresponding phase space element.

evolution of a field degree of freedom $(\hat{\phi}[f](t), \hat{\pi}[f](t))$ in an interval of time ΔT. This orthonormal set of N phase space elements $\{\tilde{\gamma}_{\phi,n}\ ,\ \tilde{\gamma}_{\pi,n}\}_{n=0\cdots N-1}$ supported at the same hypersurface t_0, are associated with a subset of modes to which each detector is sensitive in the harvesting protocol through time evolution. In order to evaluate entanglement between the two families of modes that each detector explores, we will used the tools presented in chapter 6. This means computing correlations and the covariance matrix σ, for the total system formed by the two families of modes. Subsequently, we obtain the partially transposed covariance matrix and its symplectic eigenvalues, and finally evaluate the logarithmic negativity.

Consider each family of phase-space elements $\{\tilde{\gamma}_{\phi,n}\ ,\ \tilde{\gamma}_{\pi,n}\}_{n=0\cdots N-1}$, for both subsystems A and B and let their corresponding observables be,

$$\left\{\hat{O}_{\tilde{\gamma}_{\phi,n}}\ ,\ \hat{O}_{\tilde{\gamma}_{\pi,n}}\right\}_{n=0\cdots N-1}\ . \tag{8.48}$$

For completeness, on can verify that these observables form a suitable canonical system, in the sense that

$$[\hat{O}_{\tilde{\gamma}_{\phi,l}}, \hat{O}_{\tilde{\gamma}_{\pi,m}}] = i\,\Omega_{\alpha\beta}\tilde{\gamma}^{\alpha}_{\phi,l}, \tilde{\gamma}^{\beta}_{\pi,m} = i\,\delta_{lm}\,,$$

where in the last step we used that the modes we computed using the symplectic Gram-Schmidt algorithm are orthonormal (see Appendix D). Now, we proceed to compute the covariance matrices σ_A and σ_B for each reduced subsystem, comprising the self-correlations between the N observables, (8.48). For example, for subsystem A, the correlations to compute in the Minkwoski vacuum are

$$\langle\{\hat{O}^{(A)}_{\tilde{\gamma}_{\phi,l}}, \hat{O}^{(A)}_{\tilde{\gamma}_{\phi,m}}\}\rangle\ ;\ \langle\{\hat{O}^{(A)}_{\tilde{\gamma}_{\pi,l}}, \hat{O}^{(A)}_{\tilde{\gamma}_{\pi,m}}\}\rangle\ ;\ \langle\{\hat{O}^{(A)}_{\tilde{\gamma}_{\phi,l}}, \hat{O}^{(A)}_{\tilde{\gamma}_{\pi,m}}\}\rangle\,.$$

Subsequently, we determine the covariance matrix σ for the total system, which encompasses also the cross-correlations between the two subsystems, i.e

$$\langle\{\hat{O}^{(A)}_{\tilde{\gamma}_{\phi,l}}, \hat{O}^{(B)}_{\tilde{\gamma}_{\phi,m}}\}\rangle\ ;\ \langle\{\hat{O}^{(A)}_{\tilde{\gamma}_{\pi,l}}, \hat{O}^{(B)}_{\tilde{\gamma}_{\pi,m}}\}\rangle\ ;\ \langle\{\hat{O}^{(A)}_{\tilde{\gamma}_{\phi,l}}, \hat{O}^{(B)}_{\tilde{\gamma}_{\pi,m}}\}\rangle\,.$$

As a remark, we don't have closed analytic expressions for all the components of the covariance matrix, only for some of them. The rest are computed numerically. The expressions for the correlations are quite long and not particularly enlightening, so we refrain from writing them down.

The particular geometric configuration that we use to prove that there exists *multimode entanglement* between the two sets of modes to which each detector couples in the harvesting protocol, is the same that we used in section 8.2 to analyze harvesting (see Fig. 8.1 and Fig. 8.5) with the two regions separated by the minimum distance such that they are causally disconnected. Fig. 8.8 shows the LN between the modes in each region, as a function of the number

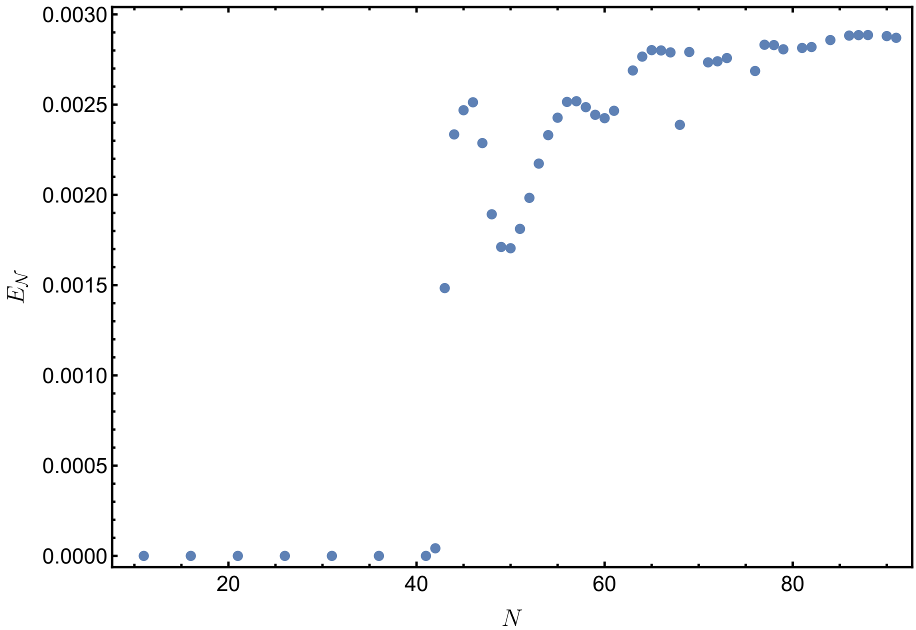

Figure 8.8: Log Neg as a function of the number of modes, N, associated which each smeared detector, when the detectors are separated a distance of $\Delta x_{AB} = \Delta T + 2R$.

of orthonormal modes we employed in region A (or B, since we chose the same modes in each region to ease the calculations). It is interesting to make a couple of remarks. First of all, we see that we need a minimum number of modes to find entanglement (in particular, we need 43 modes per subsystem in this configuration). Secondly, we observe that, as we increase the number of modes per subsystem, entanglement increases with an oscillatory behaviour, with an amplitude that decreases as we increase the number of modes. These results prove that the two discrete families of modes that the detectors explore in the harvesting results of 8.2, (see Fig. 8.2 and Fig. 8.3) are indeed entangled. In fact, the harvesting protocol explores infinitely many modes of the continuous t-families through the integrals in time controlled by the continuous switching functions.

The general results obtained here are not only particular from this configuration. We have computed other configurations where there exists multimode entanglement between two finite sets of modes. For this and other configurations, we have also checked that entanglement decreases with the distance between both subsystems but it can be greater than zero for causally disconnected regions. For the sake of simplicity we won't show more calculations here.

Chapter 9

Conclusions

This thesis compiles the author's main results achieved during his doctoral studies, in collaboration with his thesis supervisors and other researchers. The work encompasses two different disciplines within the conceptual framework of quantum field theory. The first part of the thesis investigates certain aspects of quantum field renormalization in cosmological spaces, along with the characterization of quantum states and their implications for the early Universe. The second part of the thesis explores the entanglement of the vacuum state of a quantum field theory in Minkowski spacetime. This study is conducted from an operational approach, focusing on a finite number of degrees of freedom.

In Chapter 3, we contribute to extending the point-splitting renormalization method to a pragmatic regularization method that considers subtractions within the sum of momentum modes $\vec{k}$ in a FLRW spacetime. This is useful for numerical implementation of quantum field renormalization in time-dependent cosmological spaces. Specifically, we extend the pragmatic mode-sum regularization method [36, 37] to dynamic spacetimes. This method was introduced by Levi and Ori in the context of stationary spacetimes. Our extension has been possible thanks to the isometry under spatial translations of the flat FLRW spacetime metric. The results obtained are consistent with the known adiabatic regularization prescription, which was developed by Parker and Fulling in the 1970s. Thus, adiabatic regularization can be understood as the natural renormalization mechanism that emerges when applying the point-splitting method using the spatial isometries of the FLRW metric.

In Chapter 4, we present the prescription of Low Energy States (SLE) for scalar fields [43] and contribute to extending it to spin-1/2 fields. The concept of low energy states seems to be a very useful prescription for selecting vacuum states in time-dependent spacetimes, particularly for FLRW spacetimes. This construction selects the vacuum state by minimizing the expectation value of the smeared Hamiltonian with a time-dependent window function, and its main virtue is that the resulting state satisfies the Hadamard condition.

In chapter 5 we use the formalism of low energy states to analyze the quantum vacuum state defined around the Big Bang singularity. We do this for scalar and spin-1/2 fields in a radiation-dominated Universe. This context is motivated by cosmological observations, in which the scale factor is a linear function of the conformal time τ at early times, thus allowing an analytical extension to negative times of the conformal parameter [54]. Making this extension naturally yields a temporal reversal symmetry for the metric. In this cosmological scenario, it seems natural to impose CPT symmetry at the Big Bang as an extra condition that the vacuum state of a quantum field must satisfy.

In Chapter 5, we characterize the family of low energy states that respect CPT symmetry for both scalar and spin-1/2 fields. One possible choice of vacuum state is the one proposed in [44, 45], $|0_T\rangle \propto |0_+\rangle + |0_-\rangle$. From the perspective of low-energy states, this state corresponds to defining the temporal smearing function f^2 with support at $|\tau| \to \infty$, also imposing the additional CPT symmetry. In this case, the resulting state is independent of the smearing function since its support is located in adiabatic regions of spacetime. However, this state entails providing initial conditions based on the late-time behavior of an expanding universe. An alternative option is to define the vacuum state using a temporal window around $\tau \to 0$. We have verified that this choice is fully consistent with physical requirements in the ultraviolet regime, i.e., the state satisfies the Hadamard condition for both scalar and fermionic fields. Therefore, these states are suitable candidates as effective vacua at the Big Bang from the perspective of quantum field theory. The infrared behavior of these states is sensitive to the temporal smearing function. This ambiguity could be naturally interpreted, at least heuristically, as encoding quantum gravitational effects from a more fundamental theory.

Finally, the states obtained with this method allow for some interesting physical predictions. Firstly, primordial gravitational waves can be produced even though the initial state of the Universe is well described by a radiation-dominated epoch. Secondly, in a scenario where complete cancellation of the conformal anomaly at the Big Bang is required, the mass of the natural candidate for dark matter, namely, a right-handed neutrino ν_R, is of the order of 10^8 GeV. The specific prediction for the mass slightly depends on the selection of the vacuum state.

The second part of the thesis begins in Chapter 6. It focuses on the study of entanglement of the vacuum state of a scalar field in Minkowski spacetime. In this chapter, we present a formalism for extracting field modes in a canonical way. We introduce quantum mechanics techniques for Gaussian states and continuous variable which we used in the following chapters to study entanglement. Specifically, the formalism extracts individual degrees of freedom (modes) of the field (localized in a compact region of space) by smearing the field and its conjugate momentum with compactly supported functions. Each mode defines an algebra isomorphic to the algebra of an ordinary harmonic oscillator. This strategy provides a way to extract a finite set of modes from the field in a local and covariant manner, to which standard tools of quantum mechanics can be applied to evaluate entanglement. Our strategy is free from divergences affecting other approaches. The focus on a finite number of modes is motivated by the finite capabilities of observers.

In Chapter 7, we conduct a detailed study of the entanglement of the vacuum state for a scalar field in $D+1$-dimensional Minkowski spacetime between a finite number of degrees of freedom. The specific set of modes we consider depends on the selection of smearing functions. Throughout this study, we investigate various families of these functions, focusing on common results among them. For certain smearing functions, analytical results have been obtained for D spatial dimensions, while for others, numerical methods have been used. Leveraging the Gaussian nature of the vacuum state, we calculate the reduced state defining a finite subset of modes and compute its entropy, mutual information, and entanglement. It is noteworthy that we have confirmed that the reduced state corresponding to finite-dimensional subsystems is always mixed, consistent with general results [55].

The main lesson learned from our results is that it is difficult to find entangled pairs of modes with support in spatially separated regions by a nonzero distance. This difficulty increases with spatial dimensionality. In particular, while it is relatively simple to find entangled mode pairs in $D = 1$, the task becomes significantly more challenging for $D \geq 2$. In fact, we observe that careful selection of the support regions between two modes is required to detect entanglement in $D \geq 2$. An illustrative example where entanglement is observed is when one mode is confined within a sphere while the other resides in a spherical shell surrounding it. This arrangement minimizes the separation between the modes, facilitating the detection of entanglement between them. In cases where entanglement is found between pairs or sets of modes, we have also verified that it decays rapidly with the distance between subsystems.

Overall, we can conclude that entanglement in quantum field theory is not as prevalent as commonly believed. It is ubiquitous when considering subsystems with infinite degrees of freedom but not for finite-dimensional systems. This result is consistent with the Reeh-Schlieder theorem, which guarantees that given a field mode with support in a region R_A, and a second region R_B, there is at least one mode in R_B that is entangled with the mode given in R_A [47]. However, the theorem does not indicate how many modes in R_B are entangled with the mode given in R_A, nor how complicated this mode is. Our results indicate that careful mode selection in R_B is needed to find entanglement.

The results of Chapter 7 seem to be in apparent tension with the Entanglement Harvesting mechanism in quantum field theory [49, 56]. This protocol couples the quantum field to two non-relativistic systems, acting as detectors. These detectors are turned on for a finite amount of time and are spatially separated so that they remain causally disconnected during the interval of interaction. The detectors are prepared in their respective ground states, so their initial state of the system is an unentangled product state. After the interaction, we want to know if the two detectors end up in an entangled state. If so, since the detectors do not interact with each other nor do they communicate through the field, then the only possible source of entanglement is the entanglement of the field itself, which has been transferred to the detectors through the interaction. In this sense, it is said that the detectors extract entanglement from the field. The calculations in Chapter 7 make us wonder where the entanglement acquired by the detectors in the Entanglement Harvesting protocol comes from since generic pairs of field modes are not entangled.

The answer to this question has been addressed in Chapter 8. To do so, we have carefully analyzed the temporal evolution of the field degree of freedom that couples to each detector in the Harvesting protocol. In particular, we have shown that the temporal evolution of this mode, knows about an infinite collection of modes. In fact, it can be characterized as a continuous family of modes parameterized by time t, all supported on the same hypersurface t_0. Thus, each detector in the Harvesting protocol is capable of exploring a continuum of field modes through the interaction. Consequently, although there is no entanglement for the field between any pair of modes that couple to the detectors, there can exist multimode entanglement between the two families of field modes that each detector explores. In order to demonstrate the existence of entanglement between these two families, in Chapter 8 we have proposed a specific strategy where we extract a finite set of modes from each family and calculate the entanglement between both sets using the techniques employed in Chapter 7.

Our results show the existence of entanglement between the two discrete sets of field modes that we extract from the continuous families. We prove this for a given geometric configuration where the detectors are capable of extracting entanglement with the Harvesting protocol. Furthermore, this multimode entanglement of the field seems to show a general tendency to increase as we also increase the number of modes in each subsystem, reaching an asymptotic value. This result is in agreement with the Reeh-Schlieder theorem. The two spacetime regions R_A and R_B determined by the interaction in the Harvesting protocol contain an infinite number of degrees of freedom, and both sets of these modes seem to be entangled, in accordance with the theorem. Additionally, in our calculation, we see that a minimum number of modes in each region are required to obtain entanglement, and they are distributed in a subtle manner. This is also in line with the results of Chapter 7, which indicate that the entanglement is subtly distributed, and careful mode selection between the two regions is required to find entanglement.

Altogether, we can conclude that although there isn't entanglement between any pair of field modes that couple to the detectors, there is multimode entanglement between the two families of field modes that each detector explores. Therefore, the Entanglement Harvesting protocol might be extracting entanglement from this structure of the field.

Appendix A

Adiabatic Regularization with an arbitrary μ

In this appendix, we offer a concise overview of the adiabatic regularization technique, taking into account the incorporation of a renormalization scale μ. We extend the subtraction term for the two-point function in adiabatic regularization by introducing a parameter μ. Initially proposed in [189], this method involved substituting m^2 with μ^2 at the zeroth adiabatic order. However, as outlined in [100], a more refined and physically motivated approach is to replace m^2 with $m^2 + \mu^2$. This adjustment ensures the decoupling of heavy massive fields.

The Adiabatic regularization process as described in section 3.1 can be easily extended to accomodate an arbitrary renormalization scale μ by replacing m^2 by $m^2 + \mu^2$ in the zeroth adiabatic order ω. Therefore the expansion for W_k depends now on μ

$$W_k(t) = \omega_{\text{eff}}^{(0)}(t, \mu) + \omega_{\text{eff}}^{(2)}(t, \mu) + \omega_{\text{eff}}^{(4)}(t, \mu) + \ldots \,, \tag{A.1}$$

where the leading term is $\omega_{\text{eff}}^{(0)}(t) \equiv \omega_{\text{eff}}(t) = \sqrt{k^2/a^2(t) + m^2 + \mu^2}$. The higher orders are univocally recalculated. For the second order $\omega_{\text{eff}}^{(2)}(t, \mu)$ which is enough to renormalize the two-point function we have

$$\omega_{\text{eff}}^{(2)} = \frac{5k^4\dot{a}^2}{8\omega_{\text{eff}}^5 a^6} - \frac{3k^2\dot{a}^2}{4\omega_{\text{eff}}^3 a^4} + \frac{k^2 a}{4\omega_{\text{eff}}^3 a^3} + \frac{3\xi\dot{a}^2}{\omega_{\text{eff}} a^2} + \frac{3\xi\ddot{a}}{\omega_{\text{eff}} a} - \frac{3\dot{a}^2}{8\omega_{\text{eff}} a^2} - \frac{3\ddot{a}}{4\omega_{\text{eff}} a} - \frac{\mu^2}{2\omega_{\text{eff}}} \,. \tag{A.2}$$

The additional terms proportional to μ^2 effectively eliminate the divergences, aligning with the revised definition of $\omega_{\text{eff}}^{(0)}(t,\mu)$ while preserving locality and general covariance. It's important to emphasize that μ^2 ought to be viewed as a parameter of adiabatic order 2.

Therefore, the subtraction term for the two-point function is given by

$$^{(2)}G_{Ad}(x,x) = \frac{1}{2(2\pi)^3 a^3} \int d^3k \left[\frac{1}{\omega_{\text{eff}}} - \frac{\omega_{\text{eff}}^{(2)}}{\omega_{\text{eff}}^2} \right] \,. \tag{A.3}$$

After a little bit of algebra the terms in the integral can be written like

$$^{(2)}G_{Ad}(x,x) = \frac{1}{4\pi^2 a^3} \int k^2 dk \left[\frac{1}{\omega_{\text{eff}}} + \frac{\mu^2}{2\omega_{\text{eff}}^3} + \frac{(\frac{1}{6}-\xi)R}{2\omega_{\text{eff}}^3} + \left(\frac{m_{\text{eff}}^2\dot{a}^2}{2a^2\omega_{\text{eff}}^5} + \frac{m_{\text{eff}}^2\ddot{a}}{4a\omega_{\text{eff}}^5} - \frac{5m_{\text{eff}}^4\dot{a}^2}{8a^2\omega_{\text{eff}}^7} \right) \right] \,. \tag{A.4}$$

The last terms in the parentheses are finite and can be integrated to give

$$\frac{1}{4\pi^2 a^3} \int k^2 dk \left[\frac{m_{\text{eff}}^2\dot{a}^2}{2a^2\omega_{\text{eff}}^5} + \frac{m_{\text{eff}}^2\ddot{a}}{4a\omega_{\text{eff}}^5} - \frac{5m_{\text{eff}}^4\dot{a}^2}{8a^2\omega_{\text{eff}}^7} \right] = \frac{R}{288\pi^2} \,. \tag{A.5}$$

Finally, we obtain the same subtraction term as for the pragmatic mode-sum regularization method

$$^{(2)}G_{Ad}(x,x) = \frac{1}{4\pi^2 a^3} \int_0^\infty dk k^2 \left[\frac{1}{\omega_{\text{eff}}} + \frac{(\frac{1}{6}-\xi)R}{2\omega_{\text{eff}}^3} + \frac{\mu^2}{2\omega_{\text{eff}}^3} \right] + \frac{R}{288\pi^2} \,. \tag{A.6}$$

Notice that this result agrees with (3.58) in the coincidence limit, $\epsilon \to 0$, and both agree with (3.47) when $\mu = 0$.

Appendix B

Details on the large momentum expansion of the spin-$1/2$ field modes

In this concise appendix, we present the large k expansion of the integrand of the formal vacuum expectation value of the energy density $\rho_k(\tau)$, which is defined as

$$\langle T_{00} \rangle = \frac{1}{(2\pi)^2 a^3} \int_0^\infty k^2 dk \, \rho_k(\tau) \ ,$$

for the CPT-invariant vacuum states characterized by Θ_k (for details on $\langle T_{\mu\nu} \rangle_{ren}$ for Dirac fields in spatially flat FLRW backgrounds, see Ref. [87]). By employing the techniques presented in [190], we determine the expansion.

$$\begin{aligned} m^{-1}\rho_k(\tau) \quad &\sim \cos(2\Theta_k)\left(-\tfrac{2k}{\gamma\tau} - \tfrac{\gamma\tau}{k} + \tfrac{\gamma}{2k^3\tau} + \tfrac{\gamma^3\tau^3}{4k^3} - \tfrac{\gamma\cos(2k\tau)}{2k^3\tau} + \mathcal{O}\left(\tfrac{\sin(2k\tau)}{k^4}\right) \right) \\ &+ \sin(2\Theta_k)\left(\tfrac{1}{k\tau} + \tfrac{\gamma^2\tau}{2k^3} - \tfrac{\cos(2k\tau)}{k\tau} + \tfrac{\gamma^2\tau^2\sin(2k\tau)}{3k^2} + \mathcal{O}\left(\tfrac{\cos(2\kappa\tau)}{k^3}\right) \right) . \end{aligned} \tag{B.1}$$

This expression has to be compared with the large k expansion of the adiabatic expansion of the energy density up to and including the second adiabatic order (the 4th adiabatic order is finite for spin-1/2 fields) , namely

$$m^{-1}\rho_k(\tau)^{ad} \sim -\frac{2k}{\gamma\tau} - \frac{\gamma\tau}{k} + \frac{\gamma}{4k^3\tau} - \frac{\gamma^3\tau^3}{4k^3} + \mathcal{O}\left(\frac{1}{k^5}\right) . \tag{B.2}$$

In this case, this means to find coincidence with the adiabatic expansion up to and including order $\mathcal{O}(k^{-3})$.[1] We directly see that, for $\Theta_k = 0$, there is one term in (B.1), $\gamma/(2k^3\tau)$, that does not coincide with the adiabatic expansion, generating a logarithmic divergence after renormalization. On the contrary, for $\Theta_k \sim -\frac{\gamma}{4k^2}$, and using the large k expansion of the trigonometric functions, we see that the part proportional to $\sin(2\Theta_k)$ contributes to the large k expansion in such a way that we recover the adiabatic expansion (B.2), making the energy density UV regular. Furthermore, in this case we find also cancellations for the oscillatory terms. We have also performed a similar analysis with the two-point function and the pressure, finding analogous results. We have found that, to ensure the convergence of these three quantities, the trigonometric phase should behave, at large k, as $\Theta_k \sim -\frac{\gamma}{4k^2} + \mathcal{O}(k^{-n}),\ n > 2$.

[1] Note that, $\langle\rho\rangle \propto \int dk\, k^2 \rho_k(\tau)$, and therefore, a term going as $\sim k^{-3}$ generates a logarithmic divergence.

Appendix C

Analytic correlations

In this appendix, we provide some of the details that have been omitted in section 7.1. In particular, we compute the components of the covariance matrix for a system consisting of N spacelike separated modes of a scalar field in $D+1$-dimensional Minkowski spacetime. We assume that the N-modes are supported in spacelike separated spherically symmetric regions of radius R. For simplicity, all the modes we consider are extracted using the same smearing function, which in addition we take to belong to the family presented in Eq. (7.2), that is

$$\hat{\Phi}_i = \int \mathrm{d}^D x \, f_i^{(\delta)}(\vec{x}) \, \hat{\phi}(\vec{x}) \,, \tag{C.1}$$

and

$$\hat{\Pi}_i = c \int \mathrm{d}^D x \, f_i^{(\delta)}(\vec{x}) \, \hat{\pi}(\vec{x}) \,, \tag{C.2}$$

with $i = 1, \ldots, N$ and such that $|\Delta\vec{x}_{ij}| > 2\,R$ for every $i \neq j$ (to ensure that the regions are truly disjoint).

Imposing canonical commutation relations between the operator pairs $(\hat{\Phi}_i, \hat{\Pi}_i)_{i=1,\ldots,N}$ (that is, $[\hat{\Phi}_i, \hat{\Pi}_j] = i\delta_{ij}$) allows us to compute the normalization constant A_δ for any dimension,

$$A_\delta = c^{-1/2}\, R^{-D/2} \pi^{-D/4} \sqrt{\frac{\Gamma(1 + D/2 + 2\delta)}{\Gamma(1 + 2\delta)}} \,. \tag{C.3}$$

As we already mentioned, one of the advantages of the functions (7.2) is that their D-dimensional Fourier transform has a simple expression in terms of Bessel functions. In particular, we find (see Theorem. 4.15 in Sec. IV.4 of [191])

$$\begin{aligned}\tilde{f}_i^{(\delta)}(\vec{k}) &= \int \mathrm{d}^D x\, \mathrm{e}^{i\vec{k}\cdot\vec{x}} f_i^{(\delta)}(\vec{x}) \\ &= \mathrm{e}^{i\vec{k}\cdot\vec{x}_i} A_\delta \Gamma(\delta+1) 2^\delta (2\pi)^{\frac{D}{2}} (kR)^{-(\frac{D}{2}+\delta)}\, J_{\frac{D}{2}+\delta}(kR)\,,\end{aligned}$$

where $J_{\frac{D}{2}+\delta}(kR)$ is the Bessel function of the first kind of order $\frac{D}{2}+\delta$. The relevant two-point functions in the Minkowski vacuum can be computed straightforwardly, and one finds

$$\langle\{\hat{\Phi}_i, \hat{\Phi}_j\}\rangle = R^{D+1} \int \frac{\mathrm{d}^D q}{(2\pi)^D} \frac{|\tilde{f}_i^{(\delta)}(q)|^2\, e^{i\vec{q}\cdot\vec{\rho}_{ij}}}{\sqrt{q^2+\mu^2}}\,,$$

$$\langle\{\hat{\Pi}_i, \hat{\Pi}_j\}\rangle = c^2 R^{D-1} \int \frac{\mathrm{d}^D q}{(2\pi)^D} |\tilde{f}_i^{(\delta)}(q)|^2\, e^{i\vec{q}\cdot\vec{\rho}_{ij}} \sqrt{q^2+\mu^2}\,,$$

and

$$\langle\{\hat{\Phi}_i, \hat{\Pi}_j\}\rangle = 0\,,$$

where $\vec{q} = R\vec{k}$, $\vec{\rho}_{ij} = \frac{\Delta\vec{x}_{ij}}{R} = \frac{\vec{x}_i - \vec{x}_j}{R}$ is the dimensionless distance between the centers of the spherical regions centered at $\vec{x}_i$ and $\vec{x}_j$, and $\mu = m\,R$ is the dimensionless mass.

Interestingly, in the massless limit ($\mu = 0$) the integrals in the correlation functions above can be solved analytically using the following integrals:

$$\int_0^\infty dt\, t^{-\beta} J_\nu(\alpha t) J_\mu(\alpha t) = \frac{\alpha^{\beta-1}\Gamma(\beta)\Gamma\left(\frac{\nu+\mu-\beta+1}{2}\right)}{2^\beta \Gamma\left(\frac{-\nu+\mu+\beta+1}{2}\right)\Gamma\left(\frac{\nu+\mu+\beta+1}{2}\right)\Gamma\left(\frac{\nu-\mu+\beta+1}{2}\right)}\,, \quad \text{(C.4)}$$

if $\mathrm{Re}(\nu+\mu+1) > \mathrm{Re}\,\beta > 0$, $\alpha > 0$ (Eq. 6.574.2 in [192]) and

$$\begin{aligned}&\int_0^\infty dt\, t^{\beta-1} J_\alpha(at) J_\mu(bt) J_\nu(ct) = \\ &\frac{2^{\beta-1} a^\alpha b^\mu c^{-\alpha-\mu-\beta}\Gamma\left(\frac{\alpha+\mu+\nu+\beta}{2}\right)}{\Gamma(\alpha+1)\Gamma(\mu+1)\Gamma\left(1-\frac{\alpha+\mu-\nu+\beta}{2}\right)} \\ &\times F_4\left(\frac{\alpha+\mu-\nu+\beta}{2}, \frac{\alpha+\mu+\nu+\beta}{2}; \alpha+1, \mu+1; \frac{a^2}{c^2}, \frac{b^2}{c^2}\right)\,,\end{aligned}$$

which holds if $\mathrm{Re}(\alpha+\mu+\nu+\beta)>0$, $\mathrm{Re}\beta<\frac{5}{2}$, $a>0$, $b>0$, $c>0$ and $c>a+b$ (Eq. 6.578.1 in [192]) where

$$F_4(\alpha,\beta,\gamma,\gamma';x,y)=\sum_{m=0}^{\infty}\sum_{n=0}^{\infty}\frac{(\alpha)_{m+n}(\beta)_{m+n}}{(\gamma)_m(\gamma')_n m!n!}x^m y^n\,, \tag{C.5}$$

with $|\sqrt{x}|+|\sqrt{y}|<1$, is the Appell hypergeometric function of the fourth kind [1]. Using Eqs. (C.4) and (C.5), the two point correlations in the massless limit ($\mu=0$) can be written as

$$\langle\{\hat{\Phi}_i,\hat{\Phi}_j\}\rangle=2N_\delta^2\,\frac{R}{c}\begin{cases}\mathcal{J}^D(-1,\delta) & i=j\\ \mathcal{L}^D(-1,\delta,\rho_{ij}) & i\neq j\end{cases}, \tag{C.6}$$

$$\langle\{\hat{\Pi}_i,\hat{\Pi}_j\}\rangle=2N_\delta^2\,\frac{c}{R}\begin{cases}\mathcal{J}^D(1,\delta) & i=j\\ \mathcal{L}^D(1,\delta,\rho_{ij}) & i\neq j\end{cases}, \tag{C.7}$$

where

$$\mathcal{J}^D(\lambda,\delta)=2^{-1-2\delta+\lambda}\frac{\Gamma\left(\frac{D+\lambda}{2}\right)\Gamma\left(1+2\delta-\lambda\right)}{\Gamma\left(1+\delta-\frac{\lambda}{2}\right)^2\Gamma\left(\frac{D-\lambda}{2}+2\delta+1\right)}\,, \tag{C.8}$$

$$\begin{aligned}\mathcal{L}^D(\lambda,\delta,\rho)=&\rho^{-(D+\lambda)}\frac{\Gamma\left(\frac{D+\lambda}{2}\right)\Gamma\left(D/2\right)}{2^{1+2\delta-\lambda}\Gamma\left(\frac{D}{2}+1+\delta\right)^2\Gamma\left(-\frac{\lambda}{2}\right)}\times\\ &{}_3F_2\left[\begin{matrix}1+\frac{\lambda}{2},\frac{D+\lambda}{2},\frac{D+1}{2}+\delta\\ \frac{D}{2}+1+\delta,D+1+2\delta\end{matrix};\frac{4}{\rho^2}\right]\,,\end{aligned} \tag{C.9}$$

and

$$N_\delta^2=\frac{2^{2\delta}\Gamma\left(1+\frac{D}{2}+2\delta\right)\Gamma\left(1+\delta\right)^2}{\Gamma\left(1+2\delta\right)\Gamma\left(D/2\right)}\,. \tag{C.10}$$

[1] Notice that when $x=y$ and $\gamma_1=\gamma_2$, this function reduces to a generalized hypergeometric function, that is $F_4(\alpha,\beta,\gamma,\gamma,x,x)={}_3F_2\left(\alpha,\beta,\gamma-\frac{1}{2};\gamma,2\gamma-1;4x\right)$

Appendix D

The symplectic Gram-Schmidth orthonormalization algorithm

In this appendix, we give details of the symplectic orthonormalization algorithm that we implicitly used in section 8.4 to obtain a canonical system of N independent modes (i.e commutative) from the continuous t-family of modes associated to the time evolution of a field degree of freedom $(\hat{\phi}[f](t), \hat{\pi}[f](t))$ in an interval of time ΔT.

The N-modes,

$$\left\{\gamma_{\phi,t_n} \equiv E^{-1}_{t_n,t_0}\gamma_\phi \ , \ \gamma_{\pi,t_n} \equiv E^{-1}_{t_n,t_0}\gamma_\pi\right\}_{n=0\cdots N-1} , \tag{D.1}$$

that we obtained in section 8.3.3, from (8.47), are not orthonormal, in the sense that $\langle\gamma_{\phi(\pi),t_l}, \gamma_{\phi(\pi),t_m}\rangle_\Omega := \Omega_{ij}\gamma^i_{\phi(\pi),t_l}\gamma^j_{\phi(\pi),t_m} \neq 0$ and $\langle\gamma_{\phi,t_l}, \gamma_{\pi,t_m}\rangle_\Omega \neq \delta_{lm}$. In particular, for the initial data (8.36) and (8.37) we can obtain these products analytically, for example,

$$\begin{aligned}\langle\gamma_{\phi,t_i},\gamma_{\phi,t_j}\rangle_\Omega := \Omega_{\alpha\beta}\gamma^\alpha_{\phi,t_i}\gamma^\beta_{\phi,t_j} = -2^{2\delta+2}\pi R^3\, A_\delta^2\,\Gamma(\delta+1)^2\,\Delta t\,\Theta\left(2-\left|\frac{\Delta t}{R}\right|\right)\times \\ \left(\frac{\sin(\pi\delta)\Gamma(-2\delta-2)}{\pi}\left|\frac{\Delta t}{R}\right|^{2\delta+1}{}_2F_1\left(\frac{1}{2},-\delta-1;\delta+\frac{3}{2};\frac{\Delta t^2}{4R^2}\right)\right. \\ \left.+\frac{\Gamma\left(\delta+\frac{1}{2}\right)}{4\Gamma(\delta+1)\Gamma\left(2\delta+\frac{5}{2}\right)}\,{}_2F_1\left(-2\delta-\frac{3}{2},-\delta;\frac{1}{2}-\delta;\frac{\Delta t^2}{4R^2}\right)\right)\,,\end{aligned} \tag{D.2}$$

we obtain similar involved expressions for the other modes. We can use these modes and products to find a symplectically orthonormal basis of N modes from which one can compute multi-mode entanglement. We do so using the symplectic Gram-Schmidt orhtonormalization algorithm described in Appendix A of [193]. For completeness, we briefly review the workings of this algorithm.

We use the following notation for the different basis entering the algorithm:

- Initial basis: $\{\gamma_{\phi,i},\gamma_{\pi,i}\}_{i=1,\dots,N}$.
- Symplectically orthogonal basis (auxiliary): $\{\xi_{\phi,i},\xi_{\pi,i}\}_{i=1,\dots,N}$
- Symplectic orthonormal basis: $\{\tilde\gamma_{\phi,i},\tilde\gamma_{\pi,i}\}_{i=1,\dots,N}$

The first element of the orthonormal basis is obtained from the initial basis by the following normalization:

$$\tilde\gamma_{\phi,1}=\frac{\gamma_{\phi,1}}{\sqrt{|A|}}\,,\quad \tilde\gamma_{\pi,1}=\frac{\gamma_{\pi,1}}{\mathrm{sign}(A)\sqrt{|A|}}\,,\quad A=\langle\gamma_{\Phi,1},\gamma_{\pi,1}\rangle_\Omega$$

Subsequent elements of the orthogonal basis are computed by removing the projective contributions of the elements of the initial basis with respect to the orthogonal basis,

$$\xi_{z,k}=\gamma_{z,k}-\sum_{j=1}^{k-1}\left[\langle\tilde\gamma_{\phi,j},\gamma_{z,k}\rangle_\Omega\,\tilde\gamma_{\pi,j}-\langle\tilde\gamma_{\pi,j},\gamma_{z,k}\rangle_\Omega\,\tilde\gamma_{\phi,j}\right]\,,$$

with $z\in\{\phi,\pi\}$, indicating that the symplectic orthogonalization applies equivalently for the position and momentum vectors. Finally, the elements of the orthonormal basis are computed by normalizing the elements of the auxiliary basis:

$$\tilde{\gamma}_{\phi,k} = \frac{\xi_{\phi,k}}{\sqrt{A}}\,, \quad \tilde{\gamma}_{\pi,k} = \frac{\xi_{\pi,k}}{\mathrm{sign}(A)\sqrt{A}}\,, \quad A = \langle \xi_{\phi,k}, \xi_{\pi,k} \rangle_\Omega$$

Note that orthogonalizing the modes in Eqs. (8.46) - (8.47) by using the symplectic Gram-Schmidt algorithm and then Fourier transforming the orthonormal modes, is equivalent to symplectically orthogonalizing their Fourier transforms, thanks to the linearity of the Fourier transform and Parseval's identity. In practice, we use the second method.

Finally, we notice that the orthogonalization process does not change the entanglement between the two detectors, since all the operations we perform on the original set of modes are system local.

Bibliography

[1] M. D. Schwartz, Quantum field theory and the standard model.
Cambridge university press, 2014.

[2] R. M. Wald, General Relativity.
Chicago Univ. Pr., Chicago, USA, 1984.

[3] J. Polchinski, String theory.
2005.

[4] C. Rovelli, Quantum gravity.
Cambridge university press, 2004.

[5] A. Ashtekar and E. Bianchi, "A short review of loop quantum gravity," Reports on Progress in Physics **84** (2021), no. 4, 042001.

[6] L. Parker, The creation of particles in an expanding universe.
PhD thesis, Harvard University, 1966.

[7] L. E. Parker and D. Toms, Quantum Field Theory in Curved Spacetime: Quantized Field and Gravity.
Cambridge Monographs on Mathematical Physics. Cambridge University Press, 8, 2009.

[8] N. D. Birrell and P. C. W. Davies, Quantum Fields in Curved Space.
Cambridge Monographs on Mathematical Physics. Cambridge Univ. Press, Cambridge, UK, 2, 1984.

[9] R. M. Wald,
Quantum Field Theory in Curved Space-Time and Black Hole Thermodynamics

Chicago Lectures in Physics. University of Chicago Press, Chicago, IL, 1995.

[10] L. Parker, "Particle creation in expanding universes," Phys. Rev. Lett. **21** (1968) 562–564.

[11] L. Parker, "Quantized fields and particle creation in expanding universes. 1.," Phys. Rev. **183** (1969) 1057–1068.

[12] N. Aghanim, Y. Akrami, M. Ashdown, J. Aumont, C. Baccigalupi, M. Ballardini, A. J. Banday, R. Barreiro, N. Bartolo, S. Basak, et al., "Planck 2018 results-VI. Cosmological parameters," Astronomy & Astrophysics **641** (2020) A6.

[13] S. Weinberg, Cosmology.
Oxford University Press, 2008.

[14] S. W. Hawking, "Particle Creation by Black Holes," Commun. Math. Phys. **43** (1975) 199–220. [Erratum: Commun.Math.Phys. 46, 206 (1976)].

[15] E. Martín-Martínez, "Relativistic Quantum Information: developments in Quantum Information in general relativistic scenarios," arXiv preprint arXiv:1106.0280 (2011).

[16] R. Horodecki, P. Horodecki, M. Horodecki, and K. Horodecki, "Quantum entanglement," Rev. Mod. Phys. **81** (Jun, 2009) 865–942.

[17] V. Vedral, "The role of relative entropy in quantum information theory," Rev. Mod. Phys. **74** (Mar, 2002) 197–234.

[18] B. Swingle, "Spacetime from entanglement," Annual Review of Condensed Matter Physics **9** (2018) 345–358.

[19] M. Van Raamsdonk, "Building up space–time with quantum entanglement," International Journal of Modern Physics D **19** (2010), no. 14, 2429–2435.

[20] E. Bianchi and E. R. Livine, "Loop Quantum Gravity and Quantum Information," arXiv preprint arXiv:2302.05922 (2023).

[21] N. Laflorencie, "Quantum entanglement in condensed matter systems," Physics Reports **646** (2016) 1–59.

[22] A. Kitaev and J. Preskill, "Topological Entanglement Entropy," Phys. Rev. Lett. **96** (Mar, 2006) 110404.

[23] G. Vidal, J. I. Latorre, E. Rico, and A. Kitaev, "Entanglement in Quantum Critical Phenomena," Phys. Rev. Lett. **90** (Jun, 2003) 227902.

[24] E. Witten, "APS Medal for Exceptional Achievement in Research: Invited article on entanglement properties of quantum field theory," Rev. Mod. Phys. **90** (Oct, 2018) 045003.

[25] H. Reeh and S. Schlieder, "Bemerkungen zur unitäräquivalenz von lorentzinvarianten feldern," Il Nuovo Cimento (1955-1965) **22** (1961), no. 5, 1051–1068.

[26] S. J. Summers and R. Werner, "Bell's Inequalities and Quantum Field Theory. 1. General Setting," J. Math. Phys. **28** (1987) 2440–2447.

[27] J. Preskill, "Do black holes destroy information," in Proceedings of the International Symposium on Black Holes, Membranes, Wormholes and Superstrings, S. Kalara and DV Nanopoulos, eds.(World Scientific, Singapore, 1993) pp, pp. 22–39, World Scientific. 1992.

[28] S. W. Hawking, "Information loss in black holes," Phys. Rev. D **72** (Oct, 2005) 084013.

[29] S. L. Braunstein, S. Pirandola, and K. Życzkowski, "Better Late than Never: Information Retrieval from Black Holes," Phys. Rev. Lett. **110** (Mar, 2013) 101301.

[30] J. e. Martin and V. Vennin, "Real-space entanglement in the Cosmic Microwave Background," JCAP **10** (2021) 036, `arXiv:2106.15100`.

[31] I. Agullo, B. Bonga, and P. R. Metidieri, "Does inflation squeeze cosmological perturbations?," JCAP **09** (2022) 032, `arXiv:2203.07066`.

[32] E. Martín-Martínez, E. G. Brown, W. Donnelly, and A. Kempf, "Sustainable entanglement production from a quantum field," Phys. Rev. A **88** (Nov, 2013) 052310.

[33] K. Yamaguchi, A. Ahmadzadegan, P. Simidzija, A. Kempf, and E. Martín-Martínez, "Superadditivity of channel capacity through quantum fields," Phys. Rev. D **101** (May, 2020) 105009.

[34] M. Hotta, "Quantum energy teleportation in spin chain systems," Journal of the Physical Society of Japan **78** (2009), no. 3, 034001.

[35] P. Candelas, "Vacuum polarization in Schwarzschild spacetime," Physical Review D **21** (1980), no. 8, 2185.

[36] A. Levi and A. Ori, "Pragmatic mode-sum regularization method for semiclassical black-hole spacetimes," Physical Review D **91** (2015), no. 10, 104028.

[37] A. Levi and A. Ori, "Mode-sum regularization of¡ ϕ 2¿ in the angular-splitting method," Physical Review D **94** (2016), no. 4, 044054.

[38] L. Parker and S. A. Fulling, "Adiabatic regularization of the energy momentum tensor of a quantized field in homogeneous spaces," Phys. Rev. D **9** (1974) 341–354.

[39] S. A. Fulling and L. Parker, "Renormalization in the theory of a quantized scalar field interacting with a robertson-walker spacetime," Annals Phys. **87** (1974) 176–204.

[40] S. A. Fulling, L. Parker, and B. L. Hu, "Conformal energy-momentum tensor in curved spacetime: Adiabatic regularization and renormalization," Phys. Rev. D **10** (1974) 3905–3924.

[41] A. Degner and R. Verch, "Cosmological particle creation in states of low energy," J. Math. Phys. **51** (2010) 022302, `arXiv:0904.1273`.

[42] M. Martín-Benito, R. B. Neves, and J. Olmedo, "States of Low Energy in bouncing inflationary scenarios in Loop Quantum Cosmology," Phys. Rev. D **103** (2021) 123524, `arXiv:2104.03035`.

[43] H. Olbermann, "States of low energy on Robertson-Walker spacetimes," Class. Quant. Grav. **24** (2007) 5011–5030, `arXiv:0704.2986`.

[44] L. Boyle, K. Finn, and N. Turok, "The Big Bang, CPT, and neutrino dark matter," Annals Phys. **438** (2022) 168767, `arXiv:1803.08930`.

[45] L. Boyle, K. Finn, and N. Turok, "CPT-Symmetric Universe," Phys. Rev. Lett. **121** (2018), no. 25, 251301, `arXiv:1803.08928`.

[46] R. Verch and R. F. Werner, "Distillability and positivity of partial transposes in general quantum field systems," Rev. Math. Phys. **17** (2005) 545–576.

[47] S. Hollands and K. Sanders, "Entanglement measures and their properties in quantum field theory," `arXiv:1702.04924`.

[48] A. Valentini, "Non-local correlations in quantum electrodynamics," Physics Letters A **153** (1991), no. 6-7, 321–325.

[49] B. Reznik, "Entanglement from the vacuum," Foundations of Physics **33** (2003) 167–176.

[50] B. Reznik, A. Retzker, and J. Silman, "Violating Bell's inequalities in vacuum," Physical Review A **71** (2005), no. 4, 042104.

[51] A. Pozas-Kerstjens and E. Martín-Martínez, "Entanglement harvesting from the electromagnetic vacuum with hydrogenlike atoms," Physical Review D **94** (2016), no. 6, 064074.

[52] T. R. Perche, C. Lima, and E. Martín-Martínez, "Harvesting entanglement from complex scalar and fermionic fields with linearly coupled particle detectors," Physical Review D **105** (2022), no. 6, 065016.

[53] K. Gallock-Yoshimura, E. Tjoa, and R. B. Mann, "Harvesting entanglement with detectors freely falling into a black hole," Physical Review D **104** (2021), no. 2, 025001.

[54] J. Audretsch and G. Schaefer, "Thermal Particle Production in a Radiation Dominated Robertson-Walker Universe," J. Phys. A **11** (1978) 1583–1602.

[55] M. H. Ruep, "Weakly coupled local particle detectors cannot harvest entanglement," Classical Quantum Gravity **38** (2021), no. 19, 195029.

[56] A. Pozas-Kerstjens and E. Martin-Martinez, "Harvesting correlations from the quantum vacuum," Physical Review D **92** (2015), no. 6, 064042.

[57] A. Fabbri and J. Navarro-Salas, Modeling black hole evaporation. Imperial College Press-World Scientific, London, 2005.

[58] L. Parker, "Quantized fields and particle creation in expanding universes. 2.," Phys. Rev. D **3** (1971) 346–356. [Erratum: Phys.Rev.D 3, 2546–2546 (1971)].

[59] S. A. Fulling, "Nonuniqueness of canonical field quantization in riemannian space-time," Physical Review D **7** (1973), no. 10, 2850.

[60] P. C. Davies, "Scalar production in schwarzschild and rindler metrics," Journal of Physics A: Mathematical and General **8** (1975), no. 4, 609.

[61] W. G. Unruh, "Notes on black-hole evaporation," Physical Review D **14** (1976), no. 4, 870.

[62] R. M. Wald, "EXISTENCE OF THE S MATRIX IN QUANTUM FIELD THEORY IN CURVED SPACE-TIME," Annals Phys. **118** (1979) 490–510.

[63] S. A. Fulling, Aspects of Quantum Field Theory in Curved Space-time, vol. 17.
Cambridge University Press, 1989.

[64] R. M. Wald, "On particle creation by black holes," Communications in Mathematical Physics **45** (1975), no. 1, 9–34.

[65] B. S. DeWitt, "Quantum Field Theory in Curved Space-Time," Phys. Rept. **19** (1975) 295–357.

[66] B. S. DeWitt, "Dynamical theory of groups and fields," Conf. Proc. C **630701** (1964) 585–820.

[67] S. M. Christensen, "Vacuum expectation value of the stress tensor in an arbitrary curved background: The covariant point-separation method," Physical Review D **14** (1976), no. 10, 2490.

[68] S. Christensen, "Regularization, renormalization, and covariant geodesic point separation," Physical Review D **17** (1978), no. 4, 946.

[69] B. S. Dewitt, "Covariant quantum geometrodynamics," Magic Without Magic: John Archibald Wheeler (1972) 409.

[70] D. Bernard and A. Folacci, "Hadamard function, stress tensor, and de Sitter space," Physical Review D **34** (1986), no. 8, 2286.

[71] R. Brunetti and K. Fredenhagen, "Microlocal analysis and interacting quantum field theories: Renormalization on physical backgrounds," Commun. Math. Phys. **208** (2000) 623–661, `arXiv:math-ph/9903028`.

[72] S. Hollands and R. M. Wald, "Local Wick polynomials and time ordered products of quantum fields in curved space-time," Commun. Math. Phys. **223** (2001) 289–326, `arXiv:gr-qc/0103074`.

[73] S. Hollands and R. M. Wald, "Existence of local covariant time ordered products of quantum fields in curved space-time," Commun. Math. Phys. **231** (2002) 309–345, `arXiv:gr-qc/0111108`.

[74] P. Candelas and K. Howard, "Vacuum¡ φ 2¿ in Schwarzschild spacetime," Physical Review D **29** (1984), no. 8, 1618.

[75] K. W. Howard and P. Candelas, “Quantum stress tensor in Schwarzschild space-time,” Physical review letters **53** (1984), no. 5, 403.

[76] K. W. Howard, “Vacuum¡ T μ ν¿ in Schwarzschild spacetime,” Physical Review D **30** (1984), no. 12, 2532.

[77] P. R. Anderson, “A method to compute¡ φ 2¿ in asymptotically flat, static, spherically symmetric spacetimes,” Physical Review D **41** (1990), no. 4, 1152.

[78] P. R. Anderson, W. A. Hiscock, and D. A. Samuel, “Stress-energy tensor of quantized scalar fields in static black hole spacetimes,” Physical review letters **70** (1993), no. 12, 1739.

[79] S. Khatri and M. M. Wilde, “Principles of Quantum Communication Theory: A Modern Approach,” 2020.

[80] A. Levi, “Renormalized stress-energy tensor for stationary black holes,” Physical Review D **95** (2017), no. 2, 025007.

[81] A. Lanir, A. Levi, A. Ori, and O. Sela, “Two-point function of a quantum scalar field in the interior region of a Reissner-Nordstrom black hole,” Physical Review D **97** (2018), no. 2, 024033.

[82] A. Lanir, A. Levi, and A. Ori, “Mode-sum renormalization of¡ Φ 2¿ for a quantum scalar field inside a Schwarzschild black hole,” Physical Review D **98** (2018), no. 8, 084017.

[83] A. Lanir, A. Ori, N. Zilberman, O. Sela, A. Maline, and A. Levi, “Analysis of quantum effects inside spherical charged black holes,” Physical Review D **99** (2019), no. 6, 061502.

[84] N. Zilberman, A. Levi, and A. Ori, “Quantum fluxes at the inner horizon of a spherical charged black hole,” Physical Review Letters **124** (2020), no. 17, 171302.

[85] A. Landete, J. Navarro-Salas, and F. Torrenti, “Adiabatic regularization for spin-1/2 fields,” Phys. Rev. D **88** (2013) 061501, `arXiv:1305.7374`.

[86] A. Landete, J. Navarro-Salas, and F. Torrenti, “Adiabatic regularization and particle creation for spin one-half fields,” Phys. Rev. D **89** (2014) 044030, `arXiv:1311.4958`.

[87] A. del Rio, J. Navarro-Salas, and F. Torrenti, "Renormalized stress-energy tensor for spin-1/2 fields in expanding universes," Phys. Rev. D **90** (2014), no. 8, 084017, `arXiv:1407.5058`.

[88] J. F. Barbero G., A. Ferreiro, J. Navarro-Salas, and E. J. S. Villaseñor, "Adiabatic expansions for Dirac fields, renormalization, and anomalies," Phys. Rev. D **98** (2018), no. 2, 025016, `arXiv:1805.05107`.

[89] F. J. Marañón González and J. Navarro-Salas, "Adiabatic regularization for spin-1 fields," Phys. Rev. D **108** (2023), no. 12, 125001, `arXiv:2310.11860`.

[90] J. S. Schwinger, "On gauge invariance and vacuum polarization," Phys. Rev. **82** (1951) 664–679.

[91] L. Brewin, "Riemann normal coordinate expansions using Cadabra," Classical and Quantum Gravity **26** (2009), no. 17, 175017.

[92] P. R. Anderson and L. Parker, "Adiabatic regularization in closed Robertson-Walker universes," Phys. Rev. D **36** (Nov, 1987) 2963–2969.

[93] N. Birrell, "The application of adiabatic regularization to calculations of cosmological interest," Proceedings of the Royal Society of London. A. Mathematical and Physical Sciences **361** (1978), no. 1707, 513–526.

[94] B. Hu and L. Parker, "Anisotropy damping through quantum effects in the early universe," Physical Review D **17** (1978), no. 4, 933.

[95] P. R. Anderson, "Effects of quantum fields on singularities and particle horizons in the early universe. III. The conformally coupled massive scalar field," Physical Review D **32** (1985), no. 6, 1302.

[96] S. Habib, C. Molina-Paris, and E. Mottola, "Energy-momentum tensor of particles created in an expanding universe," Physical Review D **61** (1999), no. 2, 024010.

[97] P. R. Anderson, C. Molina-Paris, D. Evanich, and G. B. Cook, "Study of the preheating phase of chaotic inflation," Physical Review D **78** (2008), no. 8, 083514.

[98] I. Agulló, J. Navarro-Salas, G. J. Olmo, and L. Parker, "Revising the predictions of inflation for the cosmic microwave background anisotropies," Physical review letters **103** (2009), no. 6, 061301.

[99] J. D. Bates and P. R. Anderson, "Effects of quantized scalar fields in cosmological spacetimes with big rip singularities," Physical Review D **82** (2010), no. 2, 024018.

[100] A. Ferreiro and J. Navarro-Salas, "Running gravitational couplings, decoupling, and curved spacetime renormalization," Physical Review D **102** (2020), no. 4, 045021.

[101] A. Ferreiro, S. Nadal-Gisbert, and J. Navarro-Salas, "Renormalization, running couplings, and decoupling for the Yukawa model in a curved spacetime," Phys. Rev. D **104** (2021), no. 2, 025003, `arXiv:2104.14318`.

[102] K.-T. Pirk, "Hadamard states and adiabatic vacua," Phys. Rev. D **48** (1993) 3779–3783, `arXiv:gr-qc/9211003`.

[103] S. Hollands, "The Hadamard condition for Dirac fields and adiabatic states on Robertson-Walker space-times," Commun. Math. Phys. **216** (2001) 635–661, `arXiv:gr-qc/9906076`.

[104] A. A. Grib, S. G. Mamaev, and V. M. Mostepanenko, "Particle Creation from Vacuum in Homogeneous Isotropic Models of the Universe," Gen. Rel. Grav. **7** (1976) 535–547.

[105] S. G. Mamaev, V. M. Mostepanenko, and A. A. Starobinsky, "Particle Creation from Vacuum Near an Homogeneous Isotropic Singularity," Zh. Eksp. Teor. Fiz. **70** (1976) 1577–1591.

[106] D. M. Chitre and J. B. Hartle, "Path Integral Quantization and Cosmological Particle Production: An Example," Phys. Rev. D **16** (1977) 251–260.

[107] S. A. Fulling, "Remarks on positive frequency and Hamiltonians in expanding universes," Gen. Rel. Grav. **10** (1979) 807–824.

[108] P. R. Anderson, C. Molina-Paris, and E. Mottola, "Short distance and initial state effects in inflation: Stress tensor and decoherence," Phys. Rev. D **72** (2005) 043515, `arXiv:hep-th/0504134`.

[109] I. Agullo, W. Nelson, and A. Ashtekar, "Preferred instantaneous vacuum for linear scalar fields in cosmological space-times," Phys. Rev. D **91** (2015) 064051, `arXiv:1412.3524`.

[110] R. Banerjee and M. Niedermaier, "Bonus properties of states of low energy," J. Math. Phys. **61** (2020), no. 10, 103511, `arXiv:2006.08685`.

[111] M. Martín-Benito, R. B. Neves, and J. Olmedo, "Non-Oscillatory Power Spectrum From States of Low Energy in Kinetically Dominated Early Universes," Front. Astron. Space Sci. **0** (2021) 133, arXiv:2104.14850.

[112] A. Álvarez-Domínguez, L. J. Garay, M. Martín-Benito, and R. B. Neves, "States of low energy in the Schwinger effect," JHEP **06** (2023) 093, arXiv:2303.15294.

[113] A. Ferreiro and S. Pla, "Instantaneous vacuum and States of Low Energy for a scalar field in cosmological backgrounds," J. Phys. Conf. Ser. **2531** (2023), no. 1, 012008, arXiv:2303.18074.

[114] R. Banerjee and M. Niedermaier, "States of Low Energy on Bianchi I spacetimes," J. Math. Phys. **64** (2023), no. 11, 113503, arXiv:2305.11388.

[115] A. Ashtekar, T. De Lorenzo, and M. Schneider, "Probing the Big Bang with quantum fields," Adv. Theor. Math. Phys. **25** (2021), no. 7, 1651–1702, arXiv:2107.08506.

[116] P. R. Anderson, E. D. Carlson, T. M. Ordines, and B. Hicks, "Semiclassical predictions regarding a preinflationary era and its effects on the power spectrum," Phys. Rev. D **102** (2020), no. 6, 063528, arXiv:2005.12370.

[117] S. Das, G. Goswami, J. Prasad, and R. Rangarajan, "Revisiting a pre-inflationary radiation era and its effect on the CMB power spectrum," JCAP **06** (2015) 001, arXiv:1412.7093.

[118] T. M. Ordines and E. D. Carlson, "Argument for the radiation-dominated behavior of matter fields in the preinflationary era," Phys. Rev. D **106** (2022), no. 10, 103537, arXiv:2209.01056.

[119] R. Penrose, "Singularities and time-asymmetry," in General Relativity: An Einstein Centenary Survey, pp. 581–638. Cambridge University Press, 1979.

[120] R. Penrose, "Gravitational collapse: The role of general relativity," Riv. Nuovo Cim. **1** (1969) 252–276.

[121] R. P. A. C. Newman, "On the Structure of conformal singularities in classical general relativity. 2. Evolution equations and a conjecture of K.P. Tod," Proc. Roy. Soc. Lond. A **443** (1993) 493–515.

[122] M. Abramowitz and I. A. Stegun, Handbook of Mathematical Functions with Formulas, Graphs and Mathematical Tables. Dover Publications, 1964.

[123] L. Alvarez-Gaume and M. A. Vazquez-Mozo, An invitation to quantum field theory, vol. 839. Springer-Verlag, Berlin, 2012.

[124] S. Weinberg, The Quantum theory of fields. Vol. 1: Foundations. Cambridge University Press, 6, 2005.

[125] L. H. Ford, "Cosmological particle production: a review," Rept. Prog. Phys. **84** (2021), no. 11, 116901, `arXiv:2112.02444`.

[126] L. Parker and S. A. Fulling, "Quantized matter fields and the avoidance of singularities in general relativity," Phys. Rev. D **7** (1973) 2357–2374.

[127] L. H. Ford, "Gravitational Particle Creation and Inflation," Phys. Rev. D **35** (1987) 2955.

[128] D. J. H. Chung, E. W. Kolb, and A. Riotto, "Superheavy dark matter," Phys. Rev. D **59** (1998) 023501, `arXiv:hep-ph/9802238`.

[129] P. R. Anderson, E. Mottola, and D. H. Sanders, "Decay of the de Sitter Vacuum," Phys. Rev. D **97** (2018), no. 6, 065016, `arXiv:1712.04522`.

[130] M. R. R. Good, P. R. Anderson, and C. R. Evans, "Time Dependence of Particle Creation from Accelerating Mirrors," Phys. Rev. D **88** (2013) 025023, `arXiv:1303.6756`.

[131] Y. Ema, K. Nakayama, and Y. Tang, "Production of Purely Gravitational Dark Matter," JHEP **09** (2018) 135, `arXiv:1804.07471`.

[132] P. Beltrán-Palau, A. Ferreiro, J. Navarro-Salas, and S. Pla, "Breaking of adiabatic invariance in the creation of particles by electromagnetic fields," Phys. Rev. D **100** (2019) 085014, `arXiv:1905.07215`.

[133] S.-S. Xue, "Massive particle pair production and oscillation in Friedman Universe: dark energy and matter interaction," 3, 2022.

[134] L. H. Ford and L. Parker, "Quantized Gravitational Wave Perturbations in Robertson-Walker Universes," Phys. Rev. D **16** (1977) 1601–1608.

[135] R. Penrose, Cycles of time: an extraordinary new view of the universe. Random House, 2010.

[136] G. 't Hooft, "Local conformal symmetry: The missing symmetry component for space and time," Int. J. Mod. Phys. D **24** (2015), no. 12, 1543001.

[137] G. 't Hooft, "Local conformal symmetry in black holes, standard model, and quantum gravity," Int. J. Mod. Phys. D **26** (2016), no. 03, 1730006.

[138] M. Paneitz, "A quartic conformally covariant differential operator for arbitrary pseudo-riemannian manifolds," Typeset by the Editors for the Proceedings of the Midwest Geometry Conference 2007 (1983) `arXiv:0803.4331`.

[139] R. J. Reigert, "A non-local action for the trace anomaly," Phys. Lett. B **134** (1984), no. 1, 56–60.

[140] G. de Berredo-Peixoto and I. L. Shapiro, "On the High derivative fermionic operator and trace anomaly," Phys. Lett. B **514** (2001) 377–384, `arXiv:hep-th/0101158`.

[141] A. Stergiou, G. P. Vacca, and O. Zanusso, "Weyl covariance and the energy momentum tensors of higher-derivative free conformal field theories," JHEP **06** (2022) 104, `arXiv:2202.04701`.

[142] V. P. Gusynin, "New Algorithm for Computing the Coefficients in the Heat Kernel Expansion," Phys. Lett. B **225** (1989) 233–239.

[143] L. Boyle and N. Turok, "Cancelling the vacuum energy and Weyl anomaly in the standard model with dimension-zero scalar fields," `arXiv:2110.06258`.

[144] J. Miller, G. E. Volovik, and M. A. Zubkov, "Fundamental scalar field with zero dimension from anomaly cancellations," Phys. Rev. D **106** (2022), no. 1, 015021, `arXiv:2202.05726`.

[145] A. I. Bogolubov N. N. Logunov, A. A. Oksak and I. T. Todorov, General Principles of Quantum Field Theory. Academic Publishers, Dordrecht, 1990.

[146] C. J. Fewster and R. Verch, "Quantum fields and local measurements," Commun. Math. Phys. **378** (2020), no. 2, 851–889.

[147] H. Bostelmann, C. J. Fewster, and M. H. Ruep, "Impossible measurements require impossible apparatus," Phys. Rev. D **103** (2021), no. 2, 025017.

[148] M. A. Nielsen and I. L. Chuang, Quantum Computation and Quantum Information: 10th Anniversary Edition.
Cambridge University Press, 2010.

[149] R. D. Sorkin, "1983 paper on entanglement entropy: "On the Entropy of the Vacuum outside a Horizon"," arXiv:1402.3589.

[150] L. Bombelli, R. K. Koul, J. Lee, and R. D. Sorkin, "A Quantum Source of Entropy for Black Holes," Phys. Rev. D **34** (1986) 373–383.

[151] M. Srednicki, "Entropy and area," Phys. Rev. Lett. **71** (1993) 666–669.

[152] S. N. Solodukhin, "Entanglement entropy of black holes," Living Rev. Relativity **14** (2011) 8.

[153] E. Bianchi and R. C. Myers, "On the Architecture of Spacetime Geometry," Classical Quantum Gravity **31** (2014) 214002.

[154] E. Bianchi and A. Satz, "Entropy of a subalgebra of observables and the geometric entanglement entropy," Phys. Rev. D **99** (2019), no. 8, 085001.

[155] R. Haag, Local Quantum Physics: Fields, Particles, Algebras.
Springer-Verlag, Berlin, 1996.

[156] L. Schwartz, Some Applications of the Theory of Distribution, vol. 1 of Lectures on Modern Mathematics.
Société mathématique de France, 1963.

[157] I. Agullo, B. Bonga, P. Ribes-Metidieri, D. Kranas, and S. Nadal-Gisbert, "How ubiquitous is entanglement in quantum field theory?," Phys. Rev. D **108** (2023), no. 8, 085005, arXiv:2302.13742.

[158] A. Ashtekar, T. De Lorenzo, and M. Schneider, "Probing the Big Bang with quantum fields," Adv. Theor. Math. Phys. **25** (2021), no. 7, 1651–1702.

[159] A. Ashtekar and A. Magnon, "Quantum Fields in Curved Space-Times," Proc. R. Soc. A **346** (1975) 375–394.

[160] J. Martin and V. Vennin, "Real-space entanglement in the Cosmic Microwave Background," J. Cosmol. Astropart. Phys. **10** (oct, 2021) 036.

[161] E. Bianchi and A. Satz, "Entropy of a subalgebra of observables and the geometric entanglement entropy," Phys. Rev. D **99** (Apr., 2019) 085001.

[162] L. Hackl and E. Bianchi, "Bosonic and fermionic Gaussian states from Kähler structures," SciPost Phys. Core **4** (2021) 025.

[163] A. Serafini, Quantum Continuous Variables: A Primer of Theoretical Methods.
CRC Press, Taylor & Francis Group, 2017.

[164] A. Peres, "Separability criterion for density matrices," Phys. Rev. Lett. **77** (1996), no. 8, 1413.

[165] M. B. Plenio, "Logarithmic negativity: A full entanglement monotone that is not convex," Phys. Rev. Lett. **95** (2005), no. 9, 090503.

[166] X. Wang and M. M. Wilde, "Cost of Quantum Entanglement Simplified," Phys. Rev. Lett. **125** (Jul, 2020) 040502.

[167] X. Wang and M. M. Wilde, "α-logarithmic negativity," Phys. Rev. A **102** (Sep, 2020) 032416.

[168] P. Calabrese and J. L. Cardy, "Entanglement entropy and quantum field theory," J. Stat. Mech. **06** (2004) P06002.

[169] T. Jacobson, "Thermodynamics of space-time: The Einstein equation of state," Phys. Rev. Lett. **75** (1995) 1260–1263.

[170] S. Ryu and T. Takayanagi, "Holographic derivation of entanglement entropy from AdS/CFT," Phys. Rev. Lett. **96** (2006) 181602.

[171] J. Martin and V. Vennin, "Quantum Discord of Cosmic Inflation: Can we Show that CMB Anisotropies are of Quantum-Mechanical Origin?," Phys. Rev. D **93** (2016), no. 2, 023505.

[172] J. Martin and V. Vennin, "Real-space entanglement of quantum fields," Phys. Rev. D **104** (Oct., 2021) 085012.

[173] L. Espinosa-Portalés and V. Vennin, "Real-space Bell inequalities in de Sitter," J. Cosmol. Astropart. Phys. **07** (jul, 2022) 037.

[174] P. Morgan, "Classical and Quantum Measurement Theory," `arXiv:2201.04667`.

[175] B. de S. L. Torres, K. Wurtz, J. Polo-Gómez, and E. Martín-Martínez, "Entanglement structure of quantum fields through local probes," J. of High Energy Phys. **05** (05, 2023) 058.

[176] R. Simon, "Peres-Horodecki Separability Criterion for Continuous Variable Systems," Phys. Rev. Lett. **84** (Mar, 2000) 2726.

[177] B. Reznik, “Entanglement from the vacuum,” Found. Phys. **33** (2003) 167–176.

[178] H.-C. Chang and L.-C. Wang.

[179] E. Martín-Martínez, M. Montero, and M. del Rey, “Wavepacket detection with the Unruh-DeWitt model,” Physical Review D **87** (2013), no. 6, 064038.

[180] Á. M. Alhambra, A. Kempf, and E. Martín-Martínez, “Casimir forces on atoms in optical cavities,” Physical Review A **89** (2014), no. 3, 033835.

[181] E. Martín-Martínez, E. G. Brown, W. Donnelly, and A. Kempf, “Sustainable entanglement production from a quantum field,” Physical Review A **88** (2013), no. 5, 052310.

[182] T. R. Perche, B. Ragula, and E. Martín-Martínez, “Harvesting entanglement from the gravitational vacuum,” Physical Review D **108** (2023), no. 8, 085025.

[183] J. G. Caribé, R. H. Jonsson, M. Casals, A. Kempf, and E. Martín-Martínez, “Lensing of vacuum entanglement near Schwarzschild black holes,” Physical Review D **108** (2023), no. 2, 025016.

[184] C. Gooding, A. Sachs, R. B. Mann, and S. Weinfurtner, “Vacuum entanglement probes for ultra-cold atom systems,” arXiv preprint arXiv:2308.07892 (2023).

[185] P. Forn-Díaz, J. J. García-Ripoll, B. Peropadre, J.-L. Orgiazzi, M. Yurtalan, R. Belyansky, C. M. Wilson, and A. Lupascu, “Ultrastrong coupling of a single artificial atom to an electromagnetic continuum in the nonperturbative regime,” Nature Physics **13** (2017), no. 1, 39–43.

[186] N. Janzen, X. Dai, S. Ren, J. Shi, and A. Lupascu, “Tunable coupler for mediating interactions between a two-level system and a waveguide from a decoupled state to the ultrastrong coupling regime,” Physical Review Research **5** (2023), no. 3, 033155.

[187] E. Tjoa and E. Martín-Martínez, “When entanglement harvesting is not really harvesting,” Physical Review D **104** (2021), no. 12, 125005.

[188] M. M. Wilde, Quantum information theory. Cambridge university press, 2013.

[189] A. Ferreiro and J. Navarro-Salas, "Running couplings from adiabatic regularization," Phys. Lett. B **792** (2019) 81–85, arXiv:1812.05564.

[190] P. Beltrán-Palau, S. Nadal-Gisbert, J. Navarro-Salas, and S. Pla, "Renormalization and a non-adiabatic vacuum choice in a radiation-dominated universe," 4, 2022.

[191] E. M. Stein and G. Weiss, Introduction to Fourier Analysis on Euclidean Spaces, vol. 1.
Princeton University Press, Princeton, NJ, 1971.

[192] I. S. Gradshteyn, I. M. Ryzhik, A. Jeffrey, and D. Zwillinger, Table of Integrals, Series, and Products, Sixth Edition.
Elsevier/Academic Press, Amsterdam, San Diego, 2000.

[193] N. Klco, D. H. Beck, and M. J. Savage, "Entanglement structures in quantum field theories: Negativity cores and bound entanglement in the vacuum," Phys. Rev. A **107** (2023), no. 1, 012415, arXiv:2110.10736.